



<https://theses.gla.ac.uk/>

Theses Digitisation:

<https://www.gla.ac.uk/myglasgow/research/enlighten/theses/digitisation/>

This is a digitised version of the original print thesis.

Copyright and moral rights for this work are retained by the author

A copy can be downloaded for personal non-commercial research or study, without prior permission or charge

This work cannot be reproduced or quoted extensively from without first obtaining permission in writing from the author

The content must not be changed in any way or sold commercially in any format or medium without the formal permission of the author

When referring to this work, full bibliographic details including the author, title, awarding institution and date of the thesis must be given

Enlighten: Theses

<https://theses.gla.ac.uk/>  
[research-enlighten@glasgow.ac.uk](mailto:research-enlighten@glasgow.ac.uk)

# **G Protein Signalling Characteristics of Human IP Prostanoid Receptors**

A THESIS PRESENTED FOR  
THE DEGREE OF  
DOCTOR OF PHILOSOPHY

BY

**CHEE-WAI FONG**



DIVISION OF BIOCHEMISTRY AND MOLECULAR BIOLOGY  
INSTITUTE OF BIOMEDICAL AND LIFE SCIENCES  
UNIVERSITY OF GLASGOW

January 1999

ProQuest Number: 10390907

All rights reserved

INFORMATION TO ALL USERS

The quality of this reproduction is dependent upon the quality of the copy submitted.

In the unlikely event that the author did not send a complete manuscript and there are missing pages, these will be noted. Also, if material had to be removed, a note will indicate the deletion.



ProQuest 10390907

Published by ProQuest LLC (2017). Copyright of the Dissertation is held by the Author.

All rights reserved.

This work is protected against unauthorized copying under Title 17, United States Code  
Microform Edition © ProQuest LLC.

ProQuest LLC.  
789 East Eisenhower Parkway  
P.O. Box 1346  
Ann Arbor, MI 48106 – 1346

## Abstract

The functional assay of agonists acting on G protein coupled receptors (GPCRs) coupled to the  $G_s\alpha$  subunit usually involves the measurement of effector (adenylate cyclase) activity. However, the activity of adenylate cyclase can be modulated by proteins other than  $G_s\alpha$ , and their levels and subtypes vary between cell lines. As such, measurement of agonist efficacy at the level of the G protein would be most ideal. This is currently not possible with traditional assays such as the [ $^{35}$ S]GTP $\gamma$ S binding and high affinity GTPase assays, since activated  $G_s\alpha$  has low rates of GTP exchange and hydrolysis (Wieland *et al.* 1994; Gierschik *et al.* 1994).

A FLAG<sup>TM</sup>-tagged form of the human IP prostanoid receptor (a  $G_s\alpha$ -coupled GPCR) was expressed stably in HEK293 cells and bound [ $^3$ H]iloprost with high affinity and stimulated cAMP production when exposed to agonist. A cDNA encoding the  $G_{i1}\alpha$  sequence but with the carboxyl-terminal six amino acids of  $G_s\alpha$  was also constructed. Co-expression of this chimeric G protein  $G_{i1}/G_{s6}\alpha$ , but not  $G_s\alpha$  or  $G_{i1}\alpha$ , resulted in robust stimulation by iloprost. This significantly high levels of agonist-stimulated [ $^{35}$ S]GTP $\gamma$ S binding and high affinity GTPase were not abolished by treatment with both cholera and pertussis toxins. This correlated with the loss of both cholera (arginine 201 of  $G_s\alpha(L)$ ) and pertussis (cysteine 351 of  $G_{i1}\alpha$ ) toxin-susceptible sites in the  $G_{i1}/G_{s6}\alpha$  protein. This clearly demonstrated the utility of chimeric G proteins to combine the high GTP exchange and hydrolysis capacity of  $G_{i1}\alpha$  with the ability to couple to a  $G_s\alpha$ -coupled GPCR.

The stoichiometry of GPCR to  $G\alpha$  can have a direct impact on the signalling cascades of GPCRs (Kenakin 1995a; 1997). In addition, there is evidence that GPCR and  $G\alpha$  may not be localised in the same microdomain of the plasma membrane (Neubig 1994). Through the use of a fusion protein between the  $\beta_2$ -adrenergic receptor and  $G_s\alpha$ , Bertin *et al.* (1994) demonstrated productive interactions between the fused partners. A fusion protein of the FLAG<sup>TM</sup>-tagged

human IP prostanoid receptor with  $G_{s\alpha}(L)(HA)$  was therefore generated and stably expressed in HEK293 cells. These cells bound [ $^3H$ ]iloprost with high affinity and also stimulated adenylate cyclase upon addition of agonist. When compared to the freely interacting IP prostanoid receptor, the fusion protein FhIPR- $G_{s\alpha}$  exhibited enhanced agonist-stimulated activities in both the [ $^{35}S$ ]GTP $\gamma$ S binding and high affinity GTPase assays. Furthermore, cholera toxin treatment diminished its capacity to hydrolyse GTP but not the incorporation of [ $^{35}S$ ]GTP $\gamma$ S.

The fidelity of signalling in GPCR- $G\alpha$  fusion proteins was established by studying the  $G\alpha$  activity of a series of FhIPR- $G\alpha$  fusions. When stably expressed in HEK293 cells and stimulated by iloprost, the FhIPR- $G_{i1\alpha}$  protein failed to elevate the low levels of high affinity GTPase and [ $^{35}S$ ]GTP $\gamma$ S binding activity. These low levels of activity were shown to be derived from activation of endogenous  $G_{s\alpha}$  but not receptor-linked  $G_{i1\alpha}$ . Substituting the carboxyl-terminal six amino acids of FhIPR- $G_{i1\alpha}$  with  $G_{s\alpha}$  resulted in the production of the FhIPR- $G_{i1}/G_{s6\alpha}$  fusion protein. This protein produced substantial elevation of both high affinity GTPase and [ $^{35}S$ ]GTP $\gamma$ S binding activity upon stimulation by iloprost. In addition, these activities were resistant to both cholera and pertussis toxin treatments, as was observed for the freely interacting  $G_{i1}/G_{s6\alpha}$  protein. This clearly demonstrated that fusing the GPCR and  $G\alpha$  did not alter their individual characteristics.

The assay of agonist activity at the G protein level for a  $G_{s\alpha}$ -coupled GPCR is now possible by using the chimeric  $G_{i1}/G_{s6\alpha}$  protein or GPCR- $G\alpha$  fusions. The GPCR- $G\alpha$  fusion approach is superior to the chimeric protein as the stoichiometry of GPCR to  $G\alpha$  is fixed at 1:1 and the interacting partners are co-targeted to the same microdomain of the plasma membrane.

## Acknowledgements

I would like to firstly thank Professor Graeme Milligan for allowing me the chance to work in his laboratory. His vision, guidance and advice is crucial to the success of this thesis. My gratitude also goes to everyone in the laboratory, for their patience, technical assistance, encouragement, friendship, co-operation and most of all, tolerance towards me.

I am greatly indebted to my sponsoring organisation, the National Science & Technology Board of Singapore, for sponsoring my studies administered under the Institute of Molecular & Cell Biology. Without their financial assistance and assurance, I would not have the opportunity to further my study here. In that aspect, I am particularly indebted to Associate Professor Miranda Yap, for her recommendations and support.

My flatmates from China, church friends from all over Asia and the congregation at Partick Free Church of Scotland had filled my days with joyous moments when I am not working. My parents and siblings also deserved to be mentioned, for their unfailing love and support all these years. My struggle in both study and daily living in the United Kingdom was also made worthwhile by the love, patience and companionship of my wife, Nancy, who has to bear with all my idiosyncrasies.

Finally, the pursuit of wisdom and knowledge will be futile if I do not give glory to our Lord God JEHOVAH:

*Proverbs 1:7 "The fear of the LORD is the beginning of knowledge..."*

# Contents

	Page
<b>Abstract</b>	I
<b>Acknowledgements</b>	III
<b>Contents</b>	IV
<b>List of Figures</b>	VIII
<b>List of Tables</b>	XII
<b>List of Publications</b>	XIII
<b>Abbreviations</b>	XIV

<b>CHAPTER 1 INTRODUCTION</b>		Page
<b>1.1</b>	<b>G-protein coupled receptors (GPCR)</b>	<b>1</b>
1.1.1	Historical Perspective	1
1.1.2	Structural Features of GPCRs	4
1.1.3	Regulation of GPCR	7
	<i>A) Desensitisation</i>	8
	<i>B) Internalisation / Sequestration</i>	10
	<i>C) Downregulation</i>	11
<b>1.2</b>	<b>The Heterotrimeric G proteins</b>	<b>12</b>
1.2.1	G Alpha Subunit	12
	<i>A) G<sub>s</sub>α subfamily</i>	16
	<i>B) G<sub>i</sub>α subfamily</i>	18
	<i>C) G<sub>q</sub>α subfamily</i>	21
	<i>D) G<sub>12</sub>α subfamily</i>	23
1.2.2	G Beta and Gamma Subunits	25

<b>1.3</b>	<b>Receptor G-protein Coupling</b>	<b>29</b>
1.3.1	Receptor domains essential for coupling	29
1.3.2	G-protein domains essential for coupling	31
1.3.3	Divergent Signalling in GPCRs	32
<b>1.4</b>	<b>Prostaglandin Receptors</b>	<b>35</b>
1.4.1	Prostaglandins and their biosynthesis	35
1.4.2	Prostaglandin Receptor Family	37
	A) <i>DP</i>	38
	B) <i>EP</i>	38
	C) <i>FP</i>	39
	D) <i>TP</i>	39
1.4.3	Prostacyclin (IP) Receptor	40
	A) <i>Physiological functions and potential therapeutic roles</i>	41
	B) <i>Agonist Studies</i>	43
<b>1.5</b>	<b>Research Objectives</b>	<b>45</b>

## CHAPTER 2 MATERIALS AND METHODS

<b>2.1</b>	<b>Materials</b>	<b>46</b>
2.1.1	General Reagents	46
2.1.2	Radiochemicals	48
2.1.3	Tissue Culture	48
2.1.4	Standard Buffers	49
2.1.5	Antisera	51
<b>2.2</b>	<b>Cell Culture</b>	<b>52</b>
2.2.1	Routine Cell Culture	52
2.2.2	Transient Transfections	52
2.2.3	Generation and Maintenance of Stable Cell Lines	53
2.2.4	Preservation of Cell Lines	54
2.2.5	Treatment with Toxins and Agonist	55
2.2.6	Cell Harvesting	55
<b>2.3</b>	<b>Molecular Biology</b>	<b>55</b>

2.3.1	Reagents for Molecular Biology	56
2.3.2	Transformation	57
	<i>A) Preparation of competent bacteria</i>	57
	<i>B) Transformation of DNA</i>	58
2.3.3	DNA Preparation	59
2.3.4	Polymerase Chain Reaction	60
2.3.5	Agarose Gel Electrophoresis	61
2.3.6	DNA Purification from Agarose Gel	61
2.3.7	DNA Sequencing	62
2.3.8	Construction of FLAG-hIPR (FhIPR)	62
2.3.9	Construction of Receptor-G $\alpha$ Fusion cDNA	63
	<i>A) FhIPR-G<math>_s\alpha</math> cDNA</i>	64
	<i>B) FhIPR-G<math>_{11}\alpha</math> cDNA</i>	64
	<i>C) FhIPR-G<math>_{11}/G_s6\alpha</math> cDNA</i>	65
<b>2.4</b>	<b>Assays</b>	<b>66</b>
2.4.1	Radioligand Binding	66
2.4.2	Adenylate Cyclase Catalytic Activity	67
2.4.3	High Affinity GTPase	69
2.4.4	GTP $\gamma$ S Binding	71
<b>2.5</b>	<b>Other Protocols</b>	<b>73</b>
2.5.1	Preparation of Cell Membranes	73
2.5.2	Western Blotting	73
	<i>A) Preparation of SDS-PAGE gel</i>	73
	<i>B) Electrophoresis of SDS-PAGE</i>	74
	<i>C) Protein transfer onto membrane</i>	75
	<i>D) Incubation with antibodies</i>	76
	<i>E) Enhanced chemiluminescence</i>	77

<b>CHAPTER 3</b>	<b>Selective Activation of a Chimeric <math>G_{i1}/G_s</math> G Protein <math>\alpha</math> Subunit by the Human IP Prostanoid Receptor</b>	
3.1	Introduction	78
3.2	Results	85
3.3	Discussion	110
<b>CHAPTER 4</b>	<b>Comparison of Signal Transduction Efficiency between the Human IP Prostanoid Receptor and the Human IP Prostanoid Receptor-<math>G_s\alpha</math> Fusion Protein</b>	
4.1	Introduction	115
4.2	Results	121
4.3	Discussion	146
<b>CHAPTER 5</b>	<b>Analysis of G Protein Coupling Specificity in the Human IP Prostanoid Receptor-<math>G\alpha</math> Fusion Proteins</b>	
5.1	Introduction	156
5.2	Results	161
5.3	Discussion	182
<b>CHAPTER 6</b>	<b>DISCUSSION</b>	190
<b>REFERENCES</b>		199

## List of Figures

Figure	Title	Page
1.1	Structure of a typical G protein coupled receptor	6
1.2	Structure of $G_{i1}\alpha$ .	15
1.3	The propeller structure of $G\beta\gamma$ subunit	26
1.4	Biosynthesis of prostaglandins	36
1.5	PG Receptor Phylogeny	37
1.6	Diagram of the human IP prostanoid receptor	42
1.7	Structure of iloprost	42
3.1	Stable expression of the FLAG <sup>TM</sup> -tagged human IP prostanoid receptor in clones of HEK293 cells	94
3.2	Stimulation of cAMP production by iloprost and forskolin in clones of HEK293 cells stably expressing FhIPR	95
3.3A	[ <sup>3</sup> H]iloprost saturation binding studies of clone 13 cells	96
3.3B	Scatchard plot of agonist saturation binding in clone 13 cells	96
3.4	Displacement of [ <sup>3</sup> H]iloprost binding in membranes of clone 13	97
3.5	Immunodetection of the FLAG <sup>TM</sup> -tagged human IP prostanoid receptor in transiently and stably transfected HEK293 cells	98
3.6	Adenylate cyclase concentration-response curve for iloprost in intact clone 13 cells	99
3.7	Sustained agonist treatment of clone 13 cells results in downregulation of $G_s\alpha$ but not $G_{i1/2}\alpha$ or $G_{q/11}\alpha$ subunits	100
3.8	Generation of $G_{i1}/G_s6\alpha$ chimeric protein	101
3.9	Immunological characterisation of $G_{i1}/G_s6\alpha$ protein	102
3.10	Expression of $G_{i1}/G_s6\alpha$ with FhIPR enhances agonist-stimulated high affinity GTPase activity	103
3.11	Immunoblot indicating expression levels of $G_i\alpha$ , $G_s\alpha$ , and	104

	$G_{i1}/G_s6\alpha$ in clone 13 cells	
3.12	Co-expression of $G_{i1}/G_s6\alpha$ with FhIPR enhances agonist-stimulated binding of [ $^{35}\text{S}$ ]GTP $\gamma$ S	105
3.13	Comparison of the effects of cholera and pertussis toxin on agonist-stimulated high affinity GTPase activity in clone 13 cells	106
3.14	The effects of combined cholera and pertussis toxin treatment on agonist-stimulated [ $^{35}\text{S}$ ]GTP $\gamma$ S binding in clone 13 cells transiently expressing various $G\alpha$ subunits	107
3.15	Sustained treatment of clone 13 cells with cholera and pertussis toxin downregulates levels of $G_s\alpha$ and modifies $G_{i1}$	108
3.16	Adenylate cyclase response in cells co-expressing FhIPR and $G_{i1}/G_s6\alpha$ protein	109
4.1	Schematic representation of FhIPR- $G_s\alpha$ fusion cDNA and protein	128
4.2	Agarose gel analysis of FhIPR- $G_s\alpha$ cDNAs	129
4.3	Stable expression of the FhIPR- $G_s\alpha$ fusion protein in clones of HEK293 cells	130
4.4	Stimulation of cAMP production by iloprost and forskolin in clones of HEK293 cells stably expressing FhIPR- $G_s\alpha$	131
4.5	Displacement of [ $^3\text{H}$ ]iloprost binding in membranes of clone 44 cells	132
4.6	Immunodetection of the FLAG <sup>TM</sup> -tagged human IP prostanoid receptor fused to $G_s\alpha$ in clone 44 cells	133
4.7	Effect of agonist treatment on clone 13 and clone 44 cells	134
4.8	Clone 44 cells exhibit enhanced agonist-stimulated high affinity GTPase activity compared to clone 13 cells	137
4.9	Immunoblot showing overexpression of $G_s\alpha(\text{L})(\text{HA})$ in clone 13 cells	138
4.10	Clone 44 cells exhibit enhanced agonist-stimulated [ $^{35}\text{S}$ ]GTP $\gamma$ S binding compared to clone 13 cells	139
4.11	Effects of cholera and pertussis toxins on agonist-stimulated high affinity GTPase activity in clone 44 cells	140

4.12	Effects of cholera and pertussis toxins on agonist-stimulated [ <sup>35</sup> S]GTP $\gamma$ S binding in clone 44 cells	141
4.13	Sustained treatment of clone 13 and clone 44 cells with cholera toxin downregulates endogenous levels of G <sub>s</sub> $\alpha$	142
4.14	Time course of adenylate cyclase response to iloprost stimulation in clone 13 and clone 44 cells	143
4.15	Comparison of adenylate cyclase concentration-response for iloprost in intact clone 13 and clone 44 cells	144
4.16	Analysis of adenylate cyclase response in clone 13 and clone 44 cells pretreated with cholera toxin	145
5.1	Schematic representation of FhIPR-G <sub>11</sub> $\alpha$ and FhIPR-G <sub>11</sub> /G <sub>s</sub> 6 $\alpha$ fusion proteins	168
5.2	Agarose gel analysis of FhIPR-G <sub>11</sub> $\alpha$ and FhIPR-G <sub>11</sub> /G <sub>s</sub> 6 $\alpha$ cDNAs	169
5.3	Stable expression of the FhIPR-G <sub>11</sub> $\alpha$ or FhIPR-G <sub>11</sub> /G <sub>s</sub> 6 $\alpha$ fusion proteins in clones of HEK293 cells	170
5.4	Immunodetection of FhIPR-G $\alpha$ fusion proteins	171
5.5	Displacement of [ <sup>3</sup> H]iloprost binding in membranes of HEK293 clones stably expressing FhIPR and FhIPR-G $\alpha$ fusion proteins	172
5.6	Adenylate cyclase concentration-response for iloprost	173
5.7	Effects of cholera and pertussis toxins on agonist-stimulated [ <sup>35</sup> S]GTP $\gamma$ S binding in HEK293 clones expressing FhIPR and FhIPR-G $\alpha$ fusion proteins	174
5.8	Effects of cholera and pertussis toxins on agonist-stimulated high affinity GTPase activity in HEK293 clones expressing FhIPR and FhIPR-G $\alpha$ fusion proteins	175
5.9	Time course of agonist-stimulated [ <sup>35</sup> S]GTP $\gamma$ S binding in HEK293 clones expressing FhIPR-G <sub>s</sub> $\alpha$ and FhIPR-G <sub>11</sub> /G <sub>s</sub> 6 $\alpha$	176
5.10	Iloprost concentration-response of [ <sup>35</sup> S]GTP $\gamma$ S binding in HEK293 clones expressing FhIPR-G <sub>s</sub> $\alpha$ and FhIPR-G <sub>11</sub> /G <sub>s</sub> 6 $\alpha$ fusion proteins	177
5.11	Time course of high affinity GTPase activity in HEK293 clones	178

expressing FhIPR-G<sub>s</sub>α and FhIPR-G<sub>i1</sub>/G<sub>s</sub>δα

5.12	Iloprost concentration-response of high affinity GTPase activity in HEK293 clones expressing FhIPR-G <sub>s</sub> α and FhIPR-G <sub>i1</sub> /G <sub>s</sub> δα fusion proteins	179
5.13	Basal and iloprost-stimulated high affinity GTPase activity at various GTP concentrations	180
5.14	Eadie-Hofstee plots of basal and iloprost-stimulated high affinity GTPase activity at various GTP concentrations	181

## List of Tables

Table	Title	Page
1.1	Classification of $G\alpha$ subunits, their distribution and effectors	13
5.1	Expression levels of HEK293 clones	162
5.2	$K_m$ and $V_{max}$ values of HEK293 cells expressing FhIPR, FhIPR- $G_s\alpha$ and FhIPR- $G_{i1}/G_{s6}\alpha$ .	167
5.3	Rates of [ $^{35}$ S]GTP $\gamma$ S incorporation	187
5.4	Rates of GTP turnover	189

## List of Publications

**Fong, C. W.**, Bahia, D. S., Rees, S., and Milligan, G. (1998) *Mol. Pharmacol.* **54**, 249-257

Milligan, G., Groarke, D. A., McLean, A., Ward, R., **Fong, C. W.**, Cavalli, A., and Drmota, T. (1999) *Biochem. Soc. Trans.* (in press)

## Abbreviations

The abbreviations used in this thesis are as set out in "Instructions to Authors" Biochemical Journal (1985) **225**, 1-26 with the following additions:

aa	amino acid
ADP	Adenosine 5'-diphosphate
App(NH)p	Adenylyl 5'-imidodiphosphate
ARF	ADP-ribosylating factor
$\beta_2$ AR	$\beta_2$ -adrenergic receptor
$B_{max}$	Maximal binding capacity
cAMP	Adenosine 3', 5'-cyclic monophosphate
cDNA	Complimentary deoxyribonucleic acid
CHO	Chinese hamster ovary
cpm	Counts per minute
CRLR	Calcitonin-receptor-like receptor
CTX	Cholera toxin
DAG	Diacylglycerol
DMEM	Dulbecco's modified of Eagle's medium
DMSO	Dimethylsulphoxide
dpm	Disintegrations per minute
DTT	Dithiothreitol
<i>E. coli</i>	<i>Escherichia coli</i>
EC	Extracellular loop of G protein coupled receptor
EC <sub>50</sub>	Median effective dose
EDTA	Ethylenediaminetetraacetic acid
FhIPR	FLAG <sup>TM</sup> -epitope tagged human IP prostanoid receptor

GAP	GTPase activating protein
GDP	Guanosine 5'-diphosphate
GEF	Guanine nucleotide exchange factor
GPCR	G protein coupled receptors
Gpp(NH)p	Guanylyl 5'-[ $\beta$ imido]diphosphate
GRK	G protein receptor kinase
GTP	Guanosine 5'-triphosphate
GTP $\gamma$ S	Guanosine 5'-[3-o-thio]triphosphate
h	Hour
HEK293	Human Embryonic Kidney 293
HEPES	4-(2-Hydroxyethyl)-1-piperazine-N' 2-ethane-sulphonic acid
hIPR	Human IP prostanoid receptor
IC	Intracellular loop of G protein coupled receptor
IC <sub>50</sub>	Median inhibitory dose
K <sub>d</sub>	Equilibrium dissociation constant
kDa	Kilodaltons
LT	Leukotriene
MEM	Minimum Essential Medium
min	Minute
mRNA	Messenger ribonucleic acid
NBCS	Newborn calf serum
NHE	Na <sup>+</sup> /H <sup>+</sup> exchanger
PAGE	Polyacrylamide Gel Electrophoresis
PCR	Polymerase chain reaction
PG	Prostaglandin
PH	Pleckstrin homology

PKA	Protein kinase A
PKC	Protein kinase C
PLA2	Phospholipase A2
PLC	Phospholipase C
PTX	Pertussis toxin
RAMP	Receptor-activity-modifying protein
<i>S. cerevisiae</i>	<i>Saccharomyces cerevisiae</i>
SDS	Sodium dodecyl sulphate
SEM	Standard error of the mean
TCA	Trichloroacetic acid
TEMED	N, N, N', N'-tetramethylethylenediamine
TM	Transmembrane segment of G protein coupled receptor
TSH	Thyrotropin receptor
Tris	Tris(hydroxymethyl)aminomethane
TX	Thromboxane

# CHAPTER 1 INTRODUCTION

## 1.1 G-protein coupled receptors (GPCR)

Receptors play a very important role in transducing extracellular signals into cells. Among the many families of receptors, G-protein coupled receptors (GPCR) are by far the largest (about 1000). Ligands that act on GPCRs range from cations, chromophores, odourous chemicals, small biogenic amines, nucleotides, lipid derived messengers and chemokines to large peptide hormones. Correlating with the broad range of ligands is the wide distribution of GPCRs in our body, mediating such diverse functions as vision, smell, neurotransmission, cardiovascular regulation, immune and inflammatory responses, pain control, growth, metabolism and even reproduction. Malfunctioning of GPCRs therefore can give rise to a variety of diseases.

GPCRs are very well studied and their basic mode of action well established. Despite this wealth of knowledge, we continue to benefit from new experimental approaches such as structural and mutational studies, undertaken to unravel their functions and mechanisms down to the molecular level. The discovery of novel classes and subtypes of GPCRs, especially among the large group of orphan receptors, also confirms the importance of GPCRs in modern medicine. Despite more than four decades of research in this field, there are still many important discoveries to be made, and many dividends may be reaped from such progress with the aid of modern techniques and novel approaches.

### 1.1.1 Historical Perspective

The discovery of GPCRs stretches back to 1957, when Sutherland and Rall (Rall *et al.* 1957; Sutherland *et al.* 1958) characterized the properties of the enzyme adenylate cyclase, which was activated by the hormones adrenaline and glucagon and by sodium fluoride. Initially, adenylate cyclase was thought to be a protein complex in which the hormone ligand directly activated the enzyme via a site on a regulatory subunit. It was not until the late 1960s that Birnbaumer and

Rodbell (1969) concluded that the hormone receptors are distinct from the enzyme from studies of fat cell adenylate cyclase.

At about the same time, a crucial role for guanine nucleotides on hormone binding and activation of adenylate cyclase was uncovered (Rodbell *et al.* 1971). Pfeuffer and Helmreich (1975) separated a GTP-binding protein from the adenylate cyclase complex, which when added back to an insensitive cyclase, restored activation by GTP and sodium fluoride (Ross and Gilman 1977). This protein is now widely known as  $G_s\alpha$  subunit, due to its stimulatory effect on cyclase.

The GTPase activity of  $G_s\alpha$  was first noted by Cassel and Selinger (1977) when they stimulated adenylate cyclase of turkey erythrocyte membranes with adrenaline. This GTPase activity was inhibited by cholera toxin, which activated adenylate cyclase by an unknown mechanism. Further experiments led them to postulate that hormone activated receptor interacted with  $G_s\alpha$  to release bound GDP and subsequently bind GTP (Cassel and Selinger 1978), thus enabling the  $G_s\alpha$  subunit to activate adenylate cyclase.  $G_s\alpha$  activity was terminated when the bound GTP was hydrolysed to GDP. Cholera toxin was able to ADP-ribosylate  $G_s\alpha$  which inhibited the hormone stimulated GTPase cycle and hence constitutively activate adenylate cyclase (Cassel and Selinger 1977).

The cellular effectors of the other partner in the heterotrimeric subunits, the  $G\beta\gamma$  dimer, were only discovered in the late 1980s. Early evidence came from Clapham's group in 1987 who showed direct activation of a muscarinic acetylcholine regulated  $K^+$  channel in cardiac atrial cells by  $G\beta\gamma$  dimer (Logethetis *et al.* 1987). There was initial contention about whether such effects were due to  $G\alpha$  or  $G\beta\gamma$  subunits, but it is now widely accepted that  $G\beta\gamma$  dimers do regulate a wide range of effectors (Clapham *et al.* 1997). The crystallography studies of  $G\beta\gamma$  subunit showed a "propeller" structure (Sondek *et al.* 1996).

On the receptor front, the bovine opsin receptor was the first GPCR cloned (Nathans *et al.* 1983), using oligonucleotide probes designed from the amino acid

sequence of bovine rhodopsin. When the mammalian  $\beta_2$ -adrenergic receptor cDNA was cloned in 1986 (Dixon *et al.* 1986), it was apparent from the deduced sequence that it exhibited a structure similar to that of the rhodopsins, and suggested the existence of a family of signal receptors. The application of new molecular cloning techniques, such as polymerase chain reaction (PCR) and homology screening, enabled rapid progress in the isolation of GPCR genes. This included many novel members for which physiological ligands are not identified, and hence they are named "orphan receptors".

Sustained agonist activation of GPCR resulted in diminished cellular response, a phenomenon known as desensitisation in the laboratory (Shear *et al.* 1976) or drug tolerance in the clinic. Initial research focused on the role second messenger activated kinases, such as protein kinase A (PKA) and protein kinase C (PKC), played in the uncoupling of  $G\alpha$  from GPCR (Hausdorff *et al.* 1990). However, understanding of the regulation of desensitisation was given new impetus with the discovery of a group of receptor kinases known as G protein receptor kinases (GRKs). Rhodopsin kinase (now known as GRK1) was the first kinase in the family to be discovered, by Kuhn in 1978. He and other co-workers realised that rhodopsin phosphorylation is light-dependent, and results in the desensitisation of the receptor. A similar kinase, known as  $\beta$ -adrenergic receptor kinase (or GRK2) was also shown to phosphorylate  $\beta$ -adrenergic receptors (Benovic *et al.* 1986). Furthermore, a protein known as  $\beta$ -arrestin was able to bind to the GRK phosphorylated receptor to cause uncoupling of the receptor from their  $G\alpha$  subunits (Lohse *et al.* 1990).  $\beta$ -arrestin is an isoform of visual arrestin, originally discovered by Pfister (Pfister *et al.* 1985) that binds to GRK phosphorylated rhodopsin.

The identification of new proteins regulating the GPCR pathway continued into the 1990s with the discovery of regulators of G protein signalling (RGS). These proteins are equivalent to the GTPase activating proteins (GAPs) of small G proteins such as RasGAP, in that they accelerate the GTP hydrolysis rate and hence "switch-off" the activated conformation of G proteins (Berman *et al.* 1998). A eukaryotic RGS homologue, SST2 was initially shown to exist in the yeast

*Saccharomyces cerevisiae* when Chan and Otte screened for mutant haploids hypersensitive to pheromone-induced cell cycle arrest (Chan *et al.* 1982). It was only in 1995 that a human homologue, GAIP was found through a yeast two-hybrid system by using  $G_{13}\alpha$  as bait (DeVries *et al.* 1995). GAIP contains the core RGS domain which is also found in products of BL34/1R20 and GOS8 cDNAs, now known as RGS1 and RGS2 respectively. Using homologous screening and expressing the cDNAs in SST2 gene deficient yeast cells, RGS3 and RGS4 were found (Druey *et al.* 1996). There are at least 19 RGS proteins identified to date.

This enormous progress in the identification and understanding of GPCRs and their signalling pathways, with their profound implications for human diseases, enabled the development of new therapies. It is without doubt that many of our most useful medicines were developed from such intensive research. As we continue to uncover the intricacies of GPCR signalling and understand their regulation and involvement with other signalling pathways, it is undeniable that such research will be important and relevant in our endless battle against diseases.

### **1.1.2 Structural Features of GPCRs**

Analysis of the amino acid sequence of GPCRs indicated seven hydrophobic domains which were shown to transverse the plasma membrane. Hence, GPCRs are also known as seven transmembrane receptors. They have an extracellular N-terminal segment, seven transmembrane segments (TM) of 20 to 27 amino acids which are linked by three intracellular (IC) and three extracellular (EC) loops, and ending in an intracellular C-terminal segment (Figure 1.1).

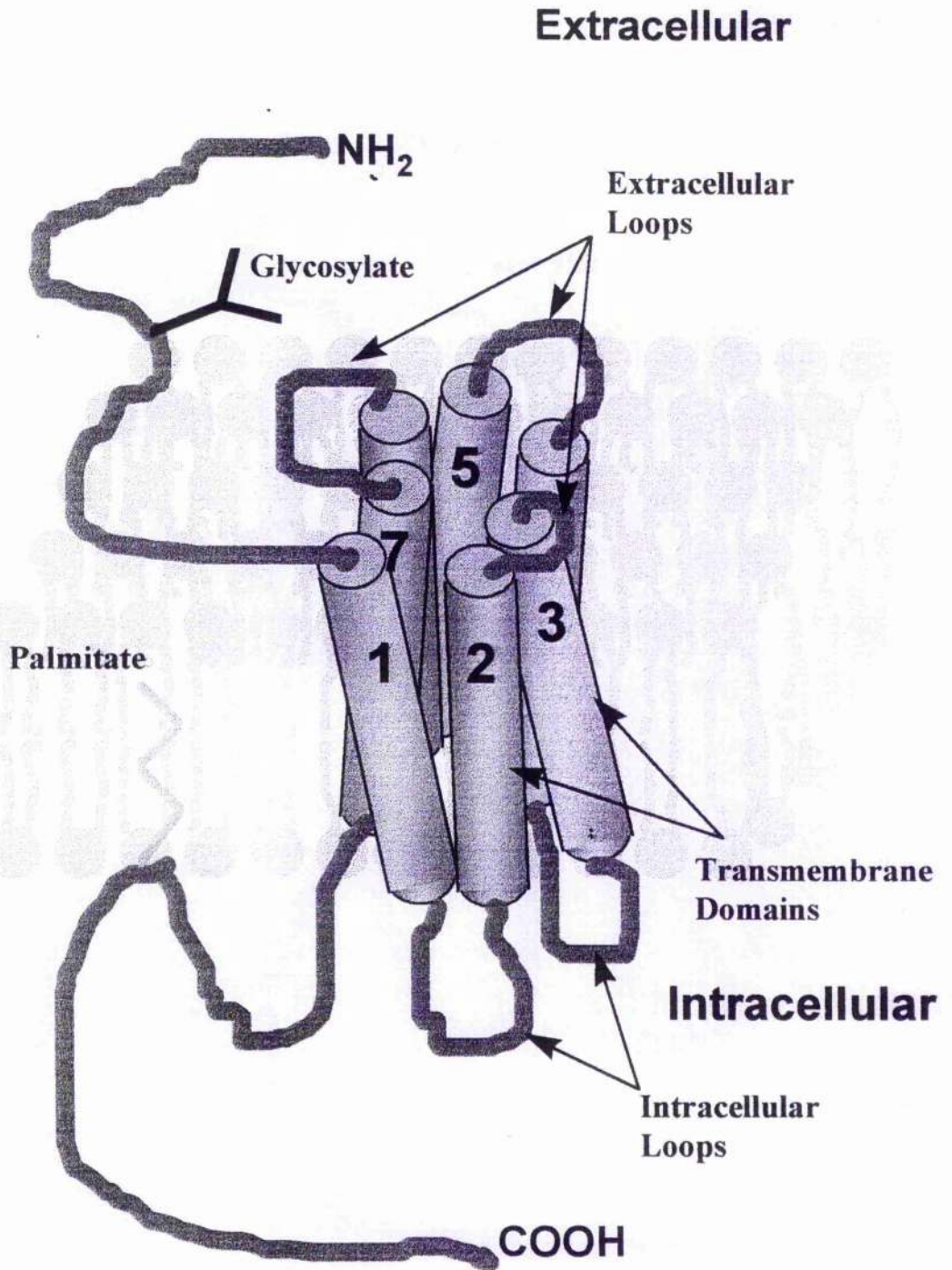
The N-terminal segment contains one to nine glycosylation consensus sequences (Asn-X-Ser/Thr), where X is any amino acid except Pro or Asp. N-glycosylation at the asparagine residue of this sequence targets the receptor to the plasma membrane (Rands *et al.* 1990). Variability in the overall length of GPCRs also occurs primarily in this domain (7-595 amino acids). This domain plays a role in ligand binding, especially for large polypeptides and glycoprotein

hormones. There is a weak correlation between the length of the domain and the size of the ligand (Ji *et al.* 1998).

Interestingly, there is a new family of single transmembrane domain proteins known as receptor-activity-modifying proteins (RAMPs) that control the transport and glycosylation of certain GPCRs (McLatchie *et al.* 1998). Co-expression of RAMP1 with calcitonin-receptor-like receptor (CRLR) presents the receptor at the cell surface as a mature glycoprotein and a calcitonin-gene-related peptide (CGRP) receptor. However, co-expression of RAMP2 with CRLR caused core-glycosylation of the receptor, and presented it as an adrenomedullin receptor. Thus, RAMPs have the capacity to regulate the pharmacological profile of GPCRs, and hence may have extensive physiological implications.

The transmembrane domains are arranged in a counter-clockwise orientation (TM 1 to 7; see Figure 1.1) when viewed from the extracellular surface, based on the structure of animal rhodopsin (Unger *et al.* 1997). Using chimeric  $\alpha_2/\beta_2$ -adrenergic receptors to identify intramolecular interactions between specific amino acids on the transmembrane domains, Mizobe *et al.* (1996) also found a similar counter-clockwise arrangement of the adrenergic receptors. The orientation of the TMs gives rise to specific stereo and geometrical selectivity of the ligands that bind to the TM core. This core is formed from the closed loop arrangement of the TMs, and is packed tightly together by extensive hydrogen bonds and salt bridges within and between the TMs (Pebay-Peyroula *et al.* 1997). The greatest degree of amino acid similarity (20 to 90%) occurs in the TM segments. Finally, the TMs are not orientated perpendicular to the plane of the plasma membrane; but with TM3 tilted at  $\sim 30^\circ$  and TMs 1,2 and 5 tilted slightly (Unger *et al.* 1997).

Figure 1.1 Structure of a typical G protein coupled receptor



The intracellular loops allow interaction of heterotrimeric G protein subunits and other regulatory proteins with the receptor. The first and second loops are relatively well conserved among the GPCRs, but the third intracellular loop is quite divergent. Both the second and third intracellular loops have been shown to be crucial for coupling to G $\alpha$  subunits, especially residues close to TM5 and TM6 in the third loop (Burstein *et al.* 1995). The third intracellular loop also may contain sites for phosphorylation by second messenger regulated kinases.

The first and second extracellular loops contain cysteine residues that form a disulphide bond in receptors for rhodopsin,  $\beta_2$ -adrenergic, muscarinic, thyrotrophin-releasing hormone, thromboxane A<sub>2</sub>, gonadotrophin releasing hormone and many others. The disulphide bonds are thought to play a crucial role in maintaining the structural integrity of GPCRs. For example, in congenital blue cone monochromacy, a point mutation of an opsin gene leading to the loss of a conserved cysteine residue in the second intradiscal loop causes congenital colour blindness (Nathans *et al.* 1989). Furthermore, the importance of the cysteine residues involved in disulphide bond formation is shown by the conservation of cysteine residues in corresponding locations in the majority of GPCRs. The first or second extracellular loop may also contain sites for N-linked glycosylation.

The intracellular C terminal segment varies considerably in length (12-359 amino acids). It is often thioacylated at the cysteine residue of a palmitoylation consensus sequence, which anchors the carboxyl tail of the receptor to the plasma membrane, and gives rise to a fourth intracellular loop (O'Dowd *et al.* 1989). The C terminal domain is usually rich in serine and threonine residues that are potential sites for phosphorylation by GRKs and second messenger regulated kinases.

### **1.1.3 Regulation of GPCR**

Binding of an extracellular ligand (or primary messenger) to the GPCR activates the receptor which then initiates a series of signalling cascades in the interior of the cell. These signalling cascades, if not kept in check, may result in

abnormal functioning of the cell, as shown by the constitutively activated mutant receptors. Furthermore, in the case of the photoreceptors, it is important that the activated receptor be reverted back quickly to its normal state so that the eye can perceive continuous changes in light intensity. It is therefore crucial that mechanisms exist to regulate the activated GPCR so that it can continue to function.

### **A) Desensitisation**

Receptor desensitisation refers to the phenomenon whereby receptors become refractory to further stimulation after an initial response, despite the continued presence of a stimulus of constant intensity (Shear *et al.* 1976). After exposure to agonists, GPCR-G $\alpha$  interactions become attenuated due to rapid uncoupling of receptors from their cognate G proteins. It can be classified into homologous desensitisation (where only the activated GPCR is affected) and heterologous desensitisation (where other GPCRs on the same cell are also affected) (Hausdorff *et al.* 1990).

Phosphorylation of the GPCR is an important mechanism whereby both types of desensitisation mediate their effects. The G-protein coupled receptor kinases (GRK) are involved in the homologous desensitisation process. The GRK family consists of 6 members to date, which are divided into 3 subfamilies: (i) GRK1 (also known as rhodopsin kinase), (ii) GRK2 consisting of GRK2 & 3 (also known as  $\beta$ ARK1 &  $\beta$ ARK2 respectively), and (iii) GRK4 consisting of GRK4, 5 & 6 (Pitcher *et al.* 1998). They are ubiquitously expressed with the exception of GRK1 (exclusively in retina) and GRK4 (significant levels only in testes).

GRKs phosphorylate serine and threonine residues predominantly in the third intracellular loop and C-terminal segment of the agonist bound receptor. So far, there is no clear GRK phosphorylation consensus sequence, although there is evidence that GRK1 and GRK2 prefer acidic residues flanking the serine or threonine sites, while GRK5 and GRK6 prefer basic residues (Pitcher *et al.* 1998). For GRKs to phosphorylate GPCRs, they must

be first localised to the plasma membrane. GRK1 is farnesylated (C15 isoprenylated) on the last cysteine residue with subsequent carboxylmethylation, while GRK4 and GRK6 are palmitoylated (C16 acylation). GRK2 and GRK3, however, are recruited to the activated receptor by binding to the dissociated G $\beta\gamma$  subunit via the pleckstrin homology (PH) domain in their carboxyl termini. GRK5 has also been shown to bind phospholipids with its carboxyl and amino terminal sequences (Krupnick *et al.* 1998).

The GRK phosphorylated receptor recruits a class of cytoplasmic inhibitory proteins known as arrestin isoforms, composing of only 3 members: visual arrestin,  $\beta$ -arrestin 1 and  $\beta$ -arrestin 2. The arrestin protein inhibits functional coupling of the GPCR to its G $\alpha$  by binding to the third intracellular loop and carboxyl terminus of the receptor, and hence terminates the GPCR signalling process (Lohse *et al.* 1990).

Second messenger kinases like PKA and PKC play important roles in the heterologous desensitisation of GPCRs (Hausdorff *et al.* 1990). These serine/threonine kinases are mobilised by the feedback effect of activated G $\alpha$  subunits dissociated from the agonist-occupied receptors. In the case of PKA, also known as cAMP dependent protein kinase, agonist treatment of the G $s\alpha$  coupled GPCR raises cAMP levels in the cell which then causes phosphorylation of the receptor on PKA consensus sequences (Lys/Arg-Arg-X-X-Ser) (Iismaa *et al.* 1995). Similarly, agonist stimulation of a G $q\alpha$  coupled GPCR results in elevation of inositol trisphosphate (IP $_3$ ) and diacylglycerol (DAG) levels due to the activation of phospholipase C (PLC) by dissociated G $q\alpha$  subunits. DAG enhances the activity of PKC, which phosphorylates PKC consensus sequences of the receptor. As phosphorylation by second messenger regulated kinases is not selective for the activated receptor, other GPCRs that carry appropriate sequences may be phosphorylated too. Hence, the response of other GPCRs to their respective ligands are also

diminished at the same time, giving rise to the phenomenon of heterologous desensitisation (Hausdorff *et al.* 1990).

### ***B) Internalisation / Sequestration***

Sustained agonist treatment of GPCR was also shown to result in redistribution of the receptor from the plasma membrane into the interior of the cell (Bohm *et al.* 1997). This phenomenon is known as receptor internalisation or sequestration, and is independent of the very rapid receptor desensitisation process described before. In the case of sequestered  $\beta_2$ -adrenergic receptors, they were co-localised in intracellular vesicles with transferrin receptors, and hence demonstrated the involvement of the endosomal sorting pathway (Von Zastrow *et al.* 1992).

Sequestration of GPCRs does not appear to require coupling to  $G\alpha$ , and is independent of second messenger kinase phosphorylation (Koenig *et al.* 1997). However, evidence is accumulating that receptor phosphorylation by GRKs may play an important role, especially in the recruitment of arrestins. Immunofluorescence studies show that the activated  $\beta_2$ AR,  $\beta$ -arrestin and clathrin all co-localise into intracellular punctate accumulations upon addition of agonist (Goodman *et al.* 1996). This result correlates well with the arrestin/clathrin interaction observed *in vitro*. Thus,  $\beta$ -arrestin and arrestin3 act as adaptor proteins by targeting the desensitised receptor to clathrin coated pits.

Although the sequestration of GPCR is distinct from desensitisation, recent studies have indicated that it may play a role in resensitisation (recovery from desensitisation) (Lefkowitz 1998). The first direct evidence came from the lack of resensitisation of  $\beta_2$ -adrenergic receptors, when their internalisation through clathrin coated pits was inhibited by treatment with concanavalin A or sucrose (Pippig *et al.* 1995). Furthermore, the central idea that dephosphorylation and subsequent recycling of functional receptors to the plasma membrane was essential for resensitisation, was confirmed by the ability of calyculin A (an inhibitor of protein phosphatases) and monensin (an

inhibitor of intracellular trafficking) to block resensitisation of the  $\beta_2$ -adrenergic receptors (Pippig *et al.* 1995). Finally, dephosphorylation may require other conditions to be present, like acidification of vesicles in the case of  $\beta_2$ AR, and the dissociation of arrestin from photoactivated rhodopsin (Krupnick *et al.* 1998).

### **C) Downregulation**

Prolonged agonist treatment (hours) of a GPCR can result in downregulation of receptor levels where there is an irreversible loss from the plasma membrane due to both internalisation and degradation, and also reduction in mRNA levels (Hausdorff *et al.* 1990). The requirements for downregulation are still not very clear, although there seems to be a requirement for functional coupling with  $G_\alpha$ , as S49 lymphoma cyc<sup>-</sup> cells lacking endogenous  $G_{s\alpha}$  exhibit very little agonist-induced downregulation (Mahan *et al.* 1985). The role of serine/threonine is conflicting, with some studies suggesting that phosphorylation by second messenger regulated kinases, but not GRK are essential in downregulating  $\beta_2$ -adrenergic receptors (Hausdorff *et al.* 1991). However, tyrosine residues in the C terminal segment of the  $\beta_2$ -adrenergic receptor appear to be crucial (Valiquette *et al.* 1990). What is clear so far is that there is instability of receptor mRNA, resulting in reduction in steady state levels. Cellular recovery to the normal level of receptor expression has been shown to take days or weeks and is dependent on new protein synthesis (Iismaa *et al.* 1995).

## 1.2 The Heterotrimeric G proteins

The heterotrimeric G proteins refer to G alpha ( $G\alpha$ ), G beta ( $G\beta$ ) and G gamma ( $G\gamma$ ) subunits, which associate together with a seven transmembrane receptor to form a functional GPCR unit at the plasma membrane of the cell. Upon agonist activation of the receptor,  $G\alpha$  subunit releases its bound GDP and exchanges it for GTP (due to the higher intracellular concentration of GTP versus GDP). The GTP bound  $G\alpha$  subunit then dissociates from the  $G\beta\gamma$  dimer, allowing both to activate their effectors. Termination of signalling occurs with the hydrolysis of GTP by the  $G\alpha$  subunit, which subsequently reassociates with the receptor and  $G\beta\gamma$  dimer. Such a simple mechanism underlies the transduction of signalling by all receptors in the GPCR superfamily. Differences in cellular effects among the GPCRs therefore are determined by the subunits: their GTP exchange rates, GTP hydrolysis rates, cellular localisation, activation of effectors, and regulation by various proteins.

### 1.2.1 G Alpha Subunit

There are 20 different mammalian  $G\alpha$  subunits to date, classified into 4 subfamilies according to the similarity of their amino acids (56% to 95%). As seen in Table 1.1, there are only 16 gene products, with splice variants of  $G_{s\alpha}$  and  $G_{o\alpha}$ , and their size ranges from 39 to 52 kDa (Iismaa<sup>1</sup> *et al.* 1995). Members of the same subfamily may activate the same effector (e.g. adenylate cyclase or phospholipase C) although this is not absolute.

**Table 1.1** Classification of G $\alpha$  subunits, their distribution and effectors

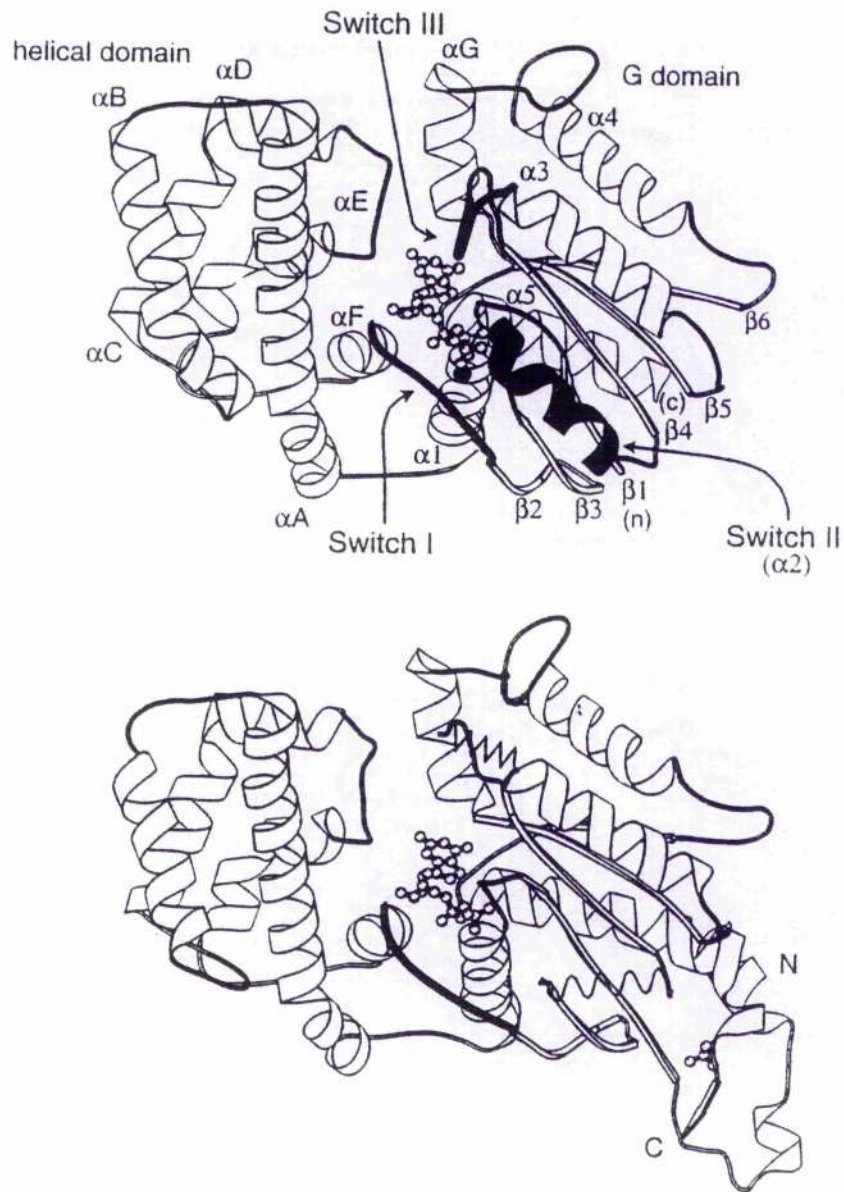
Subtype	Expression	Effectors
<b><u>G<sub>s</sub><math>\alpha</math> Subfamily</u></b>		
G <sub>s</sub> $\alpha$ (4 splice variants)	Ubiquitous	↑Adenylate Cyclase, ↑Ca <sup>2+</sup> Channels, ↓Na <sup>+</sup> Channels
G <sub>olf</sub> $\alpha$	Olfactory	↑Adenylate Cyclase
<b><u>G<sub>i</sub><math>\alpha</math> Subfamily</u></b>		
G <sub>i1</sub> $\alpha$	Widespread	↓Adenylate Cyclase, <i>etc</i>
G <sub>i2</sub> $\alpha$	Ubiquitous	↓Adenylate Cyclase, <i>etc</i>
G <sub>i3</sub> $\alpha$	Widespread	↓Adenylate Cyclase, <i>etc</i>
G <sub>o</sub> $\alpha$ (2 splice variants)	Neuroendocrine	↑K <sup>+</sup> Channels, ↓Ca <sup>2+</sup> Channels
G <sub>gust</sub> $\alpha$	Taste Buds	↑cGMP Phosphodiesterase
G <sub>i11</sub> $\alpha$	Retinal Rods	↑cGMP Phosphodiesterase
G <sub>i12</sub> $\alpha$	Retinal Cones	↑cGMP Phosphodiesterase
G <sub>z</sub> $\alpha$	Neuroendocrine	↓Adenylate Cyclase, <i>etc</i>
<b><u>G<sub>q</sub><math>\alpha</math> Subfamily</u></b>		
G <sub>q</sub> $\alpha$	Widespread	↑Phospholipase C
G <sub>11</sub> $\alpha$	Widespread	↑Phospholipase C
G <sub>14</sub> $\alpha$	Widespread	↑Phospholipase C
G <sub>16</sub> $\alpha$	Circulatory	↑Phospholipase C
<b><u>G<sub>12</sub><math>\alpha</math> Subfamily</u></b>		
G <sub>12</sub> $\alpha$	Ubiquitous	RhoGEF & others
G <sub>13</sub> $\alpha$	Ubiquitous	RhoGEF & others

The crystal structures of  $G_{i\alpha}$  and  $G_{11\alpha}$  bound with various nucleotides has yielded tremendous amounts of structural information (Sprang 1997). Basically, the structure of  $G_{\alpha}$  consists of two domains: a GTPase domain (also known as G domain) and an  $\alpha$  helical domain. The GTPase domain consists of 5  $\alpha$  helices surrounding a 6 stranded  $\beta$  sheet. This domain contains the guanine nucleotide binding pocket (making up a motif for binding GTP and  $Mg^{2+}$ ) and sites for binding the receptor, downstream effectors, and  $G\beta\gamma$  subunit. The 5 helices are designated  $\alpha 1$  to  $\alpha 5$ , while the strands of the  $\beta$  sheet are designated  $\beta 1$  to  $\beta 6$  (Figure 1.2). The five polypeptide loops in the GTPase domain (consisting of the various helices and  $\beta$  strands), form the guanine nucleotide-binding site. These five loops (G1 to G5) are also the most highly conserved elements across the G protein superfamily, which consists of both the heterotrimeric  $G_{\alpha}$  and the small G proteins.

Three segments of  $G_{i1\alpha}$  undergo substantial rearrangement upon GTP hydrolysis (Mixon *et al.* 1995). These are switch I (the loop between  $\alpha 1$  helix and the  $\beta 2$  strand; involved in  $Mg^{2+}$  coordination), switch II (the loop preceding  $\alpha 2$  helix, and the helix itself), and switch III (the loop connecting helix  $\alpha 3$  to strand  $\beta 5$ ). In the  $GTP\gamma S$  bound state (Figure 1.2 top figure), basic residues in switch II form ionic interactions with complementary residues in the switch III loop. However, upon GTP hydrolysis, both switch II and switch III are disordered or collapsed and hence these contacts are severed (Figure 1.2 bottom figure). As both switch II and III are the proposed effector-binding regions in the activated  $G_{\alpha}$ , the collapse in their structure also abrogates interactions with effectors (Sprang 1997).

**Figure 1.2 Structure of  $G_{i1}\alpha$**

The structures of  $G_{i1}\alpha$  complexed with  $GTP\gamma S.Mg^{2+}$  (top) or GDP (bottom). In the top figure, the  $\alpha$  helical domain (left) and G domain (right) of  $G_{i1}\alpha$  are shown together with the switch segments (darkened) (adapted from Sprang 1997).



The  $\alpha$  helical domain is unique for the heterotrimeric  $G\alpha$  subunits but its function is unclear. The interface between the helical domain and the GTPase domain creates a narrow crevice within which the guanine nucleotide is bound, although most of the GTP or GDP contacts are made with the 5 loops (G1 to G5) of the GTPase domain. The  $\alpha$  helical domain was shown to influence the spontaneous GDP release rate of  $G\alpha$  and hence was postulated to act as a "lid" to bury the guanine nucleotide deep between it and the GTPase domain (Hamm *et al.* 1996). Furthermore, it may also play a role in GTP hydrolysis as it helps to orient the critical arginine 174 residue of  $G_{12}\alpha$  whose side chain interacts with the guanine nucleotide terminal phosphate (Rens-Domiano *et al.* 1995).

The role of  $G\alpha$  subunits may extend beyond the GPCR family, as a number of other non-seven transmembrane receptors have been shown to activate G proteins. Examples are short peptides of the insulin-like growth factor II receptor coupled to  $G_{12}\alpha$  and epidermal growth factor receptor coupling with a  $G_{13}\alpha$ -like subunit (Spiegel 1992). The precise roles which  $G\alpha$  subunits play in the signalling pathways of these receptors are still not very clear, although a recent study has implicated  $G_{12}\alpha$  as a positive regulator of insulin action (Moxham *et al.* 1996). However, the importance of  $G\alpha$  subunits in GPCR signalling can be seen by the extensive studies of the various  $G\alpha$  subfamilies.

#### **A) $G_s\alpha$ subfamily**

The  $G_s\alpha$  subfamily is so named due to the ability of these G proteins to stimulate the enzyme adenylate cyclase upon binding of GTP. Adenylate cyclase catalyses the formation of cyclic adenosine mono-phosphate (cAMP) from adenosine triphosphate. cAMP acts as a second messenger in the cell to activate cAMP dependent protein kinase (PKA), a serine / threonine kinase with diverse functions. The activity of cAMP is terminated by cAMP phosphodiesterases, which hydrolyse cAMP to 5'-AMP.

$G_s\alpha$  is expressed in almost all cells, but has 4 splice variants, known as  $G_s\alpha 1$ ,  $G_s\alpha 2$ ,  $G_s\alpha 3$ , and  $G_s\alpha 4$  (Bray *et al.* 1986).  $G_s\alpha 1$  and  $G_s\alpha 3$  are identical

except that  $G_{s\alpha 3}$  lacks a single stretch of 15 amino acids (from exon 3).  $G_{s\alpha 2}$  and  $G_{s\alpha 4}$  are identical to  $G_{s\alpha 1}$  and  $G_{s\alpha 3}$  respectively but have 3 additional nucleotides (CAG) at the 5' end of exon 4. The longer forms ( $G_{s\alpha 1}$  &  $G_{s\alpha 2}$ ) are known as  $G_{s\alpha}$  long ( $G_{s\alpha}(L)$ ) while the shorter forms ( $G_{s\alpha 3}$  &  $G_{s\alpha 4}$ ) are known as  $G_{s\alpha}$  short ( $G_{s\alpha}(S)$ ).  $G_{s\alpha}$  can activate all 9 mammalian adenylate cyclases.

$G_{olf\alpha}$  is selectively expressed in the cilia cells of the olfactory bulb and thus *in vivo* only couples to the very large class of olfactory receptors (estimated at 400). It is grouped under the  $G_{s\alpha}$  subfamily due to its high homology with  $G_{s\alpha}$  and its ability to activate the olfactory specific adenylate cyclase type III. Activated  $G_{olf\alpha}$  elevates cAMP and also phospholipase C, leading to the opening of a cyclic nucleotide-gated cation channel (Parmentier *et al.* 1994).

Membrane association of  $G_{s\alpha}$  subunit is mediated by reversible palmitoylation of a Met-Gly-Cys motif at the amino terminus (Wedegaertner *et al.* 1995). The 16-carbon saturated fatty acid forms a thioester bond with the cysteine residue, and imparts significant hydrophobicity to the protein, which can affect both protein-lipid and protein-protein interactions. An example is the co-fractionation of palmitoylated  $G_{\alpha}$  subunits with caveolin, a protein marker for caveolae (specialised invaginations of the plasma membrane). Since palmitoylation is reversible, there are suggestions that it may be regulated, as shown by enhanced palmitate turnover when  $G_{s\alpha}$  is activated. Indeed, an acyl-protein thioesterase enzyme was recently identified and found to be regulated by the activation of the G protein (Duncan *et al.* 1998).

Members of the  $G_{s\alpha}$  subfamily are ADP-ribosylated by cholera toxin (CTX) from *Vibrio cholerae* at a crucial arginine residue (arginine 201 in  $G_{s\alpha}(L)$ ) in the GTPase domain. These ADP-ribosylated subunits are constitutively active, as their GTP hydrolysis rates are dramatically diminished (Cassel *et al.* 1977). As a result, there is a persistent activation of adenylate cyclase

and a net increase in intracellular cAMP levels. The clinical symptom of infection by *Vibrio cholerae* is excessive loss of body fluids and ions, secreted by cells in the small intestine. As CTX specifically activates  $G_{s\alpha}$  subunits but not others, it is therefore very useful in studying  $G_{s\alpha}$  regulated signalling pathways.

Receptors that couple to  $G_{s\alpha}$  subunits are very widespread, ranging from  $\beta$ -adrenergic, glucagon, secretin, VIP, corticotropin releasing factor, and certain members of the vasopressin, adenosine, dopamine, 5-HT and PG subfamilies of GPCRs. It is therefore not surprising that mutations in  $G_{s\alpha}$  would give rise to severe clinical disorders that is more generalised than mutations involving a locally expressed receptor. For example, in pseudohypoparathyroidism type Ia, loss of function mutations of the  $G_{s\alpha}$  gene cause resistance to several hormones. In McCune-Albright syndrome, mutation on the arginine 201 residue of  $G_{s\alpha}$  during embryogenesis led to pleiotropic endocrine, skin and bone manifestations of this disorder.

### **B) $G_i\alpha$ subfamily**

The  $G_i\alpha$  proteins were originally identified as inhibitory regulators of adenylate cyclase (Katada and Ui 1982a). However, after the reclassification of G protein family by amino acid sequence homology, the  $G_i\alpha$  subfamily now includes other members ( $G_o\alpha$ ,  $G_t\alpha$ ,  $G_{gust\alpha}$ ) that do not inhibit adenylate cyclase. A more common characteristic, apart from  $G_{z\alpha}$ , is their susceptibility to ADP-ribosylation catalysed by pertussis toxin (PTX) from *Bordetella pertussis* (Katada and Ui 1982b). This occurs on the last cysteine residue and results in uncoupling of  $G\alpha$  from the receptor. PTX is therefore used routinely in the laboratory to "knockout" the signalling effects arising from receptors coupled to members of the  $G_i\alpha$  subfamily (except  $G_{z\alpha}$ ).

PTX was previously known as islet-activating protein, and was discovered by Katada and Ui in 1977, when they found that perfusion of the pancreas with

the toxin abolished  $\alpha$ -adrenergic-induced hyperglycemia, and enhanced  $\beta$ -adrenergic stimulation. It was subsequently shown to specifically modify the inhibition of adenylate cyclase (Katada and Ui 1981), and ADP-ribosylate a G protein of about 41 kDa (Katada and Ui 1982a and 1982b). This conclusively proved the existence of a separate G protein apart from  $G_{s\alpha}$ , which has molecular mass of 45 or 52 kDa, that is involved in inhibiting adenylate cyclase.

The demonstration of direct inhibition of adenylate cyclase (type II and IV) by  $G_i\alpha$  subunits ( $G_{i1\alpha}$ ,  $G_{i2\alpha}$ ,  $G_{i3\alpha}$ ) was only achieved in 1993 in an *in vitro* reconstitution study (Taussig *et al.* 1993). This inhibition is non-competitive with respect to activation by  $G_{s\alpha}$ , and hence indicates separate sites of interaction for  $G_i\alpha$  and  $G_{s\alpha}$  subunits (Birnbaumer 1995). Besides their effect on adenylate cyclase,  $G_i\alpha$  subunits also activate potassium channels; an inwardly rectifying  $K^+$  channel and an ATP-sensitive  $K^+$  channel. A role for  $G_{i2\alpha}$  in regulating insulin action had been found in transgenic mice deficient in  $G_{i2\alpha}$  expression (Moxham *et al.* 1993). In further studies of cells from these mice, adipose tissue and liver deficient in  $G_{i2\alpha}$  were found to produce hyper-insulinaemia, impaired glucose tolerance and resistance to insulin *in vivo* (Moxham *et al.* 1996). Furthermore, protein-tyrosine phosphatase activity was increased and insulin-stimulated tyrosine phosphorylation of insulin-receptor substrate 1 was attenuated *in vivo*. This suggested that  $G_{i2\alpha}$  is a positive regulator of insulin action (Moxham *et al.* 1996).

$G_o\alpha$  is found predominantly in neuroendocrine tissues, accounting for about 1% of brain membrane protein. There are 2 splice variants of it, known as  $G_{o1\alpha}$  and  $G_{o2\alpha}$ , which arise from differential RNA splicing of a single  $G_o\alpha$  gene. Their C-terminal 113 aa are encoded by alternative use of duplicated exons 7 and 8 (Kaziro *et al.* 1991). The positions of the splice junctions of the human  $G_o\alpha$  gene are identical to those of the human  $G_{i2\alpha}$  and  $G_{i3\alpha}$  gene in the coding region. As the splice variants differ only in their C-terminal

region, it is possible that they may interact with different receptors. Indeed, in rat pituitary GH3 cells,  $G_{o1\alpha}$  and  $G_{o2\alpha}$  have been shown to inhibit  $Ca^{2+}$  channel by coupling to muscarinic and somatostatin receptors respectively (Kleuss *et al.* 1991).

$G_{gust\alpha}$  is involved in the perception of sweet and bitter taste at the taste buds of the tongue (McLaughlin *et al.* 1992). The G protein involved in the transduction of signal from rhodopsin and opsin receptors is  $G_t\alpha$ , also known as transducin. There are two isoforms of transducin,  $G_{t1\alpha}$  found in rod cells (coupling with rhodopsin) and  $G_{t2\alpha}$  found in cone cells (coupling with opsin receptors) (Lerea *et al.* 1986). 80% of their amino acid sequence is identical. All these G proteins found in sensory organs are believed to couple to cGMP phosphodiesterase.  $G_{gust\alpha}$  and  $G_t\alpha$  can be ADP-ribosylated by both PTX and CTX.

$G_z\alpha$  is found primarily in neurons, particularly cells with long axonal processes. It has a very slow rate of guanine nucleotide exchange, and an unusual  $Mg^{2+}$  ion dependence when compared to  $G_s\alpha$  and  $G_i\alpha$  proteins (Casey *et al.* 1990). In addition, its intrinsic guanosine triphosphatase (GTPase) activity is at least 100 times slower compared to other  $G\alpha$  subunits. The functions of  $G_z\alpha$  are only beginning to be discovered, with studies showing that it may inhibit adenylate cyclase (type I and V) and also it can couple to a number of  $G_i\alpha$  coupled receptors (Fields *et al.* 1997). An interesting study demonstrated a potential role of  $G_z\alpha$  subunits with  $\mu$  opioid receptor when the anti-nociceptive effects of  $\mu$  but not  $\delta$  opioid agonists were diminished in rats injected intracerebroventricularly with antisense oligonucleotides, which resulted in reduced expression of  $G_z\alpha$  protein in various parts of the brain (Sanchez-Blazquez *et al.* 1995). Finally,  $G_z\alpha$  is phosphorylated by PKC *in vitro*, which blocks its interaction with  $G\beta\gamma$  subunit (Kozasa and Gilman 1996).

Members of  $G_{i\alpha}$  subfamily are both palmitoylated (at cysteine3) and myristoylated (at glycine2) except  $G_{t\alpha}$  which is only myristoylated. N-myristoylation of  $G\alpha$  subunits results in the addition of the saturated 14-carbon fatty acid myristate to the N-terminal glycine residue of  $G_{i\alpha}$ ,  $G_{o\alpha}$ ,  $G_{z\alpha}$ , and  $G_{t\alpha}$  (Wedegaertner *et al.* 1995). Myristoylation, but not palmitoylation, seems to be essential for both membrane localisation and interaction with  $G\beta\gamma$  and adenylate cyclase (Taussig *et al.* 1993). Many studies have also showed that preventing myristoylation by mutation of glycine to alanine also prevented palmitoylation of members of the  $G_{i\alpha}$  subfamily (Wedegaertner *et al.* 1995).

### **C) $G_{q\alpha}$ subfamily**

Direct activation of phospholipase C- $\beta$  (PLC- $\beta$ ) is a common feature of the  $G\alpha$ 's of this subfamily. However, the potency and specificity of activation of the various PLC- $\beta$  isoenzymes differ among the members of this subfamily. Phospholipase C catalyses the breakdown of phosphatidylinositol 4,5-bisphosphate ( $PIP_2$ ), a minor lipid component of the plasma membrane, to inositol trisphosphate ( $IP_3$ ) and diacylglycerol (DAG).  $IP_3$  is water soluble and capable of diffusing through the cytosol to exert its effects by binding to the  $IP_3$  receptors on a subcompartment of the smooth endoplasmic reticulum. The  $IP_3$  receptors regulates  $Ca^{2+}$  flow from the endoplasmic reticulum to the cytosol. DAG, on the other hand, is lipophilic and hence remains associated close to the plasma membrane. PKC is activated by both DAG and  $Ca^{2+}$ , and hence its activity is usually enhanced in  $G_{q\alpha}$  signalling (Iismaa *et al.* 1995).

$G_{q\alpha}$  and  $G_{11\alpha}$  subunits differ by less than 12% in their amino acid sequences, especially in their amino terminal domains. This region is involved in determining the specificity of interaction with the  $G\beta\gamma$  subunit and the relative rate of nucleotide exchange and hydrolysis. This may give rise to differences in regulation of effector isoforms, plus variations in the amplitude and duration of signal between the two subunits (Simon *et al.* 1991).

Receptors that couple to  $G_{q\alpha}$  or  $G_{11\alpha}$  include those for  $TXA_2$ , bradykinin, thrombin, bombesin, angiotensin, histamine, vasopressin and others. Interestingly, recent evidence points to the need for tyrosine phosphorylation before receptor activation of  $G_{q\alpha}/G_{11\alpha}$  subunit (Umemori *et al.* 1997).

The importance of  $G_{q\alpha}$  in platelet activation was highlighted in a study by Gabbeta *et al.* (1997) when they found the level of  $G_{q\alpha}$  was less than 50% of normal in a patient with abnormal platelet responses. GTPase and [ $^{35}$ S]GTP $\gamma$ S binding were also diminished in platelet membranes upon stimulation with thrombin, platelet-activating factor, or the thromboxane  $A_2$  analogue, U46619. These results were further confirmed by  $G_{q\alpha}$ -deficient mice, which had increased bleeding times and were protected from collagen and adrenaline-induced thromboembolism (Offermans *et al.* 1997a). This clearly demonstrated the crucial role of  $G_{q\alpha}$  in activation of platelets, which cannot be replaced by other subunits.

Other members of the  $G_{q\alpha}$  subfamily include  $G_{14\alpha}$ , which is found in stromal and epithelial cells, and  $G_{16\alpha}$ , which is found only in some cells derived from the haematopoietic lineage. Despite the very limited expression of  $G_{16\alpha}$ , a large number of receptors were shown to be able to couple to this subunit following its heterologous expression, and there has even been a suggestion that it can function as a universal G protein adapter (Milligan *et al.* 1996).

The N-termini of  $G_{q\alpha}$  and  $G_{11\alpha}$  differ from other  $G_{\alpha}$  subunits in that they contain a unique, highly conserved 6 aa extension (MTLESI) and (MTLESM) respectively. Deletion or mutation of this N-terminal extension in  $G_{q\alpha}$  was recently shown to allow coupling with non- $G_{q\alpha}$ -coupled GPCRs (Kostenis *et al.* 1997 & 1998). Palmitoylation of  $G_{q\alpha}$  members occur on cysteine residues at the 9th or 10th positions.  $G_{q\alpha}$  subunits are not myristoylated.

#### D) $G_{12\alpha}$ subfamily

Although  $G_{12\alpha}$  and  $G_{13\alpha}$  proteins are ubiquitously expressed, their functions are only recently beginning to be understood. There is evidence implicating their involvement in regulating a range of signalling pathways. For example, both subunits stimulate  $\text{Na}^+/\text{H}^+$  exchanger (NHE), via PKC dependent ( $G_{12\alpha}$ ), and independent pathway ( $G_{13\alpha}$ ).  $G_{13\alpha}$  interacts with the Rho proteins involved in cellular actin cytoskeletal effects, and hence stimulates NHE mediated by the Rac/Cdc42 Jun N-terminal Kinase pathway (Hooley *et al.* 1996). Moreover,  $G_{12\alpha}$  was implicated in pathways that regulate cell growth, and was shown to activate NHE through a pathway dependent on Ras and the phosphatidylcholine-phospholipase / PKC network (Wadsworth *et al.* 1997). Further evidence that  $G_{12\alpha}$  and  $G_{13\alpha}$  regulate distinct, non-complementary signalling pathways was apparent in  $G_{13\alpha}$  gene knock-out studies in mice (Offermanns *et al.* 1997b). Fibroblasts from these mice were also defective in thrombin-stimulated cell migration, and hence confirmed the role of  $G_{13\alpha}$  in Rho dependent cytoskeletal effects.

$G_{12\alpha}$  was recently found to directly stimulate Bruton's tyrosine kinase (Btk) and  $\text{Gap1}^m$ , a RasGAP, *in vitro* and *in vivo* (Jiang *et al.* 1998).  $G_{12\alpha}$  interacts with a conserved domain composed of the pleckstrin-homology domain and the adjacent Btk motif, present in both Btk and  $\text{Gap1}^m$ . Overexpression of a constitutively active  $G_{12\alpha}$  (Q229L) in DT40 lymphoma cells led to increased kinase activity of endogenous Btk. Similarly, overexpression of  $G_{12\alpha}$  (Q229L) in COS-7 cells reduced the stimulation of Ras by EGF. The Rho guanine nucleotide exchange factor p115 RhoGEF, was found to be a direct effector of  $G_{13\alpha}$  (Hart *et al.* 1998). Activated  $G_{13\alpha}$  bound tightly to p115 RhoGEF and stimulated its capacity to catalyze nucleotide exchange on Rho. In contrast, activated  $G_{12\alpha}$  inhibited stimulation of p115 RhoGEF by  $G_{13\alpha}$ . Therefore,

Gap1<sup>m</sup> and p115 RhoGEF appeared to provide a link between signalling in heterotrimeric and monomeric G proteins.

A range of GPCRs are known to couple to the G<sub>12</sub>α subfamily. The thrombin receptor was among the first GPCR shown to activate both subunits in platelet membranes (Offermanns *et al.* 1994). Using a cotransfection approach, Mao *et al.* (1998) found that thromboxane A<sub>2</sub>, lysophosphatidic acid (LPA), and endothelin receptors induce serum response factor in a C3 exotoxin-dependent manner. C3 exotoxin (*Clostridium butulinum* C3 transferase) is a specific RhoA inactivator that ADP-ribosylates RhoA, but not Cdc42 or Rac1. As activated G<sub>q/11</sub>α and G<sub>12/13</sub>α but not G<sub>i</sub>α or G<sub>o</sub>α can regulate SRF activity, these cotransfection studies were done in a fibroblast cell line derived from mice lacking G<sub>q/11</sub>α. Therefore, GPCRs that induce C3-dependent SRF activation in this cell line would suggest coupling with G proteins of the G<sub>12</sub>α subfamily.

A final point to note of these Gα subunits is that their rate of nucleotide exchange is very slow ( $k = 0.01$  to  $0.02 \text{ min}^{-1}$ ) compared to most other G proteins except G<sub>z</sub>α (Fields *et al.* 1997).

## 1.2.2 G Beta and Gamma Subunits

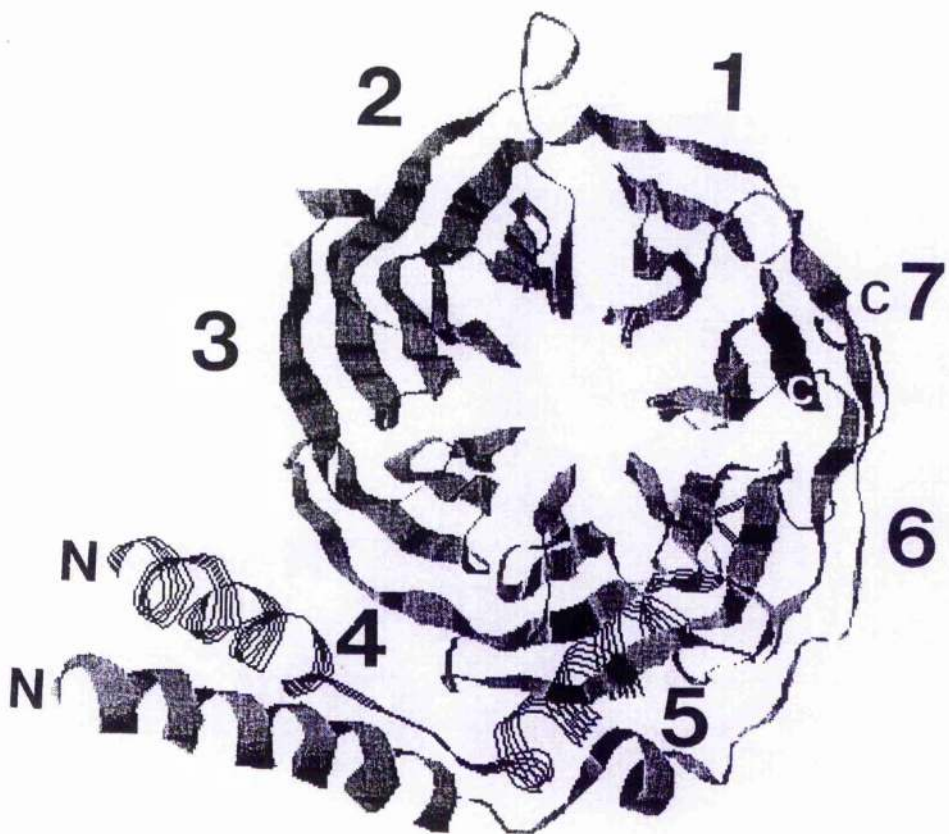
The  $G\beta\gamma$  complex is made up of two polypeptides,  $G\beta$  and  $G\gamma$ , but functionally it is a monomer as the two subunits cannot be dissociated except with denaturants. At present, 6 different  $G\beta$  and 12 different  $G\gamma$  subunits have been identified (Clapham *et al.* 1997).  $G\beta$  and  $G\gamma$  subunits are very widely expressed, with the exception of  $\gamma_1$ , present only in the photoreceptor cells, and  $\gamma_2$  and  $\gamma_3$ , restricted to the brain. While many  $G\beta\gamma$  pairs can form, not all combinations are possible. The ability of  $G\beta\gamma$  subunits to regulate effectors was relatively recently recognised (from 1987). As there are potentially more combinations of  $G\beta\gamma$  than  $G\alpha$  subtypes, there is a possibility that  $G\beta\gamma$  may play a role as important as  $G\alpha$  in mediating GPCR signalling.

Structurally, the  $G\beta\gamma$  complex has been described as a “propeller” (Figure 1.3) based on crystallography studies (Sonddek *et al.* 1996).  $G\beta$  subunit is made up of 2 structurally distinct regions, an amino terminal segment and a repeating sequence. The amino terminal segment comprises about 20 amino acids in an  $\alpha$  helix. The repeating sequence consists of 7 WD repeating motifs made up of small anti-parallel  $\beta$  strands arranged in a ring, forming a propeller structure with 7 blades.

The WD-repeat comprises a highly conserved core of about 40 amino acids, bounded by glycine-histidine and tryptophan-aspartate (WD), and a variable length region between WD and the next GH. Each blade of the propeller is made up of 4 twisted  $\beta$  strands; the conserved core making up the inner 3 while the variable length region forms the outer strand. Finally, the circular structure is held closed by the seventh blade, which is made up of both the N-terminal region (the outer strand) and the C-terminal region (the inner 3 strands), forming a kind of molecular “velcro snap” (Clapham *et al.* 1997).

**Figure 1.3 The propeller structure of  $G\beta\gamma$  subunit**

Seen from the surface that faces  $G\alpha$ .  $G\beta$  subunit is in solid gray;  $G\gamma$  subunit is in black stripes. The blades are numbered so that the first core WD repeat occurs in blade 1 (adapted from Clapham *et al.* 1997).



The N-terminus of  $G_\gamma$  forms a coiled-coil with the amino  $\alpha$ -helix of  $G_\beta$ , with the rest of the polypeptide extending across the wider surface of  $G_\beta$ , contacting residues in blades 5, 6, and 7 of the propeller structure (Sondek *et al.* 1996). Docking of the  $G_\alpha$  subunit to  $G_\beta\gamma$  involves the  $G_\alpha$  N-terminal  $\alpha$  helix (tethered to the plasma membrane by either palmitoylation or myristoylation, or both) binding to the side of the  $G_\beta$  propeller structure parallel to the central tunnel (Lambright *et al.* 1996). Furthermore, the switch II region of  $G_\alpha$ , which changes conformation upon binding GTP, is positioned directly over the central tunnel. This crucial hydrophobic region (switch II) of  $G_\alpha$  is believed to be hidden within the  $G_\alpha$  subunit upon GTP exchange, and therefore prevented from interacting with the top of the  $G_\beta$  propeller (Neer *et al.* 1996). This results in dissociation of the  $G_\alpha$  and  $G_\beta\gamma$  subunits, exposing sites for interaction with effectors.

$G_\beta\gamma$  interferes with the function of  $G_\alpha$  subunit, especially in the dissociation of bound GDP from the  $G_\alpha$  protein, a pre-requisite step for GTP exchange. This effect is  $Mg^{2+}$  dependent; at low concentration of  $Mg^{2+}$  (less than 5mM)  $G_\beta\gamma$  dimer inhibits the GTPase activity of  $G_{o\alpha}$  as it slows the dissociation of GDP. At higher concentrations, the rate of dissociation of GDP from the  $G_{o\alpha\beta\gamma}$  heterotrimer is greater than the  $G_{o\alpha}$  monomer (Higashijima *et al.* 1987). Since the intracellular  $Mg^{2+}$  concentration is about 1mM, it is postulated that the predominant effect of  $G_\beta\gamma$  in the cell would be to slow the GTPase activity of  $G_\alpha$  by stabilizing the inactive, GDP-bound state (Clapham *et al.* 1997). A further effect of  $G_\beta\gamma$  subunit on  $G_\alpha$  is in enhancing the binding of  $G_\alpha$  protein to its appropriate receptor (Higashijima *et al.* 1987). This is likely due to the isoprenylation of  $G_\gamma$  subunit (farnesylation for  $\gamma_1$ ; geranylgeranylation for other  $\gamma$ -subtypes) at the carboxyl terminus, which localises the  $G_\beta\gamma$  dimer to the plasma membrane.

The discovery that  $G_\beta\gamma$  subunits can activate the muscarinic  $K^+$  channel in pacemaker cells marked the first evidence of direct regulation of an effector by  $G_\beta\gamma$  dimers (Logothetis *et al.* 1987). However, the widespread interest in unravelling how  $G_\beta\gamma$  subunits participate in GPCR signalling started only when adenylate cyclase and phospholipase were found to be involved. Adenylate

cyclase type I activity can be inhibited by  $G\beta\gamma$ , while adenylate cyclase type II and type IV have been shown to be stimulated by  $G\beta\gamma$  subunits when the cyclases are also activated by  $G_s\alpha$  (Tang *et al.* 1991). Such difference from  $G\alpha$  regulation of effectors also extend to the activation of PLC- $\beta$ , where high nanomolar and even micromolar concentrations of  $G\beta\gamma$  dimers are required, compared to the low or sub-nanomolar concentrations for  $G\alpha$  subunits (Birnbaumer 1992). Since AC and PLC are also regulated by  $G\alpha$  subunits, such convergence of signalling on the same effector may represent a further modulation of signals within the cell arising from agonist activation of different GPCRs. However, there are also effectors (direct and indirect) specific for  $G\beta\gamma$  dimers: PLA<sub>2</sub>, GRK2 & GRK3, phosducin, phosphoinositide-3 kinase, mitogen activated kinase cascade proteins (e.g. Shc, Raf-1, Ras exchange factor), Btk, and plasma membrane Ca<sup>2+</sup> pump (Clapham *et al.* 1997).

## 1.3 Receptor G-protein Coupling

The coupling of GPCRs with heterotrimeric G proteins is generally specific. This is partly due to the differential tissue expression of GPCR and G proteins. For example, transducin ( $G_t\alpha$ ) is expressed in rod cells, which accounts for why only rhodopsin transmits extracellular signals via this  $G\alpha$  subunit. However, in a vast majority of cells, the presence of different  $G\alpha$  subunits implies that the GPCR and the  $G\alpha$  must contain specific domains that enable them to "recognise" or couple to each other. This coupling specificity of GPCR with their cognate  $G\alpha$  had long been a topic of great interest, as this directly affects the activation of secondary effectors, and ultimately the final physiological response.

### 1.3.1 Receptor domains essential for coupling

Various approaches including receptor chimeras, deletions, point mutations, and short peptides that mimic or inhibit receptor interactions with  $G\alpha$  have been employed to identify critical regions of the receptor that coupled to G proteins. These studies pointed to the importance of intracellular domains, especially the C-terminal residues of IC2, the N- and C-terminal portions of IC3, and the C-terminal tail (Bourne 1997).

Extensive studies using rhodopsin and  $\beta_2$ -adrenergic receptors were among the first to establish the involvement of the second and third IC loops in GPCR /  $G\alpha$  interactions. For the rhodopsin receptor, biochemical, mutagenesis, and peptide competition studies identified the residues 143-150 of IC2 and residues 236-239, 244-249 of IC3 as domains essential for activation of  $G_t\alpha$  (Konig *et al.* 1989). Similar segments in the  $\beta_2$ -adrenergic receptor, namely the N-terminal and C-terminal portions of IC3, plus the C-terminal cytoplasmic domain proximal to TM7 were found to be critical for activation of  $G_s\alpha$  (Savarese *et al.* 1992). The shortest segment of the intracellular loop shown to confer specificity in G protein coupling was mapped to a 4 aa epitope on the  $M_2$  muscarinic acetylcholine receptor (Liu *et al.* 1995). This epitope was predicted to be located

at the junction between IC3 and TM6, and can specifically recognise the C-terminal 5 aa of  $\alpha$  subunits of the  $G_i\alpha$  subfamily.

Most GPCRs share similar  $G\alpha$  coupling domains with the rhodopsin and  $\beta_2$ -adrenergic receptors. In instances where the coupling domains are not entirely similar, substituting regions of the cytoplasmic domain may confer additional coupling capacity to the receptor. For example, in chimeric constructs of muscarinic acetylcholine ( $M_1$  and  $M_2$ ) and  $\beta_1$ -adrenergic receptors (Wong *et al.* 1994), each parental receptor activates a single G protein exclusively:  $M_1$  muscarinic ( $G_q\alpha$ ),  $M_2$  muscarinic ( $G_i\alpha$ ), and  $\beta_1$ -adrenergic ( $G_s\alpha$ ). However, when the IC3 of both the  $M_1$  and  $M_2$  muscarinic receptor was replaced by the corresponding sequence from the  $\beta_1$ -adrenergic receptor, these chimeric receptors were able to activate all 3 types of  $G\alpha$  subunits. This effect was abolished when both IC2 and IC3 was substituted with that of  $\beta_1$ -adrenergic receptor as only  $G_s\alpha$  can be activated.

The importance of receptor C-terminal tail in GPCR/ $G\alpha$  coupling was shown by the difference in G protein coupling of bovine  $EP_3$  splice variants, where they differ only in their intracellular C-tails (Namba *et al.* 1993). Of the  $EP_3$  receptor splice variants,  $EP_{3A}$  activates the  $G_i\alpha$  subfamily, both  $EP_{3B}$  and  $EP_{3C}$  activate  $G_s\alpha$  subfamily, while the  $EP_{3D}$  activates  $G_i\alpha$ ,  $G_s\alpha$ , and  $G_q\alpha$  subfamilies. Such differences in G protein activation is not directly related to the length of the C terminal:  $EP_{3A}$  has the longest C terminal,  $EP_{3C}$  the shortest, while both  $EP_{3B}$  and  $EP_{3D}$  have similar number of residues. However, it is interesting to note that the gonadotropin-releasing hormone receptor appears to completely lack a carboxyl terminal tail (Tsutsumi *et al.* 1992) which suggests that this region is not essential for  $G\alpha$  coupling in all GPCRs.

Despite the above evidence alluding that the GPCR intracellular domains are essential for coupling to  $G\alpha$ , it must be mentioned that the overall conformation of the GPCR is rather flexible or plastic, and hence G protein

coupling can be affected by regions beyond the intracellular domains. For example, a point mutation in the extracellular loop of the luteinizing-hormone receptor abolished its ability to activate  $G_{s\alpha}$  but preserved its ability to stimulate  $G_{q\alpha}$  (Gilchrist *et al.* 1996). Furthermore, point mutations in the TM3 of  $\alpha_{1E}$ -adrenergic receptor caused selective and constitutive activation of  $G_{q\alpha}$ , but not  $G_{i\alpha}$  (Perez *et al.* 1996).

### 1.3.2 G-protein domains essential for coupling

There are at least 3 regions of  $G\alpha$  postulated to contact the receptor, with the strongest evidence pointing to the C-terminus. Similar approaches: chimeras, point mutations, and short peptides were employed to delineate the regions of  $G\alpha$  crucial for interacting with GPCR.

The importance of the extreme C-terminus was evident very early when pertussis toxin was shown to covalently modify a cysteine residue (4th aa from the C-terminus) of the  $G_{i\alpha}$  family (except  $G_{z\alpha}$ ) and hence caused uncoupling of the ADP-ribosylated  $G\alpha$  from the GPCR (West *et al.* 1985). This was followed by the discovery of an *unc* (uncoupled) mutation in which a proline residue was substituted for arginine at the 6th aa from the C-terminus of  $G_{s\alpha}$  (Sullivan *et al.* 1987). This mutated  $G_{s\alpha}$  was shown to respond normally to agents that act directly on  $G_{s\alpha}$  such as cholera toxin,  $AlF_4^-$  ion, and hydrolysis-resistant guanine nucleotides. However, activated GPCRs failed to transduce extracellular signal through the mutated  $G_{s\alpha}$  to activate adenylate cyclase.

In another study, a peptide mimicking the last 11 residues of  $G_{t\alpha}$  not only inhibited stimulation of  $G_{t\alpha}$  by rhodopsin, but also mimicked the ability of  $G_{t\alpha}$  to induce a spectral change in rhodopsin (Hamm *et al.* 1988). These and other studies using chimeric G proteins (Conklin *et al.* 1993a), antibodies (Simonds *et al.* 1989), and structural studies (Hamm 1991) further established the role of the  $G\alpha$  extreme C-terminus (last 5 to 11 aa) in receptor coupling. Despite all this evidence, it should be noted that the C-terminus of  $G\alpha$  is not the only region

interacting with the GPCR. This was shown by the fact that transducin has almost the same last 20 residues as  $G_{i\alpha}$  and  $G_{o\alpha}$  subunits, yet the  $\alpha_2$ -adrenergic receptor activated  $G_{i\alpha}$  and  $G_{o\alpha}$  but not transducin (Cerione *et al.* 1986).

Evidence that the N-terminus of  $G\alpha$  was also involved in GPCR coupling was shown by a study that a photo-affinity peptide corresponding to the IC3 region of the  $\alpha_{2A}$ -adrenergic receptor can be cross-linked to the amino terminus of  $G_{o\alpha}$  (Taylor *et al.* 1994). This confirmed previous work by Hamm *et al.* (1988) on the inhibition of interaction of  $G_{t\alpha}$  with rhodopsin using a synthetic N-terminal peptide of  $G_{t\alpha}$ . Furthermore, a chemical cross-linker attached mastoparan to a cysteine residue near the extreme N-terminus of  $G_{o\alpha}$  (Higashijima *et al.* 1991). Mastoparan is a wasp venom peptide that activates G proteins of the  $G_{i\alpha}$  subfamily. It is predicted to form an amphipathic  $\alpha$  helix that mimics the GPCR IC2 and IC3 regions.

A third region of  $G\alpha$  that may contact the receptor surface was mapped to residues 311 to 328 of  $G_{t\alpha}$  (Hamm *et al.* 1989; Hamm 1991). This peptide behaved like the last 11 residues of  $G_{t\alpha}$  in inhibiting  $G_{t\alpha}$  activation by photorhodopsin and at the same time induced spectral changes in photorhodopsin. The analogous region in Ras was postulated to be the G5 region, where the guanine ring interacts with the side chains in this region (Conklin *et al.* 1993b). There is currently no further study on the interaction of this domain with GPCRs.

### 1.3.3 Divergent Signalling in GPCRs

Although the majority of GPCRs transduce signals in a linear pathway (i.e. via a single effector system), there is emerging evidence that a number of receptors can couple to more than one  $G\alpha$  protein, and hence activate multiple effectors. Such divergent signalling can also be observed for multiple receptor subtypes that are pharmacologically indistinguishable. Alternatively, the  $G\beta\gamma$  subunit may also regulate a different effector from that of the activated  $G\alpha$ .

subunit, and hence mediate secondary effects apart from that arising from the  $G\alpha$  (Milligan 1993).

The prototypical GPCR that exhibits promiscuity in  $G\alpha$  coupling is the  $\alpha_{2A}$ -adrenergic receptor. Overexpression of this receptor in CHO (Chinese Hamster Ovary) cells indicated its association with  $G_{i\alpha}$  and  $G_{s\alpha}$  subunits from co-immunoprecipitation studies (Eason *et al.* 1992). This was further supported by the observation that agonist stimulated adenylate cyclase following pertussis toxin pretreatment. Furthermore, in co-expression studies, the  $\alpha_{2A}$ -adrenergic receptor was observed to couple to  $G_{i\alpha}$ ,  $G_{q\alpha}$ , and  $G_{s\alpha}$  subunits upon stimulation by agonists, which also demonstrated that their effective concentration at 50% response ( $EC_{50}$ ) varied between the different  $G\alpha$  (Chabre *et al.* 1994). We should however, be cautious in interpreting the significance of these results as overexpression studies tend to produce enforced coupling between the GPCR and the  $G\alpha$  (Kenakin 1997). Indeed, in the study by Eason *et al.* (1992), elevation of cAMP only occurs at more than 5 pmol/mg of  $\alpha_{2A}$ -adrenergic receptor and at high agonist concentration (micromolar).

An endogenously expressed GPCR that shows pleiotropic cellular responses is the human thyrotropin (TSH) receptor, expressed in human thyroid cells (Laugwitz *et al.* 1996). Upon receptor activation, G proteins of all 4 families ( $G_{s\alpha}$ ,  $G_{i\alpha}$ ,  $G_{q\alpha}$ , and  $G_{12\alpha}$ ) incorporated the photo-reactive GTP analogue [ $\alpha$ - $^{32}P$ ]GTP azidoanilide. This incorporation occurred at similar levels of the physiological ligand, TSH, which indicates that the TSH receptor couples equally well with the various  $G\alpha$ . This represents a naturally occurring general  $G\alpha$ -activating receptor and suggests that such promiscuous coupling may also be found in other GPCRs. Other GPCRs that couple to more than one  $G\alpha$  subunit include the  $\beta_2$ -adrenergic receptor (Xiao *et al.* 1995), the luteinizing hormone receptor (Herrlich *et al.* 1996) and many others. An unusual mechanism for the switching of  $G\alpha$  coupling in the  $\beta_2$ -adrenergic receptor was discovered recently (Daaka *et al.* 1997). In that study,  $G_{s\alpha}$  was shown to be initially activated by the

$\beta_2$ -adrenergic GPCR. Sustained agonist occupation subsequently resulted in the activation of PKA due to the elevated cAMP levels. The activated PKA then phosphorylated the  $\beta_2$ -adrenergic receptor and enabled coupling with the  $G_{i\alpha}$  subunit. It is currently not known how many GPCRs might make use of such a mechanism to switch coupling between different G proteins.

The bovine  $EP_3$  prostaglandin receptor splice variants differ at their C-terminus and were also shown to regulate different secondary effectors (see section 1.3.1). Similarly, for the human  $EP_3$  receptor isoforms, there are differences between the subtypes in their ability to mobilise  $Ca^{2+}$ . Although all the human  $EP_3$  receptor isoforms are capable of inhibiting adenylate cyclase, under conditions of high levels of expression, activation of the same receptor can also lead to stimulation of cAMP formation (Schmid *et al.* 1995). This suggests that the level of receptor expression, or the host cell, can affect the apparent differential coupling to various  $G\alpha$ . Indeed, all six C-terminal splice variants of the human  $EP_3$  receptors displayed similar binding and  $G\alpha$ -coupling characteristics when expressed in BHK-21 cells, with careful control for receptor density (Gudermann *et al.* 1996). Other examples of differential  $G\alpha$ -coupling between splice variants include the receptors for pituitary adenylate cyclase-activating polypeptide (PACAP), dopamine, calcitonin, serotonin and many others.

The last form of divergent signalling was observed from the activation of a single  $G\alpha$  subunit but with the secondary effect arising from the dissociated  $G\beta\gamma$  partner. Such divergent signalling has been observed in a large number of receptors, including the  $M_2$  and  $M_4$  muscarinic, serotonin,  $D_2$  dopamine, somatostatin and certain subtypes of the  $\alpha_2$ -adrenergic receptors (Milligan *et al.* 1993; Hildebrandt *et al.* 1997). A common characteristic of such signalling is that the effects mediated by  $G\beta\gamma$  subunits require considerably higher agonist concentrations compared to that mediated by  $G\alpha$  subunits (Birnbaumer 1992). Moreover, these effects are usually dependent on receptor abundance and host cell.

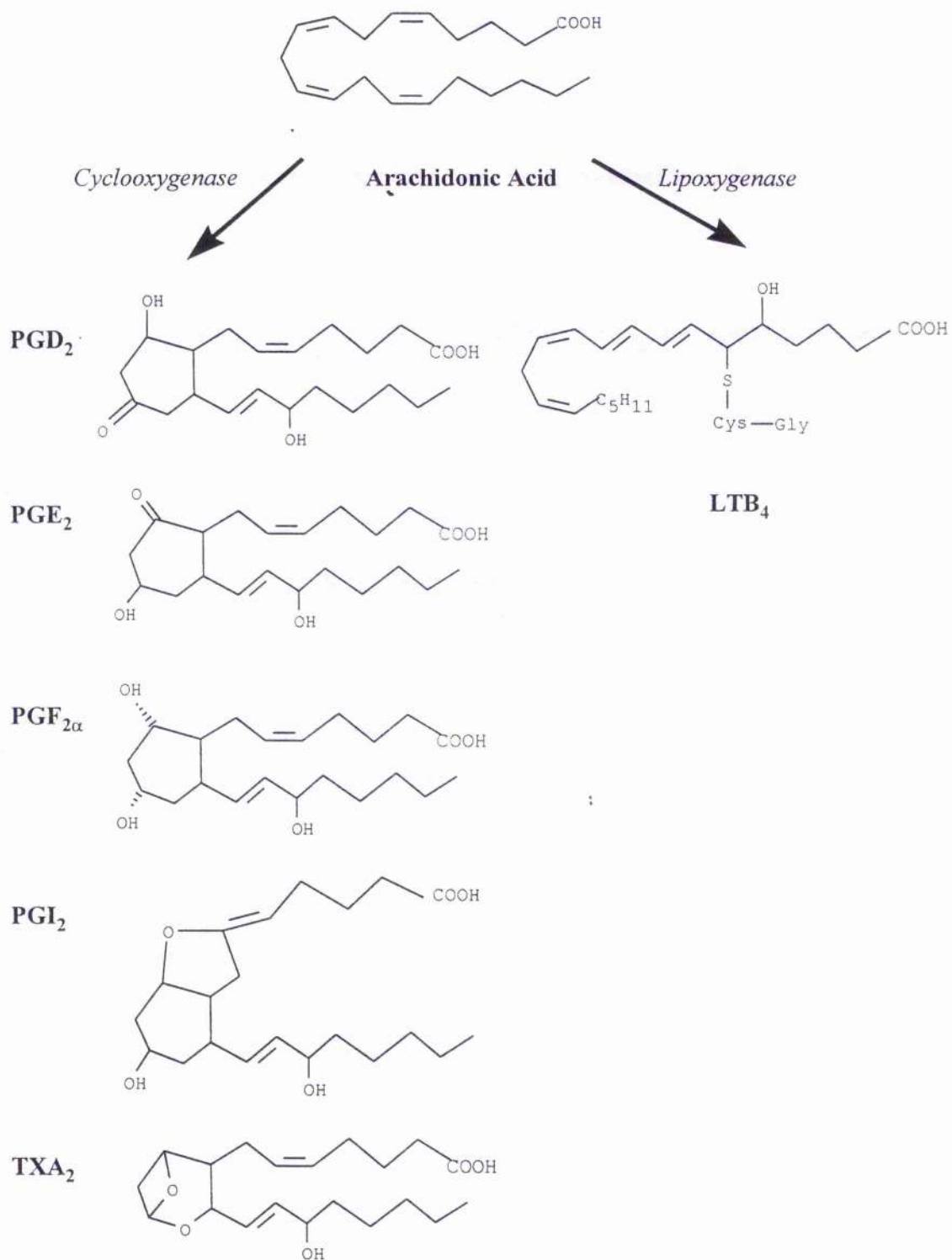
## 1.4 Prostaglandin Receptors

### 1.4.1 Prostaglandins and their biosynthesis

Prostaglandins (PGs) refer to a group of bioactive lipids with very diverse physiological functions. They were first discovered in 1930 by Kurzrok and Lieb (1930) in human seminal fluid, and shown to contract human uterus. This observation was further confirmed by other investigators and as they were thought to be produced by the prostate gland, the bioactive lipid(s) were named prostaglandin. By the 1970s most prostaglandins were isolated, and their importance in human physiology beginning to be realised. There was also much enthusiasm about their potential as drugs, especially with the discovery of  $\text{TXA}_2$  and  $\text{PGI}_2$ , which regulate platelet aggregation and thrombosis. The vast array of agents acting on prostaglandin receptors is a testimony to that enthusiasm in the 70s and 80s.

Prostaglandins and thromboxanes (TXs) are derived from arachidonic acid, release from phospholipids of cell membranes by the action of phospholipase  $A_2$  ( $\text{PLA}_2$ ) (Campbell 1990). The released arachidonic acid can activate 2 enzyme systems: cyclooxygenase and lipoxygenase. Cyclooxygenase converts arachidonic acid into cyclic endoperoxides ( $\text{PGG}_2$  and  $\text{PGH}_2$ ) that can be further converted to other PGs and TXs. Lipoxygenase catalyses arachidonic acid into hydroxyl fatty acids that can be further converted to leukotrienes (LTs). LTs are involved in inflammatory responses, especially in the chemotaxis of neutrophils and eosinophils. Figure 1.4 shows a simplified schematic diagram of the biosynthesis of PGs,  $\text{TXA}_2$ , and  $\text{LTB}_4$ . PGs are named with alphabets from A to I depending on the substitutions on the cyclopentane ring, with a suffix 1 to 3 denoting the number of double bonds in the side chains. TXs are similarly named, but has substitutions on the cyclohexane ring instead. LTs are not considered as part of the prostaglandin family and will not be discussed in detail.

Figure 1.4 Biosynthesis of prostaglandins



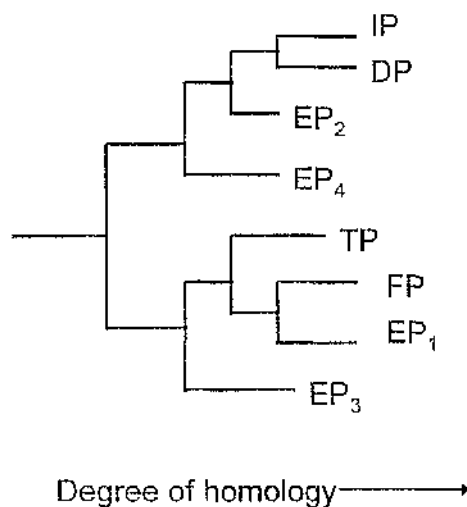
## 1.4.2 Prostaglandin Receptor Family

The mammalian prostaglandin receptor family consists of 5 subfamilies: DP, EP, FP, IP and TP, classified in accordance with their affinity for the various PGs: PGD<sub>2</sub>, PGE<sub>2</sub>, PGF<sub>2 $\alpha$</sub> , PGI<sub>2</sub>, and TXA<sub>2</sub> respectively (Coleman *et al.* 1994). There are no receptors for certain PGs as they are either unstable or intermediates of prostaglandin synthesis.

cDNAs of all known members in the PG receptor family have been cloned (Pierce *et al.* 1995). Interestingly, molecular cloning of these receptors led to the unexpected discovery of isoforms generated by alternative mRNA splicing. Some of these receptor isoforms can even couple to different effector systems. Phylogenetic analysis of PG receptor sequences led Narumiya *et al.* to the conclusion that they evolved from a precursor EP receptor into two subfamilies (see Figure 1.5) that differ with respect to their G protein coupling (Toh *et al.* 1995). The various receptor subfamilies will be briefly mentioned, while the IP prostanoid receptor will be discussed in a separate section.

Figure 1.5 PG Receptor Phylogeny

Adapted from Kedzie *et al.* 1998



### **A) DP**

The DP receptor is the least ubiquitous of the PG receptor family (Hirata *et al.* 1994). It is distributed largely in blood platelets, vascular smooth muscle, and nervous tissue including the central nervous system. Responses mediated by DP receptors are predominantly inhibitory in nature including the inhibition of platelet aggregation and inhibition of autonomic neurotransmitter release. The study of DP receptors has been facilitated by the availability of a number of rather selective and potent agonists and antagonists (Coleman *et al.* 1994). The use of these agonists and PGD<sub>2</sub> itself have shown that DP receptors can couple to G<sub>s</sub>α to stimulate adenylate cyclase.

### **B) EP**

There are 4 subtypes of EP receptors to date with splice variants for the EP<sub>3</sub> subtype (Pierce *et al.* 1995). EP<sub>1</sub> receptors mediate smooth muscle contraction of the trachea, gastrointestinal tract, uterus and bladder. Their expression is not very high compared to other EP subtypes, and is species dependent. Occupancy of EP<sub>1</sub> receptors appears to mobilise Ca<sup>2+</sup> from intracellular stores independent of IP<sub>3</sub>. EP<sub>2</sub> receptors are more widespread and mediate a wide range of responses like relaxation of smooth muscle, inhibition of mediator release in inflammatory cells, and activation of sensory afferent nerves. They are most highly expressed in ileum, then thymus, lung, spleen, heart and uterus of mouse tissue. Studies done so far imply that it is coupled to adenylate cyclase through G<sub>s</sub>α (Coleman *et al.* 1994).

EP<sub>3</sub> receptors are the most ubiquitous of all EP subtypes, with 6 splice variants in human (Pierce *et al.* 1995). These splice variants share the same amino termini and TMs and start to differ from the 11th residue of the C terminal domain. Probably because of the many isoforms, EP<sub>3</sub> receptors mediate very diverse functions like contraction of smooth muscle, inhibition of neurotransmitter release in autonomic nerves, inhibition of lipolysis,

inhibition of acid secretion from gastric mucosal cells, and also inhibition of water reabsorption from renal medulla. The EP<sub>3</sub> receptor agonist misoprostol, an anti-gastric ulcer drug, is perhaps the most useful therapeutic agent from amongst the large library of compounds acting on PG receptors. As mentioned before, splice variants of the EP<sub>3</sub> receptor are promiscuous in their coupling to G $\alpha$ , and hence activate a number of effector systems (Namba *et al.* 1993).

Finally, the EP<sub>4</sub> receptor was identified recently as having similar antagonist but not agonist (butaprost) binding properties as the EP<sub>2</sub> receptor, and it also activates the same effector system. Due to their similar characteristics, a cDNA of the EP<sub>4</sub> isoform was initially mistaken as that of EP<sub>2</sub> (Pierce *et al.* 1995).

#### **C) FP**

FP receptors mediate quite a range of functions including luteolysis of the corpus luteum and contraction of iris sphincter. It is also found in ocular tissue, and acts to lower intra-ocular pressure; hence agonists of FP receptors were found to be useful in the treatment of glaucoma. These effects were associated with elevation of intracellular Ca<sup>2+</sup> and PI turnover, suggesting coupling with the G<sub>q</sub> $\alpha$  subfamily<sup>1</sup> of G proteins (Coleman *et al.* 1994).

#### **D) TP**

Thromboxane was initially found to act on thrombocytes (platelets), which contain TP receptors. These receptors mediate inflammatory responses like vasoconstriction, platelet aggregation, bronchoconstriction *etc.* They are found in vascular smooth muscle, platelets, and airway smooth muscles (Hirata *et al.* 1991). They may also play a key physiological role in the closure of umbilical vessels at birth. Furthermore, TP receptors could be involved in wound healing and scar formation, and also in thymocyte differentiation and development. There are many antagonists of varied

structures but none are currently in clinical use. Second messenger studies on TP receptors suggest that it is coupled to  $G_q\alpha$  subunits to activate phospholipase C and mobilise  $Ca^{2+}$  (Coleman *et al.* 1994).

### 1.4.3 Prostacyclin (IP) Receptor

The cDNA of the human IP receptor was cloned only in 1994 by Abramovitz's group (Boie *et al.* 1994). It encodes a protein of 386 amino acids with a predicted molecular mass of 40,961 daltons (Figure 1.6). When expressed in *Xenopus* oocytes and challenged with agonist, it stimulated the cAMP-activated  $Cl^-$  channel. Other expression studies also indicate that the IP receptor is functionally coupled to adenylate cyclase activation via  $G_s\alpha$  (Smyth *et al.* 1996). Furthermore, the IP receptor was reported to elevate  $IP_3$  and  $Ca^{2+}$  via a pertussis toxin-insensitive G protein (Namba *et al.* 1994). This effect is seen at much higher agonist concentrations than required for elevation of cAMP and its physiological relevance is currently unclear. It seems possible that the elevation of  $IP_3$  is mediated via  $G\beta\gamma$  subunits rather than  $G_q\alpha$ , due to the characteristic higher agonist concentrations required in  $G\beta\gamma$  signalling processes. IP receptor mRNA was found most abundantly expressed in kidney, with lesser amounts in lung and liver (Boie *et al.* 1994).

The human IP receptor has two putative N-linked glycosylation sites on its N-terminal domain and the first extracellular loop (see Figure 1.6). The receptor shares 23 residues in common with other prostanoid receptors and another 10 residues in common with all GPCRs (Boie *et al.* 1994). Of interest is that the IP receptor has phenylalanine at position 292 in TM7 instead of the tyrosine which is present in virtually all other GPCRs. This tyrosine residue forms part of the N/D-PXXY sequence where it was shown recently that receptors carrying the NPXXY but not the DPXXY motif may form functional complexes with ADP-ribosylation factor (ARF) and RhoA (Mitchell *et al.* 1998). There are two PKC phosphorylation consensus sequences in the C terminus of the IP receptor (see Figure 1.6), but

recent study by Smyth *et al.* showed that serine 328 is the primary PKC phosphorylation site (Smyth *et al.* 1998).

### ***A) Physiological functions and potential therapeutic roles***

The IP prostanoid receptor was first identified in platelets, and was shown to stimulate adenylate cyclase upon activation by PGI<sub>2</sub> (Gorman *et al.* 1977). It opposes the functions of the TP receptor, and therefore acts to counteract the pro-inflammatory responses of thromboxanes. Hence, agonists acting on IP receptors have great potential as inhibitors of platelet aggregation and thrombosis. This effect is probably mediated by elevation of intracellular cAMP via G<sub>s</sub>α subunit. However, as IP receptors are also found in arterial smooth muscle, and no subtypes of IP receptors have been found to date, agonists that prevent thrombosis caused profound vasodilation effects at the same time.

IP receptors are also involved in mediating inflammatory hyperalgesia. Due to their presence in sensory neurones, they sensitise or directly activate the nerve endings upon the release of prostanoids generated by cells in response to mechanical, thermal or chemical injury and inflammatory insult (Bley *et al.* 1998). This hyperalgesic effect of IP receptors was further confirmed by studies in transgenic mice lacking the receptor (Murata *et al.* 1997). Therefore, selective antagonists of the IP receptor may act as potential blockers of inflammatory pain. This approach is currently explored by major pharmaceutical companies (Bley *et al.* 1998).

**Figure 1.6 Diagram of the human IP prostanoid receptor**

Consensus sequences for PKC phosphorylation are shown in black, while N-linked glycosylation sites are indicated in the N terminus and first extracellular loop with a Y (Adapted from Smyth *et al.* 1996).

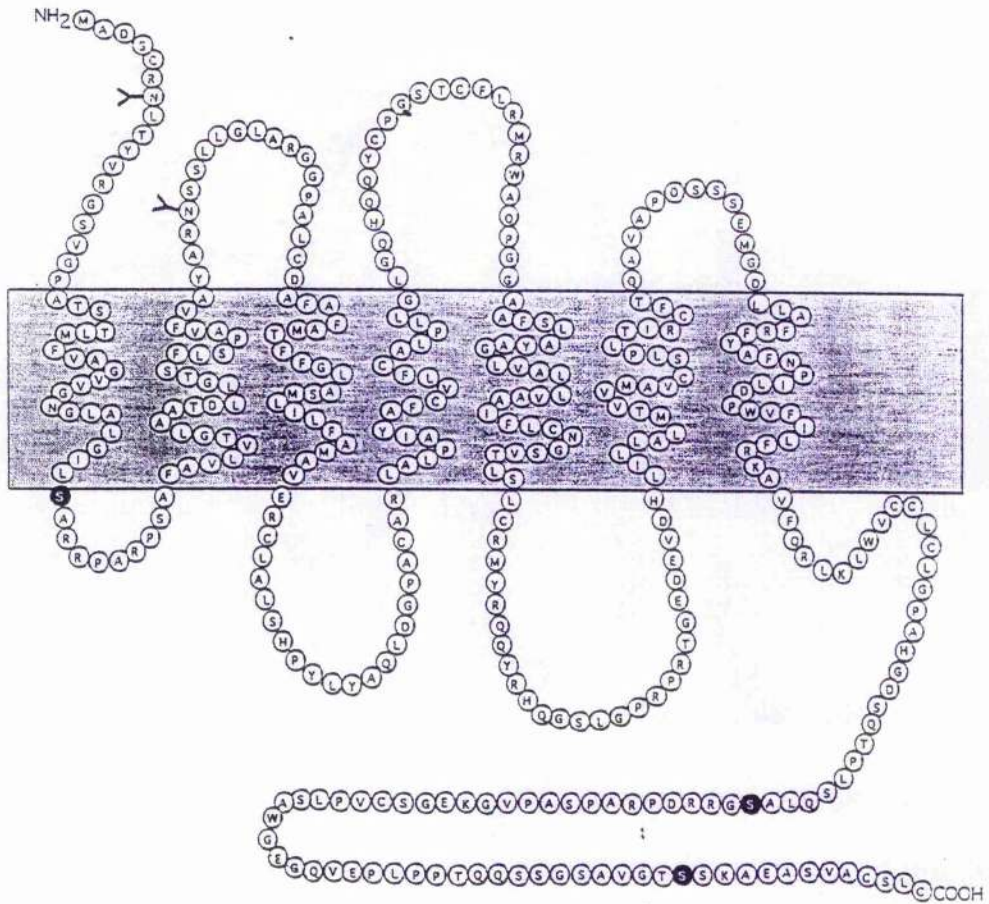
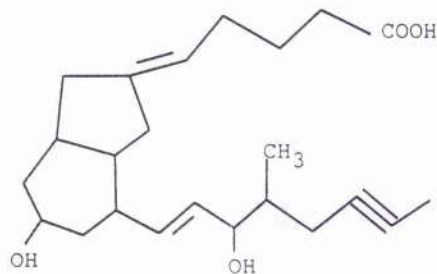


**Figure 1.7 Structure of iloprost**



## **B) Agonist Studies**

The endogenous ligand, PGI<sub>2</sub> is chemically unstable, and has a very short duration of action. Although PGE<sub>1</sub> and its 6-keto analogue are also moderately potent at the IP receptor, most prostaglandins are non-selective for the various PG receptors. Due to the potential therapeutic role of IP receptor agonists as anti-platelet agents, a range of chemically stable, potent, and selective compounds were developed by various companies in the last decade.

The first compound to combine chemical stability with high IP receptor agonist potency is iloprost, developed by Schering in the early 1980s, and is a close analogue of PGI<sub>2</sub> (Figure 1.7). It is not only at least as potent as PGI<sub>2</sub> but also more selective at the IP receptor (except for EP<sub>1</sub> subtype). Moreover, it is far more stable with an extended duration of action *in vivo*. Another compound developed by Schering is cicaprost, which is slightly more potent than iloprost but with almost no activity at other PG receptors (Coleman *et al.* 1994). Other selective compounds include octimibate, BMY 45778, BMY 42393, taprostene, TEI-9063, ONO-1301 etc. A recent study showed the rank order of potency for PGs and PG analogues for the human IP receptor expressed in COS cells as: iloprost >> carbacyclin >> PGE<sub>2</sub> > PGF<sub>2α</sub> = PGD<sub>2</sub> (Boie *et al.* 1994). Despite enormous efforts, there are still no clinically useful IP agonists; the probable reason could be their strong vasodilative effects.

Recent binding studies on chimeric mouse IP/DP (mIP/DP) receptors showed that TM6 to TM7 of mIP receptor confers the specificity to bind IP agonists such as PGE<sub>1</sub> and iloprost (Kobayahi *et al.* 1997). This was because when the region from TM6 to the carboxyl terminus of mIP receptor was replaced with the corresponding segment from mDP receptor, the chimeric receptor was able to bind IP and DP agonists indiscriminately.

When only the carboxyl terminus of mIP receptor was substituted with that of mDP receptor, binding was confined to IP agonists strictly.

A further proof of the importance of TM7 of PG receptors in agonist binding comes from a point mutation study by Kedzie *et al.* (1998). By mutating leucine 304 to tyrosine in the human EP<sub>2</sub> receptor, they were able to show functional activation of the mutant receptor by both EP receptor agonist (PGE<sub>2</sub>) and IP receptor agonist (iloprost). This study further confirmed the proposed PG receptor phylogeny (see Figure 1.5) in that PG receptors evolved functionally from an ancestral EP receptor before the development of distinct binding epitopes. This mutant receptor therefore represents a molecular "missing link" in the evolution of the IP receptor from EP<sub>2</sub> receptor (Kedzie *et al.* 1998).

Currently, there is no specific antagonist that blocks the IP receptor, and their therapeutic potential is therefore not clear. However, we can expect some compounds to be developed very soon judging from the interest shown in it.

## 1.5 Research Objectives

The primary aim of this study is to increase the G protein output of a  $G_{s\alpha}$ -coupled GPCR to a level that can be detected by assays that monitor G protein activation and termination. This will allow the measurement of agonist activity at the earliest point of the GPCR signalling cascade.

Currently, the measurement of guanine nucleotide exchange and the subsequent hydrolysis in the GPCR activated  $G_{s\alpha}$  protein is besieged with various obstacles (Wieland *et al.* 1994; Gierschik *et al.* 1994). Although such phenomena were first observed in the  $G_{s\alpha}$  proteins (through the stimulation of turkey erythrocyte membranes with adrenaline by Cassel and Selinger 1977), the activity obtained is still relatively low compared to that of the  $G_{i\alpha}$  subfamily. Therefore, agonists acting on  $G_{s\alpha}$ -coupled GPCRs are usually assayed via its secondary effector, the adenylate cyclase enzyme. The assay of this activity is reliable and highly sensitive (Wong 1994), but it can be affected by various factors including the type and level of adenylate cyclase, interference from  $G_{i\alpha}$  and  $G_{\beta\gamma}$  signalling, and also receptor expression level. These factors differ between the cell lines used and can affect the pharmacological analysis of receptor agonists even with recombinant systems (Kenakin 1997).

As the IP prostanoid receptor regulates various important functions in the body and was also shown to be an important mediator of inflammatory pain, this receptor is thus of high interest to the pharmaceutical industry and may be a potential target for high-throughput screening. Current functional assays that monitor effector activity are not compatible with high-throughput screening formats that monitor  $G_{\alpha}$  activity. Moreover, the ability to monitor  $G_{\alpha}$  activity will avoid the pitfalls associated with analysis of effector activity. By studying the G protein signalling characteristic of the human IP prostanoid receptor, it is hoped that novel assay systems may be developed that allow the monitoring of agonist-promoted  $G_{\alpha}$  activity.

# CHAPTER 2 MATERIALS AND METHODS

## 2.1 Materials

All reagents used in this study were of analytical or similar grade and were purchased from the following suppliers:

### 2.1.1 General Reagents

**Alexis Corporation Ltd.**, Bingham, Nottingham, U. K.

DTT

**Amersham International plc.**, Buckinghamshire, U. K.

Enhanced chemiluminescence reagent

**BDH**

Ammonium persulphate, glucose, glycine,  $\text{Na}_2\text{HPO}_4$

**Boehringer Mannheim U. K. Ltd.**, Lewes, East Sussex, U. K.

App(NH)p, aprotinin, creatine phosphokinase, GDP,  $\text{GTP}\gamma\text{S}$  and restriction enzymes

**Calbiochem-Novabiochem Ltd.**, Beeston, Nottingham, U. K.

Geneticin (G-418)

**Fisher Scientific Equipment**, Loughborough, U. K.

Acetic acid, DMSO, EDTA, HEPES, hydrochloric acid, KCl,  $\text{KH}_2\text{PO}_4$ ,  $\text{K}_2\text{HPO}_4$ ,  $\text{MgCl}_2$ , NaCl,  $\text{Na}_2\text{CO}_3$ ,  $\text{NaHCO}_3$ ,  $\text{NaH}_2\text{PO}_4$ , sucrose, SDS, trichloroacetic acid

**FMC BioProducts**, Rockland, USA

Agarose

**Fuji Photo Film Co. Ltd.**, Tokyo, Japan

X-ray film

**Genosys**, Cambridge, U. K.

Oligonucleotides

**Gibco BRL Life Technologies Inc**, Paisley, U. K.

Lipofectamine™, TRIS, 1 kb DNA ladder, oligonucleotides

**Invitrogen**, San Diego, CA, U. S. A.

pcDNA3

**Merck Ltd.**, Poole, Dorset, U. K.

Agar, NaOH

**Oxoid Ltd.**, Hampshire, U. K.

Tryptone, yeast extract

**Premier Beverages**, Stafford, U. K.

Marvel

**Promega Ltd.**, Southampton, U. K.

Restriction enzymes, DNA purification kits - Wizard™ Minipreps and Wizard™ Maxipreps systems

**Qiagen Ltd.**, West Sussex, U. K.

QIAquick Gel Extraction Kit

**Sigma Chemical Company**, Poole, Dorset, U. K.

Alumina, ampicillin, cholera toxin, DOWEX AG50 W-X4 (200-400 mesh), forskolin, imidazole, mineral oil, pertussis toxin, TEMED, thimerosal, TRICINE

**Stratagene Ltd.**, Cambridge, U. K.

Pfu DNA Polymerase

**Whatman International Ltd.**, Maidstone, U. K.

Brandell GF/C Glassfibre filters

### **2.1.2 Radiochemicals**

**Amersham International plc.**, Buckinghamshire, U. K.

[<sup>3</sup>H]Adenine (specific activity: 20 Ci/mmol)

[<sup>3</sup>H]Iloprost (specific activity: 11.5 Ci/mmol)

**Du Pont NEN Ltd.**, Stevenage, Hertfordshire, U. K.

[ $\gamma$ <sup>32</sup>P]GTP (specific activity: 30 Ci/mmol)

[<sup>35</sup>S]GTP $\gamma$ S (specific activity: 1250 Ci/mmol)

### **2.1.3 Tissue Culture**

**American Tissue Culture Collection**, Rockville, U. S. A.

Human Embryonic Kidney (HEK293) cells

**Costar Scientific Corporation**, Buckinghamshire, U. K.

Dishes 10 cm diameter, Flasks 25 cm<sup>2</sup> and 75 cm<sup>2</sup>, Plates 6, 12 and 24 wells,  
Disposable cell scraper

**Gibco BRL Life Technologies Inc**, Paisley, U. K.

Glutamine (2000mM), Newborn calf serum, NaHCO<sub>3</sub> (7.5% <sup>w/v</sup>), Optimem-1 medium

**Sarstedt**, Numbrecht, Germany

Cryovials

**Sigma Chemical Company**, Poole, Dorset, U. K.

Dulbecco's Modified Eagle's Medium (DMEM), Minimum Essential Medium (MEM)

**Sterilin Bibby Ltd.**, Stone, Staffordshire, U. K.

Pipettes 5 ml, 10 ml and 25 ml

#### **2.1.4 Standard Buffers**

##### **Tris Buffered Saline (TBS)**

NaCl                      150 mM

Tris/HCl                20 mM

*pH adjusted to 7.5*

This was usually made up from 20 ml of 1M Tris (pH 7.5) and 30 ml of 5M NaCl for a 1 litre solution.

##### **Tris Buffered Saline with Tween (TBST)**

As for TBS but with Tween 20 (0.1% <sup>v/v</sup>) added

### **Tris-EDTA Buffer (TE)**

Tris/HCl	10mM
EDTA	0.1mM

*pH adjusted to 7.5*

This was usually made up as a 10X stock solution and diluted when required.

### **Phosphate Buffered Saline (PBS)**

KCl	2.7 mM
KH <sub>2</sub> PO <sub>4</sub>	1.5 mM
NaCl	140 mM
NaH <sub>2</sub> PO <sub>4</sub>	8 mM

*pH adjusted to 7.4*

This was made as a 10X stock solution and diluted when required.

### **Laemmli Buffer (2X)**

DTT	0.4M
SDS	0.17M
Tris/HCl (pH8)	50mM
Urea	5M
Bromophenol Blue	0.01% <sup>w</sup> / <sub>v</sub>

This was stored in aliquots at -20°C until required.

## 2.1.5 Antisera

### Anti-FLAG M5

Mouse monoclonal antibody that binds to N-terminal methionine-FLAG proteins.

- purchased from Kodak IBI Ltd., New Haven, U. S. A.

### Anti-G $\alpha$ antisera

These antisera were generated against synthetic peptides described in Goldsmith *et al.* 1988. Conjugates of these peptides with keyhole-limpet haemocyanin were injected subcutaneously into New Zealand White rabbits. Bleeds were obtained from the ear artery. Amino acid sequence of the synthetic peptides derived from the various G $\alpha$  are listed below:

<u>Antiserum</u>	<u>Peptide Sequence</u>	<u>G<math>\alpha</math> Residues</u>	<u>Specific for:</u>
CS	RMHLRQYELL	last 10 aa of G $_s\alpha$	G $_s\alpha$
SG	KENLKDCGLF	last 10 aa of G $_i\alpha$	G $_i\alpha$ , G $_{i1}\alpha$ , G $_{i2}\alpha$
CQ	QLNLKEYNLV	last 10 aa of G $_q\alpha$	G $_q\alpha$ , G $_{q1}\alpha$
I1C	LDRIAQPNYI	159 - 168 aa of G $_{i1}\alpha$	G $_{i1}\alpha$

### Anti-mouse IgG

Goat polyclonal antibody conjugated with horseradish peroxidase, purchased from Sigma Chemical Company, Poole, Dorset, U. K.

### Anti-rabbit IgG

Donkey polyclonal antibody conjugated with horseradish peroxidase, produced by the Scottish Antibody Production Unit, Lanarkshire, U. K.

## **2.2 Cell Culture**

All tissue culture manipulations were done in laminar flow hoods designed for cell culture work, with regular cleaning and servicing schedules. Aseptic tissue culture techniques were followed strictly, and antibiotics usage was limited to medium for maintenance and selection of stable cell lines. Any contaminated cells were disposed and dealt with promptly. Finally, mycoplasma testing of all cell lines are done twice a year.

### **2.2.1 Routine Cell Culture**

The primary cell line used for the present study is Human Embryonic Kidney (HEK293) cells. It was grown in continuous monolayer culture in 75 cm<sup>2</sup> sterile tissue culture flasks in Dulbecco's Modified Eagle's Medium (DMEM) supplemented with 2 mM L-glutamine and 10% Newborn Calf Serum (NBCS). Flasks of cells were incubated in cell culture incubators (Jencons Nuaire) in a humidified atmosphere of 95% air / 5% CO<sub>2</sub> at 37°C.

Confluent cells were detached from the flasks by the addition of 1.2 ml trypsin solution (0.1% w/v trypsin, 0.025% w/v EDTA, and 10 mM glucose) after the removal of medium. When all the cells were detached, trypsinisation was terminated by the addition of 5 volumes of growth medium. The cells were centrifuged at about 800 x g for about 5 min. The cell pellet was finally resuspended in growth medium and plated out as required. For routine maintenance of cell line, HEK293 cells were split 1:16 to 1:20 per week.

### **2.2.2 Transient Transfections**

Transient transfections of DNA into HEK293 cells were achieved using Lipofectamine™ reagent (Gibco Life Technologies) according to the manufacturer's instructions.

Briefly, a 75 cm<sup>2</sup> flask of confluent HEK293 cells was split into five or six 100 mm diameter tissue culture dishes the day before transfection. On the day of

transfection, the confluency of cells should be between 60 to 80%. For each dish, about 5 µg of DNA was used, diluted in 0.4 ml of Optimem-1 medium. Lipofectamine™ was also diluted in Optimem-1 medium to give a 0.1 mg/ml solution. Equal volumes of the diluted DNA and Lipofectamine™ were then mixed together (i.e. 0.4 ml of DNA suspension + 0.4 ml of Lipofectamine™ suspension) and incubated at room temperature for about 30 min. In the meantime, cells on the dish were rinsed once in Optimem-1. Finally, 5.2 ml of Optimem-1 medium was added to the DNA / Lipofectamine™ mixture, mixed well, and then added to cells on the dish.

After 5 h incubation in a cell culture incubator, 6 ml of DMEM containing 20% NBCS was added to the dish, and left overnight in the incubator. On the following morning, the DNA / Lipofectamine™ mixture was removed and replaced with about 10 ml of growth medium. The cells were incubated for another 24 to 48 h before they were harvested or assayed.

### **2.2.3 Generation and Maintenance of Stable Cell Lines**

Generation of stably expressing cell lines involved selecting isolated colonies of cells (also known as clones) that incorporated the transfected DNA into their chromosomes. This is possible only under the presence of a selection antibiotic that kills all cells except those that have resistance conferred to them from the antibiotic resistance gene present in the transfected DNA.

The transfection protocol is the same as that for transient transfections (section 2.2.2). 48 h after DNA transfection, cells were split 1:3 into 100 mm diameter dishes, together with a dish of untransfected HEK293 cells with similar confluency (as control). Antibiotic (Geneticin G-418 in the case of pcDNA3 vector) containing medium was added to all dishes. A very high concentration of G-418 was used initially (up to 1.5 mg/ml) to select for resistant clones, and the medium changed every 3 days to maintain maximum selection pressure. After 7 to 10 days, when all the untransfected HEK293 cells in the control dish were dead, isolated clones of cells in the transfected dishes were picked. The clones (about 24 for each type of DNA transfected) were detached from the dish by scraping

with sterile blue tips and simultaneously drawing up about 0.5 ml of medium. The clones were grown in 24 well plate in 1 ml of G-418 (800 µg/ml) per well, with regular change of medium every 4 days.

After another 7 to 10 days, each confluent clone was split into a 25 cm<sup>2</sup> flask, at the same time dispensing a very small fraction into a well of a 6 well plate. When clones in the 25 cm<sup>2</sup> flask were confluent, cells were harvested for assaying their receptor levels. Once the desired clones were obtained, cells growing in the 6 well plate were expanded in medium containing lower concentration of G-418 (400 µg/ml). Routine culture of stable cell lines were in DMEM or MEM (for HEK293 stably expressing FhIPR-Gi/Gs) medium containing 350 to 400 µg/ml G-418. All mediums were prepared as in section 2.2.1.

#### **2.2.4 Preservation of Cell Lines**

Stable cell lines were preserved in the earliest passage possible. They were also tested for mycoplasma contamination before preservation. Cells in 75 cm<sup>2</sup> flasks were grown to confluency before trypsinisation as in section 2.2.1. After centrifugation, the cell pellet was suspended in 1 ml of NBCS with 10% DMSO (as a cryo-protectant). The cell suspension was transferred into 1.5 ml cryovials, and labelled clearly. These were subjected to a slow freezing process; the first 3 to 6 h in a -20°C freezer, then overnight in a -80°C freezer, and finally long term storage in liquid nitrogen tanks.

Preserved cell line can be resuscitated by thawing the cryovial in room temperature, and resuspending in 10 ml of pre-warmed medium. The cell suspension was then centrifuged at 800 x g for about 5 min to remove all traces of DMSO. The cell pellet was finally resuspended in about 13 ml of medium and grown in 75 cm<sup>2</sup> flask.

#### **2.2.5 Treatment with Toxins and Agonist**

Stable or transiently expressing cells were treated with toxins *in vivo*. Cholera toxin was used at 200 ng/ml final concentration, diluted in a small volume

of medium. It was added directly into the flasks under aseptic environment, followed by incubation for the appropriate amount of time. Pertussis toxin was added in the same manner, but at a final concentration of 25 ng/ml.

Pretreatment of cells with the agonist iloprost was done exactly the same. Iloprost was normally used at a final concentration of 1  $\mu$ M.

### **2.2.6 Cell Harvesting**

Cells were harvested by first removing the growth medium and rinsing once in cold PBS buffer. Using a disposable cell scraper, the cells were scraped off the base of the flask or dish with a small volume of PBS buffer. The cell suspension was collected into 10 ml or 50 ml tubes and centrifuged at 800 x g at 4°C for about 5 min. The cell pellets obtained were stored at -80°C until required for membrane preparation.

## **2.3 Molecular Biology**

Molecular biological manipulations were performed in a manner where contamination of DNA and DNase were kept to a minimum. This involved autoclaving all materials (e.g. pipette tips, eppendorfs, bottles, buffers, water *etc*), swapping the bench and pipettors with 70% alcohol, and using gloves for all procedures.

### 2.3.1 Reagents for Molecular Biology

#### Gel Loading Buffer (6X)

For 10 ml:

Bromophenol Blue (2%) 1.25 ml

Sucrose 4 g

These were dissolved in autoclaved water to a final volume of 10 ml. The buffer was stored in aliquots at -20°C.

#### TAE Buffer

Tris-acetate 40 mM

EDTA 1 mM

This was prepared as a 50X stock solution by adding 242 g of Tris / HCl, 57.1 ml of glacial acetic acid, and 100 ml of 0.01 M EDTA (pH 8) to deionised water in a final volume of 1 litre. This was diluted in deionised water when required.

#### Liquid Broth (LB)

For 1 litre:

Bacto-tryptone 10 g

Bacto-yeast extract 5 g

NaCl 10g

These were dissolved in deionised water and pH adjusted to 7. Sterilised by autoclaving at 126°C for 11 min.

## LB Ampicillin Agar Plates

This has the same components as LB but with bacto-agar (1.5% <sup>w/v</sup>) added. After autoclaving, it was left to cool before ampicillin was added to a final concentration of 50 µg/ml. The liquid LB agar was poured into 10 cm diameter petri dishes, and allowed to solidify before storing at 4°C. LB ampicillin agar plates can be stored for up to 3 weeks without any loss of antibiotic activity.

### 2.3.2 Transformation

The transfer of DNA into *E.coli*, known as transformation, allows multiple copies of the DNA to be produced as the bacteria replicates. The strain of *E. coli* used for transformation is DH5α, which used in conjunction with the vector pcDNA3, allows high copies of the plasmid to be made per bacteria.

#### ***A) Preparation of competent bacteria***

Before the *E. coli* can be used for DNA transformation, it must be "made receptive or competent" for foreign DNA entry. This usually involved treating the bacteria to various chemicals.

#### **Solution 1 (for 100 ml)**

Potassium acetate (1 M)	3 ml
RbCl <sub>2</sub> (1 M)	10 ml
CaCl <sub>2</sub> (1 M)	1 ml
MnCl <sub>2</sub> (1 M)	5 ml
Glycerol (80% <sup>v/v</sup> )	18.75 ml

The final volume was made up to 100 ml with deionised water and pH adjusted to 5.8 with 100 mM acetic acid. The solution was filter-sterilised and stored at 4°C.

### **Solution 2 (for 40 ml)**

MOPS (100 mM; pH 6.5)	4 ml
CaCl <sub>2</sub> (1 M)	3 ml
RbCl <sub>2</sub> (1 M)	0.4 ml
Glycerol (80% v/v)	7.5 ml

The final volume was made up with deionised water and pH adjusted to 6.5 with HCl. It was filter sterilised and stored at 4°C.

A conical flask with 250 ml of LB was inoculated with 5 ml of an overnight culture of DH5 $\alpha$  *E. coli*, and allowed to incubate at 37°C with shaking for 4 to 5 h until the optical density (at 550 nm) of the culture reached 0.48. The *E. coli* culture was then chilled on ice for 5 min, and the bacteria collected by spinning in a chilled centrifuge at low speed (~3000 rpm). The pellet was resuspended in 100 ml of solution 1 for 5 min on ice. The bacteria cells were pelleted as before, and then resuspended in 5 ml of solution 2 for 15 min on ice. The DH5 $\alpha$  bacteria is now ready for transformation or can be stored at -80°C in aliquots until required.

### **B) Transformation of DNA**

Each plasmid DNA (10-50 ng) was incubated with 50  $\mu$ l of competent bacteria in a sterile non-plastic tube for 15 min on ice. The DNA / bacteria mix was then subjected to heat shock at 42°C for 90 seconds, and plunge straight back into ice for another 2 min. 450  $\mu$ l of LB was added and the bacteria cells allowed to recover in a 37°C shaking incubator for 45 min. 100 to 200  $\mu$ l of this mix was plated out on LB ampicillin agar plate, left briefly on the bench for the agar to absorb the liquid, and finally incubated at 37°C overnight. Colonies picked from the plate can be cultured in LB for further DNA extraction, or the plate can be kept at 4°C for up to 2 weeks.

Transformed *E. coli* LB culture can also be kept as glycerol stocks by mixing 1 volume of culture with 1 volume of 50%  $v/v$  glycerol in a sterile eppendorf tube, and stored at  $-80^{\circ}\text{C}$ . Cells kept as glycerol stocks are viable for up to 2 years.

### 2.3.3 DNA Preparation

DNA was purified using the Promega Wizard™ Miniprep and Maxiprep kits according to the manufacturer's instructions. A brief description of the Miniprep protocol will be given.

The miniprep kit was used when less than 10  $\mu\text{g}$  of DNA is required. A 5 ml overnight culture of the transformed *E. coli* was first set up. 3 ml of it was transferred into two 1.5 ml eppendorf tubes and spinned at 12,000 rpm in a bench-top centrifuge for 2 min. 200  $\mu\text{l}$  of Cell Resuspension Solution (50 mM Tris/HCl pH 7.5, 10 mM EDTA, 100  $\mu\text{g}/\text{ml}$  Rnase A) was added to resuspend the cell pellet, followed by 200  $\mu\text{l}$  of Cell Lysis Solution (0.2 M NaOH, 1% SDS). The tube was gently inverted a few times until the suspension clears. 200  $\mu\text{l}$  of Neutralisation Solution (1.32 M potassium acetate pH 4.8) was added, mixed as before, and then spinned at 12,000 rpm for 5 min.

The clear supernatant thus obtained was transferred to a new 1.5 ml eppendorf tube and to it added 1 ml of Wizard™ Minipreps DNA Purification Resin. This DNA / resin mix was transferred to a disposable syringe attached to a Wizard™ Minicolumn. The mix was pulled through the column by vacuum, followed by 2 ml of Column Wash Solution. The resin which binds the DNA was now trapped in the column, and can be dried by continuing the vacuum for another 30 seconds. Finally, DNA was eluted off the resin by applying 50  $\mu\text{l}$  of preheated autoclaved water ( $65-70^{\circ}\text{C}$ ) onto the Minicolumn for 1 min. This was collected in an eppendorf tube by fitting the Minicolumn on top and spinning the whole assembly for 1 min at about 5000 rpm in a bench-top centrifuge. The DNA solution thus obtained can be stored at  $-20^{\circ}\text{C}$  for up to 3 years or more. A similar protocol for the Maxiprep kit was used.

### 2.3.4 Polymerase Chain Reaction

<b>PCR mix:</b>	Template DNA (0.1 µg/µl)	2 µl
	Primer 1 (25 pmol/µl)	1 µl
	Primer 2 (25 pmol/µl)	1 µl
	Deoxynucleotides triphosphate (2.5 mM)	5 µl
	Pfu polymerase buffer (10X)	5 µl
	Autoclaved water to	<b>50 µl</b>

The above mix was added into autoclaved thin-walled PCR tubes, with a drop of mineral oil overlayed on top. It was initially heated at 95°C for 10 min to denature the DNA double strand so that primers can hybridise onto the complementary sequences of the DNA. 0.8 µl of native Pfu enzyme was then added and the PCR cycles initiated in a Hybaid OmniGene temperature cycler.

#### PCR cycles:

<u>Denaturation</u>	<u>Annealing</u>	<u>Extension</u>	<u>Cycles</u>
95°C; 45 sec	50-60°C*; 1 min	72°C; 2.5 min	30
95°C; 45 sec	50-60°C*; 1 min	72°C; 10 min	1

\* annealing temperature was empirically determined, and was set at 50, 55 or 60°C.

At the end of the PCR cycles, the lower aqueous layer was withdrawn carefully and transferred into a clean tube.

### 2.3.5 Agarose Gel Electrophoresis

The DNA required for agarose gel electrophoresis was first diluted to the appropriate concentration with autoclaved water. Gel loading buffer (6X) was

added in the ratio 1:5 with the diluted DNA. Agarose gel was prepared by heating the appropriate amount of agarose in 30 ml TAE buffer in the microwave oven for 90 seconds. Concentrations of 0.8 to 1% w/v agarose were used depending on the size of the DNA fragments to be separated. 5 µl of ethidium bromide (10 mg/ml) was mixed well with the liquid agarose before pouring into the chamber of the electrophoresis kit (Gibco Horizon 58 with Model 200 power pack). The appropriate combs were inserted to form wells in the gel. After the gel had set, TAE buffer was added to a level that fully covered it. The prepared DNA was then loaded into the wells and the electrophoresis started. The gel was finally examined under UV light and an electronic image printed.

### **2.3.6 DNA Purification from Agarose Gel**

Purification of DNA fragments from agarose gel was performed using the QIAquick Gel Extraction kit (Qiagen, West Sussex, U. K.). Briefly, the desired DNA fragment on the agarose gel was first excised with a clean, sharp scalpel and transferred to a 1.5 ml eppendorf tube.

The gel slice was weighed and Buffer QX1 was added at a volume 3 times the gel weight. The tube was incubated at 50°C for 10 min to dissolve the gel. 1 volume of isopropanol was added to the sample and mixed by inverting. The sample was then transferred to a QIAquick column fitted on top of a 2 ml collection tube. The whole assembly was centrifuged for 1 min at about 13,000 rpm in a microcentrifuge, discarding the flow-through. 0.5 ml of QX1 was added to the QIAquick column, and centrifuged as before to remove all traces of agarose from the column. The column was washed with 0.75 ml of Buffer PE by repeating the centrifugation and discarding the waste. The column was further dried by repeating the centrifugation after discarding the waste from Buffer PE.

The QIAquick column was removed from the 2 ml collection tube and placed onto a clean and autoclaved 1.5 ml eppendorf tube. 50 µl of water was added to the QIAquick column, stand for 1 min, and centrifuged for 1 min at

13,000 rpm. The eluant contained the desired DNA fragment and can be either stored at -20°C or used immediately.

### 2.3.7 DNA Sequencing

Sequencing of DNA was done by the Molecular Biology Support Unit located at the Anderson College, Institute of Virology, University of Glasgow. An ABI dye-terminator kit was used for the PCR reaction, while a Perkin Elmer ABI 377 DNA sequencing machine was used for the electrophoresis and analysis of DNA sequences.

### 2.3.8 Construction of FLAG-hIPR (FhIPR)

The cDNA for human IP prostanoid receptor was a kind gift from Dr. M. Abramovitz of Merck Frosst, Quebec, Canada. The FLAG epitope is an 8 amino acid sequence (Asp-Tyr-Lys-Asp-Asp-Asp-Asp-Lys), where high affinity and selective antibodies are commercially available. Since there is currently no antibody raised against the human IP prostanoid receptor, tagging the N-terminus of the receptor with the FLAG epitope will be useful for immuno-detection and immuno-localisation purposes.

The set of PCR oligonucleotide primers used were:

Sense oligonucleotide 5' - AAGGATCCGCCACCATG(GACTACAAGGACGACGATGATAAG)GCGGATTCGTGCAGGAACC - 3'; the underlined bases refer to restriction sites for *Bam*H1 and *Nco*I respectively, and FLAG epitope bases are in parenthesis.

Antisense oligonucleotide 5' - AAGAATTCTCAGCTTGAAATG(TCA)GCAGAG -3'; the underlined bases refer to *Eco*RI restriction site, and the stop codon is in parenthesis.

PCR amplified fragment was purified by agarose gel (1% w/v) electrophoresis followed by gel extraction. It was digested with *Bam*HI and *Eco*RI before ligating to pcDNA3 vector through these restriction sites. Introduction of the *Nco*I site at the start codon allowed the selection of positive clones upon *Nco*I

digestion and agarose gel electrophoresis. The cDNA construct, known as FhIPR cDNA, was fully sequenced.

### **2.3.9 Construction of Receptor-G $\alpha$ Fusion cDNA**

The construction of cDNAs encoding fusions between the human IP prostanoid receptor with the various G $\alpha$  necessitates removal of the stop codon in the receptor cDNA. Furthermore, a new restriction site had to be introduced, so that the 5' end of the G $\alpha$  cDNA can be ligated in frame with the 3' end of FhIPR cDNA. It appeared that a *Xho*I sequence would be an ideal linker, as it was not present in the receptor nor all the G $\alpha$  (G $_{s\alpha}$ , G $_{11\alpha}$ , G $_{i\alpha}$ /G $_{\beta\alpha}$ ) cDNAs. Furthermore, the *Xba*I site of pcDNA3 (which is downstream of *Xho*I) is available for ligating to the 3' end of G $\alpha$  cDNAs, as this sequence is also not present in either the receptor or the G $\alpha$  cDNAs.

An oligonucleotide primer for FhIPR without the stop codon was designed:

Antisense oligonucleotide 5' - CCGCTCGAGGGAGCAGGCGACGCTGGC -3'; the underlined bases refer to *Xho*I restriction site.

PCR was repeated with the original sense oligonucleotide for FhIPR and this new antisense oligonucleotide, using FhIPR cDNA as the template. The amplified fragment was again purified by gel electrophoresis and extraction. Restriction enzymes *Bam*HI and *Xho*I were used to digest the fragment which was then ligated to pcDNA3 via these restriction sites. This cDNA was used for subsequent receptor-G $\alpha$  fusion cDNA constructs.

#### **A) FhIPR-G $_{s\alpha}$ cDNA**

To link the G $_{s\alpha}$  cDNA with the IP receptor cDNA, the 5' end was changed to a *Xho*I site, while the 3' end was changed to *Xba*I site. Hence, a set of PCR primers were designed:

Sense oligonucleotide 5' - CCGCTCGAGATGGGCTGCCTCGGCAACAG - 3'; the underlined bases refer to *Xho*I restriction site.

Antisense oligonucleotide 5' - TGCTCTAGA(TTA)GAGCAGCTCGTATTGGC - 3'; the underlined bases refer to *Xba*I restriction site and the stop codon is in parenthesis.

The template is rat  $G_{s\alpha}$ (HA), obtained from Drs M. J. Levis and H. R. Bourne, University of California at San Francisco, CA, U. S. A. It encodes the long isoform of  $G_{s\alpha}$  in which the haemagglutinin (HA) epitope (VPDYA) was constructed between amino acid residues 76-82. PCR and purification of amplified fragment were done as in section 2.3.4 & 2.3.7 respectively. The purified fragment was digested with *Xho*I and *Xba*I restriction enzymes and cloned into the corresponding sites of FhIPR (no stop codon) in pcDNA3.

#### **B) FhIPR- $G_{i1\alpha}$ cDNA**

A similar strategy was used in the construction of the FhIPR- $G_{i1\alpha}$  fusion cDNA. A set of PCR primers specific for the  $G_{i1\alpha}$  cDNA were used:

Sense oligonucleotide 5' - CCGCTCGAGGGCTGCACACTGAGCGCTG - 3'; the underlined bases refer to *Xho*I restriction site.

Antisense oligonucleotide 5' - TGCTCTAGAAGC(TTA)GAAGAGACCACAGTC - 3'; the underlined bases refer to *Xba*I restriction site and the stop codon is in parenthesis.

The template used is  $G_{i1\alpha}$  cDNA. PCR, gel extraction, digestion, and cloning were as for the above protocol.

#### **C) FhIPR- $G_{i1}/G_{s6\alpha}$ cDNA**

To construct the fusion cDNA of a chimeric G protein ( $G_{i1}/G_{s6\alpha}$ ) with the receptor, the chimeric G protein cDNA was first constructed (courtesy of Daljit Bahia). This was done by substituting the last 6 amino acids of  $G_{i1\alpha}$  with that of  $G_{s\alpha}$  using PCR primers:

Sense oligonucleotide 5' - ACGTG A A T T CGCCACCATGGGCTGCACACTG-AGCGC - 3'; the underlined bases refer to *EcoRI* restriction site.

Antisense oligonucleotide 5' - CCACGTG A A T T CTTA(TAAGAGTTCATA-TTGCCT)TAGGTTATTCTTTAT - 3'; the underlined bases refer to *EcoRI* restriction site, and bases in parenthesis refer to substitutions for  $G_s\alpha$  bases.

From this  $G_{i1}/G_{s6}\alpha$  cDNA, restriction sites at both the 5' and 3' ends were mutated to *XhoI* and *XbaI* respectively. The same strategy as that of other  $G\alpha$  cDNAs was utilised to clone the chimeric G protein cDNA in frame with that of the human IP prostanoid receptor. The sense oligonucleotide primer for the FhIPR- $G_{i1}\alpha$  fusion cDNA was used, while a new antisense oligonucleotide primer was designed:

5' - TGCTC T A G A T T A(TAAGAGTTCATATTGCCT)TAGG - 3'; the underlined bases refer to the *XbaI* restriction site and bases in parenthesis refer to  $G_s\alpha$  bases.

## 2.4 Assays

### 2.4.1 Radioligand Binding

The expression of IP prostanoid receptors in stable cell lines and transient transfected cells were assessed by [<sup>3</sup>H]iloprost binding studies. These were performed in borosilicate glass tubes in triplicates, containing the following mix:

Membrane protein (1 mg/ml)	20 $\mu$ l
Assay buffer (50 mM Tris/HCl at pH 7.5, 5 mM MgCl <sub>2</sub> )	60 $\mu$ l
[ <sup>3</sup> H]iloprost ( $\geq$ 10 nM)	10 $\mu$ l
Ilprost ( $\sim$ 10 $\mu$ M) or assay buffer	10 $\mu$ l
Total volume:	100 $\mu$ l

Reactions were incubated for 30 min at 30°C. Binding was stopped by addition of 2.5 ml ice cold wash buffer (50 mM Tris/HCl at pH 7.5, 0.25 mM EDTA), followed by vacuum filtration through GF/C filters to remove free radioligand from the membrane. The filters were washed 3 times in ice-cold wash buffer, air dried, and inserted into vials containing 5 ml of liquid scintillant. After an overnight incubation, the vials were counted in a Beckman LS6500 scintillation counter using the <sup>3</sup>H counting channel. Specific binding was determined by subtracting the counts performed in the absence of unlabelled iloprost (total counts) from that with it (non-specific counts). Receptor expression level (fmol/mg) was calculated by taking into consideration the specific activity of [<sup>3</sup>H]iloprost (34 dpm/fmol) and the amount of membrane protein used per tube.

The binding affinity of the receptors for iloprost was similarly assayed, using a concentration of [<sup>3</sup>H]iloprost close to  $K_d$  ( $\sim$ 3.4 nM) and increasing concentrations of unlabelled iloprost (from  $10^{-12}$  to  $10^{-5}$ ). Non-specific binding was taken as the counts when maximum concentration of unlabelled iloprost was used.

## 2.4.2 Adenylate Cyclase Catalytic Activity

The catalytic activity of adenylate cyclase was assayed in accordance to Wong (1994), based on the use of [<sup>3</sup>H]adenine. Cells were split into the wells of 24-well plate and incubated in medium containing [<sup>3</sup>H]adenine at 0.5  $\mu$ Ci/well for 16-24 h.

The following day, cells were washed once in assay medium make up of 1X DMEM, 2 mM L-glutamine, 20 mM HEPES (pH 7.4), 1 mM 3-isobutyl-1-methylxanthine, and 1% penicillin/streptomycin. Various concentrations of iloprost were first diluted in assay medium, and added to the wells for the required duration. During the incubation period, the plate was placed on a heated block connected to a 37°C water bath. At the end of incubation, the assay medium was aspirated and 0.5 ml of ice-cold stop solution (5%  $w/v$  TCA, 1 mM ATP, 1 mM cAMP) added to each well. The plate can be stored at -20°C or at 4°C if the columns to separate the nucleotides were ready.

Separation of cAMP from the other adenine nucleotides is based essentially on the method of Salomon *et al.* (1974). The Dowex and alumina columns were set up in accordance to Farndale *et al.* (1991). Basically, a rack of Dowex columns and a rack of alumina columns with precise alignment of the column positions were used. Columns were improvised from 5 ml syringes fitted with glass wool at the base to form a retaining mesh for the resins. Dowex resins were washed extensively in deionised water, followed by 3 washes in 1 M HCl, and again with water. It was finally resuspended 1:1 with deionised water in a beaker and kept in uniform suspension using a magnetic stirrer. 2 ml of this suspension was pipetted into the columns, giving a 1 ml bed volume. Alumina resins were washed once in water and once in 0.1 M imidazole (pH 7.3). It was similarly resuspended in deionised water and pipetted into the columns. The columns were plugged to prevent the resins from drying when not in use. Before using the columns, the Dowex columns must be primed by passing through 2 washes of 1 M HCl, followed by 2 washes of deionised water; the alumina

columns were washed twice with 0.1 M imidazole (pH 7.3) and once with deionised water.

The separation of [ $^3\text{H}$ ]cAMP from the rest of the labelled components (e.g. [ $^3\text{H}$ ]ATP, [ $^3\text{H}$ ]ADP, [ $^3\text{H}$ ]AMP, [ $^3\text{H}$ ]adenine *etc*) starts with the Dowex columns. Dowex 50 resins are negatively charged and hence are not expected to bind any of the components. However, the passage of cAMP is preferentially retarded in the column, probably by a non-specific interaction with the Dowex resin, and hence allow other labelled components to be washed away (Farndale *et al.* 1991). The alumina resin instead binds cAMP less avidly than other adenine nucleotides as the cyclisation leads to the loss of vicinal hydroxyls on the ribose ring. Imidazole, which competes for the purine binding site, can therefore displace cAMP from alumina columns.

The separation protocol involved firstly pipetting the sample (in stop solution) into the Dowex column, followed by 3 ml of deionised water. The eluant was collected in vials containing about 5 ml of liquid scintillant. This fraction contained predominantly [ $^3\text{H}$ ] labelled adenine nucleotides except [ $^3\text{H}$ ]cAMP. The rack of Dowex columns was next placed on top of the alumina columns, taking care to ensure that the eluant from the upper Dowex columns go straight into the alumina columns. The Dowex columns were next washed with 5 X 2 ml of deionised water into the alumina columns, discarding the washings. This step displaced cAMP from the Dowex to the alumina columns. The rack of Dowex columns was then removed, and 3 X 2 ml of 0.1 M imidazole (pH 7.3) added to the alumina columns. This eluant was collected in vials containing 9 ml of liquid scintillant, and labelled as the [ $^3\text{H}$ ]cAMP containing fraction. Both sets of vials were counted in Beckman scintillation counter using the  $^3\text{H}$  counting channel. Results were expressed as the ratio of [ $^3\text{H}$ ]cAMP to total [ $^3\text{H}$ ]adenine nucleotides (X100).

### 2.4.3 High Affinity GTPase

High affinity GTPase assay was performed essentially as described in Gierschik *et al.* (1994). Assay mix (for 100 tubes) was prepared as follows:

<u>Components</u>	<u>Volume (<math>\mu</math>l)</u>	<u>Final concentration</u>
Creatine Phosphate (0.4 M)	250	20 mM
Creatine Phosphokinase (2.5 U/ml)	200	0.1 U/ml
ATP (0.04 M; pH 7.5)	250	2 mM
App(NH)p (0.04 M)	25	0.2 mM
Ouabain (0.01 M)	1000	2 mM
NaCl (4 M)	250	200 mM
MgCl <sub>2</sub> (1 M)	50	10 mM
DTT (0.1 M)	200	4 mM
EDTA (0.02 M; pH 7.5)	50	0.2 mM
Tris/HCl (2 M; pH 7.5)	200	80 mM
GTP (0.1 mM)	50	1 $\mu$ M
Deionised water to final volume of	<b>5000 <math>\mu</math>l</b>	

5  $\mu$ Ci [ $\gamma$ -<sup>32</sup>P]GTP (50 nCi per assay) was added to the above mix and left on ice until ready to be added to the reaction tubes.

The assay was performed in 1.5 ml eppendorf tubes containing the following:

Membrane protein (at 0.5 mg/ml)	20 $\mu$ l
Agonist or water or GTP *	10 $\mu$ l
Deionised water	20 $\mu$ l
Assay mix	50 $\mu$ l
Total volume:	100 $\mu$ l

\* the assay was set up under 3 different conditions: agonist driven, basal, and non-specific activities, depending on whether agonist (at various concentrations), water, or GTP (1 mM) were added respectively.

The assay tubes were set up in triplicates and incubated at 37°C for 20 min. 900  $\mu$ l of ice-cold charcoal slurry (5% activated charcoal in 10 mM  $H_3PO_4$ ) was added to each tube to terminate the reaction. The charcoal was pelleted by spinning the tubes at 13,000 rpm for 5 min in a chilled microcentrifuge. 500  $\mu$ l of the supernatant (containing Pi) was withdrawn and transferred into vials for Cerenkov radiation counting in a Beckman radioisotope counter. High affinity GTP hydrolysis rate (pmol/min/mg) was obtained by subtracting the counts from GTP (1 mM) control tubes, and taking into consideration the specific activity of [ $\gamma$ <sup>32</sup>P]GTP, the concentration of unlabelled GTP in the assay (0.5  $\mu$ M), the membrane protein concentration, and finally the incubation time.

To measure enzymatic parameters like Michaelis Menton constant ( $K_m$ ) and maximum velocity ( $V_{max}$ ) of the GTPase activity, the assay can be carried out under various concentrations of GTP (the substrate). The assay mix was prepared as above with the omission of unlabelled GTP. A series of GTP dilutions was then prepared at 10X the concentration required in the final assay. The assay consisted of the following components:

Membrane protein (at 0.5 mg/ml)	20 $\mu$ l
Agonist or water	10 $\mu$ l
GTP at various concentrations	10 $\mu$ l
Deionised water	10 $\mu$ l
Assay mix (without unlabelled GTP)	50 $\mu$ l
Total volume:	100 $\mu$ l

The assay included a zero and a high concentration (1 mM) of unlabelled GTP which gave the GTPase rate at the concentration of [ $\gamma$ <sup>32</sup>P]GTP and that of non-specific respectively. The assay was performed as before and results calculated in the same manner. The data can be plotted on appropriate graphs, e.g. Eadie-Hofstee plot or Lineweaver Burke plot, to determine  $K_m$  and  $V_{max}$  values.

#### 2.4.4 GTP $\gamma$ S Binding

[<sup>35</sup>S]GTP $\gamma$ S binding studies were performed according to Wieland and Jakobs (1994). A 4X binding assay mix was first made up, consisting of 80 mM HEPES (pH 7.4), 20 mM MgCl<sub>2</sub>, 400 mM NaCl, and 20  $\mu$ M GDP (freshly added). The reaction was done in borosilicate glass tubes, with the following components:

Membrane protein (1 mg/ml)	20 $\mu$ l
Agonist or water or GTP $\gamma$ S *	10 $\mu$ l
[ <sup>35</sup> S]GTP $\gamma$ S <sup>+</sup> (0.3 to 0.5 nM)	10 $\mu$ l
Binding assay mix (4X)	25 $\mu$ l
Deionised water	35 $\mu$ l
	<b>Total volume: 100 <math>\mu</math>l</b>

\* The assay was performed under 3 conditions: agonist driven, basal, and non-specific. This depended on whether agonist (at various concentrations), water, or unlabelled GTP $\gamma$ S (200  $\mu$ M) were added respectively.

+ [<sup>35</sup>S]GTP $\gamma$ S was diluted in 10 mM Tricine (pH 7.5) and 1 mM DTT to 100 nCi/ $\mu$ l, aliquoted, and stored at -80°C. The amount used in the assay was kept constant at 50 nCi/assay by taking into account the decay of the radioisotope.

The tubes were incubated at 25°C for 60 min. Binding was stopped by the addition of 2.5 ml ice cold wash buffer (20 mM Tris/HCl at pH 7.4, 5 mM MgCl<sub>2</sub>), followed by vacuum filtration through GF/C filters to remove unbound [<sup>35</sup>S]GTP $\gamma$ S from the membrane. The filters were washed 3 times in ice-cold wash buffer, air dried, and inserted into vials containing 5 ml of liquid scintillant. These were counted in a Beckman scintillation counter using the <sup>35</sup>S counting channel.

The specific incorporation of [<sup>35</sup>S]GTP $\gamma$ S into the membranes was calculated by subtracting the non-specific counts in tubes containing high concentration (20  $\mu$ M final concentration) of unlabelled GTP $\gamma$ S.

## 2.5 Other Protocols

### 2.5.1 Preparation of Cell Membranes

Plasma membrane-containing P2 particulate fractions were prepared from cell pastes that had been stored at  $-80^{\circ}\text{C}$  since harvesting. Cell pellets were resuspended in TE buffer and rupture of the cells was achieved with 25 strokes of a hand-held Teflon-on-glass homogenizer. Unbroken cells and nuclei were removed by centrifugation at low speed (2,000 rpm) in a refrigerated microcentrifuge. The supernatant fraction was then centrifuged at 75,000 rpm for 30 min in a Beckman Optima TLX Ultracentrifuge (Palo Alto, CA) with a TLA100.2 rotor. The pellets were resuspended in TE buffer to a final protein concentration of 1-3 mg/ml and stored at  $-80^{\circ}\text{C}$  until required.

### 2.5.2 Western Blotting

#### *A) Preparation of SDS-PAGE gel*

Sodium dodecyl sulphate (SDS) polyacrylamide gel electrophoresis (PAGE) was usually performed with 10% acrylamide resolving gels. It was prepared as follows:

Water	8.3 ml
Tris/HCl (1.5M, pH 8.8), SDS (0.4% w/v)	6 ml
Acrylamide (30% w/v), bisacrylamide (0.8% w/v)	8 ml
Glycerol (50% w/v)	1.6 ml
Ammonium persulphate (10% w/v)	90 $\mu\text{l}$
TEMED	8 $\mu\text{l}$

This is sufficient for a single gel cast in a Hoefer Gel Caster with two 180 X 160 mm glass plates and 1.5 mm spacers. The gel was layered with 0.1% w/v SDS and allowed to polymerise at room temperature for about 90 min.

After the resolving gel had polymerised, the SDS layer was washed off and the stacking gel prepared as follows:

Water	9.75 ml
Tris/HCl (0.5M; pH 6.8), SDS (0.4% w/v)	3.75 ml
Acrylamide (30% w/v), bisacrylamide (0.8% w/v)	1.5 ml
Ammonium persulphate (10% w/v)	150 $\mu$ l
TEMED	8 $\mu$ l

This was layered on top of the resolving gel with a 15 well teflon comb left at the top and allowed to polymerise for about 60 min, after which, the gels were used immediately or stored at 4°C overnight.

### ***B) Electrophoresis of SDS-PAGE***

The buffer for electrophoresis of SDS-PAGE consists of 25 mM Tris/HCl, 192 mM glycine and 0.1% w/v SDS, make up to 2 litre for each electrophoresis tank. The gels were assembled into a Hoefer vertical gel electrophoresis kit, and buffer filled into the lower reservoir till the electrophoresis wire was fully immersed. Sufficient buffer was also poured into the upper reservoir, taking care not to overflow.

Protein samples (30  $\mu$ g) were diluted 1:1 in Laemmli buffer (2X) and heated to boiling for 5 min on a heating block prior to loading onto the gel. A Hamilton syringe was used to load samples into the wells of the gel. At least a sample of prestained protein markers was loaded into each gel. Any empty

wells were loaded with laemmli buffer at a volume similar to the protein samples.

Electrophoresis of each 10% SDS-PAGE gel was usually at 10 mA constant current overnight (about 16 h) or 35 mA constant current for about 4 h; the voltage was set at least 300 V and the power at least 10 W. The current was doubled for two gels:

### ***C) Protein transfer onto membrane***

After electrophoresis, the glass plates with the gel were dismantled from the electrophoresis kit. 5 litre of transfer buffer was prepared, consisting of 25 mM Tris/HCl, 192 mM glycine, and 20%  $v/v$  methanol. Nitrocellulose membranes and Whatman filter papers were also cut to the size of the gel, and pre-wetted in transfer buffer.

After the glass plates were separated from the gel, a nitrocellulose membrane was gently rolled over to cover it, taking care to avoid any air bubbles between them. This gel-nitrocellulose combination was then sandwiched between two pieces of Whatman filter paper and assembled into an LKB Transphor apparatus. The nitrocellulose membrane was positioned nearer to the positive end relative to the gel. All the transfer buffer was poured into the transfer tank.

Protein transfer from the gel to the membrane was performed at about 1.5 mA for 90 to 120 min, depending on the number of gel transfers in the apparatus. The protein transferred to the nitrocellulose membrane can be visualised by temporarily staining with a solution consisting of 0.1%  $w/v$  Ponceau S and 3%  $w/v$  trichloroacetic acid. The stain can be removed in TBST buffer.

#### ***D) Incubation with antibodies***

Prior to incubation of the membrane with antibodies, it was covered with 5% non-fat milk (Marvel) in TBS overnight at 4°C. This was necessary to remove any non-specific interaction between the membrane and the antibodies.

All antibodies were diluted in 3% Marvel in TBS and kept at 4°C with a trace of thimerosal. Membranes were incubated with each antibody for 1 to 2 h at room temperature with shaking. The membranes were washed extensively (at least 3 to 4 times) with TBST before the next antibody was added. Antibodies were reused for no more than 5 times or 3 months whichever earlier.

Dilutions of the various antibodies used were as follows:

<u>Primary antibody</u>	<u>Dilution</u>	<u>Secondary antibody</u>	<u>Dilution</u>
M5 FLAG	1:1000	Anti-mouse IgG	1:2000
CS	1:2000	Anti-rabbit IgG	1:2000
SG	1:2000	Anti-rabbit IgG	1:2000
CQ	1:2000	Anti-rabbit IgG	1:2000
I1C	1:1000	Anti-rabbit IgG	1:2000

### ***E) Enhanced chemiluminescence***

Visualisation of horse-radish-peroxidase conjugated antibodies on the nitrocellulose membrane was performed by enhanced chemiluminescence (ECL) according to the manufacturer's instructions (Amersham, U. K.). Briefly, membranes were washed extensively with wash buffer before incubation with the ECL reagent. After 3 min, excess reagent was drained off, and the membrane sandwiched between two pieces of clear plastic sheet. Care was taken to ensure that no air bubbles were trapped between the membrane and the plastic sheet.

The nitrocellulose membrane was then put into a film cassette and a light-sensitive film inserted in the darkroom. The film was developed in an automatic film developer (Kodak Xomat) after an appropriate exposure time.

## **CHAPTER 3**

# **Selective Activation of a Chimeric $G_{i1}/G_s$ G Protein $\alpha$ Subunit by the Human IP Prostanoid Receptor**

## CHAPTER 3

# Selective Activation of a Chimeric $G_{i1}/G_s$ G Protein $\alpha$ Subunit by the Human IP Prostanoid Receptor

### 3.1 Introduction

GPCRs transduce extracellular signals into the cell by activating heterotrimeric G proteins. There are currently 20  $G\alpha$ , 6  $G\beta$  and 12  $G\gamma$  subunits known. The association of G protein and GPCR is rather specific, and occurs only when specific domains and conformations are present on both the receptor and G protein. The coupling of  $G\alpha$  subunit with GPCR has been particularly well studied, and specific domains essential for coupling have been defined. Much of this work was made possible through the generation of chimeric G proteins, where codons of a  $G\alpha$  cDNA were replaced by those of another. Such chimeras represent continuous open reading frames that contain domains from 2 different  $G\alpha$  subunits. This is possible because of the high sequence homology between  $G\alpha$  subunits, which permit specific domains to be interchanged without altering the likely overall structure of the protein. As  $G\alpha$  proteins differ substantially in their handling of guanine nucleotides, activation of effectors, coupling to GPCRs, and regulation by other proteins, the substitution of certain domains will therefore generate chimeric G proteins that differ from the "parental" G protein. Careful analysis of such chimeras has yielded useful information regarding the functions and properties of the replaced domains, and their impact on the overall characteristics of the chimeric protein.

The use of chimeric G proteins in GPCR research dates back to 1988 when Masters *et al.* constructed a  $G_{i2}\alpha$  (1-212 aa) /  $G_s\alpha$  (235-394 aa) hybrid polypeptide. This was possible by digesting a conserved *Bam*HI restriction endonuclease site in the cDNA of mouse  $G_{i2}\alpha$ , that neatly separated domains I and II from domain III (the carboxyl terminus). The domains I and II fragment of

$G_{12}\alpha$  was then ligated to the domain III fragment of mouse  $G_s\alpha$ , forming a single reading frame that encoded 60% of  $G_{12}\alpha$  and 40% of  $G_s\alpha$ . This cDNA was introduced via a retroviral vector into S49 cyc<sup>-</sup> cells, which lack endogenous  $G_s\alpha$ . They found the ability of the chimeric  $G_{12}\alpha/G_s\alpha$  protein to mediate  $\beta_2$ -adrenergic receptor stimulation of adenylate cyclase was similar to that of the wild type  $G_s\alpha$ . Hence, they concluded that the carboxyl terminus of  $G_s\alpha$  contains structural features essential for interactions with the receptor and the effector enzyme, adenylate cyclase.

In the following year, a chimeric  $G\alpha$  protein,  $G_s\alpha$  (1-356 aa) /  $G_{12}\alpha$  (320-355 aa), known as  $G_{\alpha_{s/12}}$ (38) was constructed by Woon *et al.* (1989). It involved replacing the last 38 amino acids of  $G_s\alpha$  with the last 36 amino acids of  $G_{12}\alpha$ . This chimeric G protein showed 1.5 to 2.5 fold constitutively elevated cAMP levels and a 3 to 4 fold increase in PKA activity when expressed in Chinese hamster ovary (CHO) cells. Furthermore, in the presence of isobutylmethyl-xanthine, a cAMP phosphodiesterase inhibitor, cAMP levels in clones expressing the  $G_{\alpha_{s/12}}$ (38) construct were 10 to 15 fold higher than  $G_s\alpha$  expressing clones. There was also an indication of enhanced GDP dissociation rate as the lag time for maximal adenylate cyclase activation by  $GTP\gamma S$  was diminished. However, the constitutive activity of this chimeric G protein appeared to be cell line dependent, as expression in COS-1 cells did not show any constitutive activity (Osawa *et al.* 1990a).

In a further extension of the work on  $G_{12}\alpha$  (1-212 aa) /  $G_s\alpha$  (235-394 aa), Osawa *et al.* also replaced the last 38 amino acids of this hybrid polypeptide with the last 36 amino acids of  $G_{12}\alpha$  as in the  $G_{\alpha_{s/12}}$ (38) construct. Interestingly, this  $G_{12}\alpha$  (1-212 aa) /  $G_s\alpha$  (235-356 aa) /  $G_{12}\alpha$  (320-355 aa) protein did show constitutive adenylate cyclase activity when expressed in COS-1 cells (Osawa *et al.* 1990a). The  $G_s\alpha$  domain for adenylate cyclase activation was therefore mapped to isoleucine 235 to arginine 356. Besides replacing the carboxyl terminal residues of  $G_s\alpha$  with  $G_{12}\alpha$ , Osawa *et al.* also studied the effect of replacing the

amino terminal residues. They found that a chimeric G protein  $G_{i2\alpha}$  (1-54 aa) /  $G_{s\alpha}$  (55-395 aa) gave constitutive adenylate cyclase activity when expressed in COS-1 cells (Osawa *et al.* 1990b). This and other N-terminal  $G_{i2\alpha}/G_{s\alpha}$  constructs led them to the conclusion that the N-terminus of  $G_{s\alpha}$  possesses an attenuator regulatory function.

The importance of C-terminal residues of  $G\alpha$  proteins in receptor coupling was further demonstrated by Conklin *et al.* (1993a) when they generated  $G_{q\alpha}/G_{i2\alpha}$  chimeric proteins by replacing 1 to 23 amino acids of the C-terminal region of  $G_{q\alpha}$  with that of  $G_{i2\alpha}$ . When these chimeric G proteins were coexpressed with  $A_1$  adenosine or  $D_2$  dopamine receptors (both are  $G_i\alpha$  coupled GPCRs), functional coupling in HEK293 cells was shown by elevation of agonist stimulated PLC activity. The substitution of at least 3 carboxyl terminal residues was required to switch the receptor specificity of the chimeric protein from  $G_{q\alpha}$  coupled GPCR to  $G_i\alpha$  coupled GPCR (the  $A_1$  and  $D_2$  receptors) (Conklin *et al.* 1993a). Maximum coupling efficiency was seen when 4 to 9 carboxyl terminal residues were substituted. This suggested that more residues may actually hinder receptor coupling or affect the activation of PLC. Expression of chimeric  $G_{q\alpha}/G_{i2\alpha}$  proteins with 4 to 11 substitutions also caused a 2 fold increase in basal PLC activity, which was indicative of weak constitutive activity.

The benefit of switching the receptor specificity of a G protein was exploited in a study of  $G_{13\alpha}$  subunit by Voyno-Yasenetskaya *et al.* (1994).  $G_{13\alpha}$  was identified as the  $G\alpha$  subunit responsible for regulating the activity of  $Na^+-H^+$  exchanger (NHE) from transient expression studies of a mutationally activated  $G_{13\alpha}$ . However, as no GPCR was known to directly activate this subunit at that time, a chimeric protein approach was used to activate  $G_{13\alpha}$  with a  $G_i\alpha$  coupled GPCR. Hence, a  $G_{13\alpha}$  (1-372 aa) /  $G_{z\alpha}$  (351-355 aa) protein was constructed by replacing the last 5 carboxyl residues of  $G_{13\alpha}$  with those of  $G_{z\alpha}$ . This enabled the  $D_2$  dopamine receptor to couple to the  $G_{13\alpha}/G_{z\alpha}$  chimera and activate NHE using

quinpirole, a D<sub>2</sub> receptor agonist, while a dopamine antagonist, butaclamol, blocked the effect (Voyno-Yasenetskaya *et al.* 1994).

The critical carboxyl terminal residues involved in receptor coupling were further defined to be at the -3 and -4 position from the C-terminus of G $\alpha$ , using mutation studies of the G<sub>q</sub> $\alpha$ /G<sub>z</sub> $\alpha$  chimera (Conklin *et al.* 1996). However, in a study of other chimeric G proteins with substitutions of their extreme C-terminus, it was apparent that not all GPCRs were able to couple as efficiently. For example, replacement of 5 C-terminal aa of G<sub>q</sub> $\alpha$  with the equivalent G<sub>s</sub> $\alpha$  sequence permitted V2 vasopressin receptor but not  $\beta_2$ -adrenergic receptor (both Gs coupled GPCRs) to stimulate phospholipase C. Similar replacement of G<sub>s</sub> $\alpha$  aa with G<sub>q</sub> $\alpha$  permitted bombesin and V1a vasopressin receptors but not the oxytocin receptor (all G<sub>q</sub> $\alpha$  coupled GPCRs) to stimulate adenylate cyclase (Conklin *et al.* 1996).

Further evidence that the extreme carboxyl terminus of G $\alpha$  protein is not sufficient for receptor coupling comes from studies of chimeras G<sub>13</sub> $\alpha$  (1-372 aa) / G<sub>z</sub> $\alpha$  (351-355 aa) and G<sub>12</sub> $\alpha$  (1-372 aa) / G<sub>z</sub> $\alpha$  (351-355 aa) (Tsu *et al.* 1997). Signals from aminergic ( $\alpha_2$ -adrenergic and dopamine D<sub>2</sub>) receptors but not peptidergic (opioid and formyl-methionine peptide) receptors were transduced by these chimeras, despite the known G<sub>i</sub> $\alpha$  and G<sub>z</sub> $\alpha$  coupling ability of these receptors. Furthermore, G<sub>z</sub> $\alpha$  (1-319 aa) / G<sub>i</sub> $\alpha$  (315-355 aa) but not a G<sub>i</sub> $\alpha$  (1-314 aa) / G<sub>z</sub> $\alpha$  (320-355 aa) chimera couples to  $\delta$ -opioid receptor to activate adenylate cyclase type II via G $\beta\gamma$  dimers, which appears to contradict the importance of the C-terminus in receptor coupling. Similarly, C5a chemoattractant factor receptor was not able to activate a G<sub>11</sub> $\alpha$  (1-237 aa) / G<sub>16</sub> $\alpha$  (241-374 aa) chimera although it can stimulate PLC activity via full length G<sub>16</sub> $\alpha$  (Lee *et al.* 1995). Instead an additional segment encompassing residues 220-240 of G<sub>16</sub> $\alpha$  was required for functionality. Interestingly, N-terminal residues of G<sub>16</sub> $\alpha$  were sufficient to endow a G<sub>16</sub> $\alpha$  (1-209 aa) / G<sub>11</sub> $\alpha$  (207-359 aa) chimera with specificity for C5a induced

activation, although it exhibited only 40% coupling capacity of full length  $G_{16\alpha}$  (Lee *et al.* 1995). Therefore, these conflicting results indicated that not all G proteins couple to GPCRs solely via the carboxyl-terminal residues. Hence, the carboxyl terminus of  $G\alpha$  may not be the only determinant for receptor coupling.

Despite these various setbacks, it is still possible that the majority of known GPCRs activate G proteins via the extreme C-terminus (see Section 1.3.2). This probably prompted Komatsuzaki *et al.* (1997) to devise a system that reports the G proteins coupled to a GPCR by using a series of  $G_{5\alpha} / G_{x\alpha}$  chimeras ( $G_{x\alpha}$  = any  $G\alpha$ ). These chimeras were constructed by replacing the last 5 aa of  $G_{5\alpha}$  with those of  $G_{11/2\alpha}$ ,  $G_{o\alpha}$ ,  $G_{z\alpha}$ ,  $G_{q\alpha}$ ,  $G_{12\alpha}$ ,  $G_{13\alpha}$ ,  $G_{14\alpha}$ , and  $G_{16\alpha}$ . This was designed to allow the chimeric G protein to couple to the receptor under study, and hence determine the G protein(s) that are normally activated via measurement of adenylate cyclase activity. Indeed, the SSTR3 somatostatin receptor recognised the C-termini of  $G_{11/2\alpha}$ , but not  $G_{o\alpha}$  or  $G_{z\alpha}$ , and those of  $G_{14\alpha}$  and  $G_{16\alpha}$ , but not of  $G_{q\alpha}$  or  $G_{11\alpha}$ . These results were further confirmed by assaying for SSTR3 agonist stimulated PI turnover when  $G_{14\alpha}$  or  $G_{16\alpha}$  were co-transfected (Komatsuzaki *et al.* 1997). Hence, such a G protein reporting system, at least in the case of the SSTR3 somatostatin receptor, gave a similar result as co-transfection experiments and with the ease of using only a single assay end point. More studies will need to be undertaken to confirm whether this approach is applicable for other GPCRs.

This study aimed to extend the use of chimeric G proteins to assay for agonist function at the G protein level for the human IP prostanoid receptor. Activation of an agonist-occupied GPCR results in the exchange of GDP for GTP in  $G\alpha$  subunits. The activated  $G\alpha$  subunit has an intrinsic ability to hydrolyse GTP to GDP, due to the presence of a GTPase domain. This timer-controlled hydrolysis of the terminal phosphate of GTP determines the duration of the signal as GTP-bound  $G\alpha$  adopts a conformation that can activate downstream effectors. However,  $G\alpha$  subunits exhibit different rates of GTP exchange ( $k_{off}$ ) and GTP hydrolysis ( $k_{cat}$ ) (Fields *et al.* 1997). As such, assays that examine the GPCR-induced exchange of GDP for GTP or a poorly hydrolysed analogue like  $GTP\gamma S$  as

in [<sup>35</sup>S]GTP $\gamma$ S binding assays (Wieland *et al.* 1994), and the subsequent hydrolysis of GTP as in high affinity GTPase assays (Gierschik *et al.* 1994) are useful only for a subset of G proteins, in particular the pertussis toxin-sensitive subfamily of G $\alpha$ -like G proteins (Milligan 1988). The direct demonstration of guanine nucleotide binding and hydrolysis in other G $\alpha$  subunits, is often difficult to demonstrate in membrane systems, mainly due to a combination of intrinsically low GTP exchange and hydrolysis function of these subunits (Wieland *et al.* 1994; Gierschik *et al.* 1994). To assay the activation of these non G $\alpha$ -like subunits, it is important to reduce basal activity to a minimum, for example through the use of N-ethylmaleimide, a sulfhydryl group alkylating agent. N-ethylmaleimide is also a potent inhibitor of receptor-stimulated GTP hydrolysis by pertussis toxin-sensitive G proteins (Gierschik *et al.* 1994). In the [<sup>35</sup>S]GTP $\gamma$ S binding assay, pretreatment with unlabelled GTP $\gamma$ S can reduced agonist-independent binding of radiolabelled GTP $\gamma$ S, and pretreatment together with N-ethylmaleimide was found to give the best result in [<sup>35</sup>S]GTP $\gamma$ S assays of turkey erythrocyte membranes in response to  $\beta$ -adrenergic receptor agonists (Wieland *et al.* 1994). Despite these treatments, the level of agonist stimulated activity in both assays is still a fraction of that obtainable by G $\alpha$ -like subunits.

As the IP prostanoid receptor is a G $\alpha$ -coupled GPCR, conventional methods for assaying G protein activation are not ideal. Although studies on chimeric G proteins had yielded conflicting results, it may still be possible that the majority of GPCRs transduce signals to G proteins solely through residues at the carboxyl terminus of G $\alpha$ . If this is also true for the IP prostanoid receptor, then it may be possible to utilise a chimeric G $\alpha$ /G $\alpha$  protein, which has the high GTP exchange and hydrolysis capability of G $\alpha$ , but the coupling specificity of G $\alpha$ . Therefore, a G $\alpha$  (1-349 aa) / G $\alpha$  (389-394 aa) protein (known as G $\alpha$ /G $\alpha$ ) was constructed. The backbone of this chimeric G protein is essentially G $\alpha$ , while the last 6 carboxyl residues are from G $\alpha$ . It was constructed by Mr Daljit Bahia, a Ph.D. student in the laboratory, as part of a series of G $\alpha$  (1-349 aa) / G $\alpha$  (last 6 aa) chimeras. These chimeras were constructed with the intention of testing their

coupling capacity with various GPCRs. This approach will hopefully allow non-G<sub>i</sub>α coupled GPCRs to produce robust agonist-dependent regulation of high affinity GTPase and GTP<sub>γ</sub>S binding.

For ease of immunodetection, the human IP prostanoid receptor (hIPR) was FLAG<sup>TM</sup> epitope tagged on the N-terminus by PCR. The cDNA of this FLAG<sup>TM</sup> tagged receptor (FhIPR) was then stably transfected into HEK293 cells. cDNA of the G proteins G<sub>i1</sub>/G<sub>s6</sub>α, G<sub>i1</sub>α or G<sub>s</sub>α was transiently transfected into a clone of HEK293 cells stably expressing the FhIPR. GTP<sub>γ</sub>S binding and high affinity GTPase assays were utilised to monitor activation of the expressed G<sub>α</sub> by the agonist occupied FhIPR. Toxins that ADP-ribosylate G<sub>α</sub> subunits, cholera and pertussis toxins, were also employed to delineate receptor coupling with the various G proteins. Some of the results to be presented have been published in *Molecular Pharmacology* (1998) **54**, 249-257.

## 3.2 Results

### *Characterisation of HEK293 clones stably expressing FhIPR*

Incorporation of the FLAG<sup>TM</sup> epitope (Asp-Tyr-Lys-Asp-Asp-Asp-Asp-Lys) at the N-terminus of hIPR was successfully completed using PCR (see section 2.3.8). Transient transfection of this cDNA (5 µg) into HEK293 cells gave very low expression of the receptor, as assessed by [<sup>3</sup>H]iloprost binding (data not shown). The transient expression of FhIPR was not increased by using larger amounts (up to 20 µg) of cDNA. Therefore, antibiotic selection of stably expressing HEK293 clones was embarked on very early in the project.

25 HEK293 clones stably expressing the FhIPR were expanded and screened by [<sup>3</sup>H]iloprost (~10 nM) binding studies. Three of the highest expressing clones were studied in detail: clones 13, 16 and 17. Membranes of these clones and parental HEK293 cells were prepared and their level of FhIPR expression was reassessed by [<sup>3</sup>H]iloprost binding (Figure 3.1). Parental HEK293 cells expressed negligible amounts of IP prostanoid receptors (<20 fmol/mg; n=5). Clone 13 showed the highest level of specific [<sup>3</sup>H]iloprost binding at  $2957 \pm 144$  fmol/mg membrane protein (n=5), followed by clone 17 at  $1660 \pm 251$  fmol/mg (n=3) and clone 16 at  $1010 \pm 29$  fmol/mg (n=3).

The functionality of the expressed FhIPR in HEK293 clones was assessed by the ability of agonist to elevate cAMP in intact cells. This secondary messenger effect of the IP prostanoid receptor was first discovered in platelets through the action of prostacyclin (PGI<sub>2</sub>) by Gorman *et al.* (1977). In this study, the assay for adenylate cyclase activation was performed essentially according to the method of Wong (1994) in which [<sup>3</sup>H]adenine was used to label the cellular pool of adenine nucleotide. The cells were split into 12 well plates and incubated overnight with [<sup>3</sup>H]adenine at 1 µCi per well. Iloprost (1 µM) was used to stimulate the receptor while forskolin (50 µM) which directly activates adenylate cyclase, was used to assess the level of maximum cyclase activity. After 20 min incubation, the [<sup>3</sup>H]-labelled adenine nucleotides were separated as described in Section 2.4.2. All 3

clones exhibited substantial increases in cAMP when stimulated by agonist (Figure 3.2). However, agonist stimulated cAMP production in clone 16 cells was consistently lower than the rest; a possible reason being the poorer expression of FhIPR (see Figure 3.1). As clone 13 cells demonstrated maximal adenylate cyclase response to both iloprost and forskolin, and also expressed the FhIPR at high level, it was selected for detailed analysis.

Agonist saturation binding studies were performed on clone 13 cells at up to 50 nM [<sup>3</sup>H]iloprost (Figure 3.3A). A Scatchard plot showed 2-affinity binding (analysed by EBDA<sup>TM</sup>; Elsevier-BIOSOFT 1987) with dissociation constant ( $K_d$ ) of  $1.6 \pm 0.4$  nM and maximum receptor level ( $B_{max}$ ) of  $971 \pm 83$  fmol/mg membrane protein ( $n=3$ ) for receptors showing high-affinity binding and  $K_d$  of  $11.4 \pm 2.3$  nM and  $B_{max}$  of  $3202 \pm 515$  fmol/mg ( $n=3$ ) for low-affinity binding sites (Figure 3.3B).

*what the overall  
low Hill slope  
what might be 2 sites  
effect of GTP?*

Amount of [<sup>3</sup>H]iloprost that can be realistically used in the assay is 10 nM, this limited the accuracy of the  $B_{max}$  and  $K_d$  estimates. Therefore, it was decided that agonist displacement would provide a better assessment of the overall binding characteristics of clone 13 cells. From Figure 3.4, we can see that the displacement of [<sup>3</sup>H]iloprost (3.4 nM) in a concentration-dependent manner in clone 13 cells, with  $IC_{50}$  of  $6.1 \pm 0.7$  nM and  $B_0$  of 1817 fmol/mg. Applying the formalism of DeBlasi *et al.* (1989) to these data, the  $K_d$  of the high-affinity site and  $B_{max}$  was estimated at  $3260 \pm 68$  fmol/mg. The shallow slope of the displacement graph is shallow (Hill coefficient =  $0.64 \pm 0.05$ ), which is a strong indication of binding to more than one site.

Immunodetection of FLAG<sup>TM</sup> epitope in the IP prostanoid receptor was demonstrated in Figures 3.5A and 3.5B. Immunoblotting the membranes of HEK293 cells transiently expressing the FhIPR with the anti-FLAG<sup>TM</sup> monoclonal antibody M5 confirmed expression of a FLAG<sup>TM</sup>-tagged protein (Figure 3.5A) which was absent in membranes of mock transfected HEK293 cells. The predominant FLAG antibody reactive species migrated through SDS-PAGE with an apparent molecular mass of around 45 kDa. Although somewhat slower

migrating polypeptides were observed in the transiently transfected cells, these were more evident in membranes of clone 13 cells that expressed the receptor stably and at higher levels (Figure 3.5B). These probably represent differentially glycosylated forms of the FhIPR which presented as a broad complex or multiple bands ranging from 41 to 61 kDa in mass. In contrast, membranes of parental HEK293 cells from which clone 13 was derived did not show any immunoreactivity to M5 anti-FLAG™ antibody.

Agonist-stimulated adenylate cyclase activity in clone 13 cells was assessed in greater detail by studying the dose-dependent effect of iloprost (Figure 3.6). Clone 13 cells were seeded into poly-o-lysine coated 24 well plates and incubated overnight with [<sup>3</sup>H]adenine at 0.5 μCi per well. Iloprost concentrations from 10<sup>-11</sup> to 10<sup>-5</sup> M were used to stimulate the cells for 20 min. The EC<sub>50</sub> of iloprost to stimulate adenylate cyclase in clone 13 cells was estimated at 1.4 ± 0.3 X 10<sup>-10</sup> M (n=3). This result correlated well with that observed for a hemagglutinin-tagged hIPR with EC<sub>50</sub> of 0.1 nM (Smyth *et al.* 1996).

Sustained agonist treatment of cells can caused downregulation of the activated G protein(s). Therefore, iloprost (1 μM) pretreatment of clone 13 cells was attempted at various time points. Membranes of these treated cells were resolved in SDS-PAGE and immunoblotted with various anti-Gα antisera. The progressive loss of endogenous G<sub>s</sub>α with time when incubated with iloprost was clearly seen in Figure 3.7A. As stimulation of IP prostanoid receptor elevates cAMP, it is not surprising that G<sub>s</sub>α was downregulated. The long isoform of G<sub>s</sub>α was observed to be downregulated faster than the short isoform, probably due to its lower endogenous expression. However, such a time-dependent pattern of downregulation was not apparent for G<sub>11/2</sub>α or G<sub>q/11</sub>α subunits (Figures 3.7B & 3.7C respectively). Gα subunits in parental HEK293 cells were not downregulated upon iloprost treatment (1 μM for 16 h) (data not shown).

### ***Construction and immunological characterisation of a G<sub>11</sub>/G<sub>s</sub>6 $\alpha$ chimeric protein***

The C-terminal decapeptide of G<sub>s</sub> $\alpha$  differs from G<sub>11</sub> $\alpha$  in 8 residues (Figure 3.8). Conklin *et al.* (1993a) had previously shown maximum coupling efficiency when 4 to 9 carboxyl terminal residues were substituted. It was therefore possible that substituting the last 6 residues of G<sub>11</sub> $\alpha$  with those of G<sub>s</sub> $\alpha$  may confer the protein with the ability to interact with the IP prostanoid receptor. Such a chimeric protein (G<sub>11</sub>/G<sub>s</sub>6 $\alpha$ ) was constructed using a PCR-based strategy, where the last 6 codons of G<sub>11</sub> $\alpha$  cDNA were altered to encode the respective amino acids of G<sub>s</sub> $\alpha$  by changing as few bases as possible (see Section 2.3.9C).

To determine that this cDNA encoded a correct chimeric G<sub>11</sub>/G<sub>s</sub>6 $\alpha$  protein, it was transiently transfected into COS-7 cells, and the membranes assessed by a series of immunoblots. Antiserum I1C specific for an internal domain (159-168 aa) of G<sub>11</sub> $\alpha$  was firstly used. This detected strong immunoreactivity in membranes of G<sub>11</sub>/G<sub>s</sub>6 $\alpha$  transfected but not mock (pcDNA3) transfected cells (Figure 3.9A). This 41 kDa polypeptide co-migrated with an immunoreactive protein from membranes of rat brain cortex, which express high levels of G<sub>11</sub> $\alpha$ . However, SG1 antiserum, specific for the C-terminal decapeptide of G<sub>11/2</sub> $\alpha$ , failed to detect the same polypeptide in membranes of G<sub>11</sub>/G<sub>s</sub>6 $\alpha$  transfected cells (Figure 3.9B), although it did detect a low level of endogenous G<sub>11/2</sub> $\alpha$  in COS-7 cells and a high level of authentic G<sub>11/2</sub> $\alpha$  in rat brain cortex. Therefore, this showed that the "G<sub>11</sub> $\alpha$ -like" polypeptide in G<sub>11</sub>/G<sub>s</sub>6 $\alpha$  transfected cells had an altered C-terminus that failed to interact with an antiserum specific for the terminal decapeptide of G<sub>11/2</sub> $\alpha$ .

Confirmation that the chimeric G protein had acquired the immunoreactivity of the carboxyl-terminus of G<sub>s</sub> $\alpha$  can be seen from a CS immunoblot. CS antiserum was raised against the C-terminal decapeptide (RMHLRQYELL) of G<sub>s</sub> $\alpha$ . It immunoreacted with a polypeptide in G<sub>11</sub>/G<sub>s</sub>6 $\alpha$  transfected cells (Figure 3.9C; left panel). Endogenous levels of G<sub>s</sub> $\alpha$  were also detected in the G<sub>11</sub>/G<sub>s</sub>6 $\alpha$  transfected

cells (upper band). The same CS immunoreactive polypeptide also interacts with 11C antiserum (Figure 3.9C; right panel). Thus, this "G<sub>i1</sub>α-like" polypeptide is the chimeric G<sub>i1</sub>/G<sub>s</sub>6α protein. A minor point to note here is that although only 6 carboxyl residues of G<sub>s</sub>α were substituted into the corresponding segment of G<sub>i1</sub>α, the seventh carboxyl terminal residue - leucine 348, is conserved between G<sub>i1</sub>α and G<sub>s</sub>α. Therefore the last 7 residues of G<sub>s</sub>α, found in the G<sub>i1</sub>/G<sub>s</sub>6α chimera were sufficient for recognition by the CS antiserum.

### ***Transient expression of Gα proteins in clone 13 cells***

To assess the coupling capacity of the chimeric protein with the IP prostanoid receptor, cDNAs of G<sub>i1</sub>/G<sub>s</sub>6α, G<sub>s</sub>α, G<sub>i1</sub>α, and pcDNA3 were transiently transfected into clone 13 cells. Membranes from these cells were prepared and high affinity GTPase assays performed under basal and iloprost (1 μM) stimulated conditions, at a final GTP concentration of 0.5 μM. This assay detects the rate of GTP hydrolysis by Gα subunits, and hence is a measure of both G protein activation ( $k_{off}$ ) and termination ( $k_{cat}$ ) (Gierschik *et al.* 1994). As Gα subunits differ greatly in their handling of guanine nucleotides, the GTPase assay is therefore ideal to detect any "switch" of Gα coupling with the receptor.

As presented in Figure 3.10, transient expression of G<sub>i1</sub>/G<sub>s</sub>6α protein in clone 13 cells resulted in a very large increase in agonist stimulated high-affinity GTPase activity compared to mock transfected cells (unpaired t-test:  $p < 0.05$ ;  $n = 3$ ). Transient expression of G<sub>s</sub>α and G<sub>i1</sub>α in clone 13 cells did not affect the level of agonist-stimulated high affinity GTPase inherently present in these cells. Furthermore, transient transfection of parental HEK293 cells with G<sub>i1</sub>/G<sub>s</sub>6α cDNA did not result in any measurable iloprost stimulation of high affinity GTPase activity.

Since expression of high levels of protein can cause enforced coupling between G proteins and GPCRs which is not seen normally (Kenakin 1997), the level of Gα overexpression in clone 13 cells was assessed. In Figure 3.11A, the

expression level of  $G_{i1}/G_s6\alpha$  protein was similar to  $G_{i1}\alpha$  protein in transiently transfected clone 13 cells. However,  $G_{i1}/G_s6\alpha$  protein was expressed at least 3 times higher than  $G_s\alpha$  protein (Figure 3.11B). Although it may appear that the elevated GTPase response of  $G_{i1}/G_s6\alpha$  transfected cells could be attributed to the high expression of this protein, a similar level of expression of  $G_{i1}\alpha$  did not result in any increase in GTPase activity (Figure 3.10). Thus, the coupling of  $G_{i1}/G_s6\alpha$  protein with the FhIPR was specific and not a direct result of high expression levels.

The GTPase assay determines the overall activity of G proteins (a combination of activation and termination rates), while the  $GTP\gamma S$  binding assay gives only an indication of the level of activated  $G\alpha$ . This is because incorporation of a non-hydrolysable analogue of GTP ( $GTP\gamma S$ ) in  $G\alpha$  would prevent any further termination and re-activation processes (i.e.  $k_{cat} = 0$ ). With this in mind, [ $^{35}S$ ]GTP $\gamma S$  binding assays were performed on membranes of  $G_{i1}/G_s6\alpha$  transfected clone 13 and HEK293 cells, and also in untransfected clone 13 cells (Figure 3.12). Expression of  $G_{i1}/G_s6\alpha$  protein in HEK293 cells did not alter agonist-driven binding of [ $^{35}S$ ]GTP $\gamma S$  but transfection into clone 13 cells, which already express high levels of FhIPR (~3 pmol/mg), enhanced iloprost (1  $\mu M$ ) stimulated binding when compared to untransfected clone 13 cells. Thus iloprost, acting via the IP prostanoid receptor, activated a larger amount of  $G\alpha$  when  $G_{i1}/G_s6\alpha$  was co-expressed.

### ***Pretreatment with cholera and pertussis toxins***

The presence of endogenous  $G\alpha$  subunits affected the proper assessment of signalling activity arising from transfected  $G\alpha$ . Since activation of the IP prostanoid receptor resulted in cAMP production and also downregulation of endogenous  $G_s\alpha$  subunits, it is apparent that uncoupling  $G_s\alpha$  from the receptor will reduce endogenous  $G\alpha$  output and allow a true measure of  $G_{i1}/G_s6\alpha$ .

stimulation. This problem is less acute in S49 cyc<sup>-</sup> cells, which lack endogenous  $G_{s\alpha}$ , but most cell lines including HEK293, contain relatively high levels of  $G_{s\alpha}$ .

Cholera toxin has been shown to catalyse the ADP-ribosylation of  $G_{s\alpha}$  at arginine 201 and hence diminish its GTP-hydrolysis capacity (Cassel and Selinger 1977). As a result, ADP-ribosylated  $G_{s\alpha}$  is constitutively active and stimulates adenylate cyclase in the absence of agonist. Furthermore, ADP-ribosylated  $G_{s\alpha}$  is rapidly degraded, with extensive loss after 8 h treatment with cholera toxin (Chang and Bourne 1989). Using this strategy, clone 13 cells were pretreated with cholera toxin (200 ng/ml; 16 h) with the aim of reducing  $G_{s\alpha}$  activation by the IP prostanoid receptor. Alternatively, pertussis toxin catalyses the ADP-ribosylation of the last cysteine residue of G proteins of the  $G_i\alpha$  subfamily (except  $G_{z\alpha}$ ) and this modification has been shown to prevent G protein interaction with the receptor (Fields *et al.* 1997). Thus, clone 13 cells were also pretreated with pertussis toxin (25 ng/ml; 16 h) to assess its effect on endogenous  $G\alpha$  activity. Agonist-stimulated (1  $\mu$ M iloprost) high affinity GTPase assay was performed on membranes of these toxin-treated cells (Figure 3.13). The results indicated that pretreatment with cholera toxin but not pertussis toxin abolished the agonist-stimulated GTPase activity (unpaired t-test:  $p < 0.05$ ;  $n = 3$ ). This confirmed that the low level of agonist-promoted  $G\alpha$  activity was derived from activation of endogenous  $G_{s\alpha}$  and not  $G_i\alpha$ .

In the chimeric  $G_{i1}/G_{s6\alpha}$  protein both cysteine 351 of  $G_{i1\alpha}$  and arginine 201 of  $G_{s6\alpha}$  are absent (see Figure 3.8), and hence it is postulated to be resistant to both cholera and pertussis toxin treatment. Thus, clone 13 cells transiently transfected with the various  $G\alpha$  were pretreated with a combination of both cholera (200 ng/ml) and pertussis toxins (25 ng/ml) for 16 h, and [<sup>35</sup>S]GTP $\gamma$ S binding assays performed. This abolished iloprost-stimulated [<sup>35</sup>S]GTP $\gamma$ S binding in all the transfected cells except those expressing  $G_{i1}/G_{s6\alpha}$  protein (Figure 3.14). This conclusively proved that the chimeric G protein is resistant to treatment with

both toxins and that the enhancement of [<sup>35</sup>S]GTP $\gamma$ S binding in these cells was contributed by the G<sub>i1</sub>/G<sub>s6</sub> $\alpha$  protein.

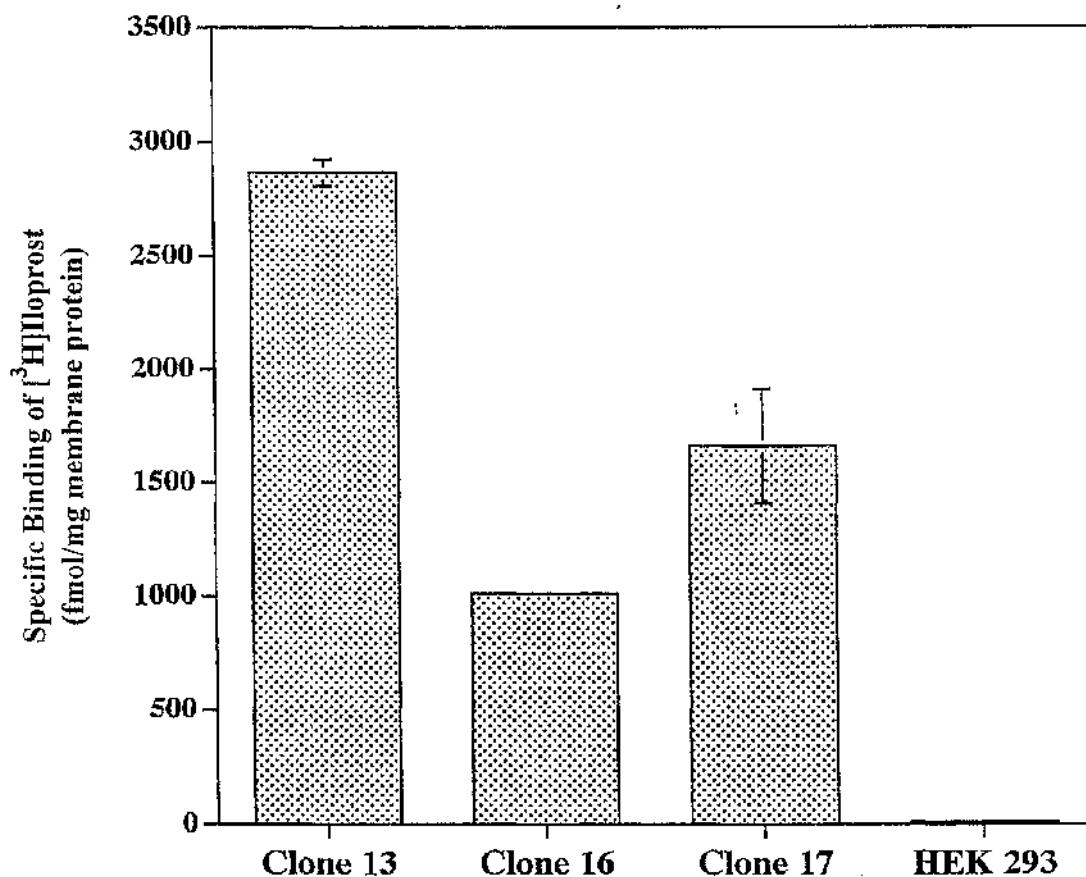
To ensure that the treatment of clone 13 cells with cholera and pertussis toxins had modified all G<sub>i</sub> $\alpha$  and G<sub>s</sub> $\alpha$  subunits, immunoblots of the membranes were performed. Immunoblotting with antiserum I1C showed retardation of the overexpressed G<sub>i1</sub> $\alpha$  protein in the presence of toxins (Figure 3.15A), indicating an increase in molecular mass arising from the covalent addition of ADP-ribose. This was however not observed in cells overexpressing G<sub>i1</sub>/G<sub>s6</sub> $\alpha$  protein. Pretreatment with toxins also resulted in the downregulation of both endogenous forms of G<sub>s</sub> $\alpha$  in all cells (Figure 3.15B), an effect of cholera toxin shown previously by various groups (Chang and Bourne 1989; MacLeod and Milligan 1990). As a higher level of the long isoform of G<sub>s</sub> $\alpha$  was expressed in cells transfected with G<sub>s</sub> $\alpha$ (L) cDNA, it was downregulated to a lesser extent by toxin treatment. Similar to that observed in the I1C immunoblot, the level of CS immunoreactive G<sub>i1</sub>/G<sub>s6</sub> $\alpha$  protein was unaffected by the action of the toxins (Figure 3.15B). These results further confirm the resistance of G<sub>i1</sub>/G<sub>s6</sub> $\alpha$  protein to both cholera and pertussis toxins under conditions where endogenous G<sub>s</sub> $\alpha$  and G<sub>i</sub> $\alpha$  subunits were downregulated and modified respectively.

As G<sub>i1</sub>/G<sub>s6</sub> $\alpha$  contains the backbone of G<sub>i1</sub> $\alpha$ , it would be expected to inhibit adenylate cyclase when activated. Clone 13 cells transfected with G<sub>i1</sub>/G<sub>s6</sub> $\alpha$  was assessed for cAMP production or inhibition upon stimulation by iloprost (1  $\mu$ M) or iloprost (1  $\mu$ M) together with forskolin (50  $\mu$ M). As seen in Figure 3.16, iloprost induced a slightly lower level of stimulation in G<sub>i1</sub>/G<sub>s6</sub> $\alpha$  transfected clone 13 cells compared to untransfected cells. However, addition of iloprost with forskolin resulted in synergistic activation of adenylate cyclase in both sets of cells. As the amount of G<sub>i</sub> $\alpha$  required to alter adenylate cyclase activity is at least 1000 fold higher than G<sub>s</sub> $\alpha$  (Taussig *et al.* 1993), it is possible that the concurrent activation of endogenous G<sub>s</sub> $\alpha$  could have masked the inhibitory action of G<sub>i1</sub>/G<sub>s6</sub> $\alpha$  on adenylate cyclase. Thus, the cells were pretreated with cholera toxin (200 ng/ml;

16 h) in an attempt to downregulate endogenous  $G_s\alpha$ . This had the effect of elevating the basal level of adenylate cyclase activity slightly and decreasing the response to iloprost in both sets of cells. However, there was still no inhibition of forskolin-stimulated adenylate cyclase activity by  $G_{i1}/G_s6\alpha$  protein upon activation by iloprost. As  $G_{i1}/G_s6\alpha$  was transiently transfected into clone 13 cells, it would mean that only 30 to 40% of all cells would express the protein (manufacturer's information leaflet on Lipofectamine<sup>TM</sup>). Therefore, even if  $G_{i1}/G_s6\alpha$  protein can inhibit adenylate cyclase activity, it would exert this effect in only 30 to 40% of clone 13 cells. It is thus not possible to properly assess the downstream signalling effects of this protein in such a scenario, and hence studies related to this were not pursued further.

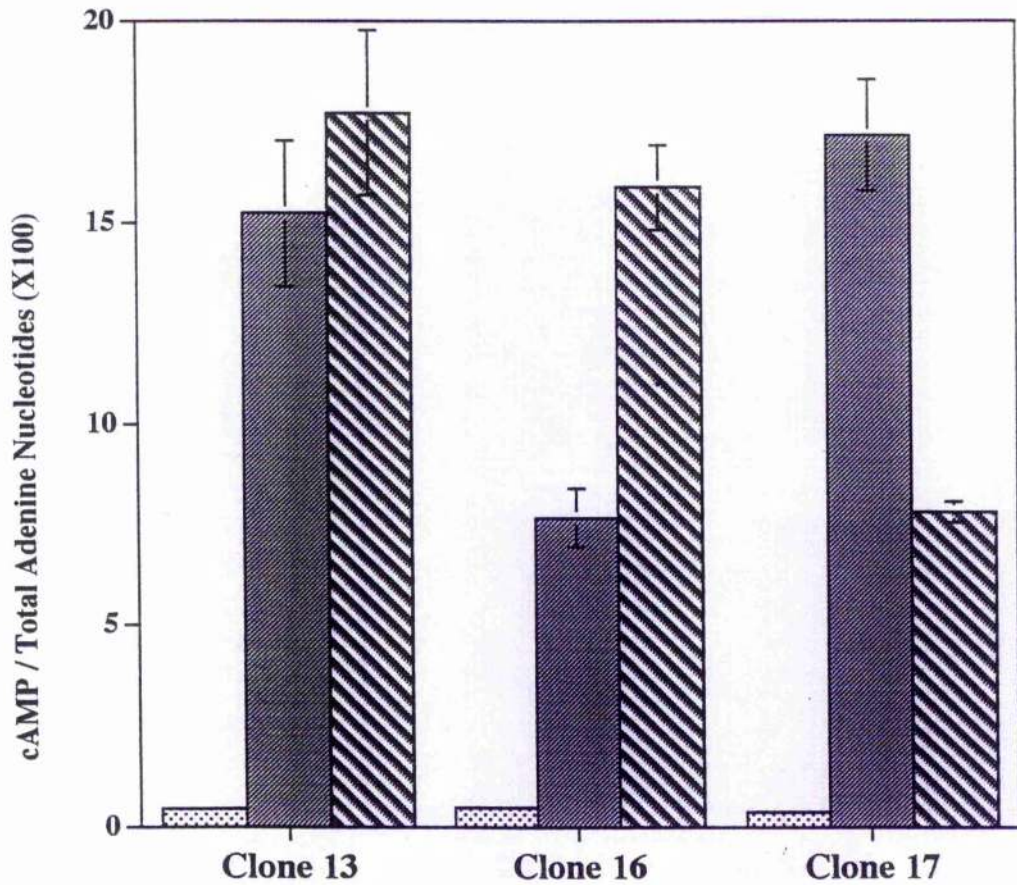
**Figure 3.1 Stable expression of the FLAG<sup>TM</sup>-tagged human IP prostanoid receptor in clones of HEK293 cells**

Following stable expression of the FhIPR cDNA into HEK293 cells, membranes from clones 13, 16, and 17 together with parental cells were prepared and assessed using ~ 10 nM [<sup>3</sup>H]iloprost. The specific binding of [<sup>3</sup>H]iloprost was obtained by subtracting non-specific counts (assessed with 5 μM unlabelled iloprost) from total counts, and normalised with the amount of membrane protein used in the assay. The data represent the mean ± SEM of 2 or more independent experiments performed in triplicate.



**Figure 3.2 Stimulation of cAMP production by iloprost and forskolin in clones of HEK293 cells stably expressing Fh1PR**

Basal adenylate cyclase activity (stippled bars) and regulation by 1  $\mu$ M iloprost (filled bars) or 50  $\mu$ M forskolin (hatched bars) were assessed in intact cells of HEK293 clones stably expressing Fh1PR (clones 13, 16 and 17). The results are expressed as the ratio of cAMP over total adenine nucleotides X 100 and represent the mean  $\pm$  SD of 2 independent experiments performed in triplicate.

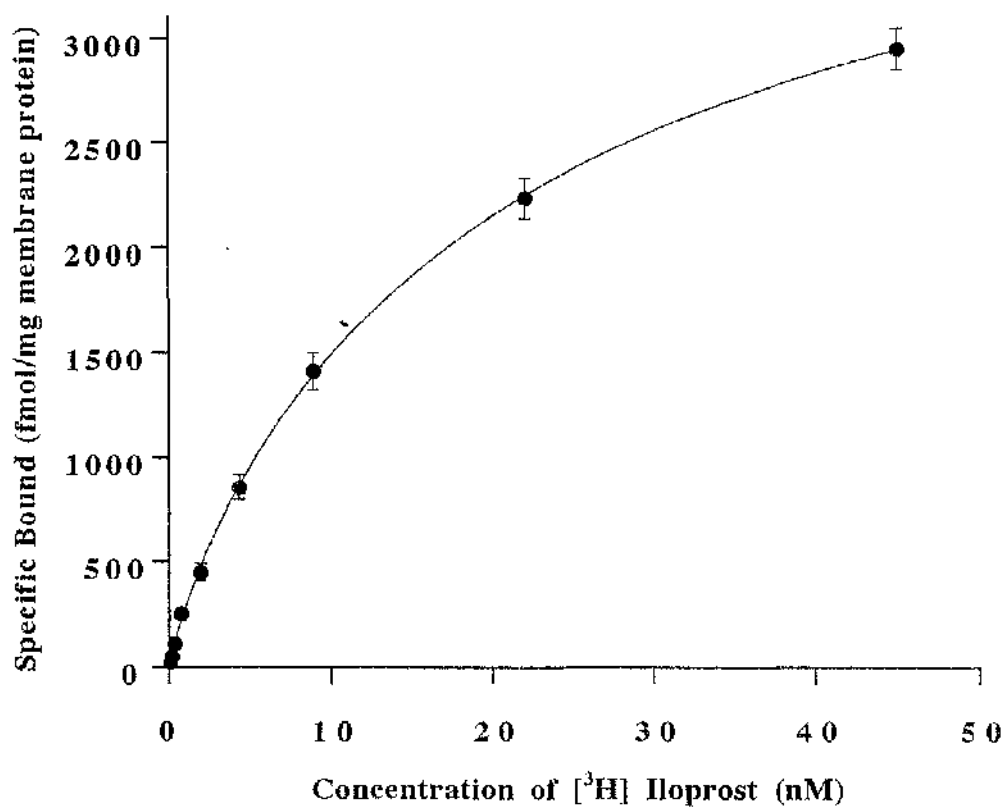
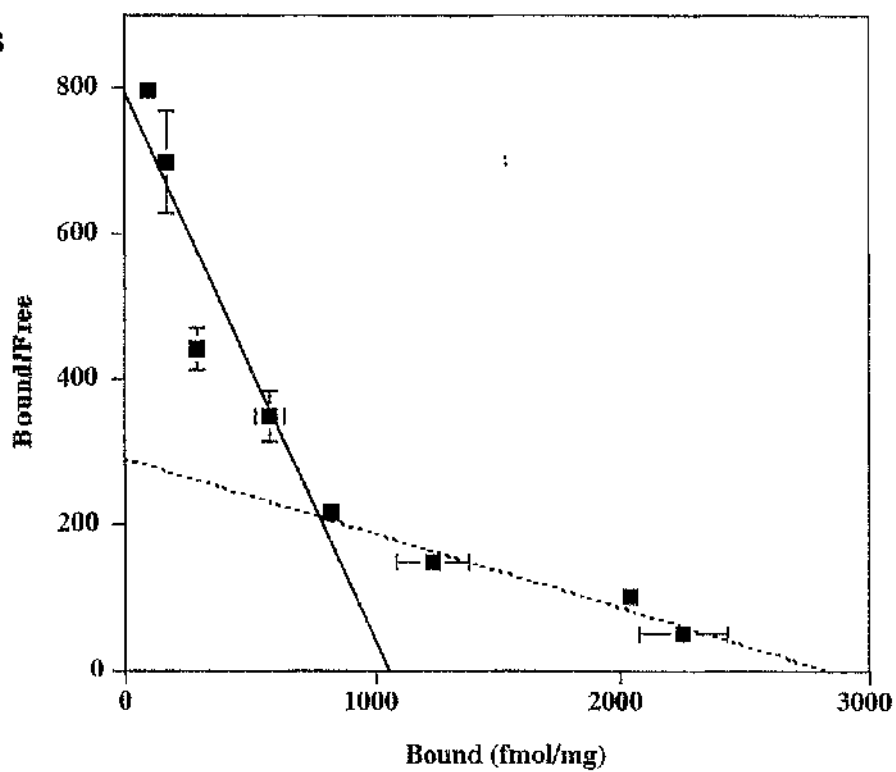


### Figure 3.3A [<sup>3</sup>H]iloprost saturation binding studies of clone 13 cells

Membranes of clone 13 cells were incubated with increasing concentrations of [<sup>3</sup>H]iloprost at 30°C for 30 min. Non-specific binding at each [<sup>3</sup>H]iloprost concentration was determined in the presence of 10 μM unlabelled iloprost. Specific binding of [<sup>3</sup>H]iloprost was obtained by subtracting non-specific binding from the total binding. Specific binding was expressed as fmol of [<sup>3</sup>H]iloprost bound per mg membrane protein by factoring in the specific activity of [<sup>3</sup>H]iloprost (34 dpm/fmol) and the amount of membrane protein used per assay (20 μg). This graph is a typical representation of 3 independent experiments performed in triplicate.

### Figure 3.3B Scatchard plot of agonist saturation binding in clone 13 cells

The binding data of Figure 3.3A was converted into concentrations of bound (fmol/mg membrane protein) and free (nM) radioligand at each [<sup>3</sup>H]iloprost concentration used. This was plotted as Bound/Free versus Bound (Scatchard Plot). The slope of the graph gave the negative inverse of  $K_d$  ( $-1/K_d$ ), while the X-intercept is the  $B_{max}$ . Analysis using EBDA (Elsevier-BIOSOFT 1987) showed 2 affinity binding. High affinity binding  $K_d$  was determined as  $1.6 \pm 0.4$  nM,  $B_{max}$  as  $971 \pm 83$  fmol/mg ( $n = 3$ ). Low affinity binding  $K_d$  was determined as  $11.4 \pm 2.3$  nM,  $B_{max}$  as  $3202 \pm 515$  fmol/mg ( $n = 3$ ). This graph is a typical representation of 3 independent experiments performed in triplicate.

**A****B**

**Figure 3.4 Displacement of [<sup>3</sup>H]iloprost binding in membranes of clone 13**

The specific binding of [<sup>3</sup>H]iloprost ( $3.4 \pm 0.2$  nM) to membranes of clone 13 cells was displaced by increasing concentrations of unlabelled iloprost. Counts obtained in the presence of  $10 \mu\text{M}$  unlabelled iloprost were treated as non-specific binding. Curve fitting by Kaleidograph™ (v3.02; Abelbeck Software 1993) indicated apparent  $B_{\text{max}}$  (also known as  $B_0$ ) of  $1817 \pm 38$  fmol/mg membrane protein and  $\text{IC}_{50}$  of  $6.1 \pm 0.7$  nM ( $n = 3$ ). Hill slope of the graph is  $0.64 \pm 0.05$ . Applying the formalism of DeBlasi *et al.* (1989),  $B_{\text{max}}$  was estimated at  $3260 \pm 68$  fmol/mg and  $K_d$  estimated at  $2.7 \pm 0.8$  nM. The data represent the mean  $\pm$  SEM of 3 independent experiments performed in triplicate.

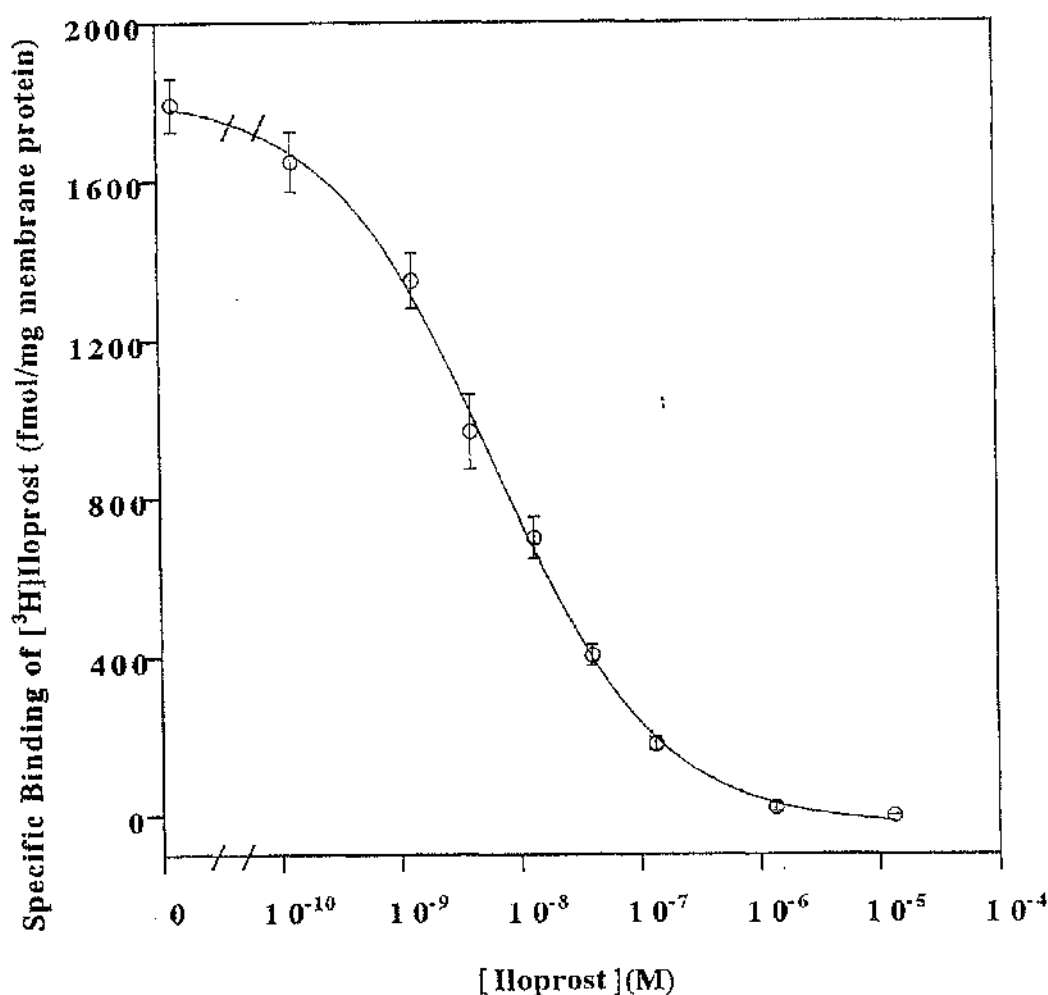


**Figure 3.5 Immunodetection of the FLAG<sup>TM</sup>-tagged human IP prostanoid receptor in transiently and stably transfected HEK293 cells**

**A.** Membranes of mock transfected (lane 1) and FhIPR transiently transfected (lane 2) HEK293 cells were resolved by 10% SDS-PAGE, transferred to nitrocellulose membrane and immunoblotted with M5 anti-FLAG<sup>TM</sup> monoclonal antibody. The predominant immunoreactive protein in lane 2 migrated with an apparent molecular mass of around 45 kDa.

**B.** Membranes of parental HEK293 (lane 1) and clone 13 (lane 2) cells were subjected to the same treatment. M5 immunoreactive proteins ranged from 41 to 61 kDa in clone 13 cells and presumably represent differentially glycosylated forms of FhIPR.

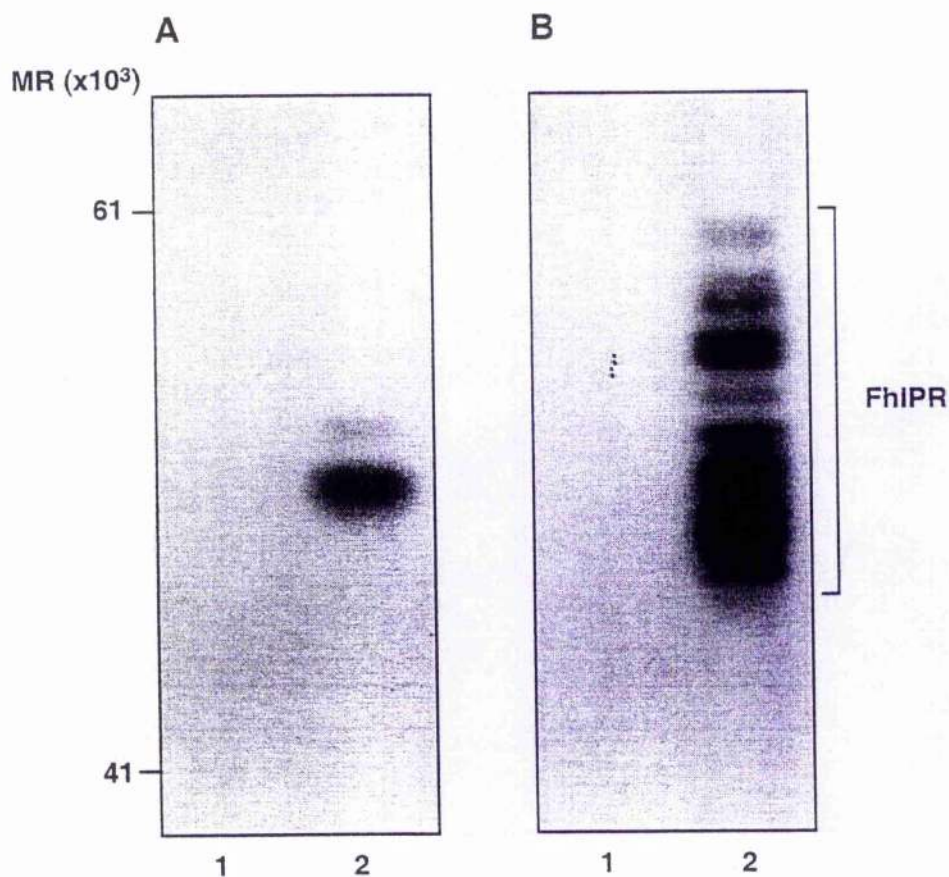


**Figure 3.6 Adenylate cyclase concentration-response curve for iloprost in intact clone 13 cells**

Intact clone 13 cells were assessed for their ability to stimulate adenylate cyclase at various concentrations of iloprost. The results are presented as in Figure 3.2 but expressed as % maximum stimulation (activity at 10  $\mu$ M iloprost treated as 100%). Effective concentration at 50% stimulation ( $EC_{50}$ ) was estimated at  $1.4 \pm 0.3 \times 10^{-10}$  M (mean  $\pm$  SEM; n =,3). This graph is representative of 3 independent experiments performed in triplicate.

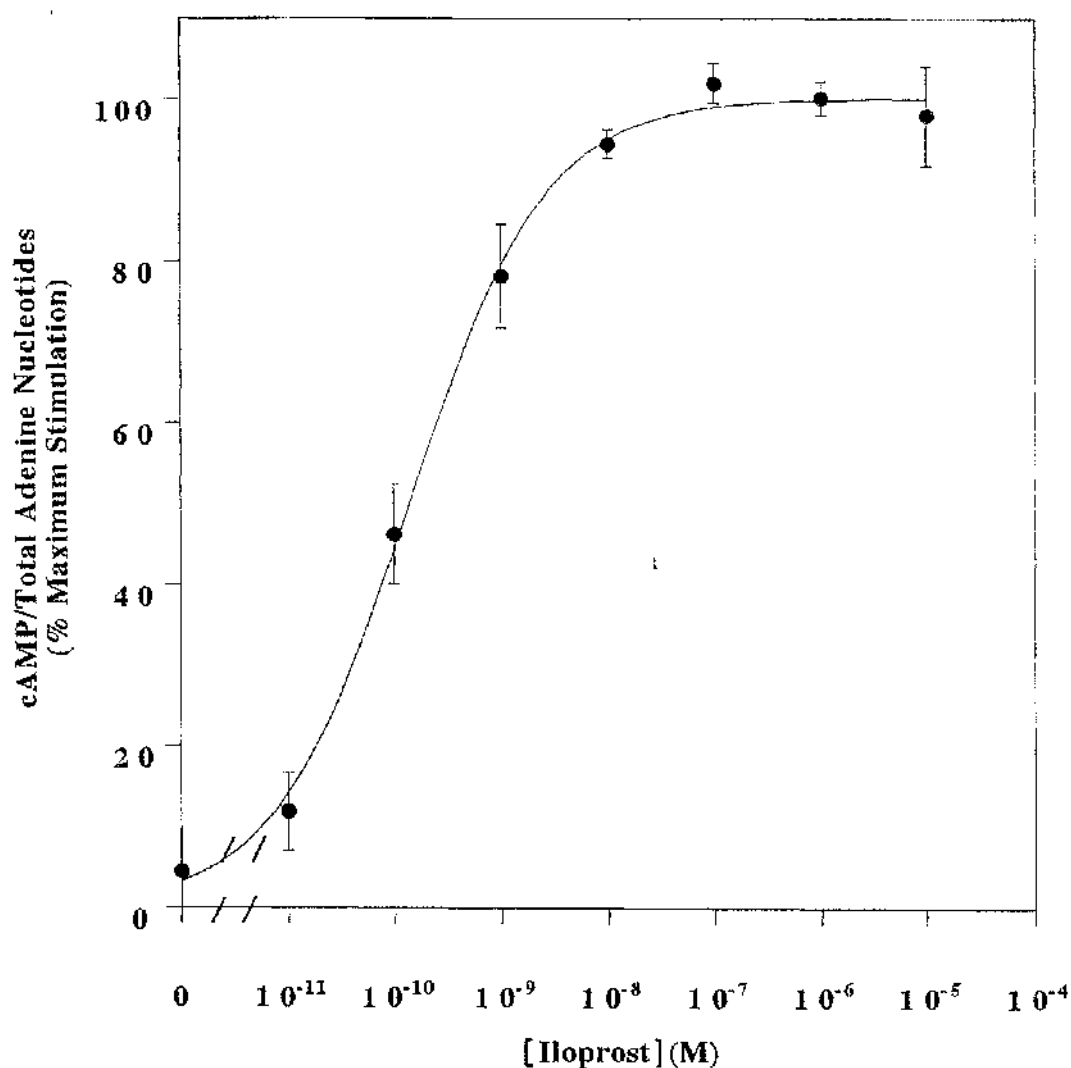
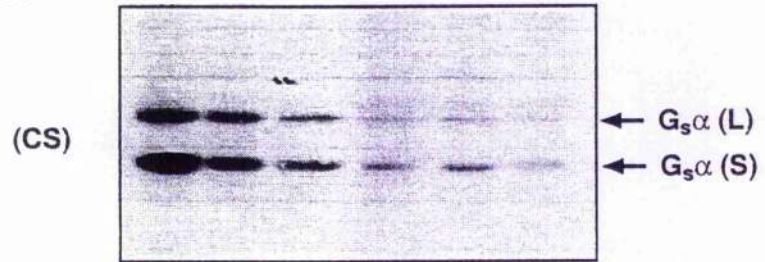


**Figure 3.7 Sustained agonist treatment of clone 13 cells results in downregulation of  $G_s\alpha$  but not  $G_{i1/2}\alpha$  or  $G_{q/11}\alpha$  subunits**

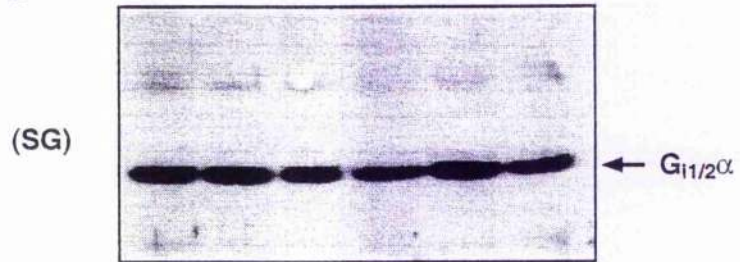
Clone 13 cells were incubated with iloprost (1  $\mu$ M) for 0, 0.5, 2, 4, 8, and 16 h. Membranes prepared from these cells were resolved by 10% SDS-PAGE, transferred to nitrocellulose membrane and immunoblotted using various anti- $G\alpha$  antisera.

- A. Immunoblotting with CS antiserum, specific for the carboxyl-terminal decapeptide of  $G_s\alpha$ , demonstrated a time-dependent downregulation of both the long and short isoforms of  $G_s\alpha$ . Downregulation occurs with just 30 min of iloprost treatment, leaving only trace amount at 16 h.
  
- B. Immunoblotting with SG antiserum, specific for the C-terminal decapeptide of  $G_{i1/2}\alpha$ , did not show any downregulation even after 16 hours of incubation with iloprost.
  
- C. Immunoblotting with CQ antiserum, specific for the C-terminal decapeptide of  $G_{q/11}\alpha$ , also did not show any time-dependent pattern of downregulation by agonist.

**A**



**B**



**C**

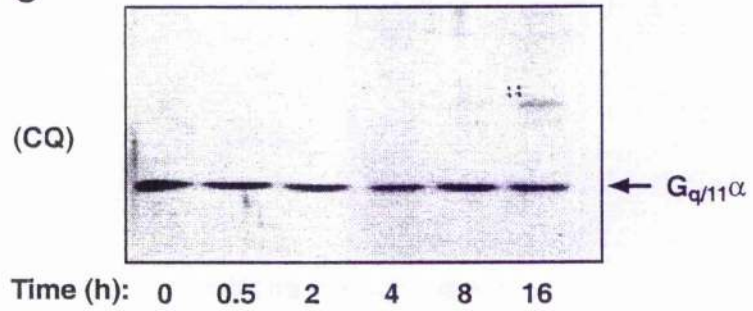


**Figure 3.8** Generation of  $G_{i1}/G_s6\alpha$  chimeric protein

The carboxyl-terminal decapeptides of  $G_{i1}\alpha$  and  $G_s\alpha$  are shown using the single letter representation of the amino acids. The ADP-ribosylation sites for pertussis toxin (cysteine 351) and cholera toxin (arginine 201) are also indicated. The chimeric  $G_{i1}/G_s6\alpha$  protein contains the last 6 residues of  $G_s\alpha$  in place of  $G_{i1}\alpha$ .

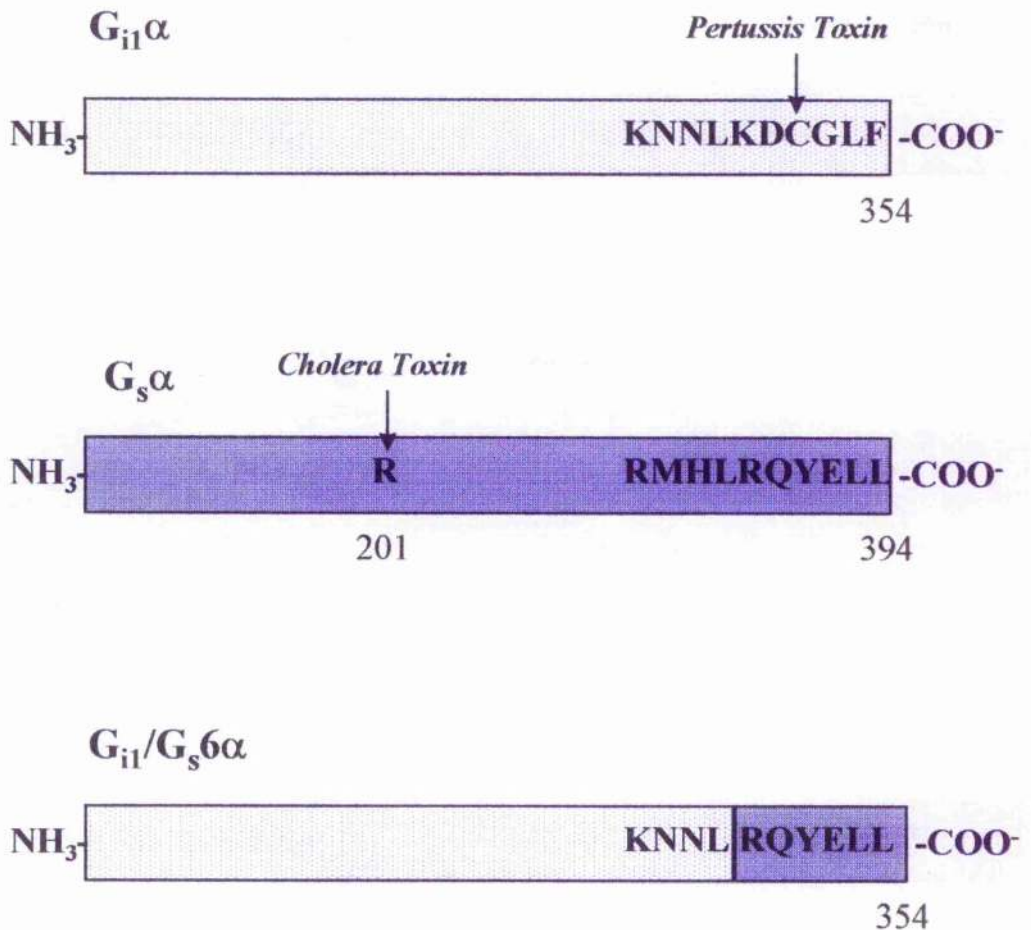
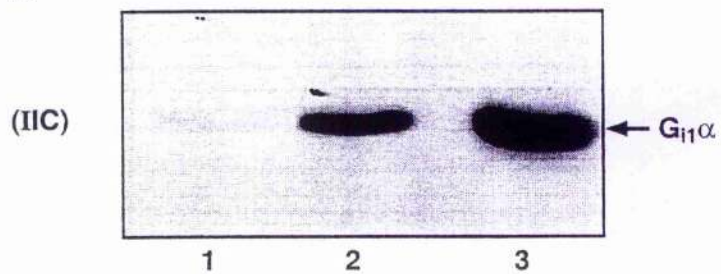


### Figure 3.9 Immunological characterisation of $G_{i1}/G_s6\alpha$ protein

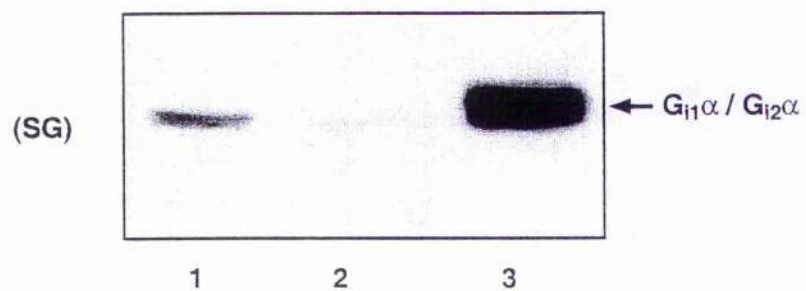
Membranes of COS-7 cells transiently transfected with pcDNA3 (1) or  $G_{i1}/G_s6\alpha$  cDNA (2) were resolved on SDS-PAGE, transferred to nitrocellulose membrane and immunoblotted with various antisera. Membranes of rat brain cortex (3) were used as positive control for  $G_{i1}\alpha$  due to its high endogenous expression.

- A. Antiserum I1C, which recognises an internal domain (159-168 aa) of  $G_{i1}\alpha$ , identified an immunoreactive protein in  $G_{i1}/G_s6\alpha$  transfected cells that co-migrated with authentic  $G_{i1}\alpha$  from rat brain cortex.
- B. Antiserum SG1, which recognises the C-terminal decapeptide of  $G_{i1/2}\alpha$ , fails to identify strong immunoreactivity in mock or  $G_{i1}/G_s6\alpha$  transfected COS-7 cells but detected high levels of  $G_{i1/2}\alpha$  in rat brain cortex.
- C. A polypeptide in  $G_{i1}/G_s6\alpha$  transfected cells together with endogenous  $G_s\alpha$  display immunoreactivity with CS antiserum, which specifically recognises the C-terminal decapeptide of  $G_s\alpha$  (left panel). The same polypeptide together with  $G_{i1}\alpha$  from rat brain cortex also display immunoreactivity with I1C antiserum (right panel). Thus this polypeptide had an internal  $G_{i1}\alpha$  domain but a C-terminal region similar to  $G_s\alpha$  and hence was identified as the  $G_{i1}/G_s6\alpha$  protein.

**A**



**B**



**C**

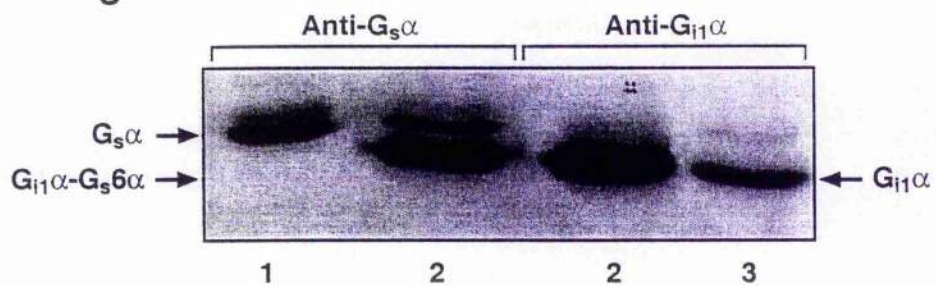


**Figure 3.10 Expression of  $G_{i1}/G_{s6}\alpha$  with FhIPR enhances agonist-stimulated high affinity GTPase activity**

Clone 13 cells were either mock transfected (with pcDNA3) or transiently transfected to express  $G_{i1}\alpha$ ,  $G_{s}\alpha$  or  $G_{i1}/G_{s6}\alpha$ . Parental HEK293 cells were also transiently transfected to express  $G_{i1}/G_{s6}\alpha$ . Membranes from these cells were assessed for basal and iloprost (1  $\mu$ M)-stimulated high affinity GTPase activity. The stimulation produced by iloprost is displayed, and is as follows (mean  $\pm$  SEM pmol/min/mg membrane protein): pcDNA3 ( $2.9 \pm 0.6$ ),  $G_{i1}\alpha$  ( $3.3 \pm 0.3$ ),  $G_{s}\alpha$  ( $3.3 \pm 0.8$ ),  $G_{i1}/G_{s6}\alpha$  ( $10.6 \pm 0.6$ ), and  $G_{i1}/G_{s6}\alpha$  in HEK293 ( $-0.4 \pm 0.3$ ). These data represent 3 independent experiments performed in triplicate.

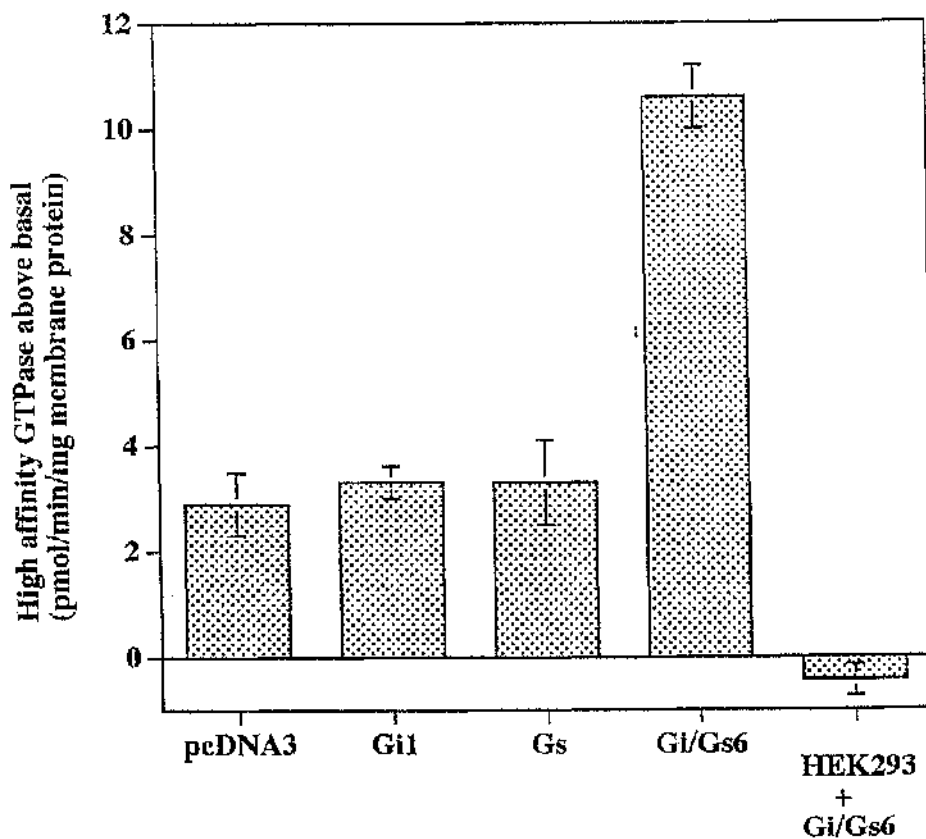


**Figure 3.11 Immunoblot indicating expression levels of  $G_{i1}\alpha$ ,  $G_s\alpha$ , and  $G_{i1}/G_s6\alpha$  in clone 13 cells**

Membranes of clone 13 cells transfected as in Figure 3.10 to express  $G_{i1}/G_s6\alpha$  (1),  $G_{i1}\alpha$  (2) and  $G_s\alpha$  (3) were resolved by 10% SDS-PAGE and immunoblotted with antisera I1C (Figure A) or CS (Figure B).  $G_{i1}/G_s6\alpha$  and  $G_{i1}\alpha$  proteins were expressed to similar levels but  $G_s\alpha$  protein was expressed at less than one third the level of  $G_{i1}/G_s6\alpha$ .

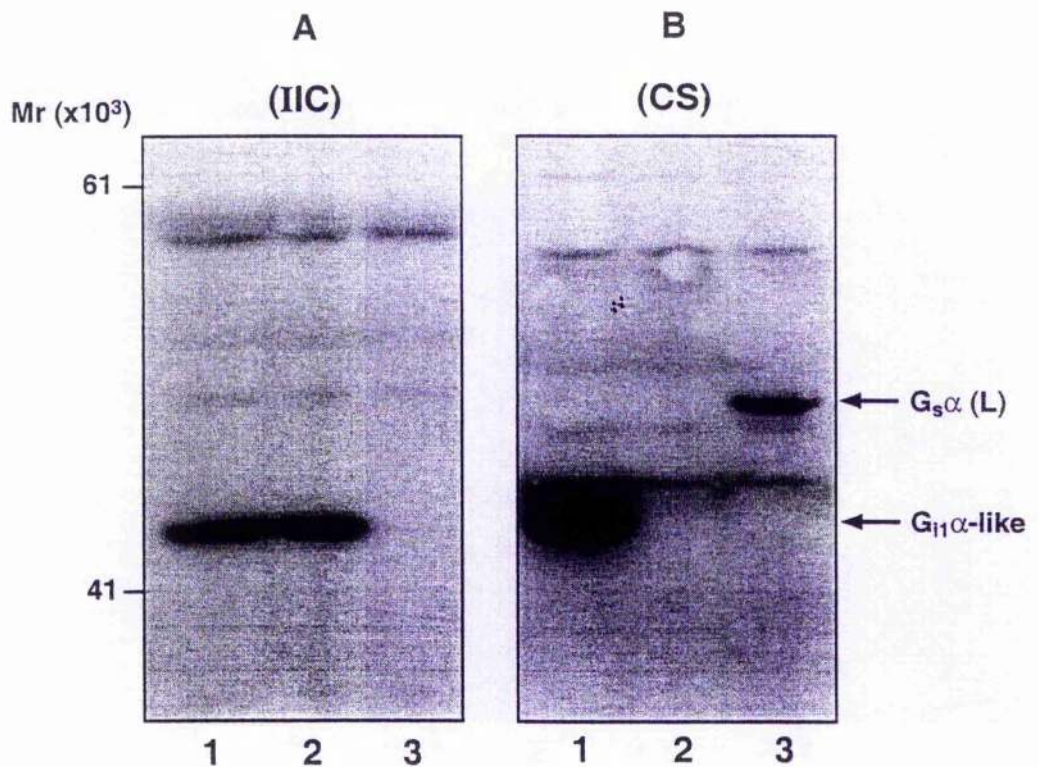


**Figure 3.12 Co-expression of  $G_{i1}/G_s6\alpha$  with FhIPR enhances agonist-stimulated binding of [ $^{35}$ S]GTP $\gamma$ S**

[ $^{35}$ S]GTP $\gamma$ S binding was assessed in membranes of  $G_{i1}/G_s6\alpha$  transfected clone 13 cells or HEK293 cells and also of untransfected clone 13 cells. Non-specific binding was obtained in the presence of 20  $\mu$ M unlabelled GTP $\gamma$ S, while agonist-stimulated binding in the presence of 1  $\mu$ M iloprost. Results are presented as [ $^{35}$ S]GTP $\gamma$ S bound (cpm) per assay (20  $\mu$ g membrane protein). Non-specific binding was similar in all cells but basal values differed slightly between clone 13 and parental HEK293 cells. This graph is a typical representation of 3 experiments performed in triplicate.

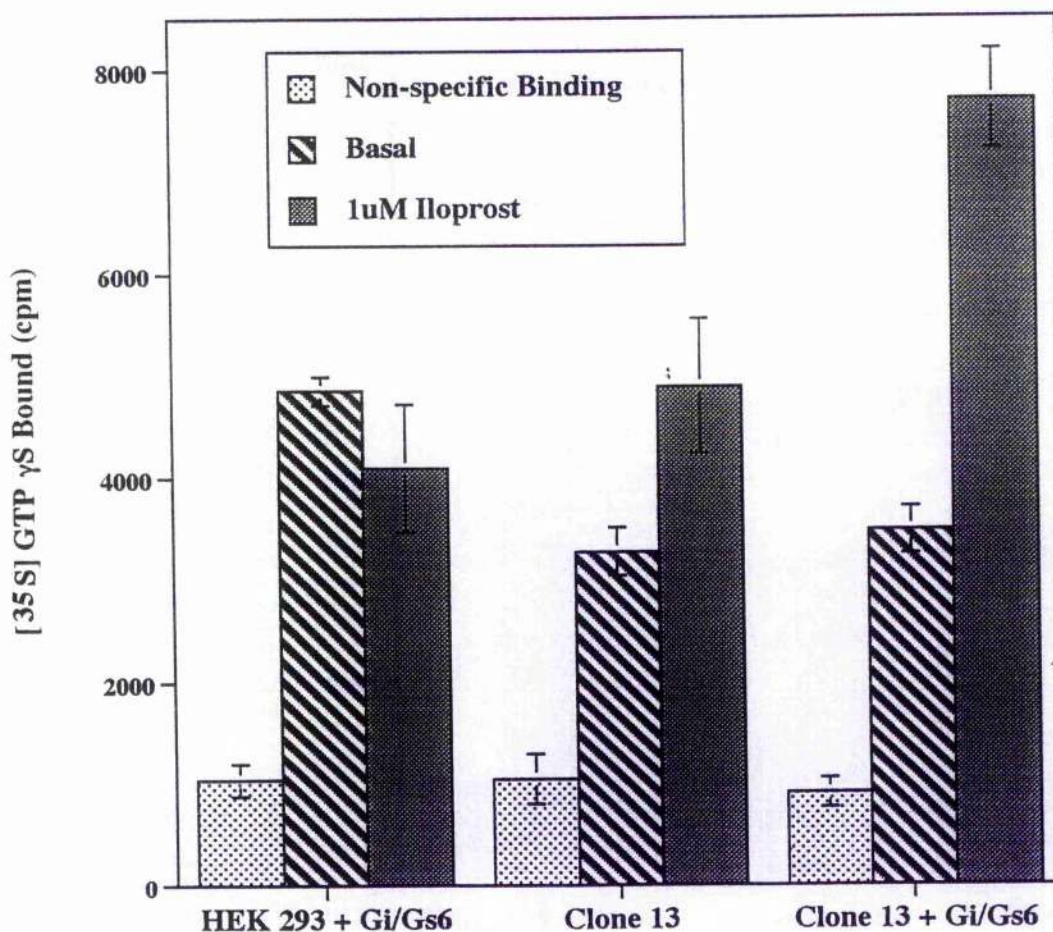


**Figure 3.13 Comparison of the effects of cholera and pertussis toxin on agonist-stimulated high affinity GTPase activity in clone 13 cells**

Clone 13 cells were treated with either vehicle (50% glycerol) or cholera toxin (200 ng/ml, 16 h) or pertussis toxin (25 ng/ml, 16 h) before harvest. Membranes from these cells were then used to measure basal high affinity GTPase activity and its stimulation by iloprost (1- $\mu$ M). Iloprost stimulated activities are displayed and as follows (pmol/min/mg membrane protein): vehicle ( $2.7 \pm 0.4$ ), cholera toxin ( $0.8 \pm 0.5$ ) and pertussis toxin ( $2.7 \pm 0.2$ ). The data represent mean  $\pm$  SEM of at least 3 experiments performed in triplicate.

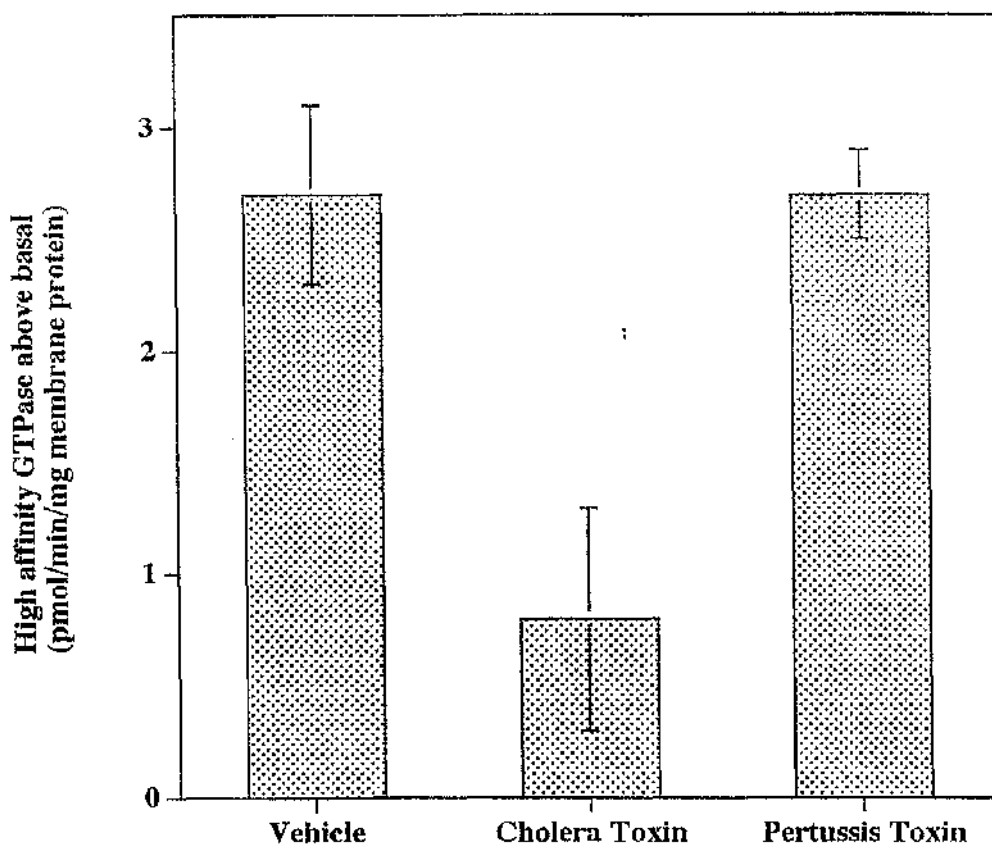


**Figure 3.14 The effects of combined cholera and pertussis toxin treatment on agonist-stimulated [<sup>35</sup>S]GTP<sub>γ</sub>S binding in clone 13 cells transiently expressing various G<sub>α</sub> subunits**

Clone 13 cells were transfected with the various G<sub>α</sub> cDNAs as in Figure 3.10 and treated with a combination of cholera toxin (200 ng/ml) and pertussis toxin (25 ng/ml) for 16 h prior to harvest. Membranes prepared from these and the untreated cells were assessed for their ability to bind [<sup>35</sup>S]GTP<sub>γ</sub>S under basal or iloprost (1 μM) stimulated conditions. The stimulation produced by iloprost is displayed. This graph represents one of three independent experiments performed in triplicate.

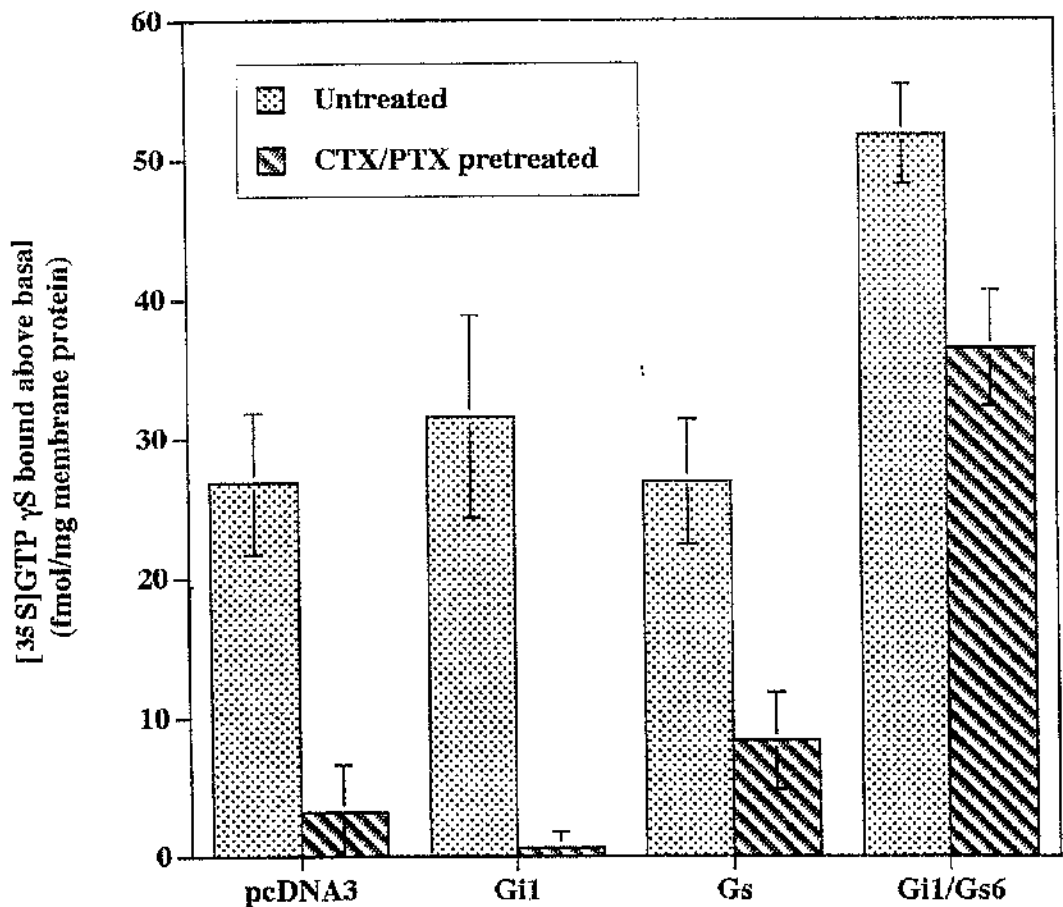


**Figure 3.15 Sustained treatment of clone 13 cells with cholera and pertussis toxin downregulates levels of  $G_s\alpha$  and modifies  $G_i\alpha$**

Membranes from Figure 3.14 were resolved on 10% SDS-PAGE, transferred to nitrocellulose and immunoblotted with either I1C antiserum (Figure A) or CS antiserum (Figure B) to assess the effect of cholera and pertussis toxins on  $G\alpha$  subunits.

- A. Retardation of overexpressed  $G_{i1}\alpha$  protein in SDS-PAGE was observed in the presence of toxins. No noticeable difference was seen in toxin-treated cells overexpressing the  $G_{i1}/G_s6\alpha$  protein.
  
- B. Endogenous levels of  $G_s\alpha$  were downregulated in the presence of toxins in all cells. The levels of  $G_{i1}/G_s6\alpha$  protein were however unaffected.

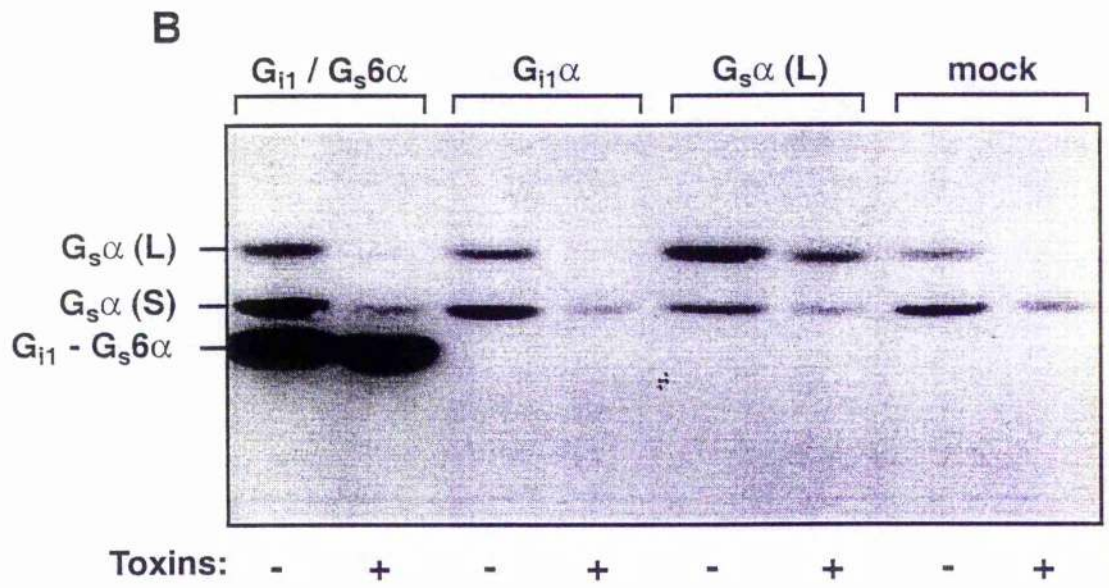
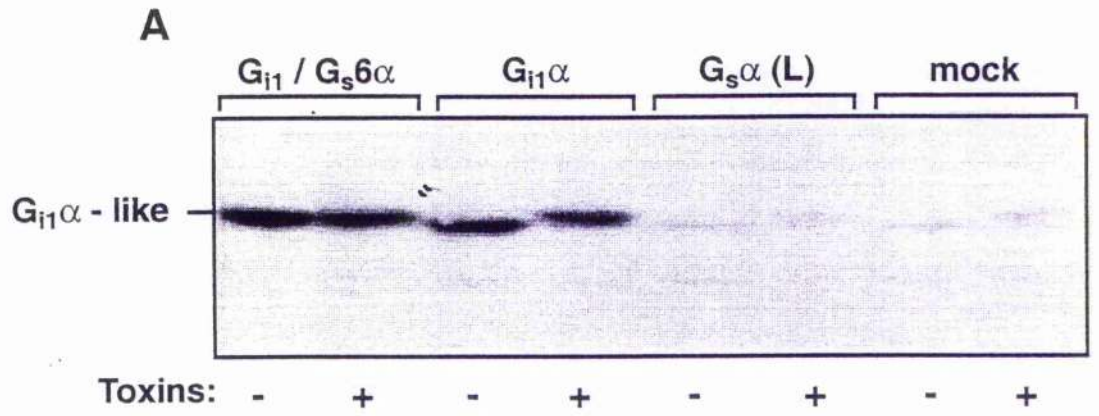
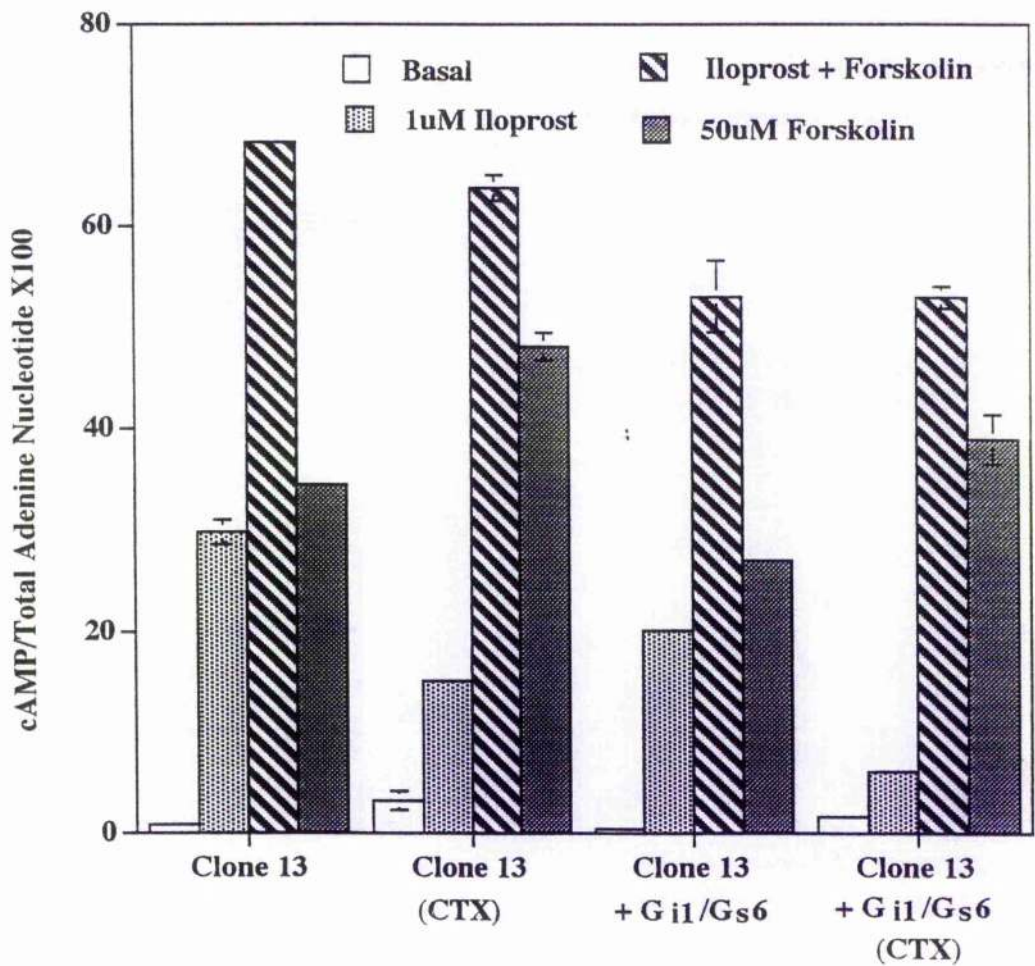


**Figure 3.16 Adenylate cyclase response in cells co-expressing Fh1PR and  $G_{i1}/G_{s6}\alpha$  protein**

$G_{i1}/G_{s6}\alpha$  was transiently transfected into clone 13 cells and their adenylate cyclase activities assessed by stimulation with iloprost (1  $\mu$ M), iloprost (1  $\mu$ M) + forskolin (50  $\mu$ M) or forskolin (50  $\mu$ M). Clone 13 cells were similarly assessed. Cholera toxin (200 ng/ml) was also incubated with both sets of cells for 16 h and their adenylate cyclase response to various activators assessed. This graph is a typical representation of two independent experiments performed in triplicate.



### 3.3 Discussion

#### *The FLAG<sup>TM</sup>-tagged human IP prostanoid receptor is similar to the parental receptor*

Epitope tagging of GPCRs allows easy immunodetection and immunolocalisation. Most often, epitope tagging of receptors is on the N-terminus, as it is extracellular and hence convenient to work with especially in immunocytochemistry. However, the N-terminus may also be involved in ligand binding and N-glycosylation. The hIPR stably expressed in clone 13 cells binds iloprost with both high and low affinity, in accordance with Boie *et al.* (1994) who expressed the parental human IP prostanoid receptor in COS-M6 cells. Their Scatchard analysis showed that [<sup>3</sup>H]iloprost binding to the hIPR conformed to a two-site model with high affinity and low affinity equilibrium dissociation constants of 1 and 44 nM respectively. This is quite similar to the results obtained in this study: high affinity  $K_d = 1.6$  nM; low affinity  $K_d = 11.4$  nM (Figure 3.3), although the accuracy of low affinity values obtained in this study is limited by the concentrations of [<sup>3</sup>H]iloprost used. Furthermore, Smyth *et al.* (1996) expressed a hemagglutinin epitope (YPYDVPDYA) tagged receptor (HAhIPR) and showed similar two-affinity site binding for [<sup>3</sup>H]iloprost (high affinity  $K_d = 0.4$  nM, low affinity  $K_d = 75$  nM). Therefore, the incorporation of FLAG<sup>TM</sup> epitope on the N-terminus of hIPR did not affect the binding affinity of the receptor.

N-glycosylation is usually not affected by epitope tagging, but instead may cause problems for immunodetecting the epitope. N-Glycosylation involved the attachment of oligosaccharides to the amine-group of asparagine residues in the extracellular segments of a GPCR. This modification facilitates the movement of the amino-terminus and extracellular domains of the receptor through the plasma membrane. The processing of N-linked oligosaccharides in the Golgi vesicles is a sequential process of removal and addition of sugar residues, with each asparagine residue modified differently. There are 3 different structures of asparagine-linked oligosaccharides: high mannose, hybrid, and complex. Thus, it is not surprising that N-glycosylated GPCRs are often presented as proteins with

various molecular masses (Figure 3.5B). The immunoblot of HAhIPR was also resolved as a broad complex with molecular mass ranging from 44 to 62 kDa (Smyth *et al.* 1996). The single immunoreactive protein in transiently transfected HEK293 cells (Figure 3.5A) was likely to be unglycosylated or represented a single form of glycosylated receptor. This compared favourably with the expected molecular mass of around 42 kDa for the FLAG<sup>TM</sup>-tagged human IP prostanoid receptor. Deglycosylation of the FhIPR in membranes of clone 13 cells was attempted by incubating with N-glycosidase F (Boehringer Mannheim) but was not successful (data not shown).

Stimulation of adenylate cyclase activity in clone 13 cells by the IP prostanoid receptor agonist iloprost was very robust and rapid. Addition of 0.14 nM iloprost resulted in 50% stimulation of adenylate cyclase activity (Figure 3.6). Furthermore, sustained treatment of clone 13 cells downregulates  $G_s\alpha$  but not  $G_{i1/2}\alpha$  or  $G_{q/11}\alpha$  (Figure 3.7). This conclusively showed that the agonist-occupied FhIPR activates  $G_s\alpha$ . The ability of prostanoid agonists to stimulate adenylate cyclase and downregulate  $G_s\alpha$  selectively was previously shown in NG108-15 neuroblastoma X glioma hybrid cells endogenously expressing the IP prostanoid receptor (McKenzie and Milligan 1990). Although there is evidence that stimulation of IP prostanoid receptor elevates  $IP_3$  level (Namba *et al.* 1994), this was not studied in detail herein. As  $G_{q/11}\alpha$  in clone 13 cells was not downregulated upon sustained iloprost treatment (Figure 3.7C), it is unlikely that elevation of  $IP_3$  is mediated via activation of  $G_q\alpha$  or  $G_{11}\alpha$ . Furthermore, most studies showing the involvement of inositol phosphate production require quite a high concentration of agonist ( $EC_{50} = 43$  nM in HAhIPR; Smyth *et al.* 1996). This is in contrast to the subnanomolar concentrations required for activation of adenylate cyclase. All these observations suggest that  $G\beta\gamma$  complex and not  $G_q\alpha$  subfamily is involved in the activation of phospholipase C. However, as the results in the current study are insufficient and not intended to address this issue, a clear conclusion on this matter cannot be drawn.

### ***Overexpression of chimeric G<sub>11</sub>/G<sub>s</sub>6 $\alpha$ protein resulted in enhanced iloprost stimulated activity***

Chimeric G proteins have been employed extensively to map the functions of specific domains in the G $\alpha$  subunit. In particular, the extreme carboxyl terminus of G $\alpha$  was shown to be essential and even sufficient for transducing signal from the receptor (Conklin *et al.* 1993a; Voyno-Yasenetskaya *et al.* 1994). This was backed up by substantial evidence showing that modification of particular residues in the carboxyl terminus resulted in loss of receptor coupling capacity. This included the pertussis toxin catalysed ADP-ribosylation of a conserved cysteine residue of G<sub>i</sub> $\alpha$  (West *et al.* 1985) and the *unc* mutation (proline 389 to arginine) of G<sub>s</sub> $\alpha$  (Sullivan *et al.* 1987). In contrast, recent studies have shown that the carboxyl terminus may not be the only determinant of receptor coupling and that the coupling domain varies between different receptors and G proteins (Tsu *et al.* 1997; Lee *et al.* 1995). As the interaction between IP prostanoid receptor and G<sub>s</sub> $\alpha$  had not been studied, it was interesting to investigate the activating capacity of a chimeric G<sub>11</sub>/G<sub>s</sub>6 $\alpha$  protein by the receptor.

The results indicate strongly that the IP prostanoid receptor can activate the G<sub>11</sub>/G<sub>s</sub>6 $\alpha$  protein which resulted in enhanced agonist-stimulated GTPase (Figure 3.10) and [<sup>35</sup>S]GTP $\gamma$ S binding (Figure 3.12). This is because activation of the IP prostanoid receptor had never previously shown measurable responses in these assays despite strong activation of adenylate cyclase and sufficiently high expression of receptors, for example in NG108-15 cells (McKenzie and Milligan 1990). While it might be argued that endogenous G<sub>s</sub> $\alpha$  is limiting in these and clone 13 cells, this is unlikely to be true. Overexpression of G<sub>s</sub> $\alpha$  in clone 13 cells did not result in increased agonist-stimulated activity in both assays (Figure 3.10 and 3.14).

The true magnitude of the iloprost-stimulated activity of G<sub>11</sub>/G<sub>s</sub>6 $\alpha$  was finally resolved through the use of cholera and pertussis toxins. Although cholera toxin is probably sufficient to remove endogenous G<sub>s</sub> $\alpha$  coupling with the receptor (Figure

3.13), the use of pertussis toxin would prevent any non-specific interaction with  $G_{i\alpha}$ -like G proteins as shown in some studies (Akam *et al.* 1997). As postulated, the  $G_{i1}/G_{s6\alpha}$  protein was not modified (Figure 3.15A) nor downregulated (Figure 3.15B) by pertussis and cholera toxin treatment. When used in combination, iloprost-stimulated  $GTP\gamma S$  binding activities were abolished in all cells except those transfected with  $G_{i1}/G_{s6\alpha}$  (Figure 3.14). Under these conditions, the remaining agonist-stimulated activity must be derived from activation of  $G_{i1}/G_{s6\alpha}$ .

The high rates of GTP exchange and hydrolysis characteristic of  $G_{i1}\alpha$  were apparently retained in the chimeric  $G_{i1}/G_{s6\alpha}$  protein. In membranes of  $G_{i1}/G_{s6\alpha}$  transiently transfected clone 13 cells, agonist stimulated GTPase activity was at least 3 fold higher while  $GTP\gamma S$  binding was about 2 fold higher than mock transfected clone 13 cells. Although the expression level of  $G_{i1}/G_{s6\alpha}$  protein is relatively high compared to endogenous  $G_{s\alpha}$  (Figure 3.15B), it should be noted that in transient transfection studies, only a small fraction of cells (30 to 40%) would express the protein. Hence, stimulation by iloprost would enable only a fraction of the total receptor to activate the chimeric protein in contrast to activation of endogenous  $G_{s\alpha}$ . The high level of activity is therefore not a result of high  $G_{i1}/G_{s6\alpha}$  expression levels, but rather an intrinsic property of the chimeric G protein. Instead, an even greater signal output might be obtained by a cell line that stably co-expresses both the receptor and the chimeric G protein.

Conklin *et al.* (1993a) were among the first to show that it is possible to switch the signalling output of a receptor by using chimeric G proteins. In that study,  $G_{i\alpha}$ -coupled GPCRs like  $D_2$  dopamine and  $A_1$  adenosine receptors activated PLC by interacting with a  $G_{q\alpha}/G_{i2\alpha}$  chimera. Similarly, Voyno-Yasenetskaya *et al.* (1994) had shown that a  $D_2$  dopamine receptor can activate NHE via a  $G_{i3\alpha}/G_{i2\alpha}$  chimera. Finally, using a series of  $G_{s\alpha}/G_{x\alpha}$  chimeras, Komatsuzaki *et al.* (1997) managed to switch the signalling output of SSTR3 somatostatin receptor from activation of PLC (via  $G_{14\alpha}$  and  $G_{16\alpha}$ ) to activation of adenylate cyclase. In this current study, I was able to show the activation of a

chimeric G protein with high rates of guanine nucleotide activities ( $k_{off}$  and  $k_{cat}$ ) by the IP prostanoid receptor, that would normally activate  $G_{s\alpha}$ , a G protein with intrinsically low guanine nucleotide activities. Therefore, this offers an alternative means to analyse agonist pharmacology at the IP prostanoid receptor. By activating only the chimeric  $G_{i1}/G_{s6\alpha}$  but not full length  $G_{i1\alpha}$ , the IP prostanoid receptor also demonstrated its selective interaction with  $G_{s\alpha}$  via the extreme carboxyl terminus. It remains to be seen how many more  $G_{s\alpha}$ -coupled GPCRs share this characteristic.

## **CHAPTER 4**

# **Comparison of Signal Transduction Efficiency between the Human IP Prostanoid Receptor and the Human IP Prostanoid Receptor- $G_s\alpha$ Fusion Protein**

## CHAPTER 4

# Comparison of Signal Transduction Efficiency between the Human IP Prostanoid Receptor and the Human IP Prostanoid Receptor- $G_s\alpha$ Fusion Protein

### 4.1 Introduction

The human IP prostanoid receptor (hIPR) belongs to the family of prostaglandin receptors that mediate the functions of prostaglandins and thromboxane  $A_2$ . The physiological ligand for the hIPR is  $PGI_2$ , which is also known as prostacyclin. Therefore, the IP prostanoid receptor has also been referred to as the prostacyclin receptor.  $PGI_2$  mediates important physiological functions including inhibition of platelet aggregation and vasodilation, and is also thought to play a role in maintaining vascular homeostasis (Moncada *et al.* 1980). These functions were confirmed in a recent study of mice lacking the IP prostanoid receptor (Murata *et al.* 1997). These knock-out mice also exhibited reduced inflammatory and pain responses, thereby implicating the IP prostanoid receptors in the mediation of inflammatory pain. Indeed, there is also other evidence linking the EP and IP prostanoid receptors with nociception, especially in post trauma and inflammation settings (Bley *et al.* 1998). Therefore, antagonists of IP prostanoid receptors may have real therapeutic applications, and their discovery are high on the agenda of some pharmaceutical companies.

Through secondary messenger studies of endogenous hIPR in human platelets (Schafer *et al.* 1979) and co-expression of the receptor with the cystic fibrosis conductance regulator (cAMP-activated  $Cl^-$  channel) in *Xenopus oocytes* (Boie *et al.* 1994), the receptor was shown to couple to  $G_s\alpha$  subunit. Most functional receptor studies therefore utilised assays for cAMP, the second messenger produced by adenylate cyclase upon binding of activated  $G_s\alpha$  (Adie *et*

*et al.* 1992; Kedzie *et al.* 1998). This assay takes advantage of the considerable signal amplification in the signalling cascade, and is particularly sensitive, as even picomolar of activated  $G_s\alpha$  can stimulate adenylate cyclase (Bourne *et al.* 1990). Constitutively activated  $G_s\alpha$  can give rise to elevated adenylate cyclase activity, for example in a  $G_s\alpha(L)$  mutant where glutamine 227 was mutated to leucine (Q227L) in the GTPase domain (Masters *et al.* 1989). This mutation diminished the GTP hydrolysing ability of  $G_s\alpha$ , and hence resulted in a failure of the mutant to "switch-off" its activation of adenylate cyclase. Pretreatment of  $G_s\alpha$  with cholera toxin also gave the same effect, when arginine 201, located in the GTPase domain, was ADP-ribosylated (Cassel and Selinger 1977).  $G_s\alpha$  coupled GPCRs that are constitutively active, for example a mutant  $\beta_2$ -adrenergic receptor (Cotecchia *et al.* 1990), can also elevate cellular cAMP levels by constantly stimulating the endogenous pool of  $G_s\alpha$ .

Previous studies have shown that the levels of receptor, G protein, and effector affect the amplitude of the transduced signal (Kenakin 1997). In neuroblastoma X glioma hybrid NG108-15 cells transfected to express high and low levels of the  $\beta_2$ -adrenergic receptor, a series of  $\beta$ -adrenergic agonists displayed higher intrinsic activity and lower  $EC_{50}$  values (from assay of membrane adenylate cyclase activity) in a clone expressing a high level of the receptor (MacEwan *et al.* 1995). Similarly, when  $G_s\alpha$  in NG108-15 cells was reduced by 35% upon treatment with ethanol (100 mM) for 48 hours, the ability of  $A_2$  adenosine and IP prostanoid receptors to stimulate adenylate cyclase were also reduced by ~30% (Mochly-Rosen *et al.* 1988). Finally, the cellular level of effector was also found to have a direct impact on signalling efficacy. Using the same NG108-15 cell line discussed above, MacEwan *et al.* (1996) co-expressed adenylate cyclase type II and  $\beta_2$ -adrenergic receptor to different levels and found the level of adenylate cyclase to be the limiting component for receptor stimulated adenylate cyclase activity. Therefore, agonist efficacy in cellular systems may vary between cell lines due to differences in the levels and ratios of the signalling components. However, an unbiased system of categorising receptor acting

compounds into full agonist, partial agonist, or neutral antagonist is currently not possible.

The assay of agonist function at the level of G protein will remove one component of the cascade that interferes with proper interpretation of agonist activity. However, for various reasons mentioned in the previous chapter, there are numerous obstacles to utilise assays that directly detect  $G_s\alpha$  activation by an agonist occupied GPCR. Interestingly, by using a chimeric G protein ( $G_{i1}/G_s\delta\alpha$ ), robust agonist stimulated GTP exchange and hydrolysis by a  $G_s\alpha$  coupled GPCR has been observed (Chapter 3 of this thesis). This offered a potential method to assay agonist activity directly at the level of the G protein. Despite this advantage, the chimeric G protein approach still fails to address an important parameter in signalling: the stoichiometry of receptor and G protein (Kenakin 1997). Through the use of a HEK293 clone stably expressing the Fh1PR, the level of receptor expressed was relatively constant and could be determined by [ $^3$ H]iloprost binding. However, as the chimeric  $G_{i1}/G_s\delta\alpha$  protein was transiently transfected into these cells, its expression level will inevitably vary between different transfections. Only very crude determination of its expression level could be performed, mainly via immunoblot comparison with known amount of G proteins.

A rather unusual approach to enhance receptor-transducer interaction was shown by Bertin *et al.* (1994) when they fused the amino terminus of  $G_s\alpha$  to the carboxyl terminus of  $\beta_2$ -adrenergic receptor, forming a receptor- $G\alpha$  fusion protein  $\beta_2AR-G_s\alpha$ . After transfecting into S49 lymphoma  $cyc^-$  cells a cDNA encoding this fusion protein, they were able to restore the defective activation of adenylate cyclase by  $\beta_2$ -adrenergic receptor. Since these cells lack endogenous  $G_s\alpha$  subunits, the adenylate cyclase activity must have derived from the receptor-fused  $G_s\alpha$ , indicating the functionality of the G protein even when covalently linked to the receptor. Moreover, the agonist-dependent activation of adenylate cyclase was more potent and productive in the  $\beta_2AR-G_s\alpha$  transfected S49  $cyc^-$  cells than in wild type S49 cells, thus leading to the conclusion that the covalent link between receptor and  $G_s\alpha$  may increase signalling efficiency over freely interacting

components (Bertin *et al.* 1994). This result must however be treated with caution, as the overall level of  $\beta_2$ -adrenergic receptor in  $\beta_2$ AR- $G_s\alpha$  transfected S49 cyc cells was higher than in wild type S49 cells.

A GPCR- $G\alpha$  fusion protein was also studied in yeast cells when Medici *et al.* (1997) expressed a fusion protein between the  $\alpha$ -factor receptor (Ste2) and the  $G\alpha$  subunit (Gpa1) into *Saccharomyces cerevisiae* devoid of endogenous STE2 and GPA1 genes. In GPA1 gene deleted yeast cells, the free  $G\beta\gamma$  complex constitutively activates the pheromone response pathway which leads to growth inhibition, and finally lethality in haploid cells. Medici *et al.* (1997) observed that the fusion protein Ste2-Gpa1, when transformed into Gpa1 deficient yeast cells, can complement efficiently the deletion of the GPA1 gene. Thus the fusion protein was able to function as normal Gpa1 by binding  $G\beta\gamma$  complex, and hence allowed normal growth to resume. Moreover when they transformed the Ste2-Gpa1 protein into cells devoid of endogenous Ste2 receptor, they found that these cells responded to  $\alpha$ -factor inhibition of growth. Therefore, the fusion protein was also able to function as a Ste2 receptor (Medici *et al.* 1997).

All  $G\alpha$  subunits are localised to the plasma membrane by post-translational modifications including palmitoylation and/or myristoylation, at sites within their amino terminus (Wedegaertner *et al.* 1995). These acylations may also play a role in interactions between the  $G\alpha$  subunit and the receptor and  $G\beta\gamma$  complex (Wedegaertner *et al.* 1993). Hence, acylation-deficient mutants usually result in reduced association with the plasma membrane. Furthermore, co-expression of a pertussis-toxin resistant and acylation-deficient  $G_{i1}\alpha$  (C3S/C351G) with the  $\alpha_{2A}$ -adrenergic receptor in COS cells failed to result in functional interactions (Wise *et al.* 1997a). However, it was unclear whether this was due to improper targeting, or altered receptor and/or  $G\beta\gamma$  interactions of the mutant  $G_{i1}\alpha$ . This problem was solved when Wise and Milligan (1997b) constructed and expressed a fusion protein between the  $\alpha_{2A}$ -adrenergic receptor and the acylation-deficient  $G_{i1}\alpha$  in COS cells, and managed to rescue the interactions between the receptor and mutant G protein. The GPCR- $G\alpha$  fusion method therefore ensures co-targeting of

G $\alpha$  with the receptor, and enables proper assessment of the capacity of receptor and transducer to interact. This is analogous to in-vitro reconstitution experiments, but much simpler and more direct.

The usefulness of receptor-G-protein fusions to detect subtle differences in G $\alpha$  protein function was recently exploited by Seifert *et al.* (1998a). The  $\beta_2$ -adrenergic receptor was linked to the short (G $_s\alpha$ (S)) and long (G $_s\alpha$ (L)) splice variants of G $_s\alpha$ , and expressed in insect Sf9 cells. The two splice variants differ by a stretch of 15 amino acids located at position 72 of the polypeptide, with an exchange of glutamine for aspartate in G $_s\alpha$ (L). Although G $_s\alpha$  splice variants are differentially expressed in various tissues, and their levels changed during various physiological and pathological processes, the precise cellular role of each splice variant is not clear. This difficulty is compounded by the strong similarity between the splice variants, and hence their interactions with receptor are influenced strongly by their relative expression levels (Kenakin 1996).

By expressing the fusion proteins  $\beta_2$ AR-G $_s\alpha$ (S) and  $\beta_2$ AR-G $_s\alpha$ (L) in Sf9 cells, which have a very low level of endogenous G $_s\alpha$ , Seifert *et al.* (1998a) were able to show that  $\beta_2$ AR-G $_s\alpha$ (L) has low basal adenylate cyclase but high basal GTP hydrolysis activity compared to  $\beta_2$ AR-G $_s\alpha$ (S). Furthermore, when stimulated by isoprenaline, a full agonist,  $\beta_2$ AR-G $_s\alpha$ (L) gave a large output of high-affinity GTPase compared to co-expression of  $\beta_2$  receptor and G $_s\alpha$ (L). The efficacy and potency of partial agonists were also found to be significantly higher for the  $\beta_2$ AR-G $_s\alpha$ (L) fusion protein than  $\beta_2$ AR-G $_s\alpha$ (S). Finally, a study of guanine nucleotide affinity between the two fusion proteins showed that  $\beta_2$ AR-G $_s\alpha$ (L) had lower GDP affinity than the short form, and hence may be more often guanine nucleotide free.

These studies elucidate the substantial benefits in receptor-G $\alpha$  fusion constructs, especially in the enhancement of G $_s\alpha$  activation to a point where traditional assays for G protein activation can be used. Furthermore, the level of expressed G $\alpha$  can be accurately quantified, and the ratio of receptor and G $\alpha$

constrained to 1:1 when endogenous  $G\alpha$  can be uncoupled from the receptor. While the Sf9 cells seem to be ideal for  $G_s\alpha$  coupled GPCR work, it is not possible to select for stably expressing clones of these cells, and hence expression level of the fusion protein will vary between transfections. Furthermore, the pattern of protein N-glycosylation had been shown to be different from that observed in vertebrate cells and is a major limitation of the baculovirus-insect cell expression system (Jarvis *et al.* 1998).

This study therefore proposed to construct a fusion protein between the FLAG<sup>TM</sup> epitope tagged human IP prostanoid receptor and its cognate  $G\alpha$ , generating a protein known as FhIPR- $G_s\alpha$ . HEK293 clones stably expressing this protein were then selected and characterised. Agonist stimulated activation of G protein was then assessed and compared with HEK293 clone 13 cells which stably express FhIPR. A comparison of the signal transduction efficiency between the freely interacting receptor/ $G\alpha$  and the covalently linked receptor- $G\alpha$  could therefore be made.

## 4.2 Results

### ***Construction of IP prostanoid receptor-G<sub>s</sub>α fusion cDNA***

The cDNA encoding the FLAG<sup>TM</sup>-tagged IP prostanoid receptor fused with G<sub>s</sub>α was constructed as described in Section 2.3.9 A. The stop codon in FhIPR cDNA was removed by an antisense primer that also encodes a *Xho*I restriction site. In the meantime, the 5' and 3' ends of G<sub>s</sub>α(L)(HA) cDNA were engineered with *Xho*I and *Xba*I sites respectively, which allowed the G<sub>s</sub>α(L)(HA) cDNA to be inserted 3' to the FhIPR (in pcDNA3), forming a continuous open reading frame. Figure 4.1 give a schematic representation of the FhIPR-G<sub>s</sub>α fusion cDNA and the protein that it encodes.

The receptor-Gα ligated cDNA was transformed into DH5α *E. coli* and clones were picked from the agar plate after overnight incubation. These were screened for the presence of FhIPR and G<sub>s</sub>α cDNAs by digesting with *Hind*III and *Xba*I (*Bam*HI was not used as it is also found in G<sub>s</sub>α cDNA). Figure 4.2A showed that clones S1 and S2 contained a digested fragment that migrates in 1% agarose gel at the combined length of FhIPR and G<sub>s</sub>α cDNAs (2.4 kilobases). Further digestion of clones S1 and S2 DNAs by *Xho*I and *Xba*I gave a 1.2 kilobase fragment, which approximates the mass of G<sub>s</sub>α cDNA. Thus, both clones S1 and S2 contained the receptor-Gα fusion cDNA. Clone S1 DNA was subsequently sent for DNA sequencing, which confirmed the sequence identity of both the IP prostanoid receptor and G<sub>s</sub>α. This DNA was then used for transfection studies.

### ***Characterisation of HEK293 clones stably expressing the FhIPR-G<sub>s</sub>α fusion protein***

The problem of low expression levels was again encountered in transient transfection of the FhIPR-G<sub>s</sub>α cDNA in HEK293 cells. Geneticin G-418 resistant clones were thus selected and expanded. Three clones (clones 41, 43 and 44) were selected for further characterisation. Their expression levels were compared

with clone 13 cells (stably expressing the FhIPR) and parental HEK293 cells. Of the three, clone 44 expressed the highest level of receptor ( $B_{\max} = 1356 \pm 143$  fmol/mg membrane protein;  $n=5$ ) when determined by [ $^3\text{H}$ ]iloprost binding studies ( $\sim 10$  nM) (Figure 4.3). Furthermore, it exhibited a relatively high level of iloprost-stimulated adenylylate cyclase activity (Figure 4.4) and was therefore selected for further studies.

Unlabelled iloprost displaced [ $^3\text{H}$ ]iloprost (3.4 nM) specifically bound to membranes of clone 44 cells in a concentration-dependent manner, with  $IC_{50}$  of  $4.8 \pm 0.5$  nM (Figure 4.5;  $n = 3$ ). Applying the formalism of DeBlasi *et al.* (1989),  $K_d$  was estimated at  $1.4 \pm 0.6$  nM. This value indicates that the iloprost binding affinity in the fusion protein is not significantly different from the isolated receptor ( $K_d = 2.7 \pm 0.8$  nM) (unpaired t-test  $p = 0.09$ ;  $n=3$ ). However, the slope of the displacement curve in clone 44 cells is less shallow (Hill coefficient =  $0.86 \pm 0.07$ ) than clone 13 cells (Hill coefficient =  $0.64 \pm 0.05$ ). This suggests that the proportion of high-affinity binding sites is higher in clone 44 than clone 13 cells.

Immunodetection of the FhIPR- $G_{s\alpha}$  fusion protein was successful with both M5 anti-FLAG<sup>TM</sup> and CS antibodies. Figure 4.6A clearly indicates the presence of a FLAG<sup>TM</sup>-tagged polypeptide migrating at the 89 kDa mark in FhIPR- $G_{s\alpha}$  expressing cells (lane 1) which was not found in cells stably expressing the FLAG<sup>TM</sup>-tagged receptor (lane 2). Instead, the differentially glycosylated forms of FhIPR were seen in membranes from these cells. The same 89 kDa polypeptide in lane 1 immunoreacted with CS antiserum (Figure 4.6B) which is specific for the carboxyl-terminal decapeptide of  $G_{s\alpha}$ . Since both the amino- and carboxyl-terminal domains of the fusion protein were shown to interact with the antisera, the FhIPR- $G_{s\alpha}$  protein was thus correctly expressed.

A comparison of the effect of sustained agonist treatment on clone 44 and clone 13 cells were made (Figure 4.7). Pretreatment with iloprost (1  $\mu\text{M}$ ) resulted in distinct downregulation of both the short and the long isoforms of endogenous  $G_{s\alpha}$  in both clones after 2 hours of incubation (Figure 4.7A). These results

demonstrated that agonist stimulation of FhIPR-G<sub>s</sub>α protein in clone 44 cells can also activate endogenous G<sub>s</sub>α. As the CS antiserum was shown to immunoreact with FhIPR-G<sub>s</sub>α fusion protein, it can thus be used to monitor the effect of agonist treatment on the fusion protein. As observed in the immunoblot, FhIPR-G<sub>s</sub>α was not downregulated by iloprost pretreatment, even up to 16 hours. This was confirmed by immunoblotting for the FLAG<sup>TM</sup> epitope, which showed consistent levels of the fusion protein and even a slightly enhanced expression at the longer times of iloprost treatment (Figure 4.7B). However, the IP prostanoid receptor was slightly downregulated after 2 hours pretreatment, with signs of recovery at 16 hours of incubation with iloprost. No discernible time-dependent pattern of agonist mediated downregulation was observed for the G<sub>11/2</sub>α (Figure 4.7C) or G<sub>q/11</sub>α (Figure 4.7D) subunits in either clone.

***Clone 44 exhibits enhanced agonist-stimulated GTP hydrolysis and GTP exchange functions when compared to clone 13***

Clone 44 cells were assessed for iloprost (1 μM) stimulated high affinity GTPase activity according to Section 2.4.3. When it was compared to clone 13 cells, membranes of clone 44 cells exhibited marked elevation of agonist-stimulated GTP hydrolysis (unpaired t-test p<0.05; n=5) (Figure 4.8). As it is possible that the overall level of G<sub>s</sub>α in clone 44 is higher than clone 13 due to expression of the FhIPR-G<sub>s</sub>α construct, clone 13 cells were transiently transfected with a cDNA encoding G<sub>s</sub>α(L)(HA) and reassessed for iloprost-stimulated GTPase activity. G<sub>s</sub>α(L)(HA) was overexpressed to a sufficiently high level (Figure 4.9) but high affinity GTPase results showed no discernible difference in the level of agonist-driven GTPase activity (Figure 4.8). Therefore, elevated agonist-stimulated GTP hydrolysis activity in clone 44 versus clone 13 cells cannot be attributed to the higher levels of G<sub>s</sub>α.

The high affinity GTPase assay monitors both the activation (GTP exchange) and termination (GTP hydrolysis) of Gα. To define exactly which step of Gα activity was enhanced in clone 44 cells, a [<sup>35</sup>S]GTPγS binding assay was

employed. Membranes in Figure 4.8 were reassessed using this assay, utilising iloprost (1  $\mu$ M) to drive the exchange of guanine nucleotides (Figure 4.10). Agonist-driven [ $^{35}$ S]GTP $\gamma$ S binding in clone 44 cells ( $226.5\% \pm 8.7$ ) was more than double that of clone 13 cells, which correlated well with results obtained in the GTPase assay. Overexpression of G $_{s\alpha}$ (L)(HA) in clone 13 cells again did not alter agonist-stimulated binding of [ $^{35}$ S]GTP $\gamma$ S. These results indicate that the elevated G $\alpha$  activity in clone 44 cells is also a result of enhanced GTP exchange. Although there is a direct correlation between the levels of receptor expression and agonist-activated G $\alpha$  activity, this is unlikely to account for the greater activity of clone 44 versus clone 13 cells. This is because clone 44 cells express FhIPR-G $_{s\alpha}$  at about 1.4 pmol/mg of membrane protein, which is less than half of the IP prostanoid receptor level ( $\sim 3$  pmol/mg) expressed in clone 13 cells. Therefore, an obvious reason for the enhanced level of activity in both the GTPase and [ $^{35}$ S]GTP $\gamma$ S binding assays must be the expression of receptor-G $\alpha$  fusion proteins in clone 44 cells.

#### ***The effect of cholera and pertussis toxins on clone 44 cells***

Treatment with cholera toxin but not pertussis toxin was previously shown to abolish agonist-stimulated GTPase activity in clone 13 cells (Chapter 3). This is due to the ADP-ribosylation of arginine 201 in G $_{s\alpha}$ , catalysed by cholera toxin, that results in diminished GTP hydrolysis capacity (Cassel and Selinger 1977). As the fusion protein contains a receptor-linked G $_{s\alpha}$  which is both functional and exhibits enhanced activity, it was of interest to examine whether it also acted as a substrate for cholera toxin.

Cells of clone 44 were thus incubated with cholera toxin (200 ng/ml) or pertussis toxin (25 ng/ml) for 16 h prior to harvest. Membranes from these cells were assessed for iloprost-stimulated GTPase activity. Indeed, treatment with cholera toxin but not pertussis toxin reduced the high level of agonist-activated G $\alpha$  activity in clone 44 cells (Figure 4.11). The level of activity in the cholera toxin treated cells ( $0.9 \pm 0.4$  pmol/min/mg membrane protein) is as low as that of similarly treated clone 13 cells ( $0.8 \pm 0.5$  pmol/min/mg), indicating almost

complete abolishment of  $G_s\alpha$  activity. This is an indirect evidence that the receptor-linked  $G_s\alpha$  can be ADP-ribosylated by cholera toxin, which diminish its GTP hydrolysis function. A direct demonstration of this event was attempted using [ $^{32}\text{P}$ ]NAD as co-factor but was unsuccessful due to the non-specific ADP-ribosylation of proteins that co-migrated with FhIPR- $G_s\alpha$  in SDS-PAGE (results not shown).

A rather different scenario was observed when membranes of the toxin-treated clone 44 cells were assessed for agonist-driven GTP exchange function. Pretreatment with cholera toxin reduced the high level of iloprost-stimulated [ $^{35}\text{S}$ ]GTP $\gamma$ S binding in clone 44 cells, but not completely as in the similarly treated clone 13 cells (Figure 4.12). This is in sharp contrast to that observed in the GTPase assay where there is almost complete abolishment of  $G_s\alpha$  activity (Figure 4.11). The similar reduction of [ $^{35}\text{S}$ ]GTP $\gamma$ S bound in cholera toxin-treated clone 44 cells ( $86.7\% \pm 18.6$ ) and clone 13 cells ( $78.4\% \pm 16.6$ ) (Figure 4.12), may however provide a clue to the cholera toxin resistance of clone 44 cells.

Although ADP-ribosylated  $G_s\alpha$  has a diminished GTPase function, no study had been done to assess its GTP exchange capability. This is partly due to the rapid degradation of ADP-ribosylated  $G_s\alpha$  (Chang and Bourne 1989) and the presumed loss of agonist-stimulated exchange function in these proteins. However, in the fusion protein construct, the receptor-linked  $G_s\alpha$  may not be degraded as rapidly as endogenous  $G_s\alpha$ . Indeed, immunoblots with CS antiserum demonstrated the continued presence of the fusion protein despite the rapid loss of endogenous  $G_s\alpha$  in membranes of cholera toxin-treated clone 44 cells (Figure 4.13). It is therefore possible that ADP-ribosylated FhIPR- $G_s\alpha$  protein maintains the capability to exchange guanine nucleotide in response to agonist, despite a diminished GTP hydrolysis function. This also highlights the dual role of cholera toxin in affecting  $G_s\alpha$  functions: catalysing the ADP-ribosylation process (which reduces GTPase activity) and subsequently enhancing the degradation (which reduced [ $^{35}\text{S}$ ]GTP $\gamma$ S bound). Reduction of [ $^{35}\text{S}$ ]GTP $\gamma$ S bound in both clone 13

and clone 44 cells upon cholera toxin treatment is therefore attributed solely to the rapid degradation of endogenous  $G_{s\alpha}$ .

### ***Analysis of secondary effector signalling in clone 44 cells***

HEK293 clones stably expressing the FhIPR- $G_{s\alpha}$  were shown to elevate the production of cAMP in the presence of iloprost (Figure 4.4). In order to compare the kinetics of adenylyate cyclase activation by receptor- $G_{\alpha}$  protein versus the isolated receptor, the level of cAMP production in intact clone 44 and clone 13 cells was monitored over time. The cells were seeded into 24 well plate and incubated overnight with [ $^3$ H]adenine at 0.5  $\mu$ Ci per well. A maximally-effective concentration of iloprost (1  $\mu$ M) and vehicle (assay medium) were added to the cells and incubated for various times up to 45 minutes. The reaction was terminated on ice and stop solution added at 0.5 ml per well. Separation of the adenine nucleotides was according to Section 2.4.2.

Results obtained show that the agonist-stimulated generation of cAMP proceed in a seemingly linear fashion for up to 45 minutes in clone 13 cells, but only for 20 minutes in clone 44 cells (Figure 4.14). Thus it appeared that the FhIPR- $G_{s\alpha}$  protein was desensitised faster than the FhIPR. The basal level of cAMP in both clones was similar and did not increase with time (less than 1% of total adenine nucleotides), and hence provides no evidence of significant constitutive activity. As adenylyate cyclase activity in clone 44 cells appeared to wane after 20 minutes of agonist stimulation, it was decided that further assays of adenylyate cyclase activity should not proceed beyond this incubation time. The dose-dependent effect of iloprost to stimulate cAMP production in clone 44 cells was assessed and compared with clone 13 cells (Figure 4.15). It was found that the  $EC_{50}$  of iloprost to stimulate adenylyate cyclase in clone 44 cells ( $1.1 \pm 0.3 \times 10^{-10}$  M; n=3) was not significantly different from clone 13 cells ( $EC_{50} = 1.4 \pm 0.3 \times 10^{-10}$  M; n=3).

To investigate the secondary effector signalling potential of the FhIPR- $G_{s\alpha}$  fusion protein, it was essential to remove endogenous  $G_{s\alpha}$  to minimise its

interaction with adenylate cyclase. Taking advantage of the earlier observation that cholera toxin-treated clone 44 cells demonstrated enhance degradation of endogenous  $G_s\alpha$  but not FhIPR- $G_s\alpha$  protein (Figure 4.13), clone 13 and clone 44 cells were similarly treated before assessing their adenylate cyclase response. Treatment with cholera toxin reduced the level of iloprost-stimulated cAMP production substantially in clone 13 cells (Figure 4.16). This correlated with the distinct downregulation of endogenous levels of  $G_s\alpha$  in these cells after 16 h of incubation with cholera toxin (Figure 4.13). Furthermore, the basal level of cAMP was also slightly increased in toxin treated clone 13 cells, which can be attributed to the constitutive active effect of the remaining ADP-ribosylated  $G_s\alpha$ , an observation shown in previous studies (MacLeod and Milligan 1990).

Cholera toxin treatment of clone 44 cells however resulted in a highly elevated basal level of cAMP (Figure 4.16) which is much higher than in similarly treated clone 13 cells (paired t-test:  $p < 0.05$ ;  $n = 3$ ). In fact, the basal cAMP level in cholera toxin-treated clone 44 cells is at such a high level that iloprost stimulation did not result in significant increase in cAMP. This major difference between clone 44 and clone 13 cells is likely due to the remaining high levels of ADP-ribosylated FhIPR- $G_s\alpha$  fusion protein but not ADP-ribosylated endogenous  $G_s\alpha$  after 16 h of cholera toxin treatment (Figure 4.13). This provides an indirect evidence that ADP-ribosylated FhIPR- $G_s\alpha$  and by inference an agonist-occupied FhIPR- $G_s\alpha$ , can signal to its secondary effector.

**Figure 4.1 Schematic representation of FhIPR- $G_s\alpha$  fusion cDNA and protein**

The incorporation of  $G_s\alpha$  within the FhIPR cDNA is shown. The last 6 residues of FhIPR and the first 6 residues of  $G_s\alpha$  are shown. There is an alteration of cysteine to glutamic acid at the last residue of the receptor due to the incorporation of *XhoI* site, required for subsequent ligation with the open reading frame of  $G_s\alpha(L)(HA)$ .

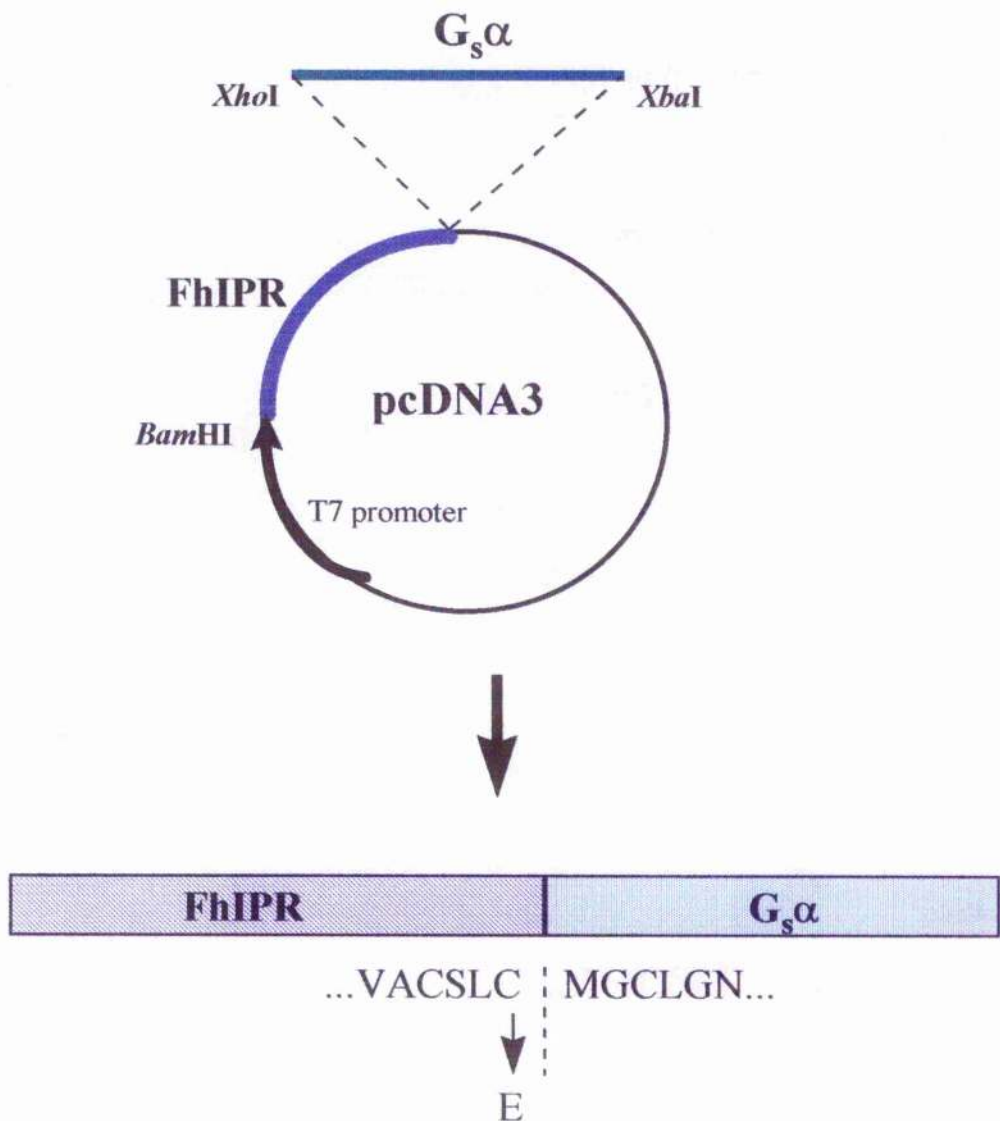


**Figure 4.2 Agarose gel analysis of FhIPR-G<sub>s</sub>α cDNAs**

**A.** DNAs from *E. coli* clones (transformed with ligated FhIPR / G<sub>s</sub>α mix) were digested with *Hind*III and *Xba*I and resolved in 1% agarose gel. Clones S1 and S2 contain a digested fragment close to the approximate length of 2.4 kb of the FhIPR-G<sub>s</sub>α cDNA.

**B.** The same DNAs from Figure A were digested with *Xho*I and *Xba*I and resolved in 1% agarose gel. As in Figure A, both clones S1 and S2 contain a digested fragment that approximates the length of G<sub>s</sub>α(L)(HA) cDNA (1.2 kb).

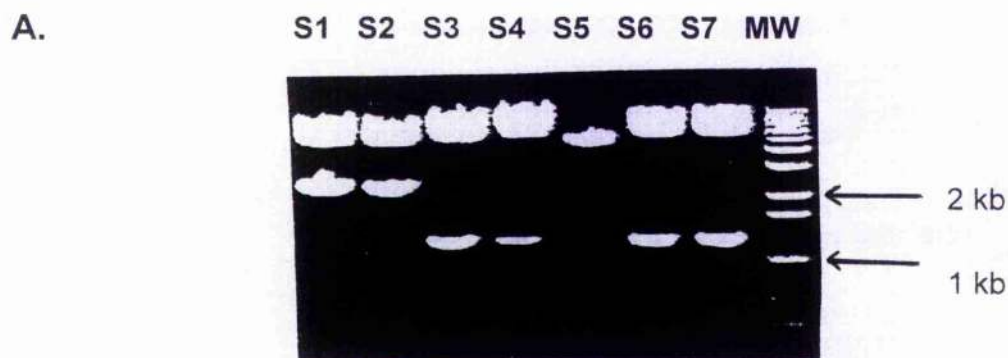


**Figure 4.3 Stable expression of the FhIPR-G<sub>s</sub>α fusion protein in clones of HEK293 cells**

Following stable expression of the FhIPR-G<sub>s</sub>α cDNA into HEK293 cells, membranes from clones 41, 42, 44 and 13, together with parental HEK293 cells were prepared and assessed using ~ 10 nM [<sup>3</sup>H]iloprost. The specific binding of [<sup>3</sup>H]iloprost was obtained by subtracting non-specific counts (assessed with 10 μM unlabelled iloprost) from total counts, and normalised with the amount of membrane protein used in the assay. Expression levels were as follows (fmol/mg membrane protein): clone 41 (1060 ± 81; n=2), clone 43 (992 ± 33; n=2), clone 44 (1356 ± 143; n=5), clone 13 and HEK293 expression levels were as in Figure 3.1.

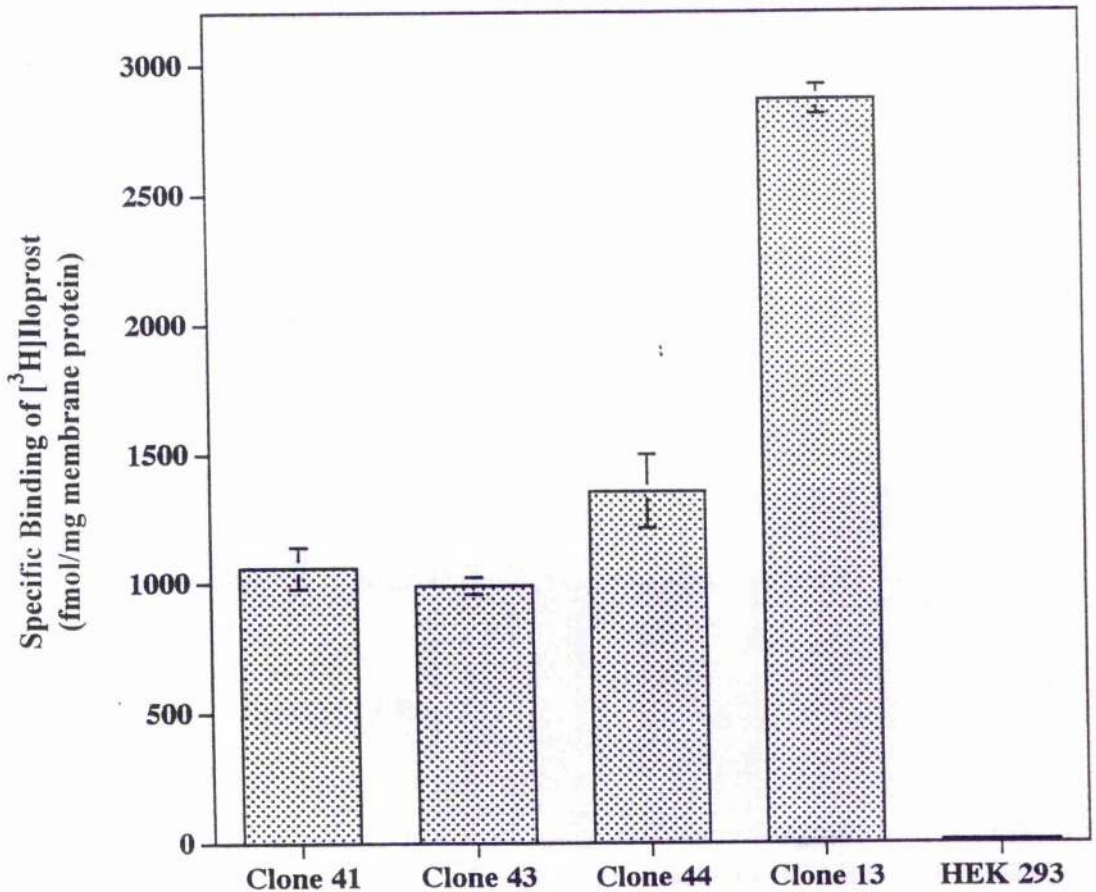


**Figure 4.4 Stimulation of cAMP production by iloprost and forskolin in clones of HEK293 cells stably expressing FhIPR-G<sub>s</sub>α**

Basal adenylate cyclase activity (stippled bars) and regulation by 1  $\mu$ M iloprost (filled bars) or 50  $\mu$ M forskolin (hatched bars) was assessed in intact cells of HEK293 clones stably expressing FhIPR-G<sub>s</sub>α (clones 41, 43 and 44). The results are expressed as the ratio of cAMP over total adenine nucleotides X 100 and represent the mean  $\pm$  SD of 2 independent experiments performed in triplicate.

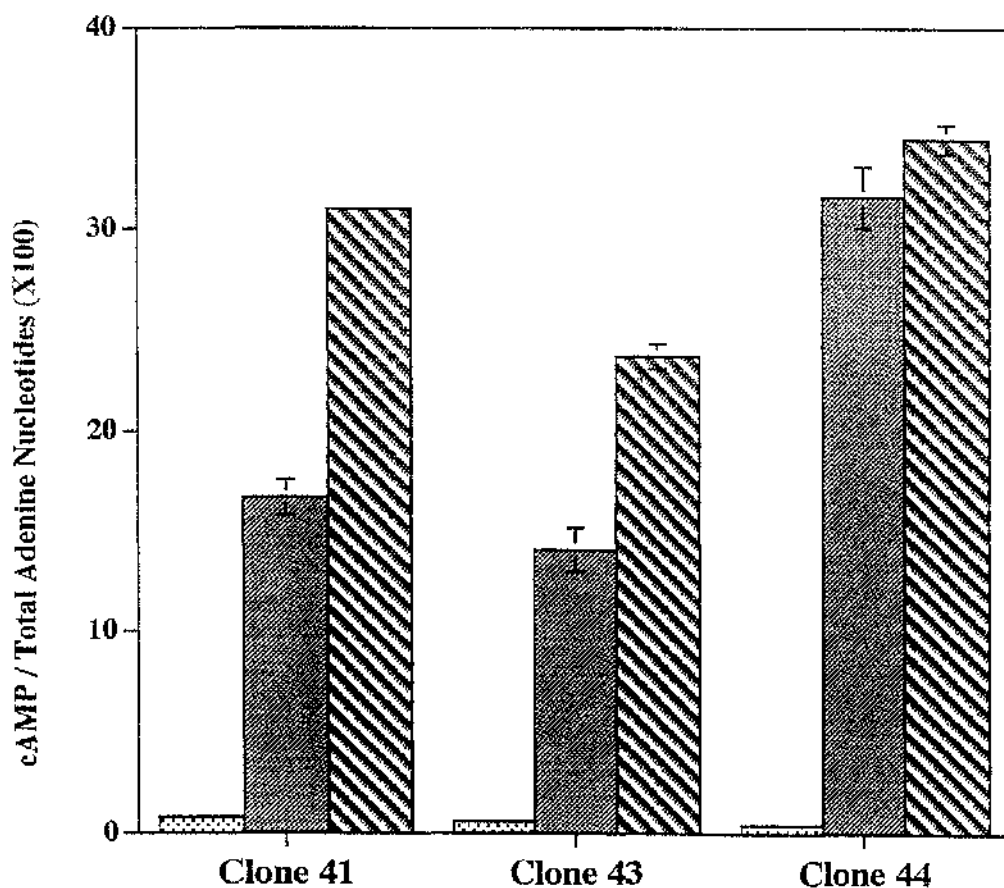


**Figure 4.5 Displacement of [<sup>3</sup>H]iloprost binding in membranes of clone 44 cells**

The specific binding of [<sup>3</sup>H]iloprost (3.4 nM) to membranes of clone 44 cells was displaced by increasing concentrations of unlabelled iloprost. Counts obtained in the presence of 10 μM unlabelled iloprost were treated as non-specific binding. Curve fitting by Kaleidograph™ (v3.02; Abelbeck Software 1993) indicated IC<sub>50</sub> of 4.8 ± 0.5 nM (n = 3). Hill slope of the graph is 0.86 ± 0.07. Data of clone 13 cells was obtained from Figure 3.4. Results are presented as %specific binding of [<sup>3</sup>H]iloprost (100% = specific binding in the absence of unlabelled iloprost). This graph is representative of 3 independent experiments performed in triplicate.

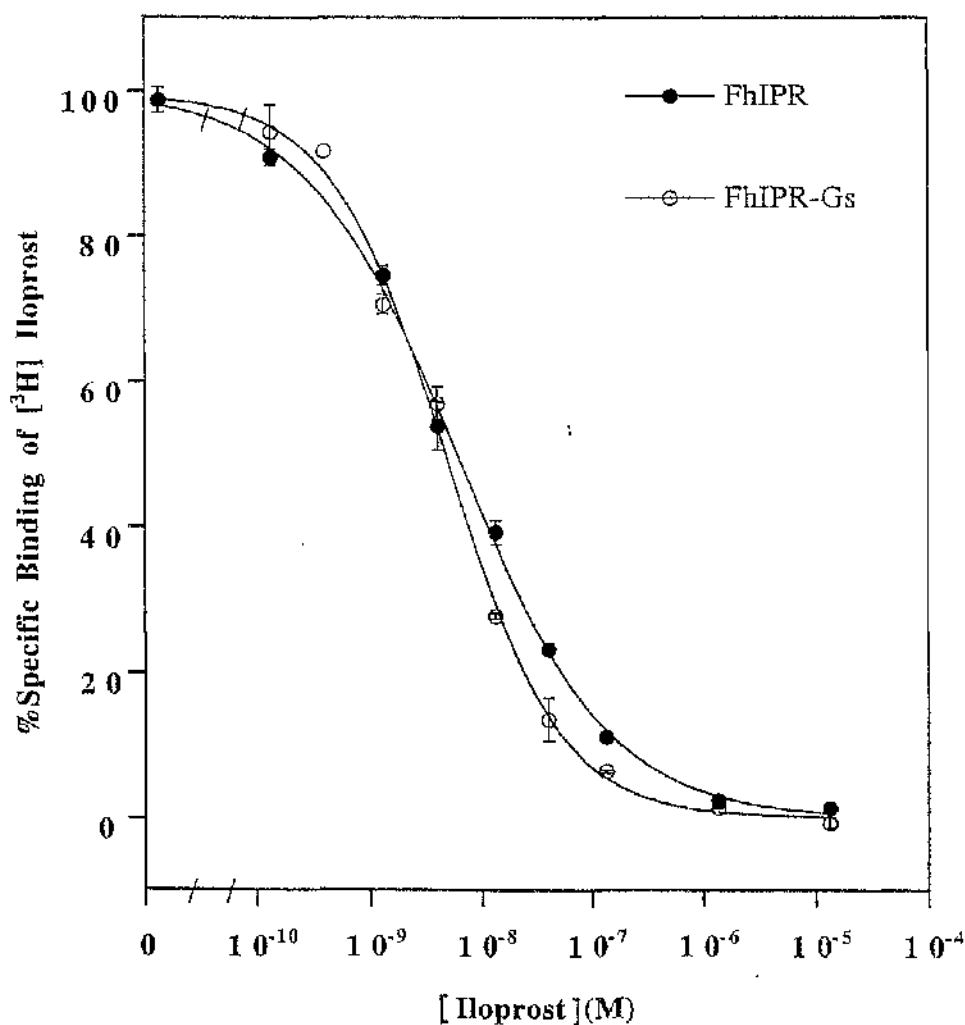


**Figure 4.6 Immunodetection of the FLAG<sup>TM</sup>-tagged human IP prostanoid receptor fused to G<sub>s</sub>α in clone 44 cells**

- A.** Membranes of clone 44 (lane 1) and clone 13 (lane 2) cells were resolved in 10% SDS-PAGE, transferred to nitrocellulose membrane and immunoblotted with M5 anti-FLAG<sup>TM</sup> monoclonal antibody. The predominant immunoreactive protein in lane 1 migrated with an apparent molecular mass of 89 kDa while a series of immunoreactive proteins ranging from 41 to 61 kDa were observed in lane 2.
- B.** The same membranes in Figure A were immunoblotted with CS antiserum, which is specific for the carboxyl-terminal decapeptide of G<sub>s</sub>α. The long and short forms of endogenously expressed G<sub>s</sub>α were detected in both lanes. However, an additional 89 kDa immunoreactive protein was detected in lane 1 but not lane 2.

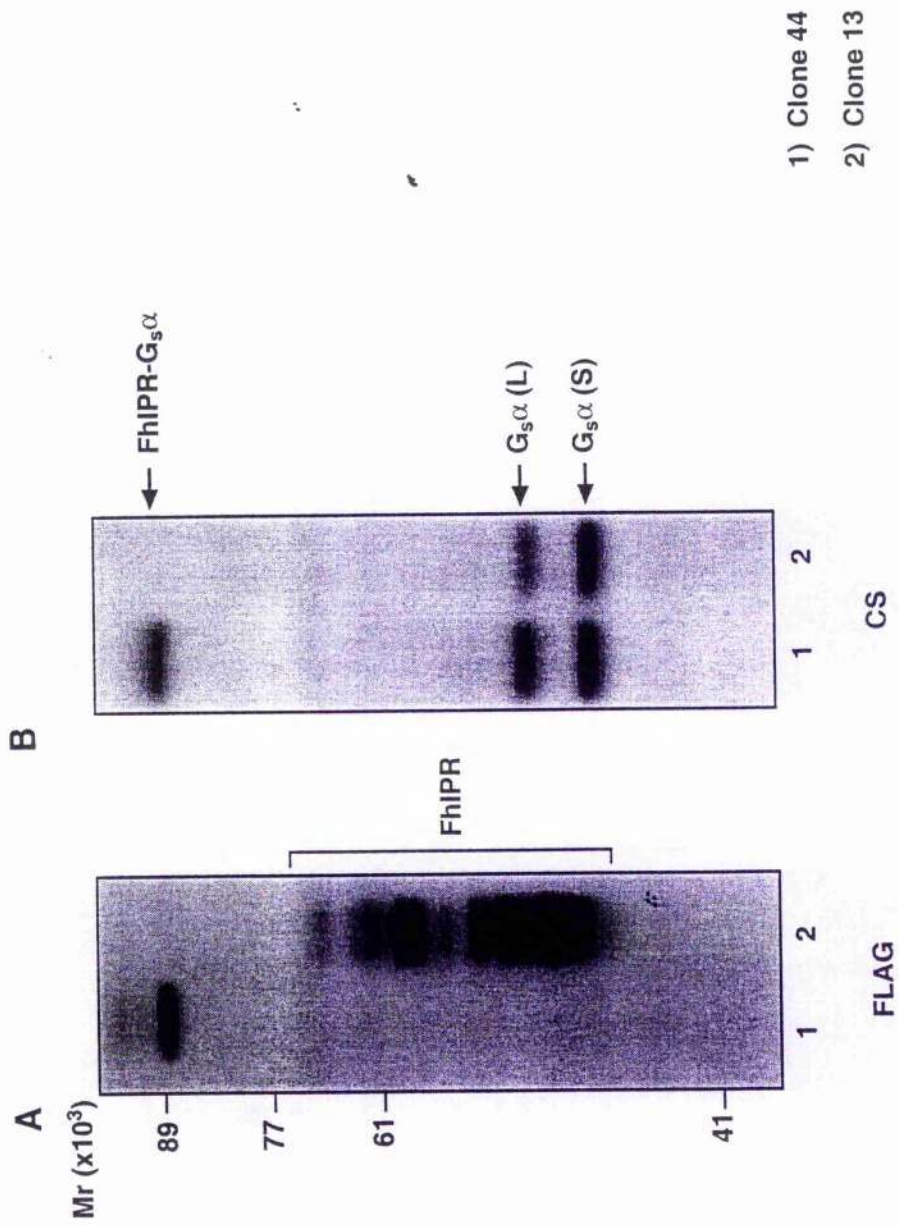


#### Figure 4.7 Effect of agonist treatment on clone 13 and clone 44 cells

Clone 13 and clone 44 cells were incubated with iloprost (1  $\mu$ M) for 0, 0.5, 2, 4, 8, and 16 h. Membranes prepared from these cells were resolved by 10% SDS-PAGE, transferred to nitrocellulose membrane and immunoblotted using various anti-G $\alpha$  antisera.

A. Immunoblotting with CS antiserum, specific for the carboxyl-terminal decapeptide of G $_s\alpha$ , demonstrated a time-dependent downregulation of both the long and short isoforms of G $_s\alpha$  but not FhIPR-G $_s\alpha$ . Downregulation of G $_s\alpha$  occurs at 30 min of iloprost treatment, with only trace amount remaining at 16h.

A

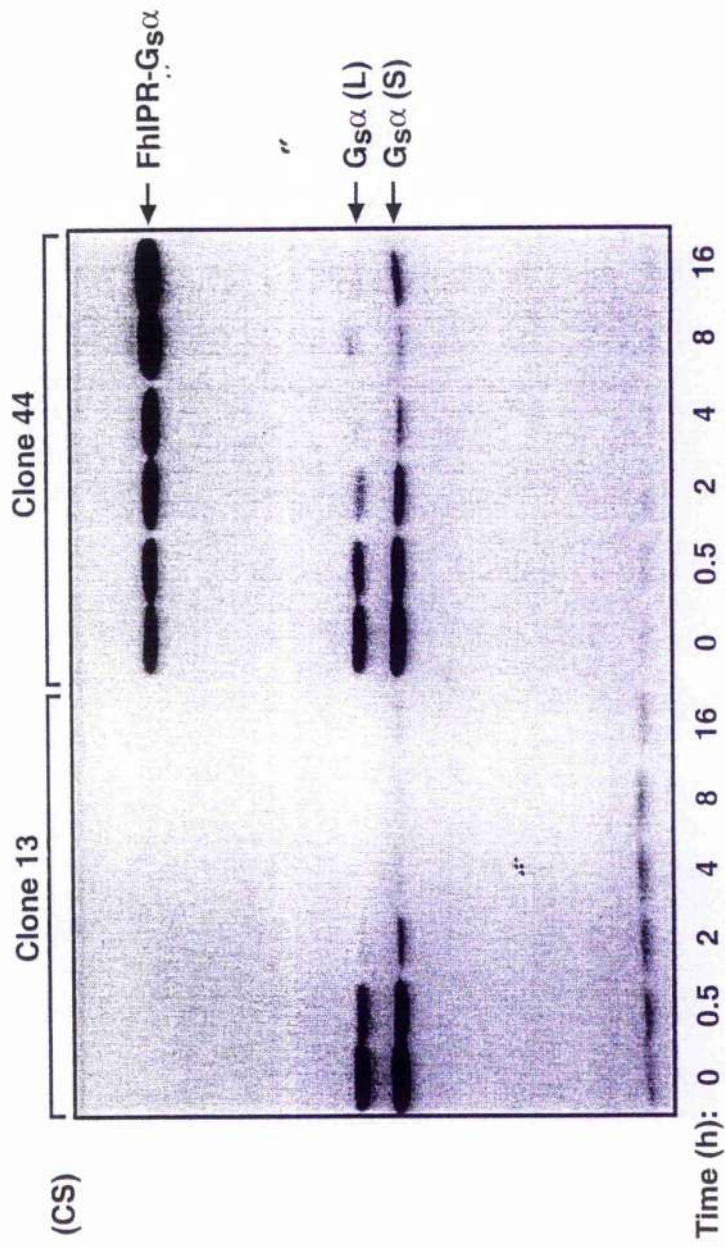


**Figure 4.7 Effect of agonist treatment on clone 13 and clone 44 cells**

- B.** Immunoblotting with M5 anti-FLAG<sup>TM</sup> antibody demonstrated that the IP prostanoid receptor was slightly downregulated after 2 h iloprost treatment but shows signs of recovery after 8 h. Expression levels of the FhIPR-G<sub>s</sub>α fusion protein were not affected by agonist treatment and there was even a slight increase at the longer times (8 and 16 h) of iloprost incubation.

**B**

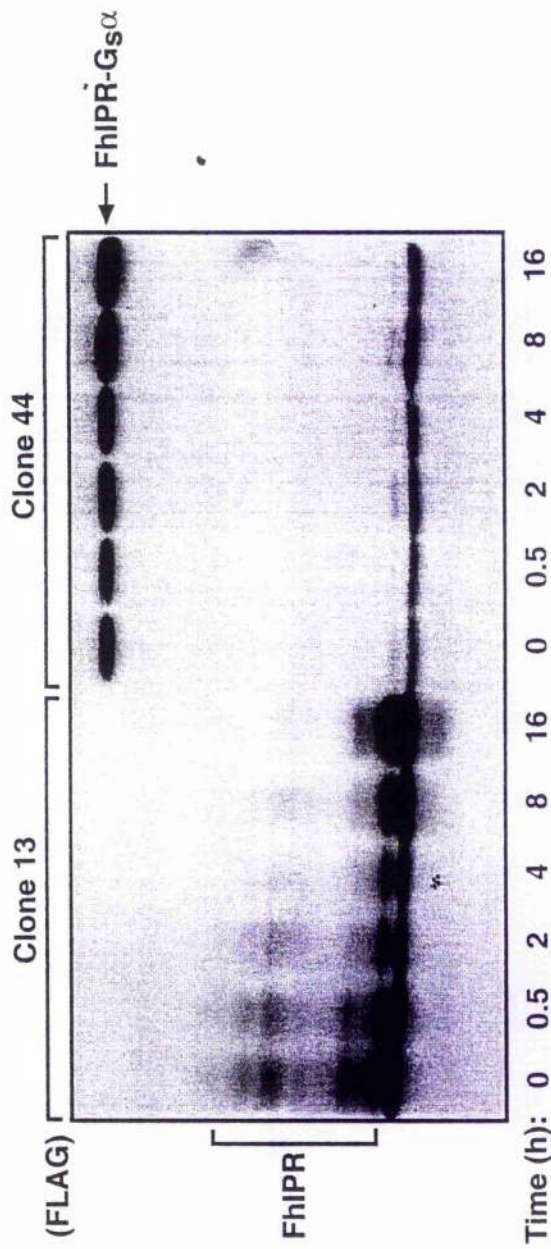


**Figure 4.7 Effect of agonist treatment on clone 13 and clone 44 cells**

C. Immunoblotting with SG antiserum, specific for carboxyl-terminal decapeptide of  $G_{11/2}\alpha$ , did not show any downregulation even after 16 h of incubation with iloprost in both sets of cells.

D. Immunoblotting with CQ antiserum, specific for the carboxyl-terminal decapeptide of  $G_{q/11}\alpha$ , also did not show any time-dependent pattern of downregulation in both sets of cells.

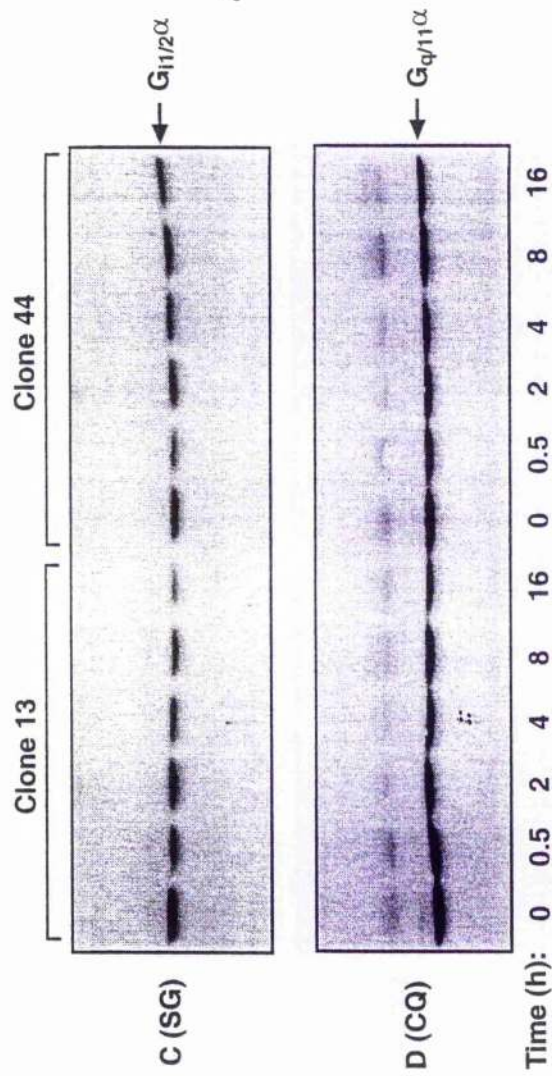


**Figure 4.8 Clone 44 cells exhibit enhanced agonist-stimulated high affinity GTPase activity compared to clone 13 cells**

Membranes of parental HEK293, clone 44, clone 13, and clone 13 transiently transfected with  $G_s\alpha(L)(HA)$  were assessed for basal and iloprost ( $1 \mu M$ )-stimulated high affinity GTPase activity. The stimulations produced by iloprost are displayed, and are as follows (mean  $\pm$  SEM pmol/min/mg membrane protein): HEK293 ( $0 \pm 0.2$ ), clone 13 ( $2.7 \pm 0.4$ ), clone 44 ( $6.0 \pm 0.3$ ), and clone 13 transfected with  $G_s\alpha(L)(HA)$  ( $2.5 \pm 0.2$ ). These data represent 3 or more independent experiments performed in triplicate.

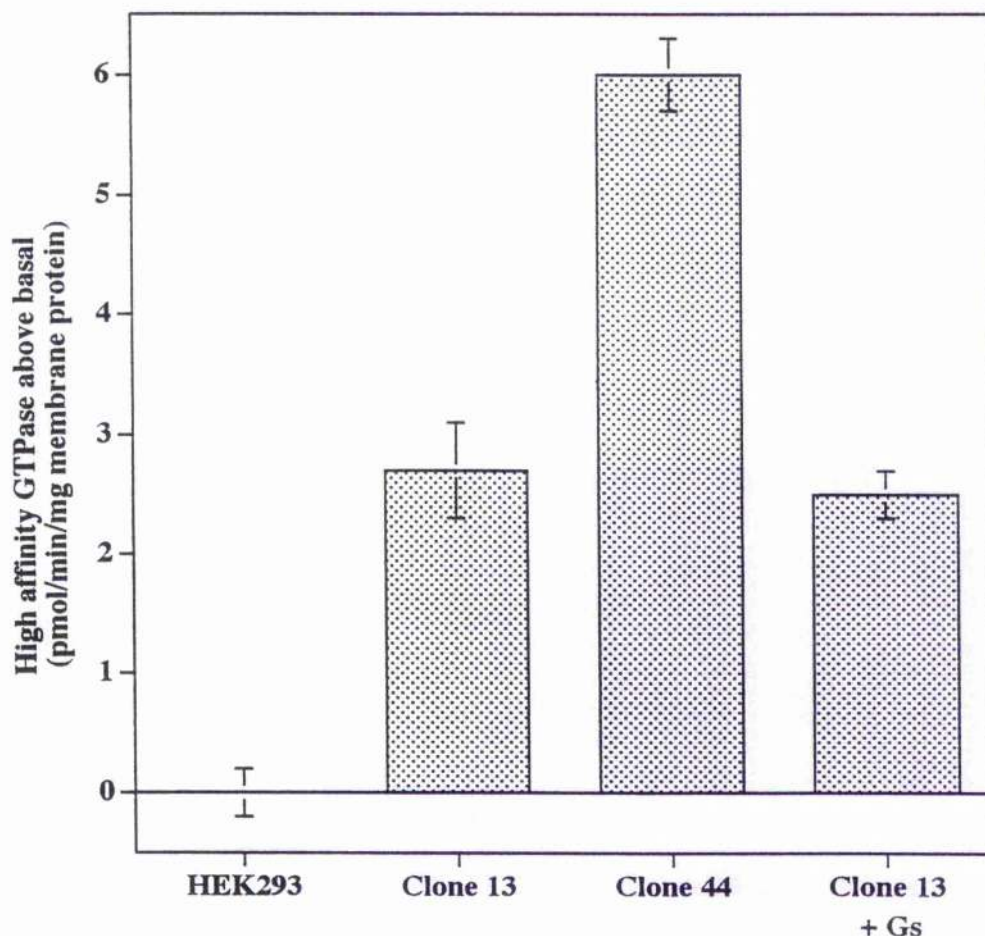


**Figure 4.9 Immunoblot showing overexpression of  $G_s\alpha(L)(HA)$  in clone 13 cells**

Membranes of clone 44 (lane 1), clone 13 (lane 2) and clone 13 cells transfected to express  $G_s\alpha(L)(HA)$  (lane 3) were resolved by 10% SDS-PAGE and immunoblotted with CS antiserum.  $G_s\alpha(L)(HA)$  migrated more slowly than endogenous  $G_s\alpha(L)$  possibly due to the differences in charge resulting from incorporation of the hemagglutinin\* epitope.

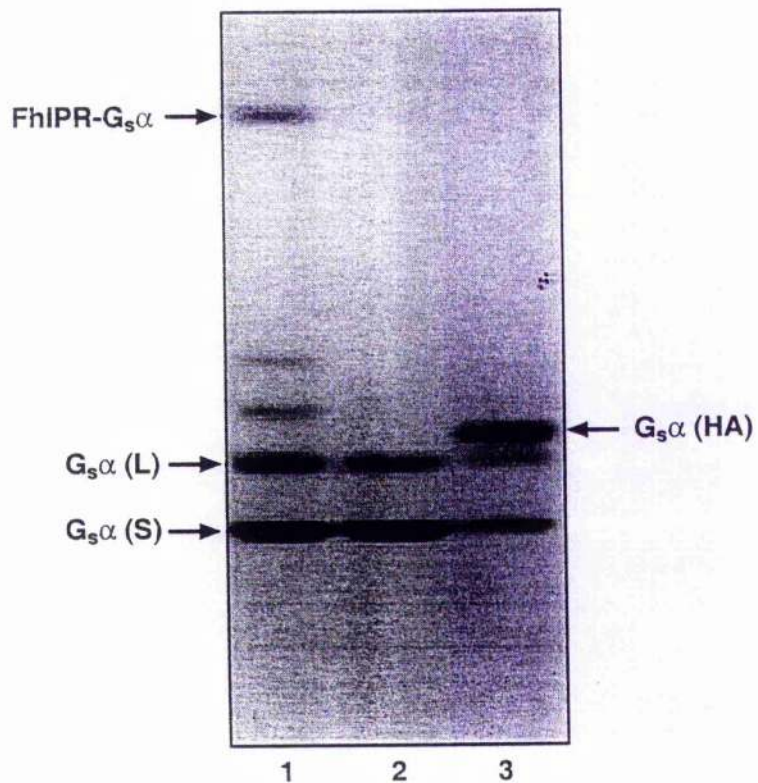


**Figure 4.10 Clone 44 cells exhibit enhanced agonist-stimulated [<sup>35</sup>S]GTP<sub>γ</sub>S binding compared to clone 13 cells**

Membranes of parental HEK293, clone 44, clone 13, and clone 13 transiently transfected with G<sub>s</sub>α(L)(HA) were assessed for basal and iloprost (1 μM)-stimulated [<sup>35</sup>S]GTP<sub>γ</sub>S binding activity. The assay was incubated at 25°C for 60 minutes. The stimulations produced by iloprost (fmol [<sup>35</sup>S]GTP<sub>γ</sub>S bound/mg membrane protein) are displayed in terms of %stimulation by untransfected clone 13 cells (100% = [<sup>35</sup>S]GTP<sub>γ</sub>S bound in clone 13). The results are as follows (mean ± SEM): HEK293 (3.7 ± 17.7), clone 13 (100 ± 16.5), clone 44 (226.5 ± 8.7), and clone 13 transfected with G<sub>s</sub>α(L)(HA) (114 ± 19). These data represent 3 or more independent experiments performed in triplicate.

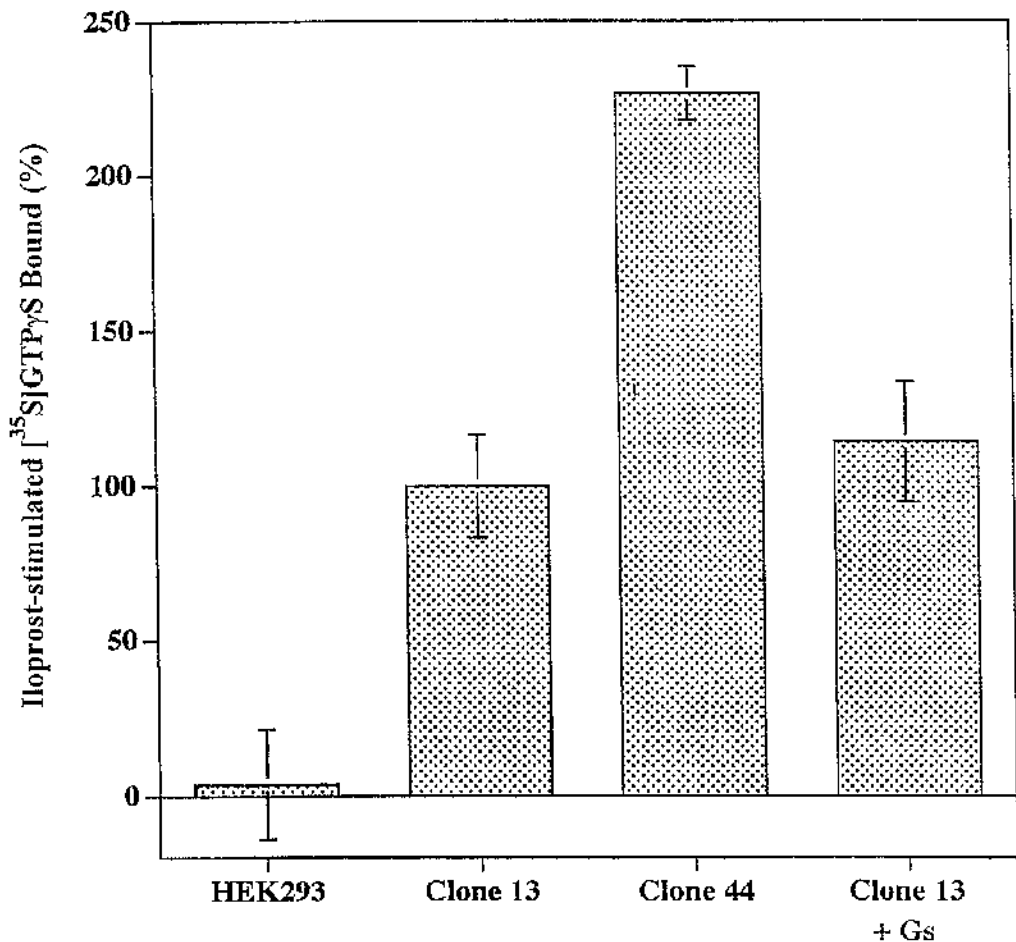


**Figure 4.11 Effects of cholera and pertussis toxins on agonist-stimulated high affinity GTPase activity in clone 44 cells**

Clone 44 cells and clone 13 cells were treated with cholera toxin (200 ng/ml, 16 h) or pertussis toxin (25 ng/ml, 16 h) before harvest. Membranes from these and untreated cells were then used to measure basal high affinity GTPase activity and its stimulation by iloprost (1  $\mu$ M). The stimulations produced by iloprost are presented and are as follows for clone 44 cells (mean  $\pm$  SEM pmol/min/mg membrane protein): untreated ( $6 \pm 0.3$ ), cholera toxin ( $0.9 \pm 0.4$ ) and pertussis toxin ( $5.9 \pm 0.3$ ). Data of clone 13 cells are from Figure 3.13. The data represent at least 3 experiments performed in triplicate.

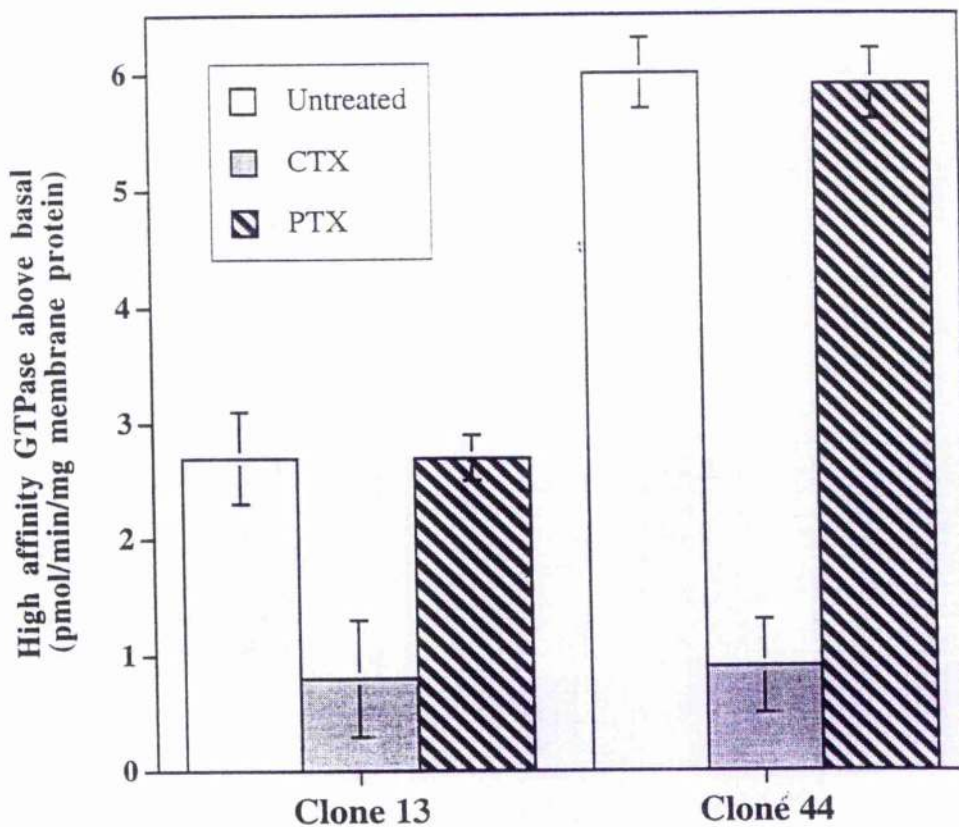


**Figure 4.12 Effects of cholera and pertussis toxins on agonist-stimulated [<sup>35</sup>S]GTP<sub>γ</sub>S binding in clone 44 cells**

Membranes from Figure 4.11 were used to measure basal and iloprost (1 μM)-stimulated binding of [<sup>35</sup>S]GTP<sub>γ</sub>S. The stimulations produced by iloprost are displayed as in Figure 4.10. The results are as follows for clone 13 cells (% stimulation ± SEM): untreated (100 ± 16.5), cholera toxin (21.6 ± 2.2), and pertussis toxin (102 ± 18). Results of clone 44 cells are as follows: untreated (226.5 ± 8.7), cholera toxin (139.6 ± 16.5), and pertussis toxin (188.7 ± 16.7). These data represent 3 independent experiments performed in triplicate.

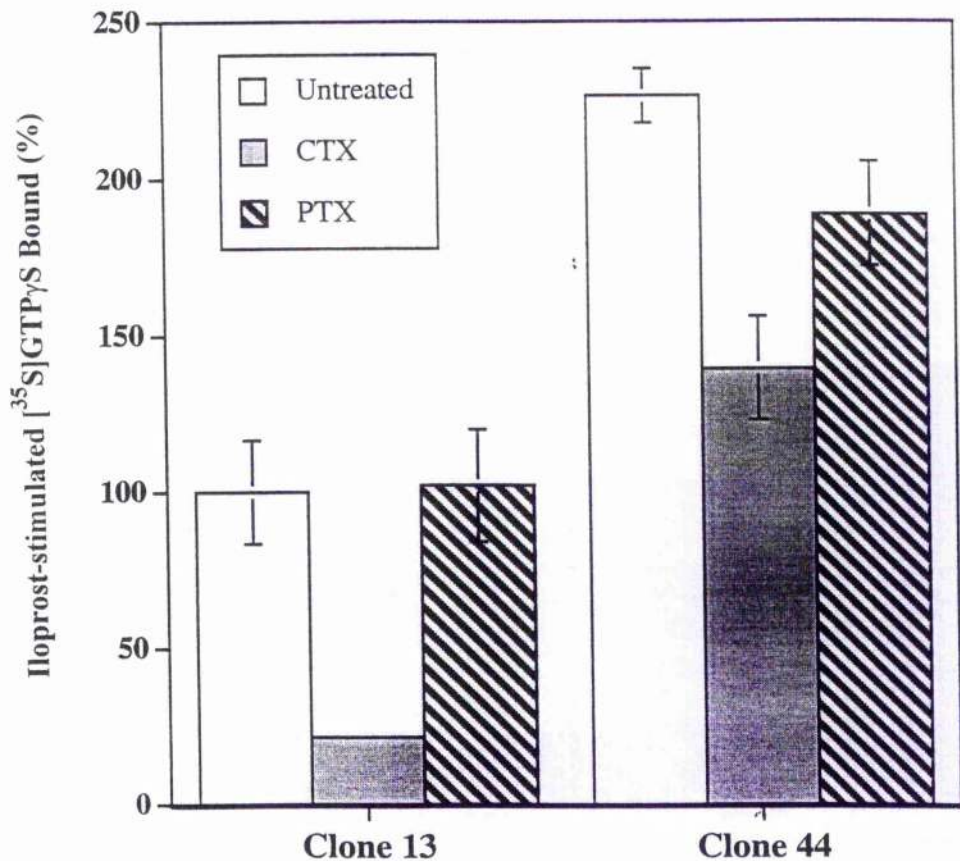


**Figure 4.13 Sustained treatment of clone 13 and clone 44 cells with cholera toxin downregulates endogenous levels of  $G_s\alpha$ .**

Cells from clone 13 and clone 44 were subjected to cholera toxin treatment (200 ng/ml) for 0, 2, 4, 8, and 16 h prior to harvest. Membranes prepared from these cells were resolved by 10% SDS-PAGE, transferred to nitrocellulose and immunoblotted with CS antiserum. Endogenous  $G_s\alpha$  was downregulated to almost undetectable levels after 8 h incubation with cholera toxin in both sets of cells. The levels of FhIPR- $G_s\alpha$  protein in clone 44 cells were however unaffected.

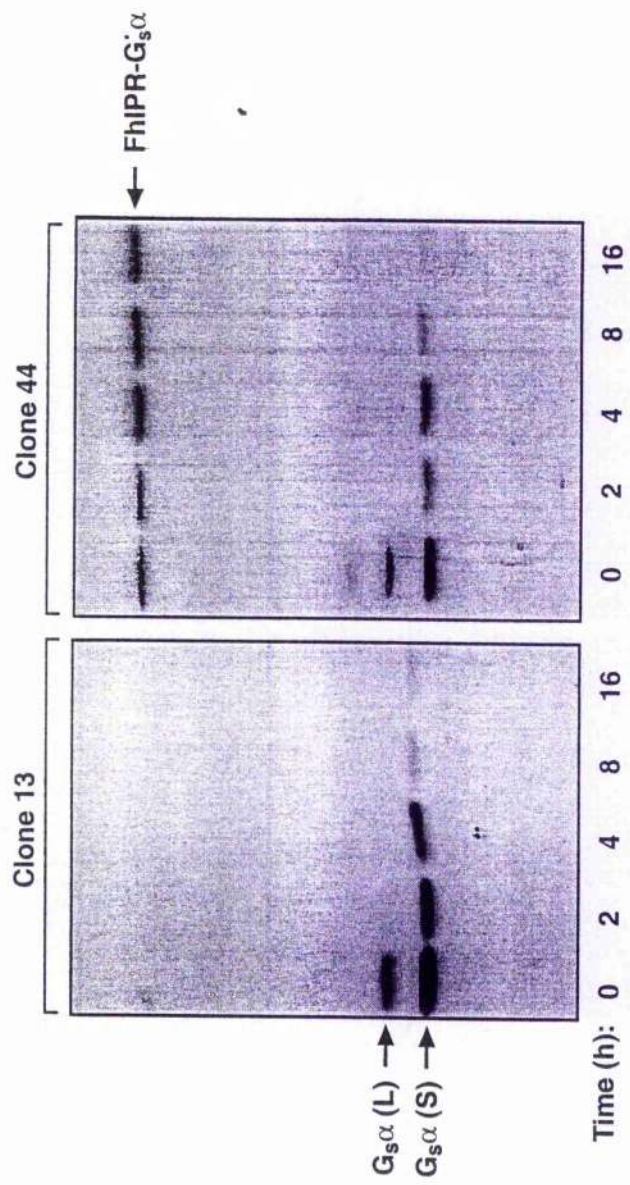


**Figure 4.14 Time course of adenylylase response to iloprost stimulation in clone 13 and clone 44 cells**

Intact clone 13 and clone 44 cells were assessed for their ability to stimulate adenylylase at various incubation times (0, 5, 10, 20, 30 and 45 min) in the absence (basal) and presence of iloprost (1  $\mu$ M). Basal cAMP levels of both clones were less than 1% of total adenine nucleotides. The iloprost-stimulated accumulation of cAMP is shown and expressed as the ratio of cAMP over total adenine nucleotides X 100. This graph is representative of 2 independent experiments performed in triplicate.

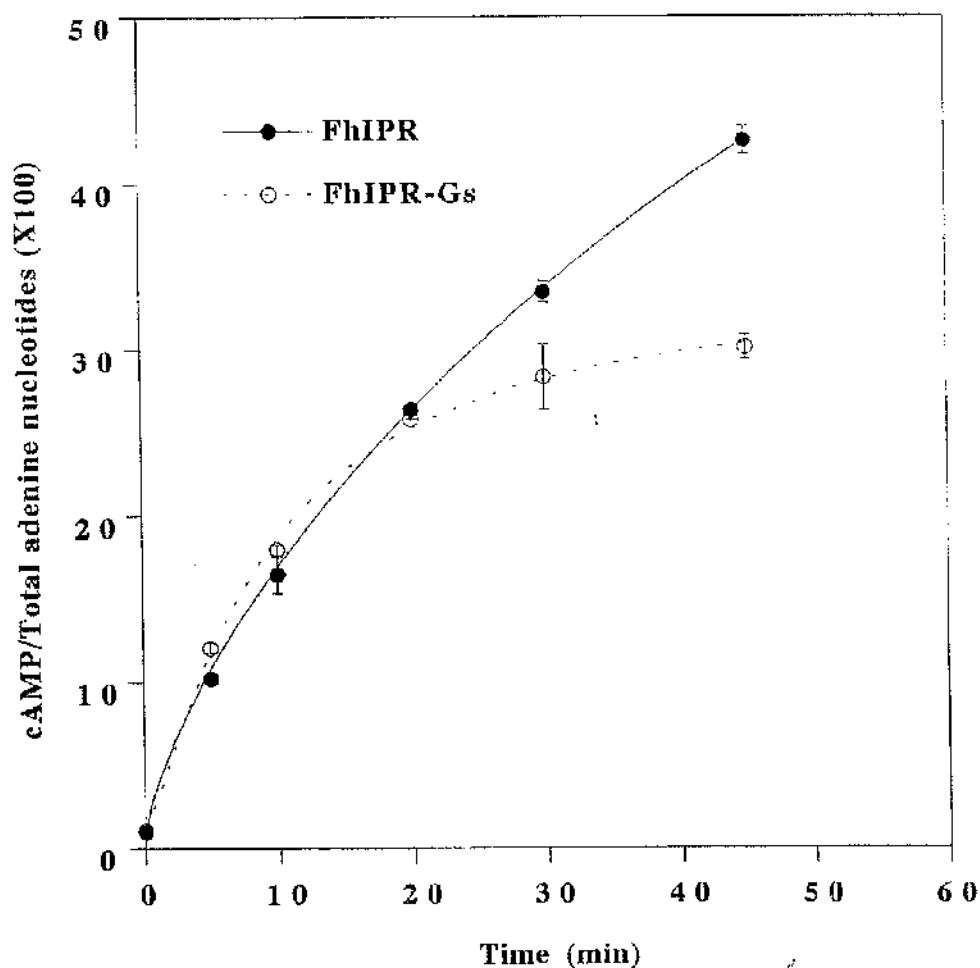


**Figure 4.15 Comparison of adenylate cyclase concentration-response for iloprost in intact clone 13 and clone 44 cells**

Intact clone 13 and clone 44 cells were assessed for their ability to stimulate adenylate cyclase at various concentrations of iloprost. The results are presented as in Figure 4.14 but expressed as % maximum stimulation (activity at 10  $\mu$ M iloprost treated as 100%). Data of clone 13 is obtained from Figure 3.6. Effective concentration at 50% stimulation ( $EC_{50}$ ) of clone 44 is estimated at  $1.1 \pm 0.3 \times 10^{-10}$  M (mean  $\pm$  SEM). This graph is representative of 3 independent experiments performed in triplicate.

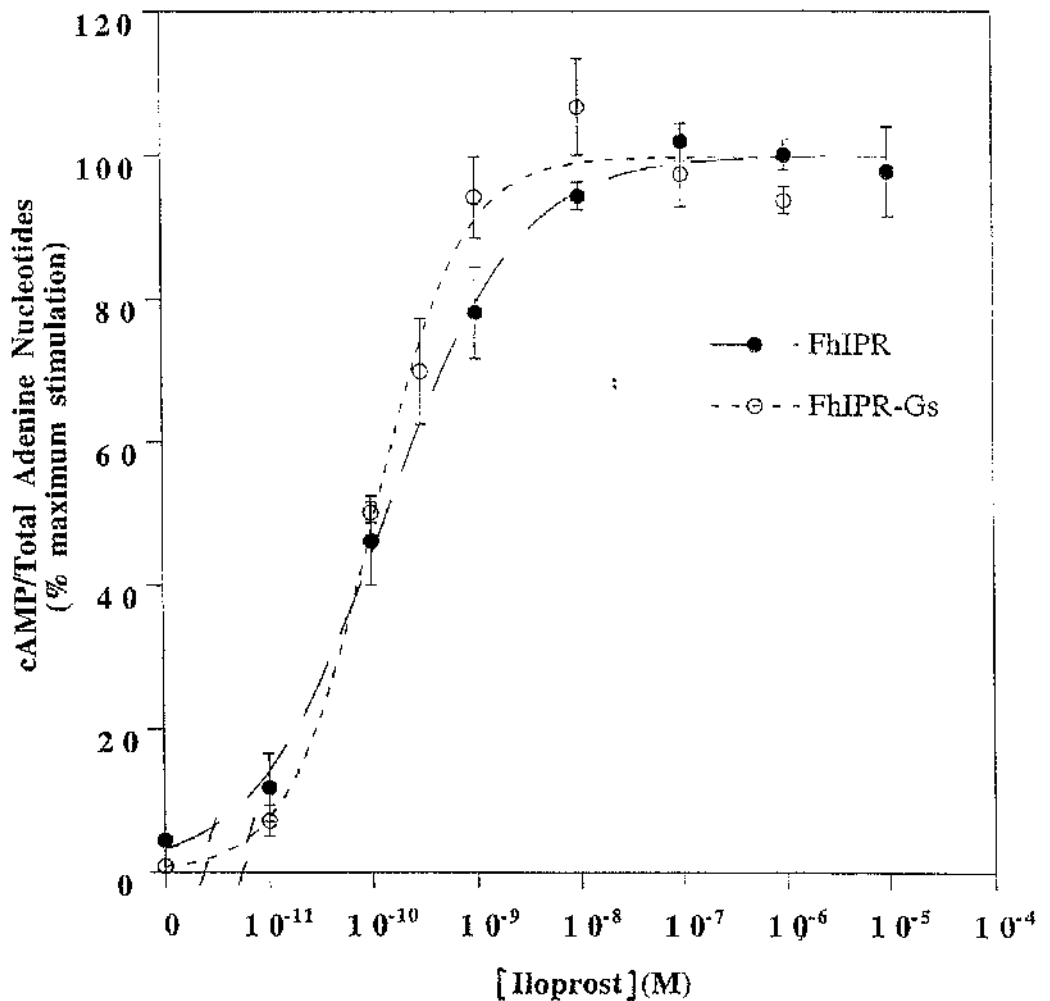
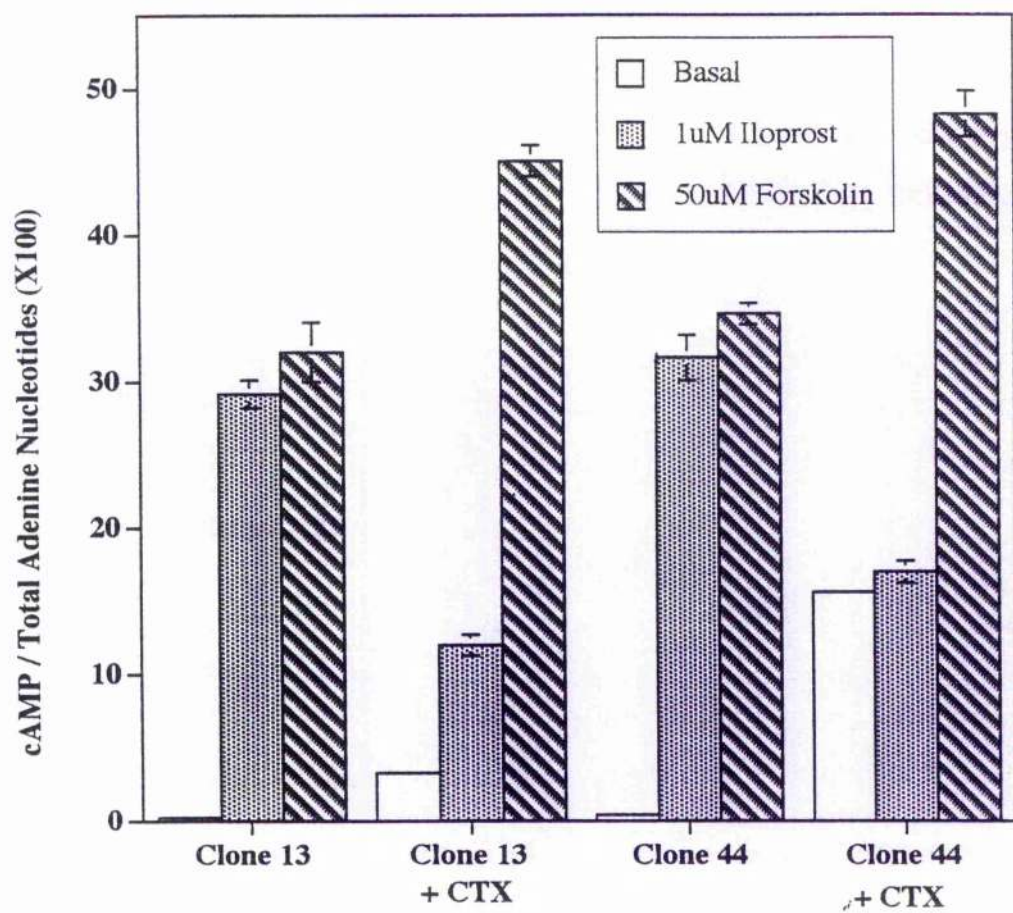


**Figure 4.16 Analysis of adenylate cyclase response in clone 13 and clone 44 cells pretreated with cholera toxin**

Adenylate cyclase activities in intact clone 13 and clone 44 cells were assessed by stimulation with iloprost (1  $\mu$ M) or forskolin (50  $\mu$ M). Cholera toxin (200 ng/ml) was also incubated with both sets of cells for 16 h and their adenylate cyclase response assessed. The results are presented as in Figure 4.4. This graph is a typical representation of 3 independent experiments performed in triplicate.



### 4.3 Discussion

#### *The FhIPR-G<sub>s</sub>α fusion protein has similar characteristics as the IP prostanoid receptor*

The construction of a cDNA encoding a fusion protein between the IP prostanoid receptor and its cognate G protein, G<sub>s</sub>α, was successful in the current study. The FhIPR cDNA was ligated in-frame with the G<sub>s</sub>α(L)(HA) cDNA by first removing the stop codon and then incorporating a restriction site that is identical to that introduced into the 5'-end of G<sub>s</sub>α(L)(HA) cDNA. The choice of the restriction site must be such that it is unique in both the receptor and G<sub>s</sub>α(L)(HA) coding sequences and does not alter many residues in either the receptor C-terminus or the Gα N-terminus. A *Xho*I restriction site (nucleotide bases: CTCGAG) was found to satisfy both criteria, causing only a change in the last residue of the receptor from cysteine to glutamic acid (Figure 4.1). As glutamic acid is negatively charged and polar, it should fit well into the cytoplasmic environment of the receptor C-terminus. The proper expression of the protein in HEK293 cells was demonstrated by antisera that interacted with both termini of the fusion protein (Figure 4.6).

HEK293 clone 44, which stably express the FhIPR-G<sub>s</sub>α at high levels was selected out of 27 clones for further characterisation and comparison with clone 13. Interestingly, although clone 44 expresses the fusion protein while clone 13 expresses the isolated receptor (FhIPR), both shared similar characteristics. Clone 44 cells bound [<sup>3</sup>H]iloprost with similar affinity as clone 13 cells when assessed in agonist displacement studies (Figure 4.5), but with a less shallow slope (Hill coefficient of clone 44 = 0.86 ± 0.07; clone 13 = 0.64 ± 0.05). The lack of an IP prostanoid receptor antagonist makes it difficult to assess the proportion of high affinity ternary complex in each clone, although the addition of the non-hydrolysable GTP analogue, Gpp(NH)p, did reduce the specific binding of [<sup>3</sup>H]iloprost to membranes of both clones (data not shown).

Immunoblotting with M5 anti-FLAG<sup>TM</sup> antibody showed multiple immunoreactive polypeptides in clone 13 which presumably reflect differentially N-

glycosylated forms of the IP prostanoid receptor. By contrast, M5 immunoblot of membranes from clone 44 showed a single well defined immunoreactive polypeptide (Figure 4.6A). It is unclear whether this reflects an unglycosylated FhIPR- $G_s\alpha$  protein or unresolved glycosylated forms of the protein due to the high molecular mass of the fusion protein (~90 kDa). In further gel-electrophoresis studies, this high molecular mass polypeptide was allowed to resolve further down the gel. Subsequent M5 immunoblots did detect multiple immunoreactive species which differ in their migration through SDS-PAGE (results not shown). Thus the FhIPR- $G_s\alpha$  protein may potentially be N-glycosylated despite the addition of a large cytoplasmic  $G\alpha$  protein.

The functionality of the FhIPR- $G_s\alpha$  fusion protein was assessed by stimulating with the IP prostanoid agonist iloprost, which resulted in distinct elevation of cAMP in HEK293 clones expressing the FhIPR- $G_s\alpha$  (Figure 4.4). A point to note is that expression of the FhIPR- $G_s\alpha$  protein did not result in elevated basal adenylate cyclase activity. This indicates that fusing the receptor and G protein together did not alter either the GPCR or the  $G\alpha$  conformation towards an activated state. Instead, stimulation by agonist is essential for the fusion protein to activate adenylate cyclase which it did so in a manner that closely resembled that of the freely interacting receptor (Figure 4.15). The spatio-orientation of the agonist binding and  $G\alpha$  interacting domains in the FhIPR- $G_s\alpha$  protein therefore mimics that of the isolated IP prostanoid receptor.

As HEK293 cells endogenously express high levels of  $G_s\alpha$ , stimulation of the fusion protein may simultaneously activate the receptor-linked and the cellular pool of  $G_s\alpha$ . Indeed, sustained agonist treatment of clone 44 cells resulted in a time-dependent downregulation of endogenous  $G_s\alpha$  (Figure 5A). This proceeded on a slightly slower time course as those of clone 13 cells, which may reflect differences in receptor expression levels. Apparently, fusing the  $G_s\alpha$  protein at the carboxyl-terminus of FhIPR did not reduce the capacity of the receptor to activate endogenous  $G_s\alpha$ . This could imply that the receptor-fused  $G_s\alpha$  is not hindering the

free movement of competing endogenous  $G_s\alpha$  subunits for coupling with the receptor. A similar observation was noted in the studies of GPCR-GFP (Green Fluorescent Protein) constructs. For example, Barak *et al.* (1997) were able to stimulate adenylate cyclase in intact HEK293 cells transiently expressing the  $\beta_2$ AR-GFP by isoprenaline in a similar manner to cells expressing  $\beta_2$ -adrenergic receptor.

The capacity of a receptor- $G\alpha$  fusion protein to activate endogenous  $G\alpha$  subunits was also previously shown by Burt *et al.* (1998). By expressing a fusion protein between the  $\alpha_{2A}$ -adrenergic receptor and a pertussis toxin-resistant mutant of  $G_{i1}\alpha$ ; (C351G) $G_{i1}\alpha$ , they demonstrated that the activation ratio of endogenous  $G_{i1}\alpha$  to receptor-linked  $G_{i1}\alpha$  is 5:1. However, recent studies by Bahia *et al.* (1998) indicated that the glycine 351 mutant of  $G_{i1}\alpha$  is activated to a much smaller extent, as it binds only 20% of the total [ $^{35}$ S]GTP $\gamma$ S bound by wild type  $G_{i1}\alpha$ , when stimulated by the  $\alpha_{2A}$ -adrenergic receptor. This would suggest that the activation ratio of endogenous  $G_{i1}\alpha$  to a  $\alpha_{2A}$ -adrenergic receptor-linked wild-type  $G_{i1}\alpha$  is closer to 1:1. The activation of endogenous  $G\alpha$  by the fusion protein is also subtype specific. Although the  $\alpha_{2A}$ -adrenergic receptor was previously shown to activate both  $G_{i1}\alpha$  and  $G_s\alpha$  subunits (Eason *et al.* 1992), the  $\alpha_{2A}$ AR- $G_{i1}$ (C351G) $\alpha$  fusion protein can only activate  $G_{i1}\alpha$  but not  $G_s\alpha$  (Sautel and Milligan 1998). As the  $EC_{50}$  for  $G_{i1}\alpha$  activation is much lower than that for  $G_s\alpha$ , this may reflect reduced affinity of endogenous  $G\alpha$  for the fusion receptor to the extent that  $G_s\alpha$  can no longer interact effectively.

A similar approach of using toxin-resistant  $G_s\alpha$  cannot be adopted for studying receptor- $G_s\alpha$  fusion proteins due to the lack of mutants that mimic the function of wild-type  $G_s\alpha$  without being a substrate for ADP-ribosylation by cholera toxin. Freissmuth and Gilman (1989) did attempt to generate such mutants by replacing the specific arginine residue, which is the site of modification by cholera toxin, to alanine, glutamic acid or lysine. However, these mutants were both

unable to hydrolyse GTP and were not totally resistant to the ADP-ribosylating action of the toxin, rendering them useless as toxin-resistant  $G_{s\alpha}$  mutants.

***Enhanced activation of  $G_{\alpha}$  in clone 44 cells is mediated by the FhIPR- $G_{s\alpha}$  fusion protein***

Despite the many similar characteristics between clone 13 and clone 44 cells, there exists a distinct difference in the amplitude of G protein signalling in these clones. Clone 44 cells show higher agonist-stimulated  $G_{\alpha}$  activity than clone 13 cells, based on the results obtained by high affinity GTPase and [ $^{35}$ S]GTP $\gamma$ S binding assays (Figure 4.8 & 4.10). Overexpression of  $G_{s\alpha}(L)(HA)$  in clone 13 cells did not result in measurable elevation of  $G_{\alpha}$  activity in both assays. This confirmed the observations in Chapter 3, where transient expression of  $G_{s\alpha}$  in clone 13 cells also did not alter agonist activity. No attempt was then made to compare the enhancement effect of  $G_{11}/G_{s6\alpha}$  protein in each assay, due to the difficulty of quantifying  $G_{11}/G_{s6\alpha}$  expression levels. However, in this study, expression levels can be assessed adequately by radioligand binding studies. These results indicated that receptor levels in the two clones are not the same: clone 13 express FhIPR at  $\sim 3$  pmol/mg membrane protein, while clone 44 express FhIPR- $G_{s\alpha}$  at  $\sim 1.4$  pmol/mg.

Iloprost-stimulated high affinity GTPase activity (pmol Pi / min / mg membrane protein) in clone 44 cells is 2.2 times that of clone 13 cells (Figure 4.8). Compensating for receptor expression levels, the increase in high affinity GTPase activity of each FhIPR- $G_{s\alpha}$  protein with respect to FhIPR is therefore:

$$\text{fold increase (membrane protein)} \times \frac{\text{expression level of FhIPR (pmol/mg)}}{\text{expression level of FhIPR-}G_{s\alpha} \text{ (pmol/mg)}}$$

Thus, the GTPase activity of each FhIPR- $G_{s\alpha}$  protein is  $2.2 \times (3/1.4) = 4.7$  times that of FhIPR. A very similar fold increase (226%) was also obtained in [ $^{35}$ S]GTP $\gamma$ S binding assay (Figure 4.10). As the agonist-stimulated binding of

$[^{35}\text{S}]\text{GTP}\gamma\text{S}$  is normally expressed as fmol  $[^{35}\text{S}]\text{GTP}\gamma\text{S}$  bound / mg membrane protein (see Figure 4.10), the increase is again understated in view of the lower receptor expression levels in clone 44 cells. Adjusting for this difference using the above formula, each iloprost-activated FhIPR- $G_s\alpha$  protein is shown to be 226% X  $(3/1.4) = 484\%$  or ~4.8 times better in stimulating the incorporation of  $[^{35}\text{S}]\text{GTP}\gamma\text{S}$  to  $G_s\alpha$  than the FhIPR protein. These results suggested that the FhIPR- $G_s\alpha$  fusion protein is more efficient in transducing signal to  $G_s\alpha$  compared to the isolated receptor.

The observation that GPCR- $G_s\alpha$  fusion proteins are more efficient signal transducing units was previously noted by Bertin *et al.* (1994) and Seifert *et al.* (1998a). They both used the same construct, a  $\beta_2\text{AR-}G_s\alpha$  fusion protein, which when overexpressed, gave higher signalling output compared to the  $\beta_2$ -adrenergic receptor. Although the results of Bertin *et al.* (1994) must be treated with caution, as S49 lymphoma *cyc<sup>-</sup>* cells, which also endogenously expressed  $\beta_2$ -adrenergic receptor were used, Seifert *et al.* (1998a) showed conclusively that expressing the  $\beta_2\text{AR-}G_s\alpha$  in insect Sf9 cells gave robust agonist-stimulated GTPase activity. As the endogenous  $G_s\alpha$  in Sf9 cells was not activated by the  $\beta_2$ -adrenergic receptor, either due to the low level of expression or species difference, this greatly facilitated their study of the subtle differences in coupling between the long and short isoforms of  $G_s\alpha$  by using  $\beta_2\text{AR-}G_s\alpha(\text{L})$  and  $\beta_2\text{AR-}G_s\alpha(\text{S})$  fusion proteins.

Despite certain advantages of using the insect cells for the study of GPCR functions, there are also numerous drawbacks. These include the processing of glycosylated proteins, the differences between insect and mammalian signalling components and the compromised metabolism of the cell resulting from the baculovirus infection (Bouvier *et al.* 1998). In addition, the recombinant receptor is expressed very late in the viral infection cycle and hence only a short window of time exists between the moment of receptor expression and cell death. As it is not possible to select for stably expressing clones, the expression of receptor will fluctuate in each transfection and will therefore affect the results of the assays. In this study, the use of stably expressing clones derived from mammalian cell lines

would therefore reflect more accurately the functions and capacities of the FhIPR- $G_{s\alpha}$  fusion protein.

***FhIPR- $G_{s\alpha}$  binds [ $^{35}$ S]GTP $\gamma$ S in the presence of cholera toxin***

The abolishment of agonist-stimulated high affinity GTPase activity in clone 44 cells upon treatment by cholera toxin (Figure 4.11) indicates that the FhIPR- $G_{s\alpha}$  only activates  $G_{s\alpha}$  protein, which is similar to that observed for the FhIPR. This is further confirmed by the lack of effect of pertussis toxin on clone 44 cells, which means that " $G_{\alpha}$ -like" proteins are not involved in the signalling of the fusion protein. Thus, the enhanced stimulation of  $G_{\alpha}$  by agonist-occupied FhIPR- $G_{s\alpha}$  certainly did not result from an altered signalling characteristic of the fusion protein compared to the FhIPR. It is also very unlikely that other  $G_{\alpha}$  subunits which are not sensitive to cholera and pertussis toxin are activated, based on the immunoblots of  $G_{\alpha}$  proteins of iloprost-treated clone 44 cells (Figure 4.7). This is a rather important point to note as elevation of inositol phosphate levels by the IP prostanoid receptor was observed in a previous study (Namba *et al.* 1994), which may implicate activation of G proteins of the  $G_{q\alpha}$  subfamily.

Direct evidence showing that receptor-linked  $G_{s\alpha}$  can act as a substrate for cholera toxin was not obtained due to the presence of co-migrating polypeptides that incorporate [ $^{32}$ P]ADP-ribose in a non-specific manner in clone 44 cells (results not shown). However, the loss of GTPase activity in cholera toxin-treated clone 44 cells indirectly infers that the receptor-linked  $G_{s\alpha}$  can be ADP-ribosylated, which diminishes its GTP hydrolysis function as for the endogenous  $G_{s\alpha}$ . This inference was put in jeopardy when it was found that cholera toxin-treated clone 44 cells still exhibit capacity to bind [ $^{35}$ S]GTP $\gamma$ S, albeit at a reduced level (Figure 4.12). This result is not that alarming when we considered carefully the  $G_{\alpha}$  activation and hydrolysis processes:

<b>Substrate</b>		<b>Product</b>	<b>Rate (<math>\text{min}^{-1}</math>)</b>
$G\alpha\text{-GDP}$	$\rightarrow$	$G\alpha + \text{GDP}$	$k_{\text{off}}(\text{GDP})$
$G\alpha + \text{GTP}$	$\rightarrow$	$G\alpha\text{-GTP}$	$k_{\text{on}}(\text{GTP})$
$G\alpha\text{-GTP}$	$\rightarrow$	$G\alpha\text{-GDP} + \text{P}_i$	$k_{\text{cat}}$

The rate constant  $k_{\text{off}}(\text{GDP})$  refers to the dissociation rate of GDP from the inactive  $G\alpha$ ,  $k_{\text{on}}(\text{GTP})$  refers to the association rate of GTP to the nucleotide free  $G\alpha$ , while  $k_{\text{cat}}$  refers to the hydrolysis rate of GTP in the activated  $G\alpha$ . As the [ $^{35}\text{S}$ ]GTP $\gamma$ S binding assay monitors the association of [ $^{35}\text{S}$ ]GTP $\gamma$ S to the inactive  $G\alpha$ , it is dependent on the rates of dissociation of GDP ( $k_{\text{off}}$ ) and the subsequent association of [ $^{35}\text{S}$ ]GTP $\gamma$ S, which closely correlate with that of GTP ( $k_{\text{on}}$ ). It is independent of alterations in the GTP hydrolysis rate, even if  $k_{\text{cat}}$  approaches zero as in the ADP-ribosylated  $G_s\alpha$ . Therefore, it is not conceptually incorrect that an ADP-ribosylated FhIPR- $G_s\alpha$  protein can bind GTP $\gamma$ S.

There is so far no known studies that support the retention of GTP binding function in ADP-ribosylated  $G_s\alpha$ . However, Freissmuth and Gilman (1989) showed that mutating the arginine residue involved in ADP-ribosylation, resulted in a loss of GTP hydrolysis but not GTP exchange function. Using the short form of  $G_s\alpha$ , they mutated arginine 187 to 3 different residues (alanine, glutamic acid and lysine). The rate constant for hydrolysis of GTP ( $k_{\text{cat}}$ ) by all these mutants was reduced approximately 100-fold compared to the wild-type protein, but the rate of association of GTP $\gamma$ S was only modestly affected and even slightly elevated. It can be inferred from these studies that ADP-ribosylated  $G_s\alpha$  would manifest the same characteristic. The current finding that cholera toxin treated FhIPR- $G_s\alpha$  can bind GTP $\gamma$ S is therefore tenable and correlates well with the  $G_s\alpha$  mutant studies. Interestingly, this also offers us an opportunity to analyse the ratio of activated endogenous  $G_s\alpha$  to receptor-linked  $G_s\alpha$  by the FhIPR- $G_s\alpha$  fusion protein.

Assuming that the dissociation rate of GDP ( $k_{off}$ ) and the association rate of GTP $\gamma$ S ( $k_{on}$ ) are not altered by the ADP-ribosylation process, this ratio was found to range from 1:1 to 1:2. This result is similar to that obtained for a  $\alpha_{2A}AR-G_{i1}(C351G)\alpha$  fusion protein when the reduced activation of the glycine mutant was taken into account.

### ***Downstream signalling events in the FhIPR-G<sub>s</sub> $\alpha$ fusion protein***

The restriction of G $\alpha$  mobility in a GPCR-G $\alpha$  fusion protein may greatly hinder the capacity of G $\alpha$  to directly act on effectors. This was investigated in the current study by selectively downregulating endogenous G<sub>s</sub> $\alpha$  by treatment with cholera toxin. As the FhIPR-G<sub>s</sub> $\alpha$  protein was not degraded after 16 h of toxin treatment (Figure 4.13), it would be expected to show signs of constitutive activity as a result of the ADP-ribosylation, which diminished its rate of GTP hydrolysis ( $k_{cat}$ ). Indeed, the basal level of cAMP was significantly increased in intact clone 44 cells after cholera toxin treatment (Figure 4.16). This conclusively demonstrated the ability of a receptor-linked G<sub>s</sub> $\alpha$  to directly activate adenylate cyclase. Such results were also obtained in previous studies of the  $\beta_2AR-G_{s\alpha}$  fusion protein in S49 lymphoma  $cyc^-$  cells and insect Sf9 cells (Bertin *et al.* 1994; Seifert *et al.* 1998a). The current result suggest that the effector signalling potential of a receptor-G $\alpha$  protein may not be cell line dependent.

Burt *et al.* (1998), however, failed to notice the downstream signalling events of a  $\alpha_{2A}AR-G_{i1}(C351G)\alpha$  fusion protein expressed in Rat-1 fibroblasts. A clone stably expressing this fusion protein was shown to activate both endogenous G<sub>i</sub> $\alpha$  and the receptor-fused G<sub>i1</sub> $\alpha$  based on high affinity GTPase studies of pertussis toxin treated cells. However, although inhibition of forskolin-stimulated adenylate cyclase activity via G<sub>i</sub> $\alpha$  subunits was observed in the presence of agonists, treatment with pertussis toxin abolished this effect. The likely conclusion is that the receptor-fused G<sub>i1</sub> $\alpha$ , which is pertussis toxin resistant, cannot directly access the adenylate cyclase enzyme. It is unclear whether this is due to the poor effector affinity or the low level of activation of the receptor-fused

mutant  $G_{i1}\alpha$ . Another possibility is that the short C-terminal tail of the  $\alpha_{2A}$ -adrenergic receptor may have constrained the spatial opportunity of the fused G protein. A further proof of the lack of downstream signalling activity of the  $\alpha_{2A}AR$ - $G_{i1}(C351G)\alpha$  fusion protein is its inability to stimulate p44 mitogen-activated protein kinase and p70 S6 kinase, which are mediated via  $G\beta\gamma$  complex (Burt *et al.* 1998).

Iloprost (1  $\mu$ M) stimulation of adenylate cyclase activity in clone 44 cells was observed to level off after 20 min incubation which suggests desensitisation of the FhIPR- $G_s\alpha$  (Figure 4.14). Interestingly, the expression levels of the fusion protein were not downregulated despite sustained agonist treatment for up to 16 h (Figure 4.7A). This indicates that the rapid desensitisation of the FhIPR- $G_s\alpha$  construct is independent of the expression levels at the plasma membrane, a phenomenon previously noted for most GPCRs (Bohm *et al.* 1997). Although FhIPR in clone 13 cells did not show any sign of desensitisation at up to 45 minutes of iloprost stimulation (Figure 4.14), this cannot be compared directly with clone 44 cells due to the huge difference in receptor expression levels.

Rapid desensitisation of receptor- $G\alpha$  fusion proteins has not been studied in detail elsewhere, but a limited study of agonist-promoted long-term desensitisation was performed by Bertin *et al.* (1994). They noted that 24 h isoprenaline (10  $\mu$ M) treatment of S49 lymphoma cyc<sup>-</sup> cells stably expressing the  $\beta_2AR$ - $G_s\alpha$  showed elevated basal activity which when re-challenged with agonist, can stimulate adenylate cyclase. Similarly treated S49 lymphoma wild type cells however, did not exhibit such properties, which led them to conclude that the fusion protein is resistant to long-term desensitisation. It is currently unclear whether the FhIPR- $G_s\alpha$  protein also behave as such, despite its resistance to downregulation by sustained agonist treatment (Figure 4.7A).

The results presented in this study conclusively show the beneficial effect of fusing the IP prostanoid receptor with  $G_s\alpha$  to form a receptor- $G\alpha$  fusion protein, FhIPR- $G_s\alpha$ . This protein has similar binding and effector activation profiles of the

freely interacting receptor, and yet gave strong agonist stimulated response at the G protein level. It was observed to rapidly stimulate  $G_s\alpha$  which resulted in elevated high affinity GTPase activity. Receptor-linked  $G_s\alpha$  can be ADP-ribosylated, based on the observation that GTP hydrolysis was abolished in clone 44 cells treated with cholera toxin. Interestingly, the ADP-ribosylated receptor-linked  $G_s\alpha$  continued to bind  $GTP\gamma S$ , a novel finding which may have implications for the ADP-ribosylated  $G_s\alpha$ . Receptor-fused  $G_s\alpha$  can also interact directly with its effector and its expression level is not reduced by long term agonist treatment.

The FhIPR- $G_s\alpha$  protein therefore offers a means to analyse agonist pharmacology using high affinity GTPase or [ $^{35}S$ ]GTP $\gamma$ S binding assays. This application is similar to that of clone 13 cells expressing the  $G_{11}/G_s6\alpha$  chimeric protein (Chapter 3), but the FhIPR- $G_s\alpha$  protein has the advantage of interacting with its cognate  $G\alpha$ , which is more physiologically relevant. In addition, the fusion protein was observed to be more refractory to agonist-induced downregulation compared to the isolated receptor. A series of agonists with varying potencies and efficacies will need to be assessed thoroughly in this system, however, before it can be utilised as a high-throughput screen for novel agonists and antagonists.

## **CHAPTER 5**

# **Analysis of G Protein Coupling Specificity in the Human IP Prostanoid Receptor-G $\alpha$ Fusion Proteins**

## CHAPTER 5

# Analysis of G Protein Coupling Specificity in the Human IP Prostanoid Receptor - G $\alpha$ Fusion Proteins

### 5.1 Introduction

A fusion protein between the human IP prostanoid receptor and G $\alpha$ <sub>s</sub> (FhIPR-G $\alpha$ <sub>s</sub>) was shown in the previous chapter to acquire higher signal transduction efficiency over freely interacting components. The reasons for this enhancement in the fusion protein are not exactly clear, but may include a combination of close proximity and co-localisation of the fused GPCR and G $\alpha$  (Burt *et al.* 1998), and lower affinity for G $\beta\gamma$  complex and guanine nucleotides in the receptor-linked G $\alpha$ <sub>s</sub> (Seifert *et al.* 1998a). It has also been suggested that covalently linking the GPCR and G $\alpha$  may replaced the role of G $\alpha$  C-terminus in bringing the G protein into close proximity with the intracellular domains of the receptor (Medici *et al.* 1997).

By expressing in Gpa1 deficient yeast cells a fusion protein between the  $\alpha$ -factor receptor (Ste2) and a chimeric G protein (Gpa1-G $\alpha$ <sub>s</sub>), Medici *et al.* (1997) were able to show functional signal transduction, which was not observed when the chimeric G protein was expressed in Ste2 positive cells. The Gpa1-G $\alpha$ <sub>s</sub> protein consists of the N-terminal 362 aa of yeast Gpa1 and C-terminal 128 aa of rat G $\alpha$ <sub>s</sub>. The junction site is within a highly conserved sequence, and therefore it is likely that this chimera would retain the G protein's normal structure. When assessed in Gpa1 deficient *S. cerevisiae*, the Gpa1-G $\alpha$ <sub>s</sub> protein was able to sequester free G $\beta\gamma$  complex and hence rescued the haploid cells from lethality, but it failed to respond to  $\alpha$ -factor. This indicated that the chimeric G protein was not able to couple productively with Ste2 receptor. However, covalent linkage between the

Ste2 receptor and the Gpa1-G<sub>s</sub>α protein seemed to overcome this problem. This led Medici *et al.* to the conclusion that it is not necessary to have a receptor recognising C-terminal region in receptor fused Gα. They also argued that the C-terminus of Gα may not have a particular role in transmitting signal from the receptor, but is mainly responsible for ensuring close contact between the G protein and the receptor (Medici *et al.* 1997).

There is unfortunately no studies on receptor-Gα fusions that support the novel findings of Medici *et al.* (1997), because all fusion proteins constructed thus far involved using receptor and G protein partners that were known to associate productively with each other physiologically (Bertin *et al.* 1994; Seifert *et al.* 1998a; Wise *et al.* 1997c). However, there could be widespread implications if the findings of Medici *et al.* (1997) were true for most receptor-Gα fusions. The C-terminus of Gα is sufficient to allow interactions with some receptors, for example, G<sub>q</sub>α/G<sub>i2</sub>α chimeras containing 4 to 9 carboxyl terminal residues of G<sub>i2</sub>α can couple to A<sub>1</sub> adenosine and D<sub>2</sub> dopamine receptors to stimulate PLC activity (Conklin *et al.* 1993a). The IP prostanoid receptor was also able to activate a G<sub>i1</sub>/G<sub>s</sub>6α chimera with the last 6 aa of G<sub>i1</sub>α replaced with those of G<sub>s</sub>α (Chapter 3). Thus, if indeed the C-terminal residues are not directly involved in transducing the signal, but only in bringing the G protein in close proximity with the receptor, then fusion proteins between the A<sub>1</sub> adenosine or D<sub>2</sub> dopamine receptor with G<sub>q</sub>α or the IP prostanoid receptor with G<sub>i1</sub>α should yield productive signal transduction proteins.

The possibility of promiscuous coupling in receptor-Gα fusion proteins may open endless opportunities for generating artificial signalling proteins. This implies that it may be possible to switch the signalling cascade of GPCRs simply by fusing the desired Gα with the receptor. For industry, this might allow development of a generic assay format in high-throughput screening of new agents acting on GPCRs, with enormous cost savings and convenience. In fact, the quest for a common reporter system for agonist screening of GPCRs had previously centred on G<sub>16</sub>α as a potential universal G protein adapter (Milligan *et al.* 1996). For academia, promiscuity of receptor-Gα coupling in fusion proteins would enable the

study of agonist activity at the G protein level, by using G proteins that give the highest output in the desired assay. Furthermore, GPCRs with unknown  $G\alpha$  coupling could also be studied in detail, and the discovery of agents acting on these receptors speeded up, which in turn would allow faster elucidation of their cellular functions. Such possibilities also extend to orphan GPCRs in the discovery of their physiological ligands, and subsequent unravelling of any novel physiological functions. Finally, fusion proteins could be constructed to attenuate the constitutive activity of the receptor in disease conditions. Thus, a receptor- $G_i\alpha$  fusion protein could perhaps abolish elevated adenylylase activity from a  $G_s\alpha$  activating GPCR, especially if it is due to sustained activation by high level of ligands (e.g. familial hyperthyroidism) or antibodies (e.g. Graves' disease and Chagas disease).

Although it may seem unlikely that such a scenario could happen, we must not forget that a number of GPCRs have already been shown to be promiscuous in G protein coupling. The  $\alpha_{2A}$ -adrenergic receptor is able to couple with  $G_i\alpha$ ,  $G_q\alpha$ , and  $G_s\alpha$  proteins (Chabre *et al.* 1994) as measured using a transient co-expression approach. The human thyrotropin (TSH) receptor can activate G proteins of all 4 families ( $G_s\alpha$ ,  $G_i\alpha$ ,  $G_q\alpha$ , and  $G_{12}\alpha$ ) to incorporate a photoreactive GTP analogue ( $[\alpha\text{-}^{32}\text{P}]\text{GTP azidoanilide}$ ) upon treatment with TSH and TSH receptor-stimulating antibodies (Laugwitz *et al.* 1996). Even the  $\beta_2$ -adrenergic receptor was recently shown to couple to a pertussis toxin-sensitive G protein in cardiac myocytes (Xiao *et al.* 1995), besides mediating most of its effects via  $G_s\alpha$ .

Though some of the studies may not be relevant in physiological settings, as overexpression studies tend to cause enforced coupling, these observations still suggest that receptor- $G\alpha$  coupling could be generally promiscuous. Perhaps there are factors that prevent such promiscuous coupling phenomena from occurring naturally, either by restricting the structural conformations that  $G\alpha$  can adopt or preventing close proximity of  $G\alpha$  with the receptor. Fusing and restraining the  $G\alpha$  protein with the receptor as in a receptor- $G\alpha$  fusion protein, may be one way to relieve these constraints, and allow the manifestation of promiscuity

between the receptor and  $G\alpha$ . Indeed, a  $G_{q\alpha}$  mutant lacking the first 6 amino acids was recently shown to couple with several different  $G_{i/o\alpha}$  or  $G_{s\alpha}$  coupled GPCRs including the  $M_2$  muscarinic,  $D_2$  dopamine,  $A_1$  adenosine, and  $\beta_2$ -adrenergic receptors (Kostenis *et al.* 1997). The N-termini of  $G_{q\alpha}$  and  $G_{11\alpha}$  differ from those of other  $G\alpha$  subunits in that they display a unique, highly conserved 6 aa extension. These residues therefore may play a critical role in constraining the receptor coupling specificity of  $G_{q\alpha}/G_{11\alpha}$  proteins.

A reassessment of current receptor- $G\alpha$  fusion studies will be needed if such a model of promiscuous coupling in receptor- $G\alpha$  fusions is true. If signals from the receptor can be transduced via a receptor-fused  $G\alpha$  that does not normally occur in physiological settings (i.e. via freely interacting  $G\alpha$ ), then this may suggest conformational changes in either or both the receptor and the G protein. Thus, studies based on fusion proteins may not truly reflect the properties of their natural counterparts. These include studies that aim to differentiate subtle differences in receptor coupling with various G proteins (Seifert *et al.* 1998a) and the assessment of agonist efficacy (Wise *et al.* 1997d).

The use of receptor- $G\alpha$  fusion proteins is in its early stages, but has shown much promise judging from the studies done. Using this approach, various groups have shown enhancement of  $G_{s\alpha}$  activation by agonist to a level that can be meaningfully assayed using [ $^{35}$ S]GTP $\gamma$ S binding and high-affinity GTPase assays (Seifert *et al.* 1998a; Chapter 4 of this thesis). Fusion proteins can also be used to overcome the problem of cellular targeting of receptor and G protein in assessing functional interactions, as in the case of acylation-deficient  $G_{i1\alpha}$  (Wise *et al.* 1997b). Furthermore, assessment of agonist efficacy can be done with full knowledge and consideration of the relative stoichiometry of receptor and G protein (Wise *et al.* 1997d). However, the work by Medici *et al.* (1997) has raised serious doubts on the fidelity of signal transduction in receptor- $G\alpha$  fusion studies, and also the role of the C-terminus of  $G\alpha$  in receptor coupling.

In view of the evidence outlined above, this study was designed to address conclusively the G protein coupling specificity of such constructs. The studies detailed in Chapter 3 had shown that the IP prostanoid receptor can couple to a chimeric  $G_{i1}/G_s6\alpha$  protein that contains only the last 6 aa of  $G_s\alpha$  on a  $G_{i1}\alpha$  subunit backbone. Medici *et al.* (1997) had suggested that the role of the C-terminus of  $G\alpha$  is merely to bring the G protein in close proximity with the receptor, but is not directly involved in transducing the signal, and this role can be fulfilled by covalently linking the receptor and G protein. Therefore, a fusion protein between the IP prostanoid receptor and full length  $G_{i1}\alpha$  might be anticipated to allow the generation of a functional signalling protein, even though these two proteins do not interact effectively when independently co-expressed. However, it was decided that a fusion protein between the IP prostanoid receptor and chimeric  $G_{i1}/G_s6\alpha$  should also be constructed, in case promiscuity of coupling did not occur. It would then be useful to study the ability of the C-terminus of  $G_s\alpha$  to restore functional coupling in the FhIPR- $G_{i1}\alpha$  fusion. The cDNAs of these fusion proteins were thus generated and stably transfected into HEK293 cells. The agonist-stimulated response of these fusion proteins in the [ $^{35}$ S]GTP $\gamma$ S binding and high affinity GTPase assays were measured, with the aid of cholera and/or pertussis toxin pretreatment to delineate the  $G\alpha$  involved. The efficiency of coupling between the GPCR and  $G\alpha$  in these proteins was also examined by performing agonist concentration-response studies.

## 5.2 Results

### ***Construction of FhIPR-G<sub>11</sub>α and FhIPR-G<sub>11</sub>/G<sub>s</sub>6α fusion cDNAs***

The construction of cDNAs encoding the FhIPR-G<sub>11</sub>α or FhIPR-G<sub>11</sub>/G<sub>s</sub>6α was similar to that of FhIPR-G<sub>s</sub>α in Chapter 4 and is shown in Figure 5.1. Receptor-Gα ligated mix was transformed into DH5α *E. coli* cells and clones were picked for inoculation into LB mini-cultures. DNAs extracted from these cultures were analysed for the proper incorporation of Gα cDNAs into the pcDNA3 vector containing the FhIPR (no stop codon). Among *E. coli* clones transformed with FhIPR / G<sub>11</sub>α ligation mix, clones I1 and I5 were found to contain a fragment of ~2.2 kilobases when digested with *Hind*III and *Xba*I restriction enzymes (Figure 5.2A). Similar digestion of DNAs from *E. coli* clones transformed with FhIPR/ G<sub>11</sub>/G<sub>s</sub>6α ligation mix indicated clones C1, C2 and C4 contained a similar size fragment (Figure 5.2B). Subsequent DNA sequencing of clones I1 and C1 confirmed the nucleotide sequence of FhIPR-G<sub>11</sub>α and FhIPR-G<sub>11</sub>/G<sub>s</sub>6α respectively.

### ***Characterisation of HEK293 clones stably expressing FhIPR-G<sub>11</sub>α and FhIPR-G<sub>11</sub>/G<sub>s</sub>6α fusion protein***

Transient expression of FhIPR-G<sub>11</sub>α and FhIPR-G<sub>11</sub>/G<sub>s</sub>6α proteins in HEK293 cells resulted in low expression levels as was observed for FhIPR and FhIPR-G<sub>s</sub>α proteins (see Chapters 3 and 4). Selection with geneticin (G-418) was carried out on transfected cells and high expressing clones were selected. A number of these clones are presented in Figure 5.3. HEK293 clones expressing FhIPR-G<sub>11</sub>α at sufficiently high levels for study were Gi9, Gi13, and Gi16; clones expressing FhIPR-G<sub>11</sub>/G<sub>s</sub>6α at appropriately high levels were Gi/Gs10, Gi/Gs14, and Gi/Gs19. The expression levels of these clones were lower than clone 13 and clone 44 which express FhIPR and FhIPR-G<sub>s</sub>α respectively. All the highest expressing HEK293 clones and their expression levels are tabulated in Table 5.1,

based on [<sup>3</sup>H]iloprost (~10 nM) binding studies of 5 independent experiments performed in triplicate:

**Table 5.1** Expression levels of HEK293 clones

Protein expressed	Clone	Receptor level (fmol/mg membrane protein)
FhIPR	13	2957 ± 144
FhIPR-G <sub>s</sub> α	44	1356 ± 143
FhIPR-G <sub>i1</sub> α	Gi16	900 ± 107
FhIPR-G <sub>i1</sub> /G <sub>s6</sub> α	Gi/Gs14	915 ± 118

To avoid confusion among the many clones, all future references to HEK293 cells expressing the various proteins will refer to the highest expressing clones as stated in the table.

Confirmation of the expression of FhIPR-G<sub>i1</sub>α and FhIPR-G<sub>i1</sub>/G<sub>s6</sub>α proteins in the HEK293 clones was shown by immunoblotting with antisera directed against the amino and carboxyl-termini of these proteins. M5 anti-FLAG™ antibody detected the presence of immunoreactive peptides in membranes of HEK293 cells expressing FhIPR-G<sub>s</sub>α, FhIPR-G<sub>i1</sub>α, and FhIPR-G<sub>i1</sub>/G<sub>s6</sub>α (Figure 5.4A). Immunoreactive peptides in cells expressing FhIPR-G<sub>i1</sub>α and FhIPR-G<sub>i1</sub>/G<sub>s6</sub>α migrated at a faster pace than FhIPR-G<sub>s</sub>α. This correlated well with the lower molecular mass of G<sub>i1</sub>α and G<sub>i1</sub>/G<sub>s6</sub>α (both ~41 kDa) compared to G<sub>s</sub>α(L)(HA)(~47 kDa). Furthermore, multiple immunoreactive peptides were observed in these membranes, which may suggest differential N-glycosylation of the fusion proteins.

The carboxyl-termini of FhIPR-G<sub>s</sub>α and FhIPR-G<sub>i1</sub>/G<sub>s6</sub>α were detected by CS antiserum, which is specific for the carboxyl-terminus of G<sub>s</sub>α (Figure 5.4B). This indicates that the FhIPR-G<sub>i1</sub>/G<sub>s6</sub>α protein contains a CS immunoreactive

carboxyl-terminus, which is characteristic of the  $G_{i1}/G_{s6}\alpha$  chimera but not the  $G_{i1}\alpha$  protein (Figure 3.9). The presence of an internal domain of  $G_{i1}\alpha$  was clearly shown in HEK293 cells expressing FhIPR- $G_{i1}\alpha$  and FhIPR- $G_{i1}/G_{s6}\alpha$  (Figure 5.4C). The relative migration of these 3 fusion proteins through 10% SDS-PAGE, as seen in the M5 immunoblot, was again demonstrated in the CS and I1C immunoblots, in that the FhIPR- $G_{s6}\alpha$  protein always migrated at a slower rate than the others.

The agonist binding affinities of FhIPR- $G_{i1}\alpha$  and FhIPR- $G_{i1}/G_{s6}\alpha$  were compared with FhIPR and FhIPR- $G_{s6}\alpha$  using iloprost displacement studies (Figure 5.5). The iloprost binding profile of FhIPR- $G_{i1}\alpha$  mimics closely that of FhIPR- $G_{s6}\alpha$ , with almost identical  $K_d$  values when applying the formalism of DeBlasi *et al.* (1989): FhIPR- $G_{i1}\alpha$  ( $1.5 \pm 0.7$  nM), FhIPR- $G_{s6}\alpha$  ( $1.4 \pm 0.6$  nM). In contrast, the [ $^3$ H]iloprost displacement curve of FhIPR- $G_{i1}/G_{s6}\alpha$  was moved to the right ( $K_d = 8.5 \pm 2.2$  nM) and is significantly different from the other fusion proteins (unpaired t-test;  $p < 0.05$ ;  $n = 3$ ). The Hill coefficients of the agonist displacement curves of all 3 fusion proteins are very similar and are significantly higher than the IP prostanoid receptor.

Cells expressing FhIPR- $G_{i1}\alpha$  or FhIPR- $G_{i1}/G_{s6}\alpha$  were able to activate adenylate cyclase in a dose-dependent manner upon stimulation by iloprost (Figure 5.6). These effects of iloprost, were however less potent when compared to the response observed in cells expressing the FhIPR- $G_{s6}\alpha$  protein; iloprost activity in cells expressing FhIPR- $G_{i1}\alpha$  is at least 5 fold less potent, while that of FhIPR- $G_{i1}/G_{s6}\alpha$  is 2 fold less potent (unpaired t-test;  $p < 0.05$  in both proteins). As the receptor-linked  $G\alpha$  in both fusion proteins cannot have an activating effect on adenylate cyclase, it is presumably the endogenous  $G_{s6}\alpha$  that is involved in signalling to the enzyme. In Chapter 4, the FhIPR- $G_{s6}\alpha$  protein was shown to downregulate endogenous  $G_{s6}\alpha$  upon long-term treatment with iloprost (Figure 4.7A), although a similar experiment was not performed using HEK293 cells

expressing FhIPR-G<sub>11</sub>α or FhIPR-G<sub>11</sub>/G<sub>s</sub>6α. While it may be argued that the Gβγ complex could be involved in activating adenylate cyclase, this would still require G<sub>s</sub>α, as it is a pre-requisite for Gβγ activation of adenylate cyclase (Tang *et al.* 1991). Thus, endogenous G<sub>s</sub>α is likely to be activated by all the FhIPR-Gα fusions.

***Cells expressing FhIPR-G<sub>11</sub>/G<sub>s</sub>6α but not FhIPR-G<sub>11</sub>α exhibit enhanced GTP exchange and hydrolysis activities***

In previous chapters, the activation of Gα by the IP prostanoid receptor or the FhIPR-G<sub>s</sub>α was investigated by [<sup>35</sup>S]GTPγS binding and high affinity GTPase assays, together with the use of cholera and pertussis toxins to delineate between G<sub>s</sub>α and G<sub>i</sub>α signalling. Using the same approach, cells expressing FhIPR-G<sub>11</sub>α or FhIPR-G<sub>11</sub>/G<sub>s</sub>6α were pretreated with either cholera toxin, pertussis toxin, or a combination of both. Membranes made from these toxin-treated cells were assessed together with membranes from untreated cells for their capacity to activate Gα subunits.

Agonist-stimulated binding of [<sup>35</sup>S]GTPγS was clearly enhanced in cells expressing the FhIPR-G<sub>11</sub>/G<sub>s</sub>6α when compared to FhIPR expressing cells, and was not abolished by either cholera toxin, pertussis toxin or a combination of both (Figure 5.7). This observation was previously noted in FhIPR expressing cells (clone 13) transiently transfected with G<sub>11</sub>/G<sub>s</sub>6α protein (Figure 3.14). Therefore, covalently linking the chimeric G<sub>11</sub>/G<sub>s</sub>6α protein to the IP prostanoid receptor did not alter its characteristics. Fusing the G<sub>11</sub>α protein to the receptor, as in the FhIPR-G<sub>11</sub>α fusion protein, reduced the overall level of Gα activation as shown by the small level of [<sup>36</sup>S]GTPγS bound in the presence of iloprost. This small level of [<sup>35</sup>S]GTPγS binding was completely abolished when the cells were pretreated with cholera toxin or a combination of both cholera and pertussis toxin, but not pertussis toxin alone (Figure 5.7).

A very similar scenario was observed when the same membranes were assayed for basal and agonist-stimulated high affinity GTPase activity (Figure 5.8). Iloprost-stimulated high affinity GTPase activity was at least 4 times higher in cells expressing FhIPR-G<sub>11</sub>/G<sub>s</sub>6 $\alpha$  than FhIPR (unpaired t-test:  $p < 0.05$ ;  $n = 3$ ) and 2 times higher than cells expressing FhIPR-G<sub>s</sub> $\alpha$  (unpaired t-test:  $p < 0.05$ ;  $n = 3$ ). As observed in the [<sup>35</sup>S]GTP $\gamma$ S binding assay, pretreatment with neither cholera nor pertussis toxin removed the agonist-stimulated activity. Similarly, cells expressing FhIPR-G<sub>11</sub> $\alpha$  did not produce robust elevation of agonist-stimulated GTPase, and pretreatment with cholera but not pertussis toxin completely removed this low level of activity. This small level of agonist-stimulated G $\alpha$  activity is thus very likely to be contributed by endogenous G<sub>s</sub> $\alpha$  subunits. When the GTPase result was analysed in combination with the [<sup>35</sup>S]GTP $\gamma$ S binding assay, it is apparent that the intrinsic property of the receptor-fused G $\alpha$  was not altered for the FhIPR-G<sub>11</sub>/G<sub>s</sub>6 $\alpha$  and FhIPR-G<sub>11</sub> $\alpha$  proteins.

***Comparison of iloprost stimulated activity in FhIPR-G<sub>s</sub> $\alpha$  and FhIPR-G<sub>11</sub>/G<sub>s</sub>6 $\alpha$  fusion protein expressing cells***

The time-course of agonist-stimulated [<sup>35</sup>S]GTP $\gamma$ S binding in cells expressing FhIPR-G<sub>s</sub> $\alpha$  and FhIPR-G<sub>11</sub>/G<sub>s</sub>6 $\alpha$  was studied in greater detail as both gave higher activity than the FhIPR. Over a period of 120 minutes, cells expressing FhIPR-G<sub>s</sub> $\alpha$  and FhIPR-G<sub>11</sub>/G<sub>s</sub>6 $\alpha$  stimulate [<sup>35</sup>S]GTP $\gamma$ S binding in a seemingly linear fashion and are not significantly different from each other (Figure 5.9). This confirmed that the observations noted earlier (Figure 5.7), performed at an incubation time of 60 min, are representative of their activity and did not arise from selective sampling at a particular incubation time. The iloprost dose-response of [<sup>35</sup>S]GTP $\gamma$ S binding indicates that the FhIPR-G<sub>11</sub>/G<sub>s</sub>6 $\alpha$  is less responsive to agonist stimulation as its EC<sub>50</sub> is 30 times higher than FhIPR-G<sub>s</sub> $\alpha$  (Figure 5.10). In addition, the iloprost activation profile of G<sub>11</sub>/G<sub>s</sub>6 $\alpha$  ( $n_H = 1.6 \pm 0.2$ ) is more steep than FhIPR-G<sub>s</sub> $\alpha$  ( $n_H = 0.9 \pm 0.1$ ).

The time course of iloprost-stimulated high affinity GTPase in cells expressing FhIPR-G<sub>s</sub>α and FhIPR-G<sub>i1</sub>/G<sub>s</sub>6α was also investigated and showed that the FhIPR-G<sub>i1</sub>/G<sub>s</sub>6α expressing cells consistently gave more robust activity (Figure 5.11). In both sets of cells, the increase in GTPase activity starts to plateau off after 30 min stimulation, contrary to the steady increase in [<sup>35</sup>S]GTPγS binding for up to 120 min. (Figure 5.9). A possible reason for this difference is the rapid denaturation of protein in the GTPase assay which was incubated at 37°C, compared to the lower incubation temperature for the [<sup>35</sup>S]GTPγS binding assay (at 25°C). Taking this into consideration, an incubation time of 20 min was used for all GTPase assays in this study. Iloprost concentration response studies again show that FhIPR-G<sub>i1</sub>/G<sub>s</sub>6α is less responsive to agonist stimulation than FhIPR-G<sub>s</sub>α (Figure 5.12), although the difference in their EC<sub>50</sub> values (16 fold) is less than that in the [<sup>35</sup>S]GTPγS binding assay (Figure 5.10).

As the hydrolysis of GTP to GDP and Pi (inorganic phosphate) is an enzymatic reaction (the Gα being the enzyme), it is possible to determine the maximum activity ( $V_{max}$ ) and Michaelis Menton Constant ( $K_m$ ) of this process by varying the substrate (GTP) concentration. Such enzyme kinetic measurements would show up any subtle differences in their maximum hydrolysing capacity and substrate affinity. By diluting [<sup>32</sup>P]GTP with increasing concentrations of unlabelled GTP and assessing basal and iloprost (1 μM)-stimulated high affinity GTPase activity, direct plots of the GTPase activity versus GTP concentrations were obtained for cells expressing FhIPR, FhIPR-G<sub>s</sub>α, and FhIPR-G<sub>i1</sub>/G<sub>s</sub>6α (Figure 5.13 A, B & C). When the graph was extrapolated to infinite substrate concentration, maximum activity ( $V_{max}$ ) could be obtained, while the Michaelis Menton constant,  $K_m$ , could be read off the x-axis at half maximal activity. However, such linear plots of the activity-substrate concentration profile are prone to error due to the grouping of data at the lower end of the scale and the difficulty in extrapolation. Hence, other plots like the Lineweaver-Burke plot (also known as the double reciprocal plot i.e. velocity<sup>-1</sup> versus substrate<sup>-1</sup>) or the Eadie-Hofstee plot (velocity versus velocity/substrate) are more commonly employed. From the

Eadie-Hofstee plots of cells expressing FhIPR, FhIPR-G<sub>s</sub>α, and FhIPR-G<sub>i1</sub>/G<sub>s</sub>6α (Figures 5.14 A, B & C), K<sub>m</sub> and V<sub>max</sub> values were obtained and tabulated into Table 5.2:

**Table 5.2** K<sub>m</sub> and V<sub>max</sub> values of HEK293 cells expressing FhIPR, FhIPR-G<sub>s</sub>α and FhIPR-G<sub>i1</sub>/G<sub>s</sub>6α. These results represent the means ± SEM of 3 or more independent experiments performed in triplicate.

Protein	Basal K <sub>m</sub> (μM)	Agonist-stimulated K <sub>m</sub> (μM)	V <sub>max</sub> (pmol/min/mg)
FhIPR	0.49 ± 0.03	0.48 ± 0.04	7.3 ± 0.6
FhIPR-G <sub>s</sub> α	0.52 ± 0.02	0.67 ± 0.03	18.0 ± 2.2
FhIPR-G <sub>i1</sub> /G <sub>s</sub> 6α	0.64 ± 0.03	0.63 ± 0.03	19.3 ± 2.3

The results indicated that the V<sub>max</sub> of FhIPR-G<sub>s</sub>α and FhIPR-G<sub>i1</sub>/G<sub>s</sub>6α are significantly higher than that of FhIPR (unpaired t-test: p<0.05). Interestingly, while both the basal and agonist-stimulated K<sub>m</sub> of cells expressing FhIPR and FhIPR-G<sub>i1</sub>/G<sub>s</sub>6α are similar (Figure 5.14A & C), the iloprost-stimulated K<sub>m</sub> of cells expressing the FhIPR-G<sub>s</sub>α protein is slightly higher than its basal K<sub>m</sub> (Figure 5.14B). This could give rise to higher agonist-stimulated GTPase activities when the assay is performed at GTP concentrations greater than 0.5 μM, the concentration used in routine assays. This altered K<sub>m</sub> of FhIPR-G<sub>s</sub>α also contributes to give a V<sub>max</sub> value close to that of FhIPR-G<sub>i1</sub>/G<sub>s</sub>6α (Table 5.2). As basal GTPase activity is mainly derived from "G<sub>i</sub>α-like" proteins (Gierschik *et al.* 1994), the altered K<sub>m</sub> of FhIPR-G<sub>s</sub>α likely reflects the activation of non-"G<sub>i</sub>α-like" subunits, which are the endogenous and receptor-linked G<sub>s</sub>α (Chapter 4).

**Figure 5.1 Schematic representation of FhIPR-G<sub>i1</sub>α and FhIPR-G<sub>i1</sub>/G<sub>s</sub>6α fusion proteins**

The last 6 residues of the receptor, and the first and last 6 residues of Gα are shown. There is an alteration of cysteine to glutamic acid at the last residue of the receptor due to the incorporation of a *Xho*I site, required for subsequent ligation with the open reading frame of G<sub>i1</sub>α and G<sub>i1</sub>/G<sub>s</sub>6α.

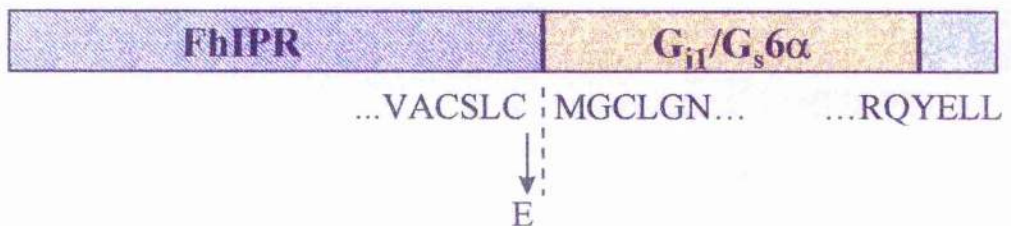
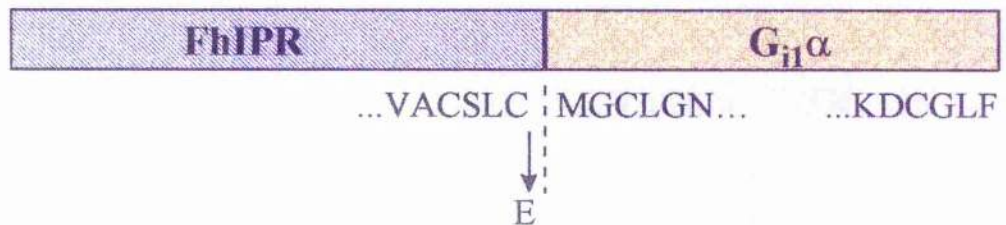


**Figure 5.2 Agarose gel analysis of FhIPR-G<sub>i1</sub>α and FhIPR-G<sub>i1</sub>/G<sub>s6</sub>α cDNAs**

**A.** DNAs from *E. coli* clones (transformed with ligated FhIPR / G<sub>i1</sub>α mix) were digested with *Hind*III and *Xba*I and resolved on a 1% agarose gel. Clones I1 and I5 contain a digested fragment close to the approximate length of 2.2 kb of the FhIPR-G<sub>i1</sub>α cDNA.

**B.** DNAs from *E. coli* clones (transformed with ligated FhIPR / G<sub>i1</sub>/G<sub>s6</sub>α mix) were similarly digested and resolved. Clones C1, C2 and C4 contain a digested fragment close to the approximate length of 2.2 kb of the FhIPR-G<sub>i1</sub>/G<sub>s6</sub>α cDNA.

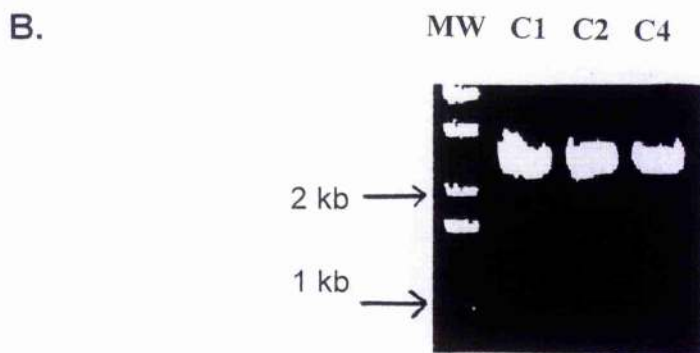
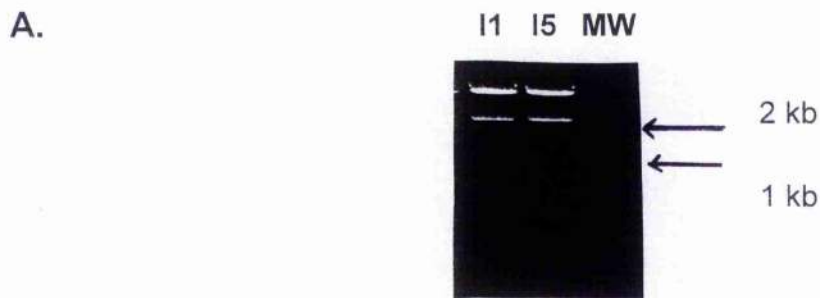


**Figure 5.3 Stable expression of the FhIPR-G<sub>i1</sub> $\alpha$  or FhIPR-G<sub>i1</sub>/G<sub>s6</sub> $\alpha$  fusion proteins in clones of HEK293 cells**

Following stable expression of the FhIPR-G<sub>i1</sub> $\alpha$  or FhIPR-G<sub>i1</sub>/G<sub>s6</sub> $\alpha$  cDNAs into HEK293 cells, membranes from clones expressing FhIPR-G<sub>i1</sub> $\alpha$ : Gi9, Gi13 and Gi16, and clones expressing FhIPR-G<sub>i1</sub>/G<sub>s6</sub> $\alpha$ : Gi/Gs10, Gi/Gs14, and Gi/Gs19, together with clone 13 and clone 44 cells were prepared and assessed using ~10 nM [<sup>3</sup>H]iloprost. The specific binding of [<sup>3</sup>H]iloprost was obtained by subtracting non-specific counts (assessed with 10  $\mu$ M unlabelled iloprost) from total counts, and normalised with the amount of membrane protein used in the assay. This graph is representative of 2 or more experiments performed in triplicate.

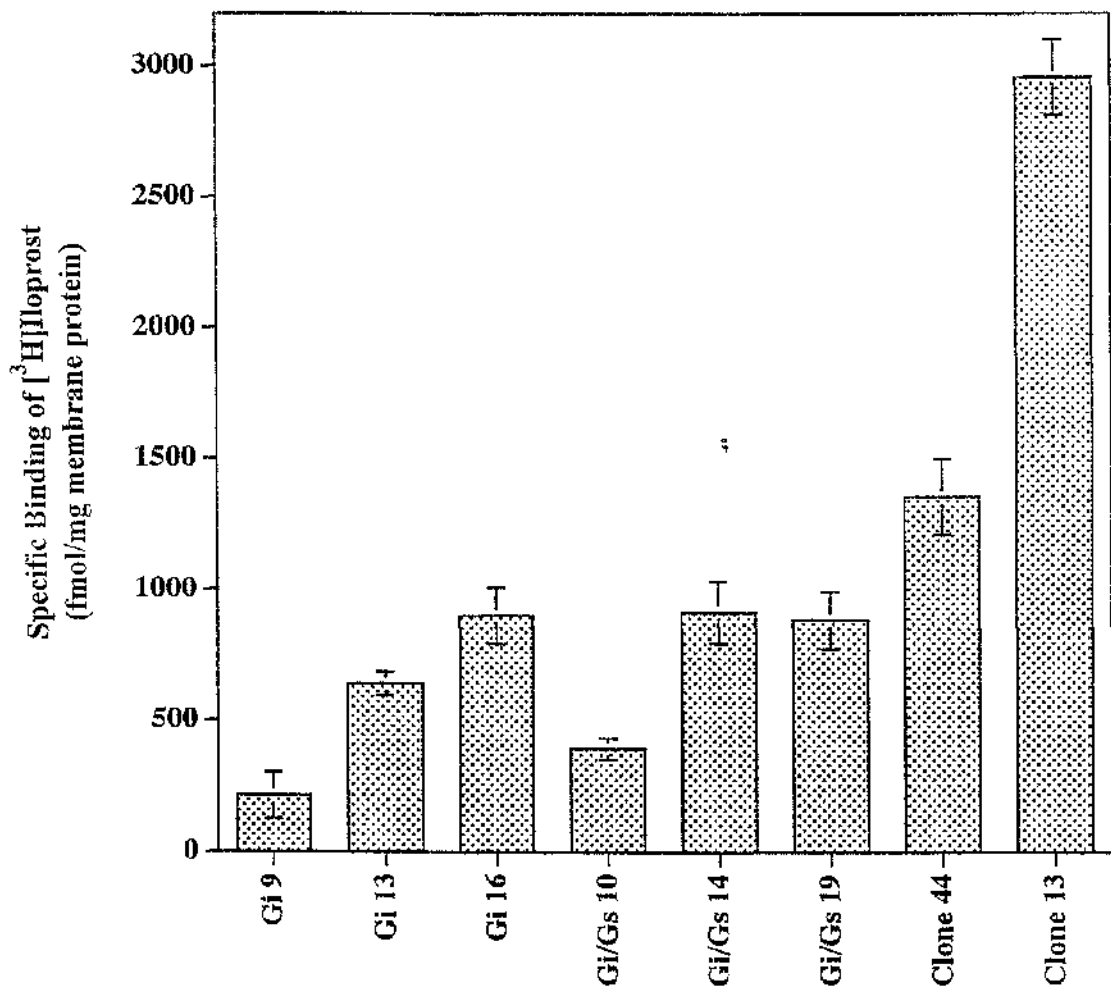
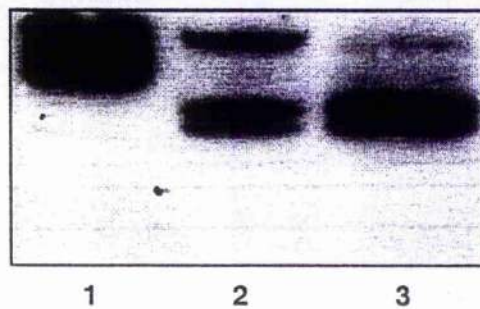


#### **Figure 5.4 Immunodetection of FhIPR-G $\alpha$ fusion proteins**

Membranes of HEK293 clones expressing FhIPR-G<sub>s</sub> $\alpha$  (lane 1), FhIPR-G<sub>i1</sub> $\alpha$  (lane 2), and FhIPR-G<sub>i1</sub>/G<sub>s6</sub> $\alpha$  (lane 3) were resolved in 10% SDS-PAGE, transferred to nitrocellulose membrane and immunoblotted with various antisera.

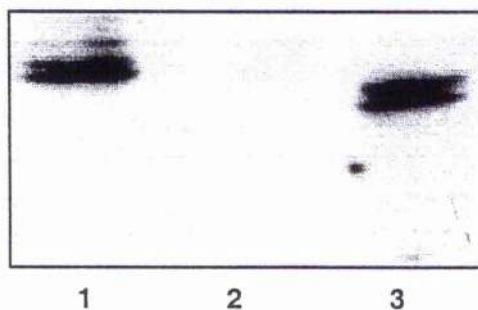
- A.** Immunoblotting with M5 anti-FLAG<sup>™</sup> monoclonal antibody indicated multiple immunoreactive proteins that migrated with apparent molecular mass of 89 kDa in lane 1. M5 immunoreactive proteins in lanes 2 and 3 were observed to co-migrate at a faster pace than lane 1.
- B.** Immunoblotting with CS antiserum, which is specific against the carboxyl-terminal decapeptide of G<sub>s</sub> $\alpha$ , detected the same immunoreactive proteins seen in Figure A, but only in lanes 1 and 3.
- C.** Immunoblotting with I1C antiserum, which is specific against an internal domain (159-168 aa) of G<sub>i1</sub> $\alpha$ , also detected the same immunoreactive proteins seen in Figure A, but only in lanes 2 and 3.

**A**



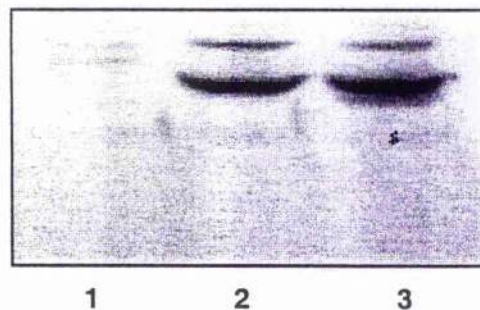
**FLAG**

**B**



**CS**

**C**

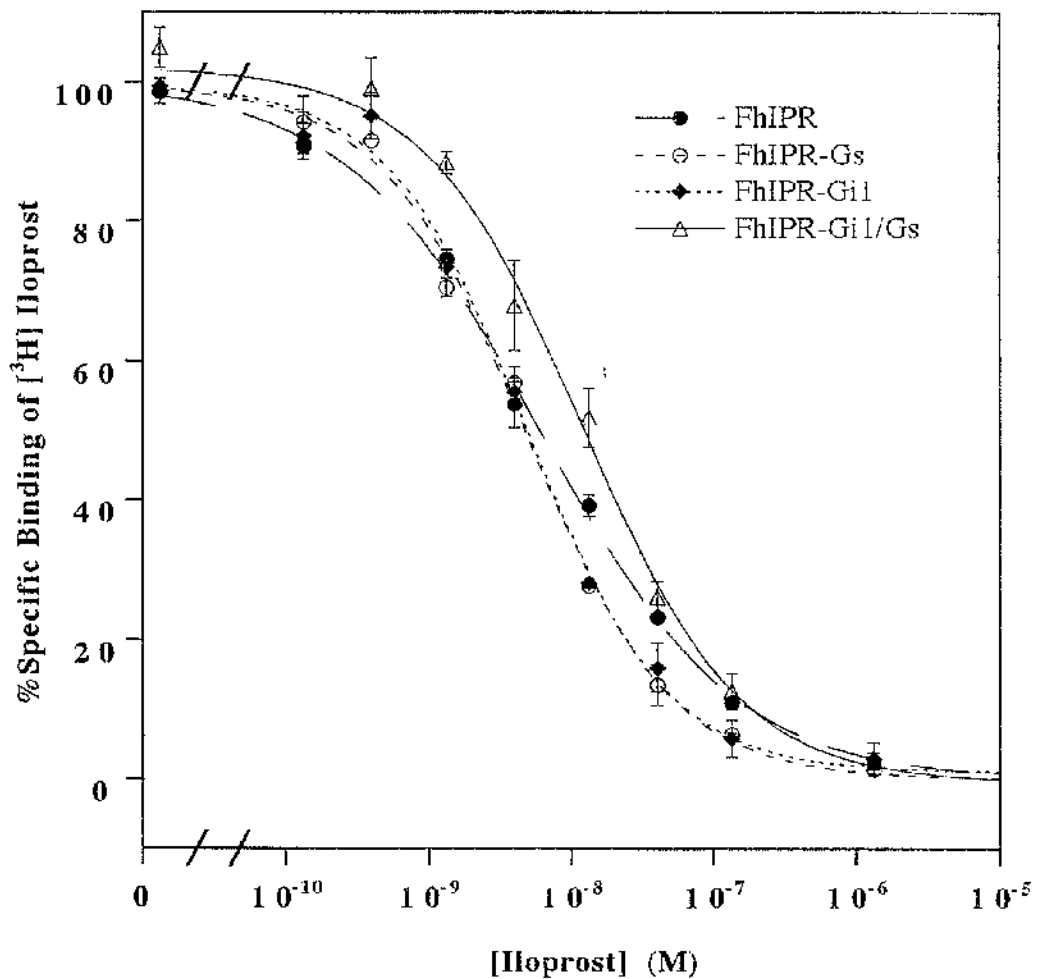


**I1C**

- 1) FhIPR-G<sub>s</sub>α
- 2) FhIPR-G<sub>i1</sub>α
- 3) FhIPR-G<sub>i1</sub>/G<sub>s</sub>6α

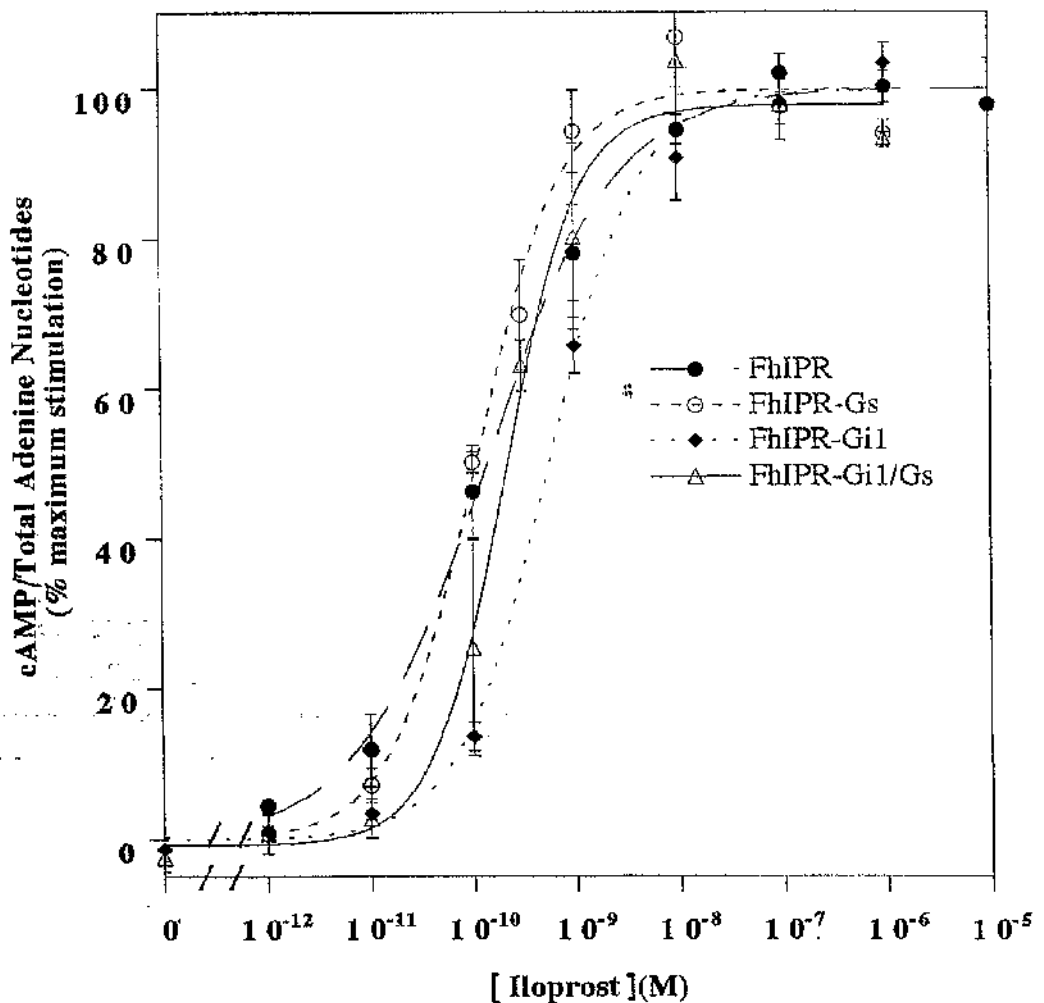
**Figure 5.5 Displacement of [<sup>3</sup>H]iloprost binding in membranes of HEK293 clones stably expressing FhIPR and FhIPR-G $\alpha$  fusion proteins**

The specific binding of [<sup>3</sup>H]iloprost (3.4 nM) to membranes of HEK293 clones stably expressing FhIPR-G<sub>11</sub> $\alpha$  and FhIPR-G<sub>11</sub>/G<sub>s</sub>6 $\alpha$  were displaced by increasing concentrations of unlabelled iloprost as in Figure 4.5. Results of FhIPR and FhIPR-G<sub>s</sub> $\alpha$  were obtained from Figure 4.5 and Figure 3.4. The IC<sub>50</sub> of FhIPR-G<sub>11</sub> $\alpha$  was estimated as 4.9  $\pm$  0.6 nM and Hill slope at 0.89  $\pm$  0.09, while the IC<sub>50</sub> of FhIPR-G<sub>11</sub>/G<sub>s</sub>6 $\alpha$  was estimated as 11.9  $\pm$  2.2 nM and Hill slope at 0.79  $\pm$  0.11. Results are presented as %specific binding of [<sup>3</sup>H]iloprost (100% = specific binding in the absence of unlabelled iloprost). This graph is representative of 3 independent experiments performed in triplicate.



**Figure 5.6 Adenylate cyclase concentration-response for iloprost**

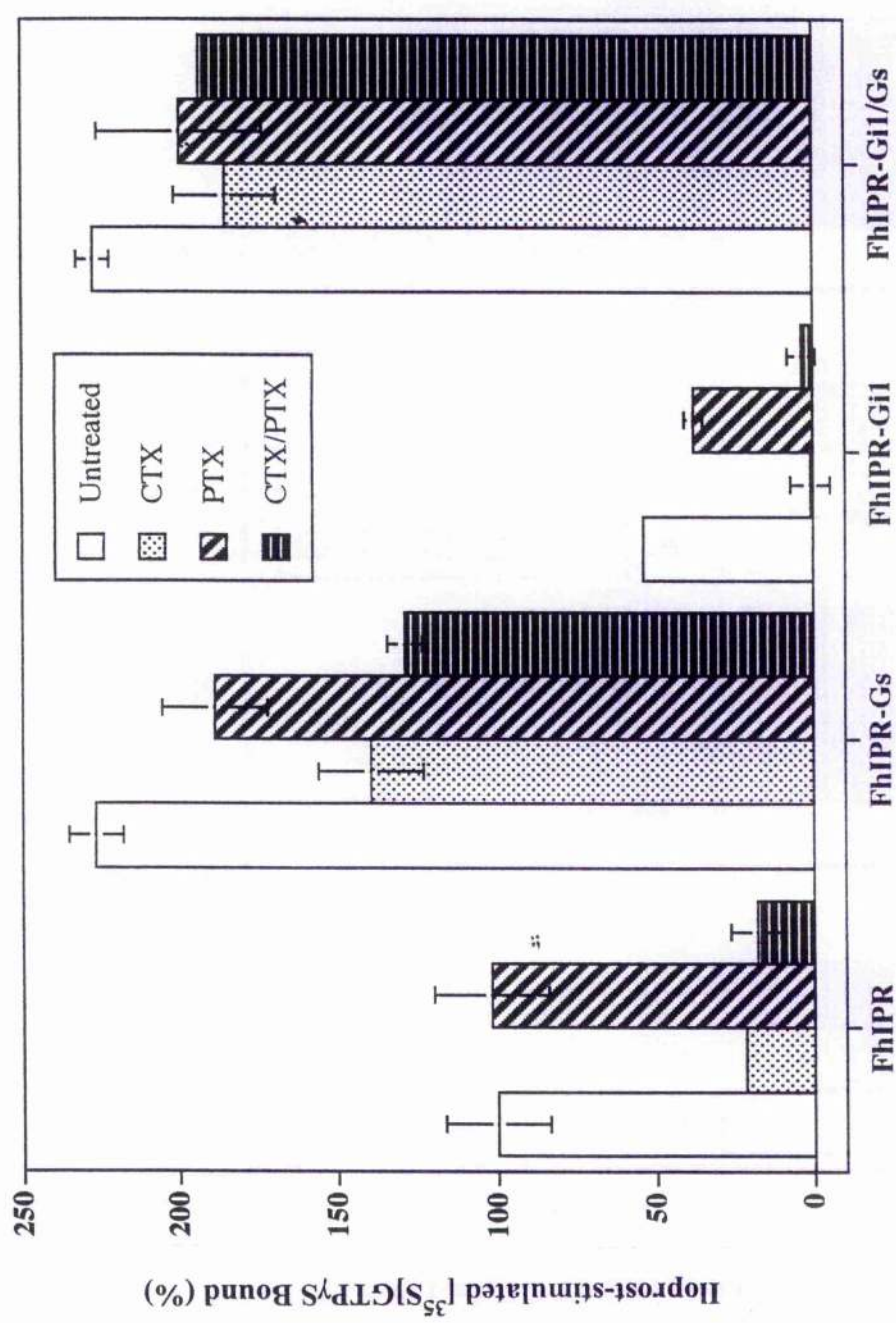
Intact cells of HEK293 clones stably expressing the various proteins were assessed for their ability to stimulate adenylate cyclase at various concentrations of iloprost. The results are calculated as the ratio of cAMP over total adenine nucleotides ( $\times 100$ ) but expressed as % maximum stimulation (activity at  $1 \mu\text{M}$  iloprost treated as 100%). Results of cells expressing FhIPR and FhIPR- $G_{s\alpha}$  were obtained from Figure 4.15.  $EC_{50}$  of iloprost activity in cells expressing FhIPR- $G_{i1\alpha}$  is estimated as  $5.5 \pm 0.8 \times 10^{-10}$  M and that of cells expressing FhIPR- $G_{i1}/G_{s6\alpha}$  is estimated as  $2.1 \pm 0.3 \times 10^{-10}$  M. This graph is representative of 3 independent experiments performed in triplicate.



**Figure 5.7 Effects of cholera and pertussis toxins on agonist-stimulated [<sup>35</sup>S]GTP<sub>γ</sub>S binding in HEK293 clones expressing FhIPR and FhIPR-G<sub>α</sub> fusion proteins**

HEK293 clones expressing FhIPR and various FhIPR-G<sub>α</sub> fusion proteins were treated with cholera toxin (200 ng/ml), pertussis toxin (25 ng/ml) or a combination of both for 16 h before harvest. Membranes from these and untreated cells were assayed for basal and iloprost (1 μM)-stimulated binding of [<sup>35</sup>S]GTP<sub>γ</sub>S. The stimulations produced by iloprost (fmol [<sup>35</sup>S]GTP<sub>γ</sub>S bound / mg membrane protein) are expressed as %stimulation (100% = [<sup>35</sup>S]GTP<sub>γ</sub>S bound in cells expressing FhIPR).

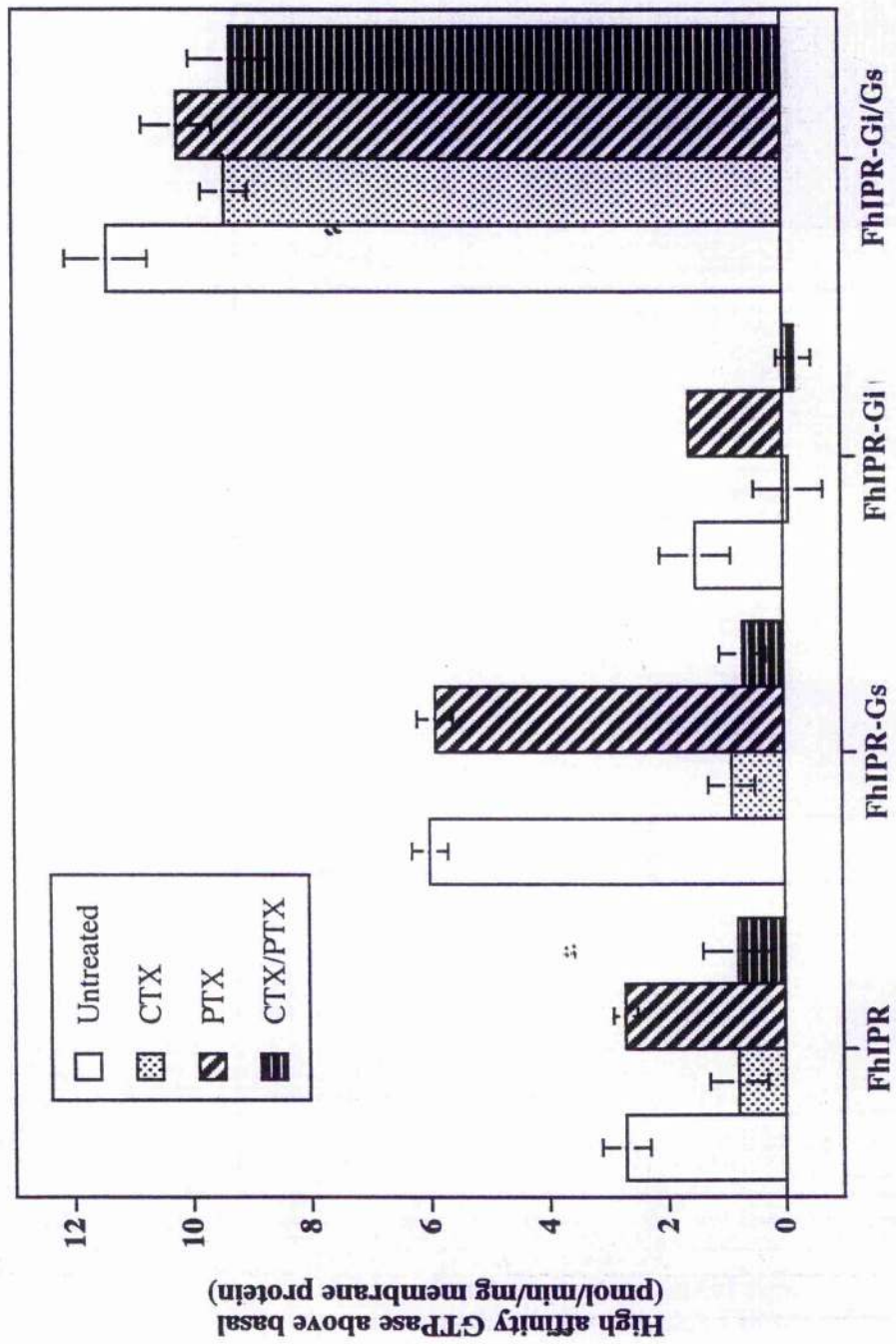
The results for cells expressing FhIPR and FhIPR-G<sub>s</sub>α were obtained from Figure 4.10, with the exception of combined toxins treatment: FhIPR (17.8 ± 8.5) and FhIPR-G<sub>s</sub>α (129 ± 5.5). The results for cells expressing FhIPR-G<sub>i1</sub>α are: untreated (53.8 ± 0.2), cholera toxin (0.9 ± 6.2), pertussis toxin (37.8 ± 3), and combined toxins (3.6 ± 4.4). Results of cells expressing FhIPR-G<sub>i1</sub>/G<sub>s</sub>6α are: untreated (227.1 ± 5.3), cholera toxin (185.2 ± 16.1), pertussis toxin (199.6 ± 26.2), and combined toxins (193.3 ± 1.1). These data represent the means of 3 independent experiments ± SEM, performed in triplicate.



**Figure 5.8 Effects of cholera and pertussis toxins on agonist-stimulated high affinity GTPase activity in HEK293 clones expressing FhIPR and FhIPR-G $\alpha$  fusion proteins**

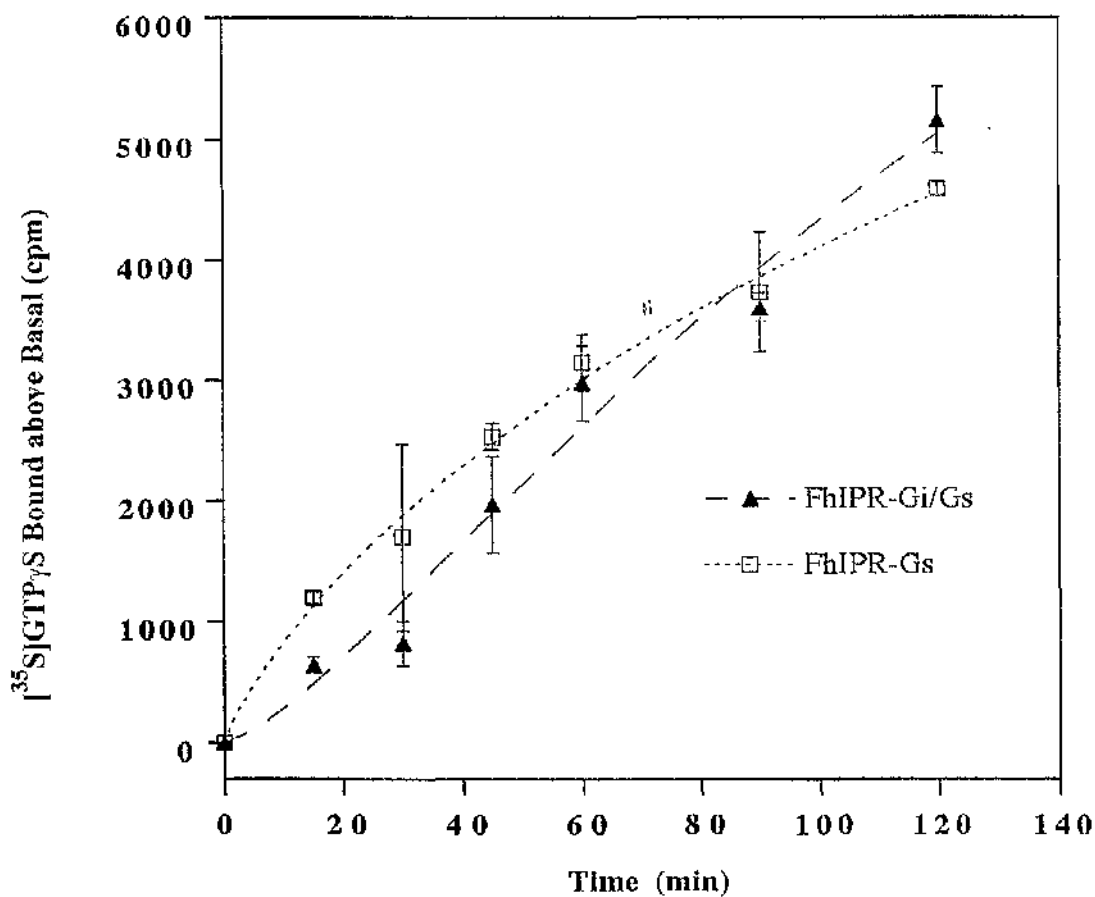
Membranes from Figure 5.7 were used to measure basal high affinity GTPase activity and its stimulation by iloprost (1  $\mu$ M). The stimulations produced by iloprost (mean  $\pm$  SEM pmol/min/mg membrane protein) are presented.

Results for cells expressing FhIPR and FhIPR-G $\alpha$  were obtained from Figure 4.8, with the exception of combined toxins treatment: FhIPR (0.8  $\pm$  0.5) and FhIPR-G $\alpha$  (0.7  $\pm$  0.4). The results for cells expressing FhIPR-G $\alpha$  are: untreated (2.0  $\pm$  0.6), cholera toxin (-0.2  $\pm$  0.6), pertussis toxin (1.6  $\pm$  0.1), and combined toxins (-0.2  $\pm$  0.3). Results of cells expressing FhIPR-G $\alpha$ /G $\beta$  are: untreated (11.4  $\pm$  0.7), cholera toxin (9.4  $\pm$  0.4), pertussis toxin (10.2  $\pm$  0.6), and combined toxins (9.3  $\pm$  0.7). These data represent the means of 3 or more independent experiments performed in triplicate.



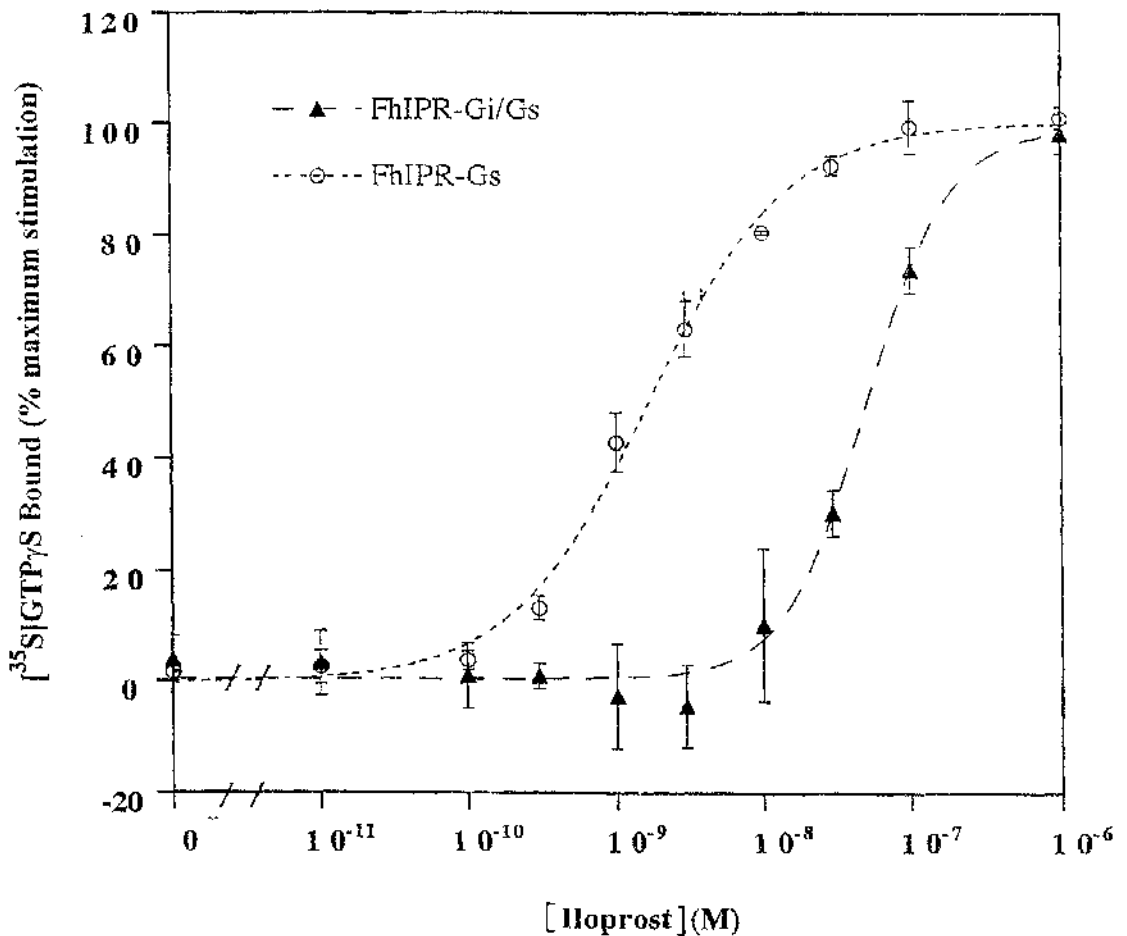
**Figure 5.9** Time course of agonist-stimulated [ $^{35}$ S]GTP $\gamma$ S binding in HEK293 clones expressing FhIPR-G $_s\alpha$  and FhIPR-G $_{i1}/G_{s6\alpha}$

Membranes of HEK293 cells stably expressing FhIPR-G $_s\alpha$  and FhIPR-G $_{i1}/G_{s6\alpha}$  (pretreated with a combination of 200 ng/ml cholera and 25 ng/ml pertussis toxins for 16 h) were assessed for their incorporation of [ $^{35}$ S]GTP $\gamma$ S at various incubation times (0, 15, 30, 45, 60, 90 and 120 min) in the absence (basal) and presence of iloprost (1  $\mu$ M). Levels of agonist-stimulated [ $^{35}$ S]GTP $\gamma$ S binding are presented as cpm / assay (20  $\mu$ g membrane protein per assay). This graph is representative of 2 independent experiments performed in triplicate.



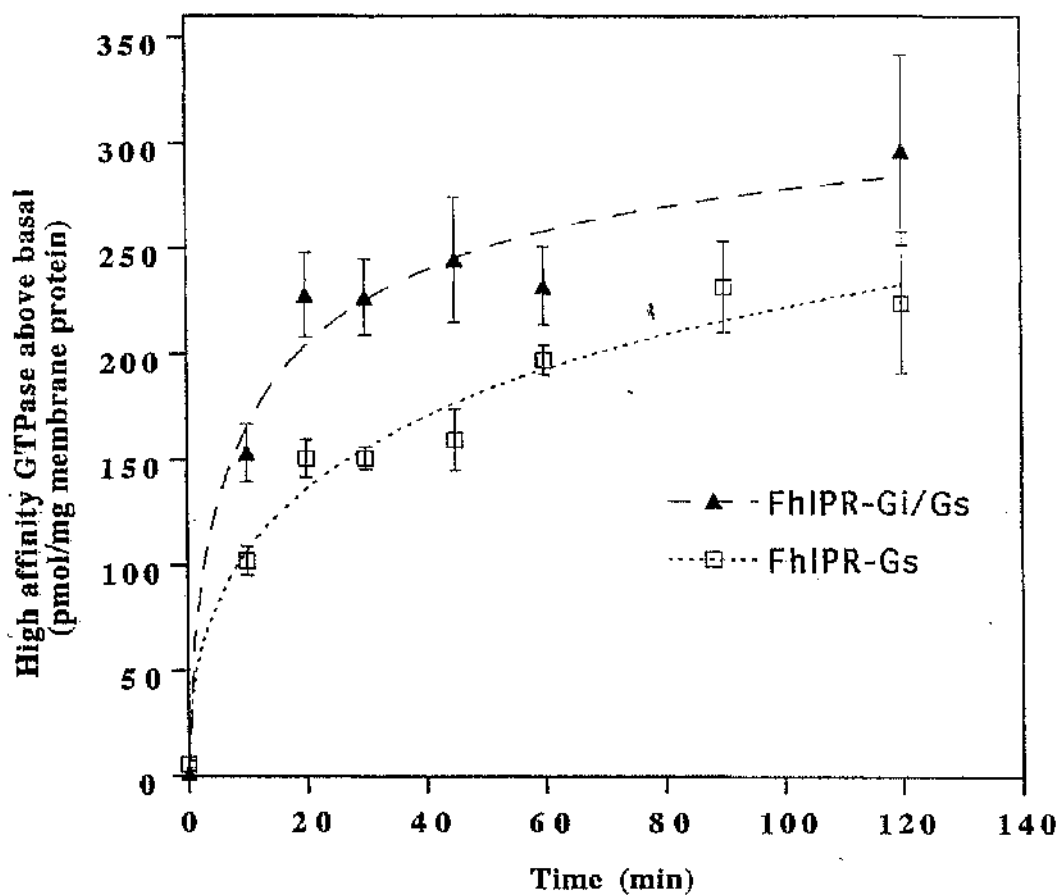
**Figure 5.10 Iloprost concentration-response of [<sup>35</sup>S]GTP<sub>γ</sub>S binding in HEK293 clones expressing FhIPR-G<sub>s</sub>α and FhIPR-G<sub>i1</sub>/G<sub>s</sub>6α fusion proteins**

Membranes from Figure 5.9 were assessed for their ability to incorporate [<sup>35</sup>S]GTP<sub>γ</sub>S at various concentrations of iloprost. The stimulations produced by iloprost are expressed as %maximum stimulation (activity at 1 μM iloprost treated as 100%). EC<sub>50</sub> of iloprost stimulated [<sup>35</sup>S]GTP<sub>γ</sub>S binding in cells expressing FhIPR-G<sub>s</sub>α is estimated as 1.7 ± 0.2 nM and that of cells expressing FhIPR-G<sub>i1</sub>/G<sub>s</sub>6α is estimated as 50.6 ± 5.3 nM. This graph is representative of 3 or more independent experiments performed in triplicate.



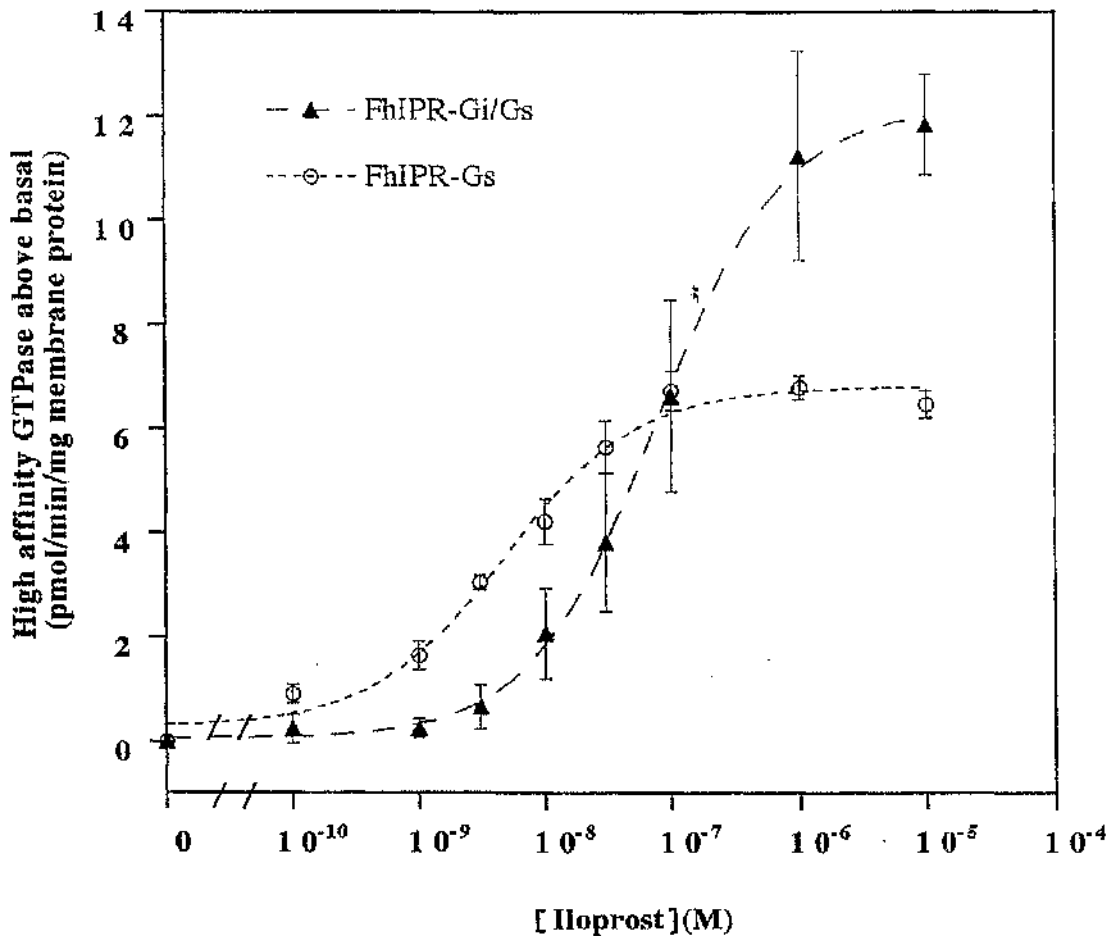
**Figure 5.11 Time course of high affinity GTPase activity in HEK293 clones expressing FhIPR-G<sub>s</sub>α and FhIPR-G<sub>i1</sub>/G<sub>s</sub>6α**

Membranes of HEK293 cells stably expressing FhIPR-G<sub>s</sub>α and FhIPR-G<sub>i1</sub>/G<sub>s</sub>6α (pretreated by a combination of cholera and pertussis toxins as in Figure 5.9) were assessed for their basal and iloprost (1 μM)-stimulated high affinity GTPase activity at various incubation times (0, 10, 20, 30, 45, 60, 90 and 120 min). Levels of iloprost-stimulated GTPase activity are presented as pmol Pi / mg membrane protein. This graph is representative of 2 independent experiments performed in triplicate.



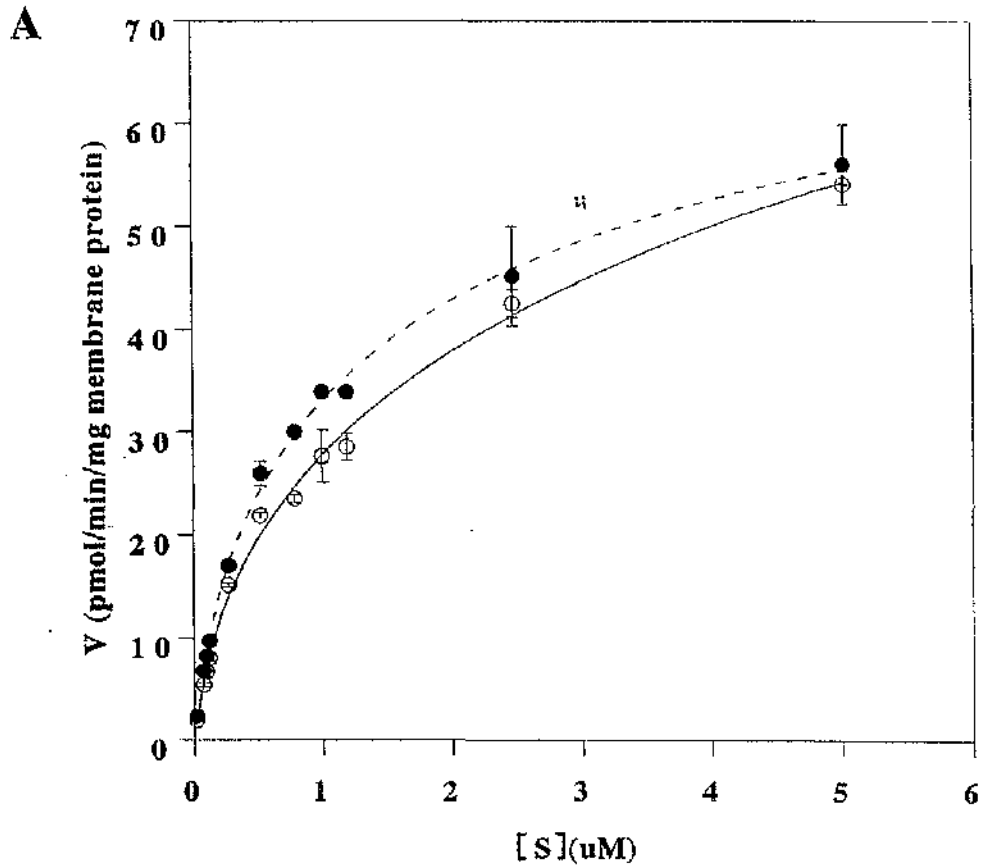
**Figure 5.12 Iloprost concentration-response of high affinity GTPase activity in HEK293 clones expressing FhIPR-G<sub>s</sub>α and FhIPR-G<sub>11</sub>/G<sub>s</sub>6α fusion proteins**

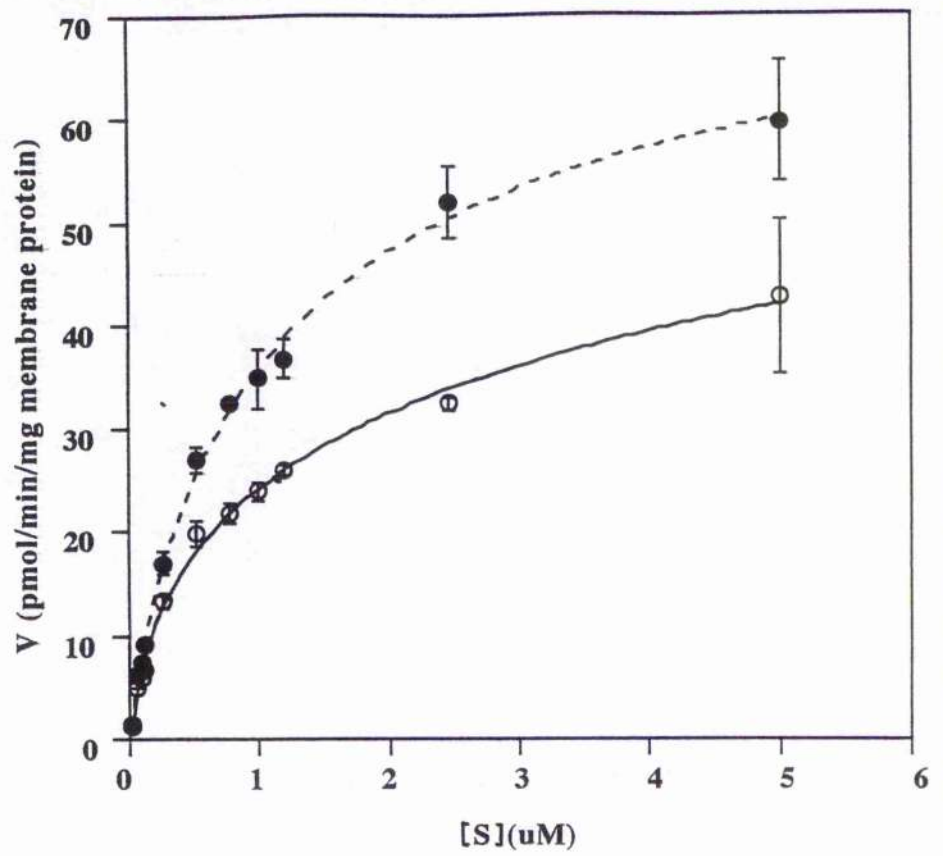
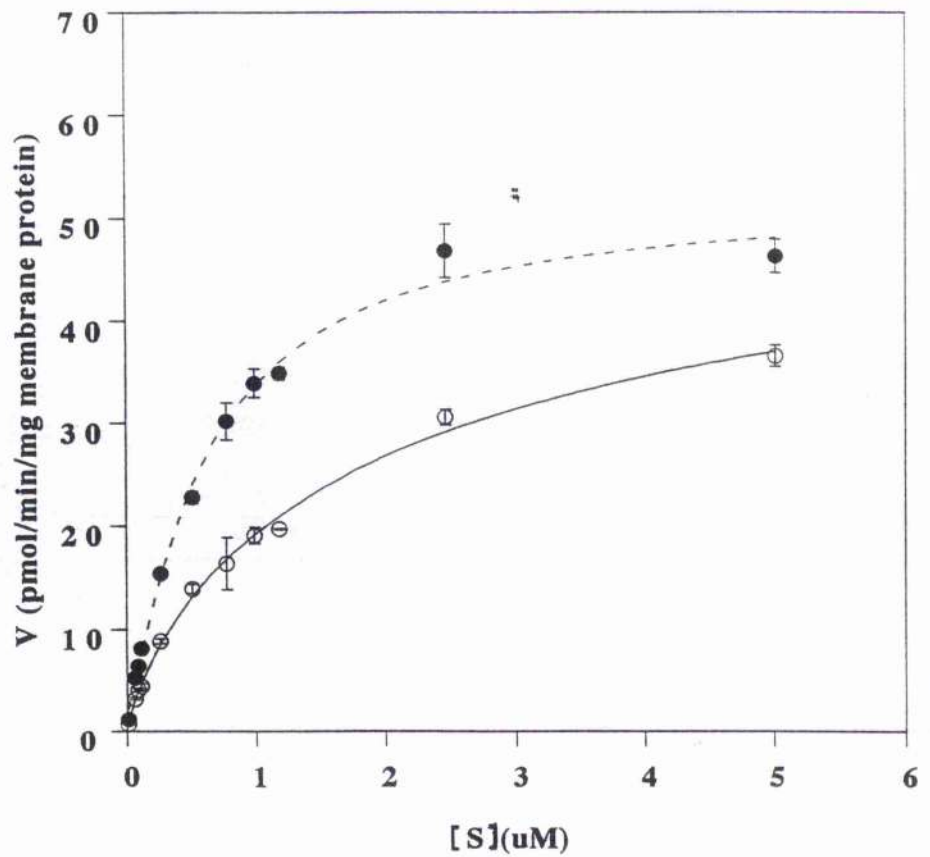
Membranes from Figure 5.11 were assessed for their ability to stimulate high affinity GTPase activity at various concentrations of iloprost. The stimulations produced by iloprost are expressed as % maximum stimulation (100% = activity at 10 μM iloprost). EC<sub>50</sub> of iloprost-stimulated GTPase activity in cells expressing FhIPR-G<sub>s</sub>α is estimated as 4.8 ± 1.2 nM and that of cells expressing FhIPR-G<sub>11</sub>/G<sub>s</sub>6α is estimated as 76.5 ± 6.6 nM. This graph is representative of 3 or more independent experiments performed in triplicate.



**Figure 5.13 Basal and iloprost-stimulated high affinity GTPase activity at various GTP concentrations**

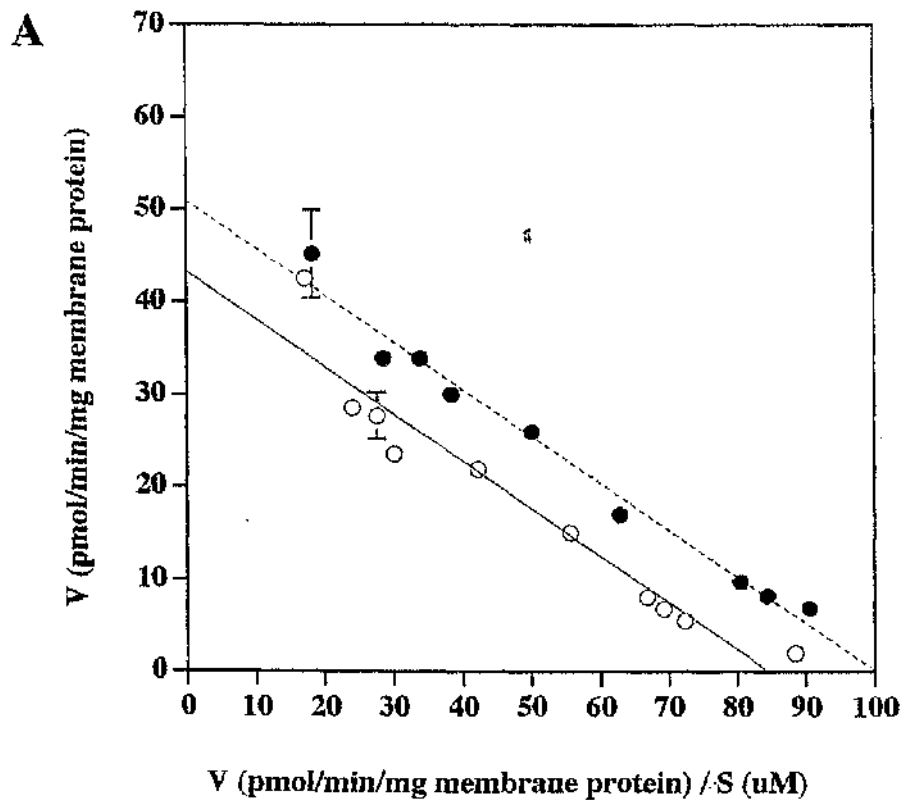
Membranes of HEK293 clones expressing FhIPR (A), FhIPR- $G_{s\alpha}$  (B), and FhIPR- $G_{i1}/G_{s6\alpha}$  (C) were assessed for their basal (open circles) and 1  $\mu$ M iloprost (closed circles)-stimulated high affinity GTPase at various concentrations of GTP. Cells expressing FhIPR- $G_{i1}/G_{s6\alpha}$  were pretreated with a combination of toxins as in Figure 5.9 before harvesting. The graphs are direct plots of GTPase activity (V) versus GTP concentrations (S) and represent a typical experiment among 3 or more performed in triplicate.

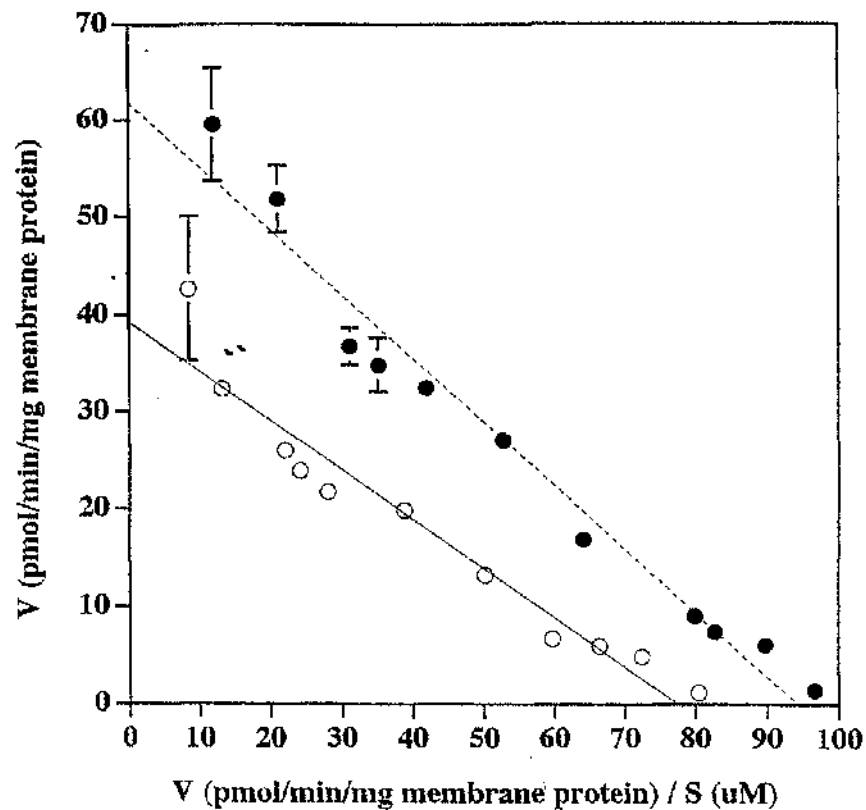
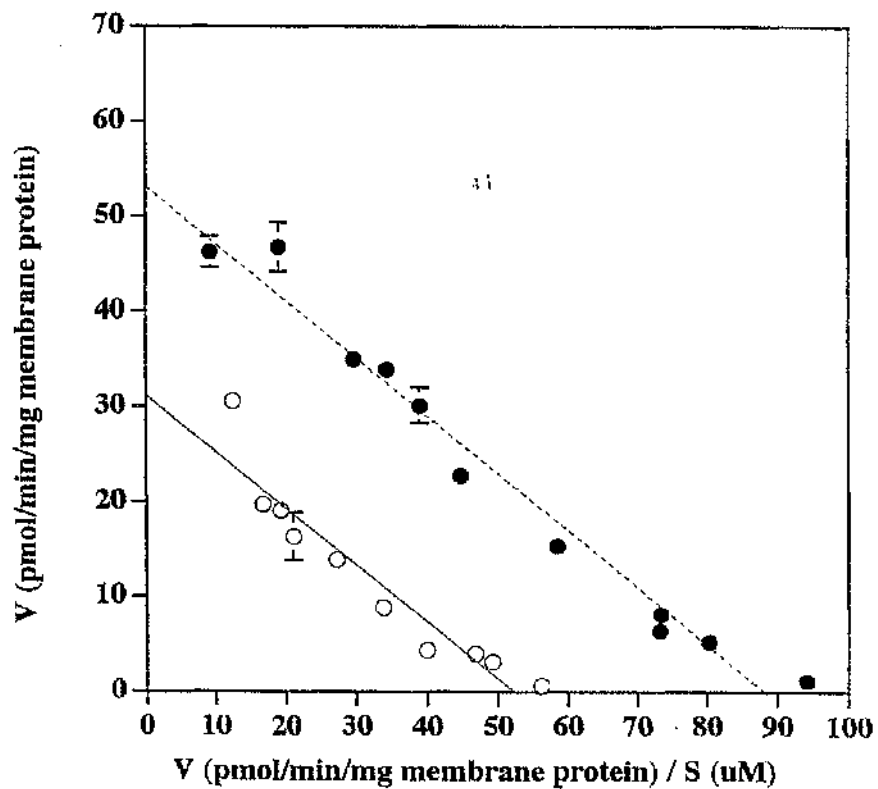


**B****C**

**Figure 5.14 Eadie-Hofstee plots of basal and iloprost-stimulated high affinity GTPase activity at various GTP concentrations**

Figures 5.13 A, B & C were transformed into Eadie Hofstee-plots: (A) FhIPR , (B) FhIPR- $G_{s\alpha}$  , and (C) FhIPR- $G_{i1}/G_{s\beta\alpha}$ . The maximum velocity ( $V_{max}$ ) is obtained by the difference in y-intercept between the basal (open circles) and iloprost (closed circles) stimulated activity, while the Michaelis Menton constant ( $K_m$ ) is obtained by the negative value of the slope of the graph. Each graph represents a typical experiment among 3 or more performed in triplicate.



**B****C**

## 5.3 Discussion

### ***Cells stably expressing FhIPR-G<sub>11</sub> $\alpha$ or FhIPR-G<sub>11</sub>/G<sub>s</sub>6 $\alpha$ fusion proteins exhibit similar characteristics as FhIPR-G<sub>s</sub> $\alpha$***

FhIPR-G<sub>11</sub> $\alpha$  and FhIPR-G<sub>11</sub>/G<sub>s</sub>6 $\alpha$  proteins exhibit certain similar characteristics as FhIPR-G<sub>s</sub> $\alpha$ . Immunological detection of their N-termini FLAG<sup>TM</sup>-epitope and their G $\alpha$  C-termini or internal domains was successful using the M5 anti-FLAG<sup>TM</sup> antibody and the appropriate anti-G $\alpha$  antisera (Figures 5.4 A, B & C). N-glycosylated forms (doublets) of these fusion proteins were apparent in the M5 and CS blots, but not so with the I1C antiserum. The N-glycosylated forms of the isolated receptor (FhIPR) was previously shown in Figure 3.5B in stably expressing HEK293 cells. As the glycosylation of asparagine residues is essential for proper targeting and expression of transmembrane receptors, it is therefore gratifying to note that these FhIPR-G $\alpha$  fusion proteins can also be glycosylated in a similar manner as FhIPR. However, multiple forms of the glycosylated fusion proteins are not as apparent in these blots as observed for the FhIPR.

Cells expressing the various FhIPR-G $\alpha$  fusion proteins bind [<sup>3</sup>H]iloprost with high affinity with the FhIPR-G<sub>11</sub>/G<sub>s</sub>6 $\alpha$  being the least among them (Figure 5.5). As agonists demonstrate high affinity for receptor states due to the promotion of G protein coupling (Colquhoun 1985), poor coupling efficiency between the GPCR and G $\alpha$ , as in the FhIPR-G<sub>11</sub>/G<sub>s</sub>6 $\alpha$  fusion protein (Figures 5.10 & 5.12), may contribute to its lower agonist affinity. Agonist binding affinity of FhIPR-G<sub>11</sub> $\alpha$  protein may not be affected as the receptor-fused G<sub>11</sub> $\alpha$  did not have any affinity for the receptor (Figures 5.7 & 5.8) and hence presumably only endogenous G<sub>s</sub> $\alpha$  interacts with the receptor.

The lack of [<sup>3</sup>H]antagonists acting at the IP prostanoid receptor restricted the assessment of receptor expression levels to radioligand binding studies using [<sup>3</sup>H]iloprost or [<sup>3</sup>H]PGE<sub>1</sub>. [<sup>3</sup>H]iloprost is the preferred radioligand due to its higher affinity and selectivity at the IP prostanoid receptor (Coleman *et al.* 1994). Routine

estimates of receptor levels using [ $^3$ H]iloprost (Table 5.1) at concentrations of 3 times or more  $K_d$  are sufficiently accurate for the various proteins except the FhIPR- $G_{i1}/G_s6\alpha$ . This is because the concentration of [ $^3$ H]iloprost used ( $\sim 10$  nM) is only slightly more than the estimated  $K_d$  of cells expressing FhIPR- $G_{i1}/G_s6\alpha$  (8.5 nM) and hence may cause an underestimation of expression level. Assuming that only 60% of the total level of FhIPR- $G_{i1}/G_s6\alpha$  specifically binds [ $^3$ H]iloprost at 10nM, the estimated receptor expression level would be closer to  $\sim 1.5$  pmol/mg membrane protein.

All the FhIPR- $G\alpha$  fusion proteins stimulated adenylate cyclase in the presence of iloprost in a concentration-dependent manner (Figure 5.6). A significantly higher concentration of iloprost (unpaired t-test:  $p < 0.05$ ;  $n = 3$ ) was required to stimulate 50% activity in cells expressing FhIPR- $G_{i1}\alpha$  ( $EC_{50} = 5.5 \pm 0.8 \times 10^{-10}$  M) compared to FhIPR- $G_s\alpha$  ( $EC_{50} = 1.1 \pm 0.3 \times 10^{-10}$  M), despite their similar affinities to bind [ $^3$ H]iloprost. This poorer activity of FhIPR- $G_{i1}\alpha$  could be attributed to the inability of receptor-linked  $G_{i1}\alpha$  to be activated by the fused receptor (Figures 5.7 & 5.8) which may hinder the access of endogenous  $G_s\alpha$  to the activated receptor. Furthermore, agonist promoted accumulation of cAMP in cells expressing the FhIPR- $G_s\alpha$  protein can be mediated via the combined effect of receptor-linked and endogenous  $G_s\alpha$ . Strangely, although the affinity for [ $^3$ H]iloprost in cells expressing FhIPR- $G_{i1}/G_s6\alpha$  is about 6 times weaker than FhIPR- $G_s\alpha$ , iloprost potency in FhIPR- $G_{i1}/G_s6\alpha$  expressing cells is only 2 times lower (Figure 5.6). Furthermore, the adenylate cyclase inhibitory effect of receptor-linked  $G_{i1}/G_s6\alpha$  should reduce the activity of adenylate cyclase and hence further lower the potency of iloprost. It is therefore unclear why the adenylate cyclase activity of FhIPR- $G_{i1}/G_s6\alpha$  did not correlate well with its affinity for agonist. A possible reason for it may be the differential accessibility of endogenous  $G_s\alpha$  to these FhIPR- $G\alpha$  fusion proteins upon stimulation by iloprost.

### ***Specificity of coupling in the FhIPR-G $\alpha$ fusion proteins***

Results obtained from the [ $^{35}$ S]GTP $\gamma$ S binding and high affinity GTPase assays, which monitor G $\alpha$  activity, demonstrate that the receptor-linked G $_{i1}\alpha$  of the FhIPR-G $_{i1}\alpha$  protein cannot be activated (Figures 5.7 & 5.8). While co-expression of G $_{i1}\alpha$  and FhIPR also did not result in activation of G $_{i1}\alpha$  (Chapter 3), it was thought that the covalent fusion of these 2 components might enable productive interactions to occur, as suggested by Medici *et al.* (1997). This is particularly the case as a chimeric G protein, G $_{i1}/G_s6\alpha$ , which is predominantly G $_{i1}\alpha$  except the last 6 aa (from G $_s\alpha$ ), was shown to interact productively with the IP prostanoid receptor (Chapter 3). As the C-terminus of G $\alpha$  was suggested to fulfil the role of bringing the G protein in close proximity with the receptor, this C-terminal sequence is therefore not crucial in a GPCR-G $\alpha$  fusion construct (Medici *et al.* 1997). However, the results obtained in this study with the FhIPR-G $_{i1}\alpha$  protein proved otherwise.

Substituting the last 6 aa of G $_s\alpha$  into the FhIPR-G $_{i1}\alpha$ , as in the FhIPR-G $_{i1}/G_s6\alpha$  protein, promoted functional interactions between the 2 fused partners. The authenticity of receptor-linked G $_{i1}/G_s6\alpha$  activation is shown by its resistance to both cholera and pertussis toxins in the [ $^{35}$ S]GTP $\gamma$ S binding and high affinity GTPase assays (Figures 5.7 & 5.8), a phenomenon previously observed when the G $_{i1}/G_s6\alpha$  protein was co-expressed with FhIPR (Chapter 3). Thus, it appears that the last 6 aa of G $_s\alpha$  is still critical for transduction of signal from the GPCR to the G $\alpha$  subunit in a fusion construct. These results further proved that the covalent link is not sufficient to enforce interaction between the FhIPR and a G $\alpha$  subunit that it does not interact with physiologically, unless a recognition sequence is also present at the C-terminus of the G $\alpha$  subunit.

Fusing the FhIPR with G $\alpha$  did not affect the characteristics of the receptor-linked G $\alpha$ . The activity of FhIPR-G $_s\alpha$  was shown in the previous chapter to be modulated by the ADP-ribosylating action of cholera toxin. The activity of FhIPR-

$G_{i1}/G_s6\alpha$  however, is resistant to both cholera and pertussis toxins, an observation also noted of the freely interacting  $G_{i1}/G_s6\alpha$  protein (Chapter 3). As the various FhIPR- $G\alpha$  fusion proteins also bind [ $^3H$ ]iloprost with high affinity and activate adenylate cyclase, this implies that covalently linking the receptor and  $G\alpha$  subunit did not alter the characteristics of either the receptor or the  $G\alpha$ .

***Receptor- $G\alpha$  interaction is more efficient in the FhIPR- $G_s\alpha$  than FhIPR- $G_{i1}/G_s6\alpha$***

Agonist promoted receptor- $G\alpha$  interactions were studied in greater detail in cells expressing FhIPR- $G_s\alpha$  and FhIPR- $G_{i1}/G_s6\alpha$ . Iloprost concentration response studies of membranes from these cells in either GTPase or [ $^{35}S$ ]GTP $\gamma$ S binding assays indicated that the FhIPR- $G_{i1}/G_s6\alpha$  protein is 16 to 30 times less responsive to iloprost stimulation than the FhIPR- $G_s\alpha$  protein (Figures 5.10 & 5.12). A partial explanation for the poor sensitivity of FhIPR- $G_{i1}/G_s6\alpha$  to iloprost stimulation could be its lower affinity for the agonist (Figure 5.5). However, the 6 fold difference in binding affinity between the FhIPR- $G_{i1}/G_s6\alpha$  and FhIPR- $G_s\alpha$  proteins cannot fully account for the large difference in activation of  $G\alpha$ . As the cells expressing FhIPR- $G_{i1}/G_s6\alpha$  were pretreated with a combination of both cholera and pertussis toxins to remove coupling with endogenous  $G_s\alpha$  and  $G_i\alpha$ -like subunits, the activation profile observed only reflects the activation of receptor-linked  $G_{i1}/G_s6\alpha$ . This is however not the case for cells expressing FhIPR- $G_s\alpha$ , which is untreated and hence would activate a combination of both endogenous and receptor-linked  $G_s\alpha$  (Chapter 4). This may suggest that the activation of receptor-linked  $G\alpha$  is less sensitive in general.

However, the most probable reason for the observed difference in iloprost potencies is that activation of  $G\alpha$  by the GPCR may be mediated via other domain(s) of  $G\alpha$  apart from the C-terminus. Various studies have implicated the involvement of the extreme N-terminus of  $G\alpha$  and a region mapped to residues 311 to 328 of  $G_{i1}\alpha$  (see Section 1.3.2). In particular, the N-terminus of  $G_o\alpha$  was

shown to be cross-linked to the the IC3 region of the  $\alpha_{2A}$ -adrenergic receptor (Taylor *et al.* 1994) and to mastoparan (Higashijima *et al.* 1991), while a synthetic N-terminal peptide of  $G_{i1}\alpha$  inhibited interaction of  $G_{i1}\alpha$  with rhodopsin (Hamm *et al.* 1988). It is therefore very likely that these domains of the  $G_{i1}/G_{s6}\alpha$  protein, which differ from  $G_{s5}\alpha$ , may contribute to the poor interactions with the receptor at sub-optimal agonist concentrations. Therefore, while these domains of  $G_{i1}\alpha$  may substitute for the corresponding domains of  $G_{s5}\alpha$ , the transduction of signal from the FhIPR may not be as efficient. It will be interesting to map the exact locations of these domains of  $G_{s5}\alpha$  by substituting into the FhIPR- $G_{i1}/G_{s6}\alpha$  fusion construct and reassessment of their receptor- $G\alpha$  interactions.

***Fusion proteins are more productive signal transducers than the isolated receptor***

The enhancement of signal transduction by the FhIPR- $G_{s5}\alpha$  fusion protein was clearly shown in Chapter 4. One of the reasons for such enhancement is the elevated activity of the receptor-linked  $G\alpha$ . Through the use of cholera toxin, which downregulates endogenous  $G_{s5}\alpha$  but not FhIPR- $G_{s5}\alpha$ , the ratio of activated endogenous  $G_{s5}\alpha$  to receptor-linked  $G_{s5}\alpha$  was found to range from 1:1 to 1:2 (Section 4.3). The predominance and enhanced activity of receptor-linked  $G\alpha$  in the FhIPR- $G_{i1}/G_{s6}\alpha$  protein was also apparent. By comparing the agonist promoted activities of untreated and toxins-treated cells (Figures 5.7 and 5.8), the ratio of activated endogenous  $G\alpha$  versus receptor-linked  $G\alpha$  in the FhIPR- $G_{i1}/G_{s6}\alpha$  expressing cells was observed to range from 1:4 to 1:5. The high dominance of receptor-linked  $G\alpha$  activity in the FhIPR- $G_{i1}/G_{s6}\alpha$  protein is likely a feature of the  $G_{i1}/G_{s6}\alpha$  protein.

The enhancement of signal transduction by the  $G_{i1}/G_{s6}\alpha$  protein was not studied in detail in co-expression systems in Chapter 3 due to the difficulty of assessing expression levels of the  $G_{i1}/G_{s6}\alpha$ . However, through the use of FhIPR- $G\alpha$  fusion proteins in the current study, the expression levels of  $G_{i1}/G_{s6}\alpha$  can be

accurately determined by receptor binding studies. This enabled a comparison to be made with cells expressing the FhIPR and FhIPR-G<sub>s</sub>α proteins, despite differences in their levels of expression. As presented in Table 5.1, the receptor expression levels of all 4 clones expressing the FhIPR and the fusion proteins are not uniform. By compensating for the amount of receptor expressed, the true "benefit" or "enhancement" of signal transduction of each fusion protein can be determined with respect to the isolated IP prostanoid receptor.

Iloprost (1 μM) stimulation resulted in enhanced binding of [<sup>35</sup>S]GTPγS to the fusion proteins FhIPR-G<sub>s</sub>α and FhIPR-G<sub>i1</sub>/G<sub>s</sub>6α (Figure 5.7). The concentration of [<sup>35</sup>S]GTPγS used in the assay ranged from 0.3 to 0.5 nM and was not diluted with unlabelled GTPγS to give a high concentration due to the low window of counts (2000 to 3000 cpm) in the assay. As such, the incorporation of [<sup>35</sup>S]GTPγS is not saturating and does not reflect the maximum amount bound at equilibrium. The counts obtained in the present assay at a fixed incubation time (60 min), would therefore give an indication of the rate of [<sup>35</sup>S]GTPγS incorporated by the various proteins. Comparison of this rate among the various proteins after normalising for their expression levels is tabulated below:

**Table 5.3** Rates of [<sup>35</sup>S]GTPγS incorporation

Protein	[ <sup>35</sup> S]GTPγS Bound (% of FhIPR / mg membrane protein)	[ <sup>35</sup> S]GTPγS Bound (%) at equal expression level	Rate of Gα activation
FhIPR	100	100	1
FhIPR-G <sub>s</sub> α	226.5	494	4.9
FhIPR-G <sub>i1</sub> /G <sub>s</sub> 6α	227.1	440*	4.4

\* The expression level of FhIPR-G<sub>11</sub>/G<sub>s</sub>6 $\alpha$  was re-estimated at 1.5 pmol/mg by assuming that only 60% of it binds [<sup>3</sup>H]iloprost at ~10 nM in view of its high K<sub>d</sub> (8.5 nM).

The rate of [<sup>35</sup>S]GTP $\gamma$ S incorporation clearly indicates that the fusion proteins activate G $\alpha$  subunits at a much faster rate than the isolated FhIPR. The similar rates of G $\alpha$  activation for the FhIPR-G<sub>s</sub> $\alpha$  and FhIPR-G<sub>11</sub>/G<sub>s</sub>6 $\alpha$  proteins suggest of a common characteristic of the FhIPR-G $\alpha$  fusion protein to stimulate GTP exchange in such constructs.

The comparison of high affinity GTPase activity by the fusion proteins is best achieved by comparing their respective V<sub>max</sub>. This is because the GTPase activity is strongly influenced by the concentration of GTP used in the assay, especially for G proteins with different K<sub>m</sub> values (Table 5.2). Differences in K<sub>m</sub> values indicate differential affinity for GTP and hence imply that unless the GTP concentration used is at least 3 times of K<sub>m</sub>, results obtained from such assays cannot be used to compare the relative activity of different G $\alpha$  subunits. In routine GTPase assays, a final GTP concentration of 0.5  $\mu$ M was used due to the need to consider both the velocity and the specific activity of [<sup>32</sup>P]GTP in the reaction. As this concentration is very close to the K<sub>m</sub> values of FhIPR and the fusion proteins, the results were not utilised for comparison of FhIPR-G<sub>s</sub> $\alpha$  and FhIPR-G<sub>11</sub>/G<sub>s</sub>6 $\alpha$  with FhIPR. Instead, the V<sub>max</sub> values obtained by the Eadie-Hofstee plots (Figures 5.14A, B & C) were used.

A relatively simple measure of the GTP binding and hydrolysing capacities of G $\alpha$  subunits is to measure their ability to bind and hydrolyse GTP per unit time per molecule, known as the GTP turnover number (Wise *et al.* 1997c). Hence, by using the V<sub>max</sub> (pmol/min/mg) values of each construct and dividing this by their expression levels (pmol/mg), the turnover number (min<sup>-1</sup>) is obtained and presented in Table 5.4:

**Table 5.4** Rates of GTP turnover

Protein	V <sub>max</sub> (pmol/min/mg)	Expression levels (pmol/mg)	Turnover number (min <sup>-1</sup> )	Ratio of turnover number
FhIPR	7.3	3.0	2.5 ± 0.2	1
FhIPR-G <sub>s</sub> α	18.0	1.4	13.3 ± 1.6	5.3
FhIPR-G <sub>i1</sub> /G <sub>s</sub> 6α	19.3	1.5*	12.9 ± 1.5	5.1

\* The expression levels of FhIPR-G<sub>i1</sub>/G<sub>s</sub>6α differ from Table 5.1 for the reasons mentioned in Table 5.3

A comparison of their GTP turnover number again strongly suggests that fusion proteins are more efficient than the isolated receptor in binding and hydrolysing GTP. This result, together with that obtained in the [<sup>35</sup>S]GTPγS binding assay, conclusively show that the fusion proteins are more productive signal transducers.

In summary, this study is the first to show that coupling specificity is retained in the FhIPR-Gα fusion proteins. Furthermore, this study also illustrates the importance of the C-terminus of G<sub>s</sub>α in restoring the coupling between FhIPR and Gα, a role which cannot be replaced by covalently linking them as suggested by Medici *et al.* (1997). In addition, it is apparent that the characteristics of the receptor and Gα in these FhIPR-Gα fusion proteins are similar to that of the freely interacting components. Finally, functional FhIPR-Gα fusion proteins exhibit much higher activity than the isolated FhIPR when assessed by both [<sup>35</sup>S]GTPγS binding and high affinity GTPase assays.

## **CHAPTER 6**

## **DISCUSSION**

## CHAPTER 6 DISCUSSION

GPCRs transduce extracellular signals into the cell by activating heterotrimeric G proteins. Both the  $G\alpha$  and  $G\beta\gamma$  complex have been shown to act on a variety of effectors ranging from enzymes (adenylate cyclase, phospholipase C & cGMP phosphodiesterase) to ion channels ( $K^+$ ,  $Ca^{2+}$  &  $Na^+$  channels). As signals are amplified down the signalling cascade, most functional assays measure the activity of the downstream effectors either directly or via reporter genes and reporter proteins. However, although these functional assays are sensitive, analysis of the resulting output can be complex and subject to the type of tissue or cell line used, mainly due to variations in their downstream signalling components. The stoichiometry of the GPCRs, G proteins and effectors also differs greatly between cell lines, and this can give rise to different functional responses (Kenakin 1995a). This particularly affects GPCRs that are promiscuous in their coupling, as the stoichiometry of GPCRs to the various  $G\alpha$  can determine the signalling cascades to be activated. This phenomenon can also be observed in recombinant systems by expressing GPCRs and  $G\alpha$  subunits to different levels (Kenakin 1997).

The determination of agonist efficacy at the earliest point of the signalling pathway (i.e. at the level of G protein activation) is besieged with various problems for GPCRs that do not couple to " $G_{i\alpha}$ -like" subunits (Wieland *et al.* 1994; Gierschik *et al.* 1994). However, through the use of a chimeric  $G_{i1}/G_{s6\alpha}$  protein, high levels of activity were observed upon stimulation by the IP prostanoid receptor (Chapter 3). The retention of intrinsically high rates of GTP exchange and hydrolysis of the  $G_{i1}\alpha$  subunit enabled the detection of IP prostanoid receptor agonist activity based on conventional assays that measure G protein output. By activating only the chimeric  $G_{i1}/G_{s6\alpha}$  but not full length  $G_{i1}\alpha$ , the IP prostanoid receptor also demonstrated its selective interaction with  $G_{s\alpha}$  via the extreme carboxyl terminus.

This study therefore allowed the opportunity to study agonist function at the level of the G protein for a  $G_{s\alpha}$ -coupled GPCR. Traditionally, assays that detect

activation of  $G_s\alpha$  frequently involved measuring the activity of adenylate cyclase, a downstream effector of activated  $G_s\alpha$ . While this assay is generally sensitive and reliable, there are various drawbacks to its use for assessing agonist efficacy. There are currently 9 isoforms of mammalian adenylate cyclase known. Although all 9 isoforms can be activated by  $G_s\alpha$ , not all the isoforms have been carefully assessed for their sensitivity to  $G_s\alpha$ . In addition, the type of isoforms and their levels of expression will naturally vary between cell lines, and their activity can be modulated by various proteins including  $G_i\alpha$  and  $G_z\alpha$  subunits, and the  $G\beta\gamma$  complex. All these factors make it difficult to directly compare the efficacy of agonists across different cell lines based on the measurement of adenylate cyclase activity (Birnbaumer 1992).

Furthermore, there appears to be distinct differences in the capacity to activate adenylate cyclase among the splice variants of  $G_s\alpha$ . The short isoform of  $G_s\alpha$  ( $G_s\alpha(S)$ ) was previously shown to be more effective in activating adenylate cyclase than the long isoform ( $G_s\alpha(L)$ ) in both co-expression and GPCR- $G\alpha$  fusion studies (Walseth *et al.* 1989; Seifert *et al.* 1998). While agonist trafficking of GPCRs had been studied in some detail (Kenakin 1995b), the ability of agonists to promote preferential coupling of the splice variants of  $G_s\alpha$  is currently unclear. As such, it is rather crucial that agonist activity be determined at the level of  $G\alpha$ , as this would circumvent the inherent problems associated with measuring secondary effector activity.

The finding that the IP prostanoid receptor activates  $G_s\alpha$  via a recognition sequence located at the C-terminus extends the list of GPCRs that have been shown to exhibit this property (Conklin *et al.* 1993a; Voyno-Yasenetskaya *et al.* 1994). There is as yet no clear pattern as to why certain GPCRs show such a characteristic, while others do not. This short fragment involved in the coupling between GPCR and  $G\alpha$  suggests that selective uncoupling can be achieved with either short peptides or even small molecule entities. Such selective uncoupling may confer a therapeutic advantage over an antagonist that acts on the GPCR and hence blocks all signalling processes. Indeed, various studies have

concentrated on discovering selective antagonists of GPCR and  $G\alpha$  coupling (Hohenegger 1998; Freissmuth *et al.* 1996). However, as most of the currently available antagonists are analogues of suramin, which is a non-selective inhibitor of GDP/GTP exchange for  $G\alpha$ , they do not particularly discriminate between the various  $G\alpha$  subunits. Furthermore, as very high micromolar concentrations are required, it is unlikely that these compounds block the interactions between the GPCR and  $G\alpha$  via the  $G\alpha$  C-terminus. This is especially in view that subnanomolar of  $G_s\alpha$  and submicromolar of  $G_i\alpha$  are sufficient to exert their effect on adenylate cyclase (Taussig *et al.* 1993). The use of chimeric G proteins, such as the  $G_{i1}/G_s6\alpha$  chimera, to screen for selective antagonists acting at the C-terminus of  $G\alpha$  may instead yield more useful and discriminating compounds.

It is very interesting that functional chimeric G proteins can be generated to combine the desired properties of another  $G\alpha$  and yet retain coupling to the GPCR under study (Conklin *et al.* 1993a; Komatsuzaki *et al.* 1997; Chapter 3 of this thesis). As the pharmaceutical industry is always in search of generic assay formats for the different  $G\alpha$  activating GPCRs, the use of chimeric G proteins may greatly facilitate this development. In the current study, high levels of activity in both the [ $^{35}$ S]GTP $\gamma$ S binding and high affinity GTPase assays were obtained for a  $G_s\alpha$ -coupled GPCR acting via the chimeric  $G_{i1}/G_s6\alpha$  protein. This concept can therefore be extended to GPCRs that couple to  $G\alpha$  subunits other than  $G_s\alpha$ . As the [ $^{35}$ S]GTP $\gamma$ S binding assay can be adapted as a high-throughput screen through the use of SPA<sup>TM</sup> (Scintillation Proximity Assay) and Flashplate<sup>TM</sup> assay formats, it may thus be possible to use a series of  $G_{i1}/G_x\alpha$  ( $x =$  any  $G\alpha$ ) chimeras as adapter proteins for the screening of novel agonists acting at any GPCR.

The search for a common  $G\alpha$  reporter protein had previously centred on  $G_{16\alpha}$  and the use of the  $Ca^{2+}$  / aequorin system as a generic screen for GPCRs (Milligan *et al.* 1996; Stables *et al.* 1997). Recent studies had however indicated that  $G_{16\alpha}$  may not be capable of coupling to all GPCRs (Lee *et al.* 1998). While such a promiscuous  $G\alpha$  subunit may not be found in nature as it would be difficult to regulate its effect in the cell, detailed mutagenesis of the C-terminal residues of

$G\alpha$  may eventually yield a truly promiscuous mutant  $G\alpha$ . This is supported by the recent finding that an N-terminal truncation of  $G_q\alpha$ , which lacks the first 6 aa, enabled it to couple with various  $G\alpha$ -activating GPCRs (Kostenis *et al.* 1997). In addition, the promotion of GTP exchange in the  $G\alpha$  subunits may be non-specific in nature, as shown by the capacity of mastoparan and its related amphiphilic peptides and hydrophobic amines to catalyse the exchange in a number of  $G\alpha$  subunits (Higashijima *et al.* 1990).

The impact of varying stoichiometry of GPCR to  $G\alpha$  in signalling was reduced to the minimum through the use of GPCR- $G\alpha$  fusion proteins. The covalent fusion of the IP prostanoid receptor with  $G_s\alpha$ , to form the FhIPR- $G_s\alpha$ , also resulted in a highly productive signal transducing protein when compared to the freely interacting receptor (Chapter 4). As a result, this fusion protein also offers a means to analyse agonist pharmacology using high affinity GTPase or [ $^{35}$ S]GTP $\gamma$ S binding assays and with the advantage of interacting with its cognate  $G\alpha$ . As the increase in agonist-stimulated high affinity GTPase activity correlated well with that observed in the [ $^{35}$ S]GTP $\gamma$ S binding assay, it is very likely that a faster level of activation of  $G_s\alpha$  is the main reason contributing to the elevated activity. Cholera toxin treatment of HEK293 cells expressing the FhIPR- $G_s\alpha$  was shown to downregulate the level of endogenous  $G_s\alpha$  but not the FhIPR- $G_s\alpha$  protein. Therefore, the agonist-promoted incorporation of [ $^{35}$ S]GTP $\gamma$ S into the membranes of such toxin-treated cells indicates that the enhanced activity is a result of activating the receptor-linked  $G_s\alpha$ .

Overexpression of  $G_s\alpha$  in the FhIPR expressing cells did not result in elevated activity (Chapters 3 & 4). This suggests that either the close proximity or the co-targeting of GPCR and  $G\alpha$  could have accounted for the ease with which receptor-linked  $G\alpha$  can be activated. There is substantial evidence suggesting that GPCR and  $G\alpha$  subunits may not be located in the same microdomain at the plasma membrane (Neubig 1994). In particular,  $G\alpha$  subunits were found to be associated with caveolae, which are vesicular invaginations of the plasma

membrane characterised by the presence of caveolin proteins (Okamoto *et al.* 1998). Besides the endothelin receptor, few GPCRs are currently known to associate with caveolae. However, recent studies showed that the M2 muscarinic (Feron *et al.* 1997) and B2 bradykinin receptors (Weerd *et al.* 1997) translocate to caveolin-rich fractions upon stimulation by agonists but not antagonists. This suggests that such agonist-induced translocation is an essential step in the initiation of signalling cascades, as many downstream transducers of GPCRs are localised to the caveolae fractions (Okamoto *et al.* 1998).

Caveolin proteins were also found to have an inhibitory effect on the activation of  $G\alpha$  subunits. An N-terminal cytoplasmic domain of caveolin-1 (residues 61-101) binds  $G\alpha$  and suppresses the basal GTPase activity of purified  $G\alpha$  by inhibiting GDP/GTP exchange (Li *et al.* 1995). In contrast, the analogous region of caveolin-2 possesses GTPase-activating protein activity with regard to heterotrimeric G proteins (Scherer *et al.* 1996). The functions of these proteins therefore act to maintain the  $G\alpha$  subunits in the inactive GDP-liganded state. While agonist-induced translocation of FhIPR or FhIPR- $G_{s\alpha}$  into caveolin-rich fractions was not observed in the present study, sucrose density fractionations of Triton X-100 treated FhIPR and FhIPR- $G_{s\alpha}$  expressing cells clearly indicate that both proteins did not associate with caveolin-rich fractions (results not shown). This could have accounted for the enhanced activity of receptor-linked  $G_{s\alpha}$  in the FhIPR- $G_{s\alpha}$  protein as it is not under the influence of the caveolin proteins. More studies however will need to be performed to substantiate these preliminary findings.

The covalent fusion of the C-terminus of a GPCR with the N-terminus of  $G\alpha$  could affect the conformation and functions of these termini. The C-terminus of the IP prostanoid receptor contains sites for PKC phosphorylation (Figure 1.6), which are essential for regulating desensitisation of the receptor (Smyth *et al.* 1996). Recent evidence showed that serine 328 is the primary site for PKC phosphorylation of hIPR (Smyth *et al.* 1998). A reassessment of these results may be necessary for desensitisation studies of the FhIPR- $G_{s\alpha}$  fusion construct. The

N-terminus of  $G\alpha$ , was previously shown in crystallographic studies to be in direct contact with the  $G\beta\gamma$  complex, although the switch II region is also involved in the binding (Lambright *et al.* 1996). Furthermore, N-terminal truncations of various  $G\alpha$  subunits (Neer *et al.* 1988; Graf *et al.* 1992) including  $G_s\alpha$  (Journot *et al.* 1991) abrogates their ability to bind  $G\beta\gamma$ . As the  $G\beta\gamma$  complex prevents dissociation of GDP from  $G\alpha$  (Higashijima *et al.* 1987), it would be anticipated that loss of  $G\beta\gamma$  binding might result in a faster exchange of GDP for GTP (Sprang 1997). However, the  $G\beta\gamma$  complex also stabilises the GPCR/ $G\alpha$  interface and enhances binding of  $G\alpha$  to its appropriate receptor (Kleuss *et al.* 1992 & 1993), which makes the effect of N-terminal  $G\alpha$  truncates more difficult to assess *in vivo*. This may not pose a problem for GPCR- $G\alpha$  fusions as their interactions may not require any further facilitation by the  $G\beta\gamma$  complex. The question arising therefore is whether the enhanced GDP/GTP exchange observed in the FhIPR- $G_s\alpha$  is a result of loss of  $G\beta\gamma$  binding.

The association of the  $G\beta\gamma$  complex with GPCR- $G\alpha$  fusion proteins has been a question of debate. The expression of a Ste2-Gpa1 fusion in Gpa1 deficient yeast cells clearly shows that it can bind  $G\beta\gamma$ , as the haploid cells were rescued from lethality (Medici *et al.* 1997). However, Burt *et al.* (1998) failed to activate both the p44 mitogen-activated protein kinase and p70 S6 kinase in pertussis toxin treated  $\alpha_{2A}AR$ - $G_{i1}\alpha$ (C351G) fusion protein expressing cells, results which would be consistent with a loss of association with  $G\beta\gamma$ . On the other hand, co-expression of  $G\beta\gamma$  increased the GTPase activity of the  $\alpha_{2A}AR$ - $G_{i1}\alpha$ (G2A/C351G) fusion (Wise *et al.* 1997b) but not the  $\beta_2AR$ - $G_s\alpha$  fusion (Seifert *et al.* 1998b). These contradictory findings suggest that the affinity of  $G\beta\gamma$  with each fusion protein may differ. Detailed analysis will therefore need to be performed to ascertain whether a loss or lower affinity of  $G\beta\gamma$  complex could have accounted for the enhanced activity of the FhIPR- $G_s\alpha$  protein.

The fidelity of signalling in GPCR- $G\alpha$  fusion proteins was confirmed by a series of FhIPR- $G\alpha$  fusions, which also showed that the characteristics of both the

receptor and  $G\alpha$  were not altered by the covalent linkage (Chapter 5). This refuted the claim by Medici *et al.* (1997) that the covalent fusion of GPCR with  $G\alpha$  could replace the function of the C-terminus and hence re-established the importance of this domain in transducing signal from the receptor, even in a fusion construct. There is no doubt that this finding will mean it is not possible to generate promiscuous signal transducing proteins and hence reduces the utility of GPCR- $G\alpha$  fusions for such purposes, as discussed in Section 5.1. However, there are other studies where such fusion proteins may be useful.

Firstly, the study of GPCR coupling with various  $G\alpha$  can be determined with "equal opportunity" by using the fusion protein approach. As the expression level of  $G\alpha$  is equal to the receptor in the GPCR- $G\alpha$  fusion, their relative stoichiometry would be 1:1 when endogenous  $G\alpha$  coupling can be eliminated. Furthermore, by taking into account the expression level of each GPCR- $G\alpha$  fusion construct, the activation of various receptor-linked  $G\alpha$ s can be directly compared and analysed as demonstrated in Section 5.3. Moreover, the fusion construct does not suffer from any interference arising from differential localisation or compartmentalisation of the GPCR and  $G\alpha$  at the plasma membrane (Neubig 1994). Finally, as the coupling of  $G\alpha$  with the appropriate receptor can also be affected by the  $G\beta$  (Kleuss *et al.* 1992) and  $G\gamma$  subunits (Kleuss *et al.* 1993), the use of GPCR- $G\alpha$  fusions will not require the presence of appropriate  $G\beta\gamma$  complexes in the cell line under study. Such "controlled" studies of  $G\alpha$  coupling are analogous to reconstitution studies where the appropriate amount of receptor and  $G\alpha$  are allowed to interact in an artificially created environment. The GPCR- $G\alpha$  fusion approach is however more akin to the cellular system, simpler to perform and offers better control of expression levels.

The GPCR- $G\alpha$  fusion approach may also enable the detailed study of interactions between GPCR and  $G\alpha$  to be done at a level that is not possible before. Previous structural mapping studies of domains critical for effective coupling were mainly performed through the expression of mutant or chimeric receptor and  $G\alpha$ . While such expression studies provided a good assessment of the construct under study, they failed to differentiate between the affinity and

exchange capacity of the mutants. Productive coupling between the GPCR and  $G\alpha$  can only occur when both partners are brought into close proximity, through the acylation of  $G\alpha$  and the C-terminus of GPCR, and enhancement by specific  $G\beta\gamma$  complex. The generation of certain mutants or chimeric proteins may therefore destroy such functions in either partner and hence abrogate coupling. A good example is the truncation of the N-terminus of  $G_{s\alpha}$ , which removed its palmitoylation and association with  $G\beta\gamma$  complex, and therefore caused a failure to activate adenylate cyclase (Journot *et al.* 1991). Others include modifying the residue for acylation (Wise *et al.* 1997a) or exchanging the N-terminus of  $G\alpha$  (Osawa *et al.* 1990b).

The ability of the GPCR- $G\alpha$  fusion protein to discriminate between affinity and exchange capacity could be applied to the study of  $G\alpha$  coupling in receptor splice variants. A prototypical example is the distinct coupling characteristics of the 4 splice variants of the bovine  $EP_3$  prostanoid receptor, which differ only in their intracellular C-termini (Namba *et al.* 1993; see Section 1.3.1). It is very likely that the C-termini are involved in bringing the various  $G\alpha$  in close association with the receptor, while the intracellular loops are responsible for catalysing the exchange of GDP/GTP in the various  $G\alpha$  subunits. By constructing fusion proteins between a C-terminal truncated form of the  $EP_3$  receptor linked to the various  $G\alpha$  proteins by a linker sequence and monitoring their activation, evidence can be collected to support or destroy this hypothesis. Hence, GPCR- $G\alpha$  fusion proteins may be applied in the mapping of GPCR domains involved in  $G\alpha$  association and  $G\alpha$  activation.

Finally, there is no reason why such a fusion approach cannot be extended to the study of other signalling proteins. There is evidence that  $G\alpha$  subunits can be activated by receptors not belonging to the GPCR superfamily. For example, short peptides of the insulin-like growth factor II receptor were shown to couple with  $G_{12\alpha}$ , while the epidermal growth factor receptor was observed to couple with a  $G_{1\alpha}$ -like subunit (Spiegel 1992). Fusions between such proteins may unravel the capacity of non-GPCRs to activate  $G\alpha$  which could not be observed either due to

a low level of activity or occur under circumstances where their detection may be difficult.

A recent study also suggests direct interaction between GPCRs and small G proteins (Mitchell *et al.* 1998). In that study, GPCRs that contain the amino acid sequence AsnProXX Tyr in their TM7 domain and activate phospholipase D, do so in a ARF and RhoA-dependent manner. Furthermore, these small G proteins were co-immunoprecipitated with the receptor on exposure to agonists. Interestingly, there are also GPCRs that activate phospholipase D independent of these small G proteins, but contain the sequence AspProXX Tyr in their TM7 domain. Mutating the aspartic acid to asparagine in the corresponding TM7 sequence of the gonadotropin-releasing hormone receptor confers sensitivity to an inhibitor of ARF. These results strongly suggest that receptors carrying the AsnProXX Tyr motif may form functional complexes with ARF and RhoA. It will therefore be very interesting to link GPCRs with these small G proteins and investigate the possibility of direct interactions between them by using the appropriate assays and inhibitors.

In conclusion, this study achieved the objective of setting up systems for improving G protein output to a level detectable by conventional assays, for a  $G_s\alpha$ -coupled GPCR, the human IP prostanoid receptor. While the chimeric  $G_{11}/G_{s6\alpha}$  protein showed substantial elevated activity upon stimulation by an agonist acting on the IP prostanoid receptor, it is difficult to control its expression level. The generation of FhIPR- $G_s\alpha$  and FhIPR- $G_{11}/G_{s6\alpha}$  fusion proteins produced highly productive signal transducing proteins, which have the advantage of defined GPCR/ $G\alpha$  stoichiometry and co-targeting of the interacting proteins. It is envisaged that such systems will be used in the screening of novel compounds acting on the human IP prostanoid receptor and various other GPCRs.

## REFERENCES

## REFERENCES

- Adie, E. J., Mullaney, I., McKenzie, F. R., and Milligan, G. (1992) *Biochem. J.* **285**, 529-536
- Akam, E. C., Carruthers, A. M., Nahorski, S. R., and Challis, R. A. (1997) *Br. J. Pharmacol.* **121**, 1203-1209
- Barak, L. S., Ferguson, S. S. G., Zhang, J., Martenson, C., Meyer, T., and Caron, M. G. (1997) *Mol. Pharmacol.* **51**, 177-184
- Benovic, J. L., Strasser, R. H., Caron, M. G., and Lefkowitz, R. J. (1986) *Proc. Natl. Acad. Sci, U. S. A.* **83**, 2797-2801
- Berman, D. M. and Gilman, A. G. (1998) *J. Biol. Chem.* **273**, 1269-1272
- Bertin, B., Freissmuth, M., Jockers, R., Strosberg, A. D., and Marullo, S. (1994) *Proc. Natl. Acad. Sci, U. S. A.* **91**, 8827-8831
- Birnbaumer, L., and Rodbell, M. (1969) *J. Biol. Chem.* **244**, 3477-3482
- Birnbaumer, L. (1992) *Cell* **71**, 1069-1072
- Birnbaumer, L., and Birnbaumer, M. (1995) *J Receptor & Signal Transduction Research* **15**, 213-252
- Bley, K. R., Hunter, J. C., Eglen, R. M., and Smith, J. A. M. (1998) *Trends Pharmacol. Sci.* **19**, 141-147
- Boie, Y., Rushmore, T. H., Darmon-Goodwin, A., Grygorczyk, R., Slipetz, D. M., Metters, K. M., and Abramovitz, M. (1994) *J. Biol. Chem.* **269**, 12173-12178
- Bohm, S. K., Grady, E. F., and Bunnett, N. W. (1997) *Biochem. J.* **322**, 1-18
- Bourne, H. R., Sanders, D. A., McCormick, F. (1990) *Nature* **348**, 125-128
- Bourne, H. R. (1997) *Curr. Opin. Cell Biology* **9**, 134-142

- Bouvier, M., Menard, L., Dennis, M., and Marullo, S. (1998) *Curr. Opin. Biotechnology* **9**, 522-527
- Bray, P., Carter, A., Simons, C., Guo, V., Puckett, C., Kamholz, J., Spiegel, A., and Nirenberg, M. (1986) *Proc. Natl. Acad. Sci, U. S. A.* **83**, 8893-8897
- Burt, A. R., Sautel, M., Wilson, M. A., Rees, S., Wise, A., and Milligan, G. (1998) *J. Biol. Chem.* **273**, 10367-10375
- Burstein, E. S., Spalding, T. A., Hill-Eubanks, D., and Brann, M. R., (1995) *J. Biol. Chem.* **270**, 3141-3146
- Campbell, W. B. (1990) in *Goodman and Gilman's the Pharmacological Basis of Therapeutics* (Gilman, A. G., Rall, T. W., Nies, A. S., and Taylor, P., eds) 8<sup>th</sup> Ed., p600-617, Pergamon Press, New York
- Cassel, D., and Selinger, Z. (1977) *Proc. Natl. Acad. Sci, U. S. A.* **74**, 3307-3311
- Cassel, D., and Selinger, Z. (1978) *Proc. Natl. Acad. Sci, U. S. A.* **75**, 4155-4159
- Cassey, P. J., Fong, H. K. W., Simon, M. I., and Gilman, A. G. (1990) *J. Biol. Chem.* **265**, 2383-2390
- Cerione, R. A., Regan, J. W., Nakata, H., Codina, J., Benovic, J. L., Gierschik, P., Somers, R. L., Spiegel, A. M., Birnbaumer, L., and Lefkowitz, R. J. (1986) *J. Biol. Chem.* **261**, 3901-3909
- Chabre O., Conklin, B. R., Brandon, S., Bourne, H. R., and Limbird, L. E. (1994) *J. Biol. Chem.* **269**, 5730-5734
- Chan, R. K., and Otte, C. A. (1982) *Mol. Cell. Biol.* **2**, 11-29
- Chang, F.-H. and Bourne, H. R. (1989) *J. Biol. Chem.* **264**, 5352-5357
- Clapham, D. E., and Neer, E. J. (1997) *Annu. Rev. Pharmacol. Toxicol.* **37**, 167-203

- Coleman, R. A., Smith, W. L., and Narumiya, S. (1994) *Pharmacol. Rev* **46**, 205-229
- Colquhoun, D. (1985) *Trends Pharmacol. Sci.* **6**, 197
- Conklin, B. R., Farfel, Z., Lustig, K. D., Julius, D., and Bourne, H. R. (1993a) *Nature* **363**, 274-276
- Conklin, B. R. and Bourne, H. R. (1993b) *Cell* **73**, 631-641
- Conklin, B. R., Herzmark, P., Ishida, S., Voyno-Yasenetskaya, T. A., Sun, Y., Farfel, Z., and Bourne, H. R. (1996) *Mol. Pharmacol.* **50**, 885-890
- Cotecchia, S., Exum, S., Caron, M. G., and Lefkowitz, R. J. (1990) *Proc. Natl. Acad. Sci, U. S. A.* **87**, 2896-2900
- DeBlasi, A., O'Reilly, K., and Motulsky, H. J. (1989) *Trends Pharmacol. Sci.* **10**, 227-229
- DeVries, L., Mousli, M., Wurmser, A., and Farquhar, M. G. (1995) *Proc. Natl. Acad. Sci, U. S. A.* **92**, 11916-11920
- Dixon, R. A., Kobilka, B. K., Strader, D. J., Benovic, J. L., Dohlman, H. G., Frielle, T., Bolanowski, M. A., Bennett, C. D., Rands, E., Diehl, R. E., *et al.* (1986) *Nature* **321**, 75-79
- Druey, K. M., Blumer, K. J., Kang, V. H., and Kehrl, J. H. (1996) *Nature* **379**, 742-746
- Duncan, J. A., and Gilman, A. G. (1998) *J. Biol. Chem.* **273**, 15830-15837
- Eason, M. G., Kurose, H., Holt, B. D., Raymond, J. R., and Liggett, S. B. (1992) *J. Biol. Chem.* **267**, 15795-15801
- Famdale, R. W., Allan, L. M., and Martin, B. R. (1991) in: *Signal Transduction A Practical Approach*, Oxford University Press, U. K. , 75-103

- Feron, O., Smith, T. W., Michel, T., and Kelly, R. A. (1997) *J. Biol. Chem.* **272**, 17744-17748
- Fields, T. A., and Casey, P. J. (1997) *Biochem J* **321**, 561-571
- Freissmuth, M. and Gilman, A. G. (1989) *J. Biol. Chem.* **264**, 21907-21914
- Freissmuth, M., Boehim, S., Beindl, W., Nickel, P., Ijzerman, A. P., Hohenegger, M., and Nanoff, C. (1996) *Mol. Pharmacol.* **49**, 602-611
- Gabbeta, J., Yang, X., Kowalska, M. A., Sun, L., Dhanasekaran, N., and Rao, A. K. (1997) *Proc. Natl. Acad. Sci, U. S. A.* **94**, 8750-8755
- Gierschik, P., Bouillon T., and Jakobs, K. H. (1994) *Methods Enzymol* **237**, 13-26
- Gilchrist, R. L., Ryu, K., Ji, I., and Ji, T. H. (1996) *J. Biol. Chem.* **271**, 19283-19287
- Gilman, A. G. (1987) *Annu. Rev. Biochem.* **56**, 615-649
- Goldsmith, P., Backlund, P. S., Rossiter, K., Carter, A., Milligan, G., Unson, C. G., and Spiegel, A. M. (1988) *Biochemistry* **27**, 7085-7090
- Goodman, O. B. Jr, Krupnick, J. G., Santini, F., Gurevich, V. V., and Penn, R. B. (1996) *Nature* **383**, 447-450
- Gorman, R. R., Bunting, S., and Miller, O. V. (1977) *Prostaglandins* **13**, 377-388
- Graf, R., Mattera, R., Codina, J., Estes, M. K., and Birnbaumer, L. (1992) *J. Biol. Chem.* **267**, 24307-24314
- Graziano, M. P., Freissmuth, M., and Gilman, A. G. (1989) *J. Biol. Chem.* **264**, 409-418
- Gudermann, T., Kalkbrenner, F., and Schultz, G. (1996) *Ann. Rev Pharmacol. Toxicol.* **36**, 429-459

- Hamm, H. E., Deretic, D., Arendt, A., Hargrave, P. A., Koenig, B., and Hofmann, K. P. (1988) *Science* **241**, 832-835
- Hamm, H. E. (1991) *Cell. Mol. Neurobiol.* **11**, 563-578
- Hamm, H. E. and Gilchrist, A. (1996) *Curr. Opin. Cell Biology* **8**, 189-196
- Hart, M. J., Jiang, X., Kozasa, T., Roscoe, W., Singer, W. D., Gilman, A. G., Sternweis, P. C., and Bollag, G. (1998) *Science* **280**, 2112-2114
- Hausdorff, W. P., Caron, M. G., and Lefkowitz, R. J. (1990) *FASEB J.* **4**, 2881-2889
- Hausdorff, W. P., Campbell, P. T., and Ostrowski, J. (1991) *Proc. Natl. Acad. Sci, U. S. A.* **88**, 2979-2983
- Herrlich, A. (1996) *J. Biol. Chem.* **271**, 16764-16772
- Higashijima, T., Ferguson, K. M., Smigel, M. D., and Gilman, A. G. (1987) *J. Biol. Chem.* **262**, 757-761
- Higashijima, T., Burnier, J., and Ross, E. M. (1990) *J. Biol. Chem.* **265**, 14176-14186
- Higashijima, T. and Ross, E. M. (1991) *J. Biol. Chem.* **266**, 12655-12661
- Hildebrandt, J. D. (1997) *Biochem. Pharmacol.* **54**, 325-339
- Hirata, M., Hayashi, Y., Ushikubi, F., Yokota, Y., Kageyama, R., Nakanishi, S., and Narumiya, S. (1991) *Nature* **349**, 617-620
- Hirata, M., Kakizuka, A., Aizawa, M., Ushikubi, F., and Narumiya, S. (1994) *Proc. Natl. Acad. Sci, U. S. A.* **91**, 11192-11196
- Hohenegger, M., Waldhoer, M., Beindl, W., Boing, B., Kreimeyer, A., Nickel, P., Nanoff, C., and Freissmuth, M. (1998) *Proc. Natl. Acad. Sci, U. S. A.* **95**, 346-351

- Hooley, R., Yu, C-Y., Symons, M., and Barber, D. L. (1996) *J. Biol. Chem.* **271**, 6152-6158
- Iismaa, T. P., Biden, T. J., and Shine, J. (1995) in: *G Protein-Coupled Receptors*, R. G. Landes, Austin, Texas, U. S. A.
- Jarvis, D. L., Kowar, Z. S., and Hollister, J. R. (1998) *Curr. Opin. Biotechnology* **9**, 528-533
- Ji, T. H., Grossmann, M., and Ji, I. (1998) *J. Biol. Chem.* **273**, 17299-17302
- Jiang, Y., Ma, W., Wan, Y., Kozasa, T., Hattori, S., and Huang, X.-Y. (1998) *Nature* **395**, 808-813
- Journat, L., Pantaloni, C., Bockaert, J., and Audigier, Y. (1991) *J. Biol. Chem.* **266**, 9009-9015
- Katada, T. and Ui, M. (1977) *Endocrinology* **101**, 1247-1255
- Katada, T., and Ui, M. (1981) *J. Biol. Chem.* **256**, 8310-8317
- Katada, T., and Ui, M. (1982a) *J. Biol. Chem.* **257**, 7210-7216
- Katada, T., and Ui, M. (1982b) *Proc. Natl. Acad. Sci, U. S. A.* **79**, 3129-3133
- Kaziro, Y., Itoh, H., Kozasa, T., Nakafuku, M., and Satoh, T. (1991) *Ann. Rev. Biochem.* **60**, 349-400
- Kedzie, K. M., Donello, J. E., Krauss, H. A., Regan, J. W., and Gil, D. W. (1998) *Mol. Pharmacol.* **54**, 584-590
- Kenakin, T. (1995a) *Trends Pharmacol. Sci.* **16**, 188-192
- Kenakin, T. (1995b) *Trends Pharmacol. Sci.* **16**, 232-238
- Kenakin, T. (1996) *Pharmacol. Rev.* **48**, 413-463
- Kenakin, T. (1997) *Trends Pharmacol. Sci.* **18**, 456-464

Kleuss, C., Hescheler, J., Ewel, C., Rosenthal, W., Schultz, G., and Wittig, B. (1991) *Nature* **353**, 43-48

Kleuss, C., Scherubl, H., Hescheler, J., Schultz, G., and Wittig, B. (1992) *Nature* **358**, 424-426

Kleuss, C., Scherubl, H., Hescheler, J., Schultz, G., and Wittig, B. (1993) *Science* **259**, 832-834

Kobayashi, T., Kiriya, M., Hirata, T., Hirata, M., Ushikubi, F., and Narumiya, S. (1997) *J. Biol. Chem.* **272**, 15154-15160

Koenig, J. A., and Edwardson, J. M. (1997) *Trends Pharmacol. Sci.* **18**, 276-287

Konig, B., Arendt, A., McDowell, J. H., Kahlert, M., Hargrave, P. A., and Hofmann, K. P. (1989) *Proc. Natl. Acad. Sci, U. S. A.* **86**, 6878-6882

Kostenis, E., Degtyarev, M. Y., Conklin, B. R., and Wess, J. (1997) *J. Biol. Chem.* **272**, 19107-19110

Kostenis, E., Zeng, F.-Y., and Wess, J. (1998) *J. Biol. Chem.* **273**, 17886-17892

Kozasa, T., and Gilman, A. G. (1996) *J. Biol. Chem.* **271**, 12562-12567

Krupnick, J. G., and Benovic, J. L. (1998) *Annu. Rev. Pharmacol. Toxicol.* **38**, 289-319

Kuhn, H. (1978) *Biochemistry* **17**, 4389-4395

Kurzrok, R., and Lieb, C. C. (1930) *Proc. Soc. Exp. Biol. Med.* **28**, 268-272

Lambright, D. G., Sondak, J., Bohm, A., Skiba, N. P., Hamm, H. E., and Sigler, P. B. (1996) *Nature* **379**, 311-319

Laugwitz, K.-L., Allgeier, A., Offermanns, S., Spicher, K., Sande, J. V., Dumont, J. E., and Schultz, G. (1996) *Proc. Natl. Acad. Sci, U. S. A.* **93**, 116-120

Lee, C. H., Katz, Arieh, and Simon, M. I. (1995) *Mol. Pharmacol.* **47**, 218-223

- Lee, J. W., Joshi, S., Chan, J. S., and Wong, Y. H. (1998) *J. Neurochem.* **70**, 2203-2211
- Lefkowitz, R. J. (1998) *J. Biol. Chem.* **273**, 18677-18680
- Lerea, C. L., Somers, D. E., and Hurley, J. B. (1986) *Science* **234**, 77-80
- Li, S., Okamoto, T., Chun, M., Sargiacomo, M., Casanova, J. E., Hansen, S. H., Nishimoto, I., and Lisanti, M. P. (1995) *J. Biol. Chem.* **270**, 15693-15701
- Liu, J., Conklin, B. R., Blin, N., Yun, J., and Wess, J. (1995) *Proc. Natl. Acad. Sci. U. S. A.* **92**, 11642-11646
- Logothetis, D. E., Kurachi, Y., Galper, J., Neer, E. J., and Clapham, D. E. (1987) *Nature* **325**, 321-326
- Lohse, M. J., Benovic, J. L., Codina, J., Caron, M. G., and Lefkowitz, R. J. (1990) *Science* **248**, 1547-1550
- MacEwan, D. J., Kim, G.-D., and Milligan, G. (1995) *Mol. Pharmacol.* **48**, 316-325
- MacEwan, D. J., Kim, G.-D., and Milligan, G. (1996) *Biochem. J.* **318**, 1033-1039
- MacLeod, K. G. and Milligan, G. (1990) *Cellular Signalling* **2**, 139-151
- McKenzie, F. R. and Milligan, G. (1990) *J. Biol. Chem.* **265**, 17084-17093
- Mahan, L. C., Koachman, A. M., and Insel, P. A. (1985) *Proc. Natl. Acad. Sci. U. S. A.* **82**, 129-133
- Mao, J., Yuan, H., Xie, W., Simon, M. I., and Wu, D. (1998) *J. Biol. Chem.* **273**, 27118-27123
- Masters, S. B., Sullivan, K. A., Miller, R. T., Beiderman, B., Lopez, N. G., Ramachandran, J., and Bourne, H. R. (1988) *Science* **241**, 448-451
- Masters, S. B., Miller, T. R., Chi, M.-H., Chang, F.-H., Biederman, B., Lopez, N. G., and Bourne, H. R. (1989) *J. Biol. Chem.* **264**, 15467-15474

- McLatchie, L. M., Fraser, N. J., Main, M. J., Wise, A., Brown, J., Thompson, N., Solari, R., Lee, M. G., and Foord, S. M. (1998) *Nature* **393**, 333-339
- McLaughlin, S. K., McKinnon, P. J., and Margolskee, R. F. (1992) *Nature* **357**, 563-569
- Medici, R., Bianchi, E., Segni, G. D., and Tocchini-Valentini, G. P. (1997) *EMBO J.* **16**, 7241-7249
- Milligan, G. (1988) *Biochem J* **255**, 1-13
- Milligan, G. (1993) *Trends Pharmacol. Sci.* **14**, 239-244
- Milligan, G., Marshall, F., and Rees, S. (1996) *Trends Pharmacol. Sci.* **17**, 235-237
- Mitchell, R., McCulloch, D., Lutz, E., Johnson, M., MacKenzie, C., Fennell, M., Fink, G., Zhou, W., and Sealfon, S. C. (1998) *Nature* **392**, 411-414
- Mixon, M. B., Lee, E., Coleman, D. E., Berghuis, A. M., Gilman, A. G., and Sprang, S. R. (1995) *Science* **270**, 954-960
- Mizobe, T., Mervyn Maze, M., Lam, V., Suryanarayana, S., and Kobilka, B. (1996) *J. Biol. Chem.* **271**, 2387-2389
- Mochly-Rosen, D., Chang, F. H., Cheever, L., Kim, M., Diamond, I., and Gordon, A. S. (1988) *Nature* **333**, 848-850
- Moncada, S., and Vane, J. R. (1980) *Adv. Prostaglandin Leukotriene Res.* **6**, 43-60
- Moxham, C. M., Hod, Y., and Malbon, C. C. (1993) *Science* **260**, 991-995
- Moxham, C. M. and Malbon, C. C. (1996) *Nature* **379**, 840-844

Murata, T., Ushikubi, F., Matsuoka, T., Hirata, M., Yamasaki, A., Sugimoto, Y., Ichikawa, A., Aze, Y., Tanaka, T., Yoshida, N., Ueno, A., Oh-ishi, S., and Narumiya, S. (1997) *Nature* **388**, 678-682

Namba, T., Sugimoto, Y., Negishi, M., Irie, A., Ushikubi, F., Kakizuka, A., Ito, S., Ichikawa, A., and Narumiya, S. (1993) *Nature* **365**, 166-170

Namba, T., Oida, H., Sugimoto, Y., Kakizuka, A., Negishi, M., Ichikawa, A., and Narumiya, S. (1994) *J. Biol. Chem.* **269**, 9986-9992

Nathans, J., and Hogness, D. S. (1983) *Cell* **34**, 807-814

Nathans, J., Davenport, C. M., and Maumenee, I. H. (1989) *Science* **245**, 831-838

Neer, E. J., Pulsifer, L., and Wolf, L. G. (1988) *J. Biol. Chem.* **263**, 8996-9000

Neer, E. J. and Smith, T. F. (1996) *Cell* **84**, 175-178

Neubig, R. R. (1994) *FASEB J.* **8**, 939-946

O' Dowd, B. F., Hnatowich, M., Caron, M. G., Lefkowitz, R. J., and Bouvier, M. (1989) *J. Biol. Chem.* **264**, 7564-7569

Offermanns, S., Laugwitz, K. L., Spicher, K., and Schultz, G. (1994) *Proc. Natl. Acad. Sci, U. S. A.* **91**, 504-508

Offermanns, S., Toombs, C. F., Hu, Y.-H., and Simon, M. I. (1997a) *Nature* **389**, 183-186

Offermanns, S., Mancino, V., Revel, J-P., and Simon, M. I. (1997b) *Science* **275**, 533-536

Okamoto, T., Schlegel, A., Scherer, P. E., and Lisanti, M. P. (1998) *J. Biol. Chem.* **273**, 5419-5422

Osawa, S., Dhanasekaran, N., Woon, C. W., and Johnson, G. L. (1990a) *Cell* **63**, 697-706

- Osawa, S., Heasley, L. E., Dhanasekaran, N., Gupta, S. K., Woon, C. W., Berlot, C., and Johnson, G. L. (1990b) *Mol. Cell. Biol.* **10**, 2931-2940
- Parmentier, M., Schurmans, S., Libert, F., Vanderhaeghen, P., and Vassart, G., (1994) in: *Handbook of Receptors and Channels*, CRC Press, U. S. A., Chapter 19
- Pebay-Peyroula, E., Rummel, G., Rosenbusch, J., and Landau, E., (1997) *Science* **277**, 1676-1681
- Perez, D. M., Hwa, J., Gaivin, R., Mathur, M., Brown, F., and Graham, R. M. (1996) *Mol. Pharmacol.* **49**, 112-122
- Pfeuffer, T., and Helmreich, E. J. M. (1975) *J. Biol. Chem.* **250**, 867-876
- Pfister, C., Chabre, M., Plouet, J., Tuyen, V. V., and DeKozak, Y. (1985) *Science* **228**, 891-893
- Pierce, K. L., Gil, D. W., Woodward, D. F., and Regan, J. W. (1995) *Trends Pharmacol. Sci.* **16**, 253-256
- Pippig, S., Andexinger, S., and Lohse, M. J. (1995) *Mol. Pharmacol.* **47**, 666-676
- Pitcher, J. A., Freedman, N. J., and Lefkowitz, R. J. (1998) *Annu. Rev. Biochem* **67**: 653-92
- Rall, T. W., Sutherland, E. W., and Berthet, J. (1957) *J. Biol. Chem.* **224**, 463-475
- Rands, E., Candelore, M. R., Cheung, A. H., Hill, W. S., Strader, C. D., Dixon, R. A. F. (1990) *J. Biol. Chem.* **265**, 759-764
- Rens-Domiano, S., and Hamm, H. E. (1995) *FASEB J.* **9**, 1059-1066
- Rodbell, M., Birnbaumer, L., Pohl, S. L., and Krans, H. M. J. (1971) *J. Biol. Chem.* **246**, 1877-1882
- Ross, E. M., and Gilman, A. G. (1977) *J. Biol. Chem.* **252**, 6966-6969

- Salomon, Y., Londos, C., and Rodbell, M. (1974) *Anal. Biochem.* **58**, 541-548
- Sanchez-Blazquez, P., Garcia-Espana, A., and Garzon, J. (1995) *J. Pharm. Exp. Ther.* **275**, 1590-1596
- Sautel, M. and Milligan, G. (1998) *FEBS Lett.* **436**, 46-50
- Savarese, T. M. and Fraser, C. M. (1992) *Biochem. J.* **283**, 1-19
- Schafer, A. I., Cooper, B., O'Hara, D., and Handin, R. I. (1979) *J. Biol. Chem.* **254**, 2914-2917
- Scherer, P. E., Okamoto, T., Chun, M., Nishimoto, I., Lodish, H. F., and Lisanti, M. P. (1996) *Proc. Natl. Acad. Sci, U. S. A.* **93**, 131-135
- Schmid, A., Thierauch, K., Schleuning, W., and Dinterr, H. (1995) *Eur. J. Biochem.* **228**, 23-30
- Seifert, R., Wenzel-Seifert, K., Lee, T. W., Gether, U., Sanders-Bush, E., and Kobilka, B. K. (1998a) *J. Biol. Chem.* **273**, 5109-5116
- Seifert, R., Lee, T. W., Lam, V. T., and Kobilka, B. K. (1998b) *Eur. J. Biochem.* **255**, 369-382
- Shear, M., Insel, P. A., Melmon, K. L., and Coffind, P. (1976) *J. Biol. Chem.* **251**, 7572-7576
- Simon, M. I., Strathmann, M. P., and Gautam, N. (1991) *Science* **252**, 802-808
- Simonds, W. F., Goldsmith, P. K., Codina, J., Unson, C. G., and Spiegel, A. M. (1989) *Proc. Natl. Acad. Sci, U. S. A.* **86**, 7809-7813
- Smyth, E. M., Nestor, P. V., and FitzGerald, G. A. (1996) *J. Biol. Chem.* **271**, 33698-33704
- Smyth, E. M., Li, W. H., and FitzGerald, G. A. (1998) *J. Biol. Chem.* **273**, 23258-23266

- Sondek, J., Bohm, A., Lambright, D. G., Hamm, H. E., and Sigler, P. B. (1996) *Nature* **379**, 369-374
- Spiegel, A. M. (1992) *Curr. Opin. Cell Biology* **4**, 203-211
- Sprang, S. R. (1997) *Annu. Rev. Biochem.* **66**, 639-678
- Stables, J., Green, A., Marshall, F., Fraser, N., Knight, E., Sautel, M., Milligan, G., Lee, M., and Rees, S. (1997) *Analytical Biochem.* **252**, 115-126
- Sullivan, K. A., Miller, R. T., Masters, S. B., Beiderman, B., Heideman, W., and Bourne, H. R. (1987) *Nature* **330**, 758-760
- Sutherland, E. W., and Rall, T. W. (1958) *J. Biol. Chem.* **232**, 1077-1091
- Tang, W.-J., and Gilman, A. G. (1991) *Science* **254**, 1500-1503
- Taussig, R., Iniguez-Lluhi, J. A., and Gilman, A. G. (1993) *Science* **261**, 218-221
- Taylor, J. M., Jacob-Mosier, G. G., Lawton, R. G., Remmers, A. E., and Neubig, R. R. (1994) *J. Biol. Chem.* **269**, 27618-27624
- Toh, H., Ichikawa, A., and Narumiya, S. (1995) *FEBS Lett.* **361**, 17-21
- Tsu, R. C., Ho, M. K. C., Yung, L. Y., Joshi, S., and Wong, Y. H. (1997) *Mol. Pharmacol.* **52**, 38-45
- Tsutsumi, M., Zhou, W., Millar, R. P., Mellon, P. L., Roberts, J. L., Flanagan, C. A., Dong, K., Gillo, B., and Sealfon, S. C. (1992) *Mol. Endocrinol.* **6**, 1163-1169
- Umemori, H., Inoue, T., Kume, S., Sekiyama, N., Nagao, M., Itoh, H., Nakanishi, S., Mikoshiba, K., and Yamamoto, T. (1997) *Science* **276**, 1878-1881
- Unger, V., Hargrave, P., Baldwin, J., and Schertler, G. (1997) *Nature* **389**, 203-206
- Valiquette, M., Bonin, H., Hnatowich, M., Caron, M. G., and Lefkowitz, R. J. (1990) *Proc. Natl. Acad. Sci. U. S. A.* **87**, 5089-5093

- Vassaux, G., Gaillard, D., Ailhaud, G., and Negrel, R. (1992) *J. Biol. Chem.* **267**, 11092-11097
- Von Zastrow, M., and Kobilka, B. K. (1992) *J. Biol. Chem.* **267**, 3530-3538
- Voyno-Yasenetskaya, T., Conklin, B. R., Gilbert, R. L., Hooley, R., Bourne, H. R., and Barber, D. L. (1994) *J. Biol. Chem.* **269**, 4721-4724
- Wadsworth, S. J., Gebauer, G., Rossum, G. D. V., and Dhanasekaran, N. (1997) *J. Biol. Chem.* **272**, 28829-28832
- Walseth, T. F., Zhang, H.-J., Olson, L. K., Schroeder, W. A., and Robertson, R. P. (1989) *J. Biol. Chem.* **264**, 21106-21111
- Weerd, W. F. and Leeb-Lundberg, L. M. (1997) *J. Biol. Chem.* **272**, 17858-17866
- Wedegaertner, P. B., Chu, D. H., Wilson, P. T., Levis, M. J., and Bourne, H. R. (1993) *J. Biol. Chem.* **268**, 25001-25008
- Wedegaertner, P. B., Wilson, P. T., and Bourne, H. R. (1995) *J. Biol. Chem.* **270**, 503-506
- West, R. E., Moss, J., Vaughan, M., Liu, T., and Liu, T. Y. (1985) *J. Biol. Chem.* **260**, 14428-14430
- Wieland, T. and Jakobs, K. H. (1994) *Methods Enzymol* **237**, 3-13
- Wise, A., Grassie, M. A., Parenti, M., Lee, M., Rees, S., and Milligan, G. (1997a) *Biochemistry* **36**, 10620-10629
- Wise, A. and Milligan, G. (1997b) *J. Biol. Chem.* **272**, 24673-24678
- Wise, A., Carr, I. C., and Milligan, G. (1997c) *Biochem. J.* **325**, 17-21
- Wise, A., Carr, I. C., Groarke, D. A., and Milligan, G. (1997d) *FEBS Lett.* **419**, 141-146
- Wong, S. K. and Ross, E. M. (1994) *J. Biol. Chem.* **269**, 18968-18976

Wong, Y. H. (1994) *Methods Enzymol* **238**, 81-94

Woon, C. W., Soparkar, S., Heasley, L., and Johnson, G. L. (1989) *J. Biol. Chem.* **264**, 5687-5693

Xiao, R., Ji, X., and Lakatta, E. G. (1995) *Mol. Pharmacol.* **47**, 322-329

